NASA TECHNICAL NOTE

NASA TN D-5792

STAGNATION-POINT SOLUTIONS FOR INVISCID RADIATING SHOCK LAYERS

by Walter B. Olstad

Langley Research Center
Hampton, Va. 23365

NATIONAL AERONAUTICS AND SPACE ADMINISTRATION • WASHINGTON, D. C. • JUNE 1970

1. Report No.	2. Government Accession No.	3. Recipient's Catalog No.
NASA TN D-5792		

4. Title and Subtitle
STAGNATION-POINT SOLUTIONS FOR INVISCID RADIATING SHOCK LAYERS

5. Report Date
June 1970

6. Performing Organization Code

7. Author(s)
Walter B. Olstad

8. Performing Organization Report No.
L-5111

9. Performing Organization Name and Address
NASA Langley Research Center
Hampton, Va. 23365

10. Work Unit No.
129-01-22-03-23

11. Contract or Grant No.

12. Sponsoring Agency Name and Address
National Aeronautics and Space Administration
Washington, D.C. 20546

13. Type of Report and Period Covered
Technical Note

14. Sponsoring Agency Code

15. Supplementary Notes
This report is a slightly revised version of a thesis presented to the Division of Engineering and Applied Physics, Harvard University, in partial fulfillment of the requirements for the doctor of philosophy degree in Applied Mathematics, April 1966.

16. Abstract

Four approximate analytic solutions are presented which are valid in the following situations: (1) the effects of radiation can be treated as small perturbations; (2) the optical thickness of the shock layer is small; (3) the optical thickness of the shock layer is large; and (4) radiation is the principal mode of energy transport. The first two solutions include the effects of variable thermodynamic properties, variable and nongray optical properties, and body surface reflectivity. The third and fourth solutions are restricted to gray gases.

The various solutions were used to indicate the effect of the radiation cooling parameter, the Bouguer number, the enthalpy dependence of the absorption coefficient, and surface reflectivity on the shock-layer enthalpy distribution, the stagnation-point radiant heat-transfer rate, and the shock standoff distance. A discussion of the effect of radiation cooling on the stagnation-point convective heating rate is also included. The results indicate that at every altitude and velocity, there is a finite value of body nose radius for which the rate of radiant heat transfer is a maximum. Also a significant reduction in the computed value of the radiant heating results when the nongray character of the absorption coefficient is taken into account.

17. Key Words (Suggested by Author(s))	18. Distribution Statement
Radiative heat transfer Shock layers Stagnation point	Unclassified – Unlimited

19. Security Classif. (of this report)	20. Security Classif. (of this page)	21. No. of Pages	22. Price*
Unclassified	Unclassified	181	$3.00

*For sale by the Clearinghouse for Federal Scientific and Technical Information
Springfield, Virginia 22151

CONTENTS

STAGNATION-POINT SOLUTIONS FOR INVISCID RADIATING SHOCK LAYERS[1]

By Walter B. Olstad
Langley Research Center

SUMMARY

Four approximate analytic solutions are presented which are valid in the following situations: (1) the effects of radiation can be treated as small perturbations; (2) the optical thickness of the shock layer is small; (3) the optical thickness of the shock layer is large; and (4) radiation is the principal mode of energy transport. The first two solutions include the effects of variable thermodynamic properties, variable and nongray optical properties, and body surface reflectivity. The third and fourth solutions are restricted to gray gases.

The various solutions were used to indicate the effect of the radiation cooling parameter, the Bouguer number, the enthalpy dependence of the absorption coefficient, and surface reflectivity on the shock-layer enthalpy distribution, the stagnation-point radiant heat-transfer rate, and the shock standoff distance. A discussion of the effect of radiation cooling on the stagnation-point convective heating rate is also included. The results indicate that at every altitude and velocity, there is a finite value of body nose radius for which the rate of radiant heat transfer is a maximum. Also a significant reduction in the computed value of the radiant heating results when the nongray character of the absorption coefficient is taken into account.

INTRODUCTION

As the exploration of space progresses from the near-earth environment to the moon and the planets of the solar system, study of the atmospheric entry of objects in excess of escape velocity (about 11 km/sec) becomes necessary. In addition to studies concerning man-made objects, there is considerable interest in the entry of meteoroids into the

[1]This report is a slightly revised version of a thesis presented to the Division of Engineering and Applied Physics, Harvard University, in partial fulfillment of the requirements for the doctor of philosophy degree in Applied Mathematics, April 1966.

earth's atmosphere at velocities from 20 to 70 km/sec. At these large speeds, radiant-energy transfer is an important factor governing the behavior of the hot-shock-layer gas enveloping the object.

Consequently, a number of investigators have addressed themselves to the problem of the radiating shock layer. The first analyses assumed that the flow processes were unaffected by (or uncoupled from) the transfer of energy by radiation. (See, for example, refs. 1 and 2.) Thermodynamic and flow properties were calculated by neglecting radiation. The radiant energy flux was then calculated from measured or theoretically determined optical properties for these conditions. Although this approach provided acceptable engineering estimates at speeds less than escape velocity, it was not sufficient to describe the effects of radiation at higher speeds. The next step was to take into account the loss of energy from the shock layer due to radiation. This cooling of the shock layer tends to reduce the emergent radiant energy flux. This reduction is often termed "radiation decay." Radiation decay was studied by a number of authors. (See, for example, refs. 3 to 8.) All the cited works, with the exception of reference 8, used the transparent approximation,[2] which neglects absorption within the shock layer, and assumed that the radiation cooling of the shock layer gas was small and did not influence the mass transport. The process of absorption by a gray[3] gas was studied in reference 8. However, the flow model used in that investigation only roughly approximates the flow in the stagnation region of a shock layer. Consequently, the analysis was unable to describe details of conditions in the shock layer or to provide reliable quantitative results.

Perhaps the most ambitious analysis to appear to date is the work of Howe and Viegas (ref. 9). (This statement was true at the time of first writing. Since then, however, a number of papers which treat the same complexities, some in more detail, and which include nongray effects have been published.) They obtained numerical solutions to the integro-differential system of equations governing the flow in the stagnation region including the effects of radiation decay, absorption by a gray gas, viscosity, and surface mass injection.

All the works discussed are restricted to velocities less than about 20 km/sec, although the work of Howe and Viegas was so restricted simply because they did not choose to make calculations for higher velocities. Fay, Moffatt, and Probstein (ref. 10) undertook an analysis of meteoroid entry, in the speed range of 20 to 70 km/sec. Since they were interested only in obtaining upper bound estimates of radiant heating, they

---

[2]It was so-called because the shock-layer gas is considered to be transparent to its own radiation.

[3]A gray gas is one for which the optical properties are independent of the photon energy or wavelength.

ignored radiation decay and absorption (except that they did not allow the radiant energy flux to exceed the black-body limit), both of which can be very important at these speeds.

Although the existing studies (which include many works in addition to those cited) have contributed much to the qualitative and quantitative understanding of the physical processes taking place in radiating shock layers, a great amount of work remains. For example, parametric studies of absorption in a realistic shock-layer flow are lacking, the effects of surface reflectivity have been generally ignored, and there have been no reported attempts (at least in the knowledge of this investigator) to study shock-layer gases with nongray optical properties. At the time this paper was first prepared Lick (ref. 11) and Greif (ref. 12) considered nongray optical properties in their studies of combined radiation and conduction. Their results indicate that nongray effects can be significant.

The investigation reported herein was undertaken to provide a parametric study of the influence of radiation on blunt objects large and small, traveling at speeds up to 70 km/sec. The approach was to seek simple approximate solutions where available in the hope that they would lead to a better understanding of the physical processes involved. The parameters studied included the radiation cooling parameter ϵ (which characterizes the relative importance of radiation as an energy transport mechanism compared with convection), the Bouguer number (which indicates the importance of absorption in radiant transport), the surface reflectivity (which is indicative of the ability of the surface of the object to accept the incident radiant energy flux), and the spectral variation of the absorption coefficient. (There is no single quantity or even group of quantities which characterizes the important effect of spectral variation on the flow.) Definitions of these parameters and their role in influencing the flow is discussed in greater detail in subsequent sections.

In order to facilitate this investigation without sacrificing physical significance, the analysis was limited to the stagnation region and the following conditions were assumed to apply: (1) the shock-layer gas is in local thermodynamic and chemical equilibrium, (2) the body geometry is axisymmetric, (3) there is no mass addition to the flow from the body surface, (4) the thicknesses of the shock and the viscous boundary layer are small in comparison with the shock standoff distance, and (5) absorption in the free stream ahead of the object is negligible.

In this investigation, solutions were obtained for four limiting cases of the radiation cooling parameter and the Bouguer number. The first of these is a small-perturbation expansion in the radiation cooling parameter ϵ, which is valid when the influence of radiation is small. The second solution holds when the shock layer is optically thin. This solution is presented as a small-perturbation expansion in the Bouguer number. A solution valid when the shock layer is optically thick (Bouguer number $\gg 1$) and the final solution, which is restricted to the case when radiation is the principal mode of energy

transport within the shock layer, are also presented. The first and second solutions have been formulated to include the effects of nongray radiation. The third and fourth solutions are restricted to the gray case. In each of the four limiting cases, it is possible to approximate the governing integro-differential system of equations by a purely differential system which leads to a singular perturbation problem.

The results obtained by means of the various approximations are combined to give the radiant-heat-transfer rate and an estimate of the effect of radiation on the convective heating rate at the stagnation points of blunt objects traversing a gray model earth atmosphere. The effects of the nongray character of air on these results are discussed.

In appendix A, a boundary-layer analysis is performed on the integro-differential system to determine the form of the equations in the inviscid region and the viscous boundary layer. Mathematical developments for optically thin shock layers and radiation-depleted shock layers are presented in appendixes B and C. The symbols used in the analyses are given in appendix D.

Since this work was completed in early 1966 a number of studies which include the effects of radiation decay and nongray absorption have appeared in the literature. The importance of atomic line radiation was recognized and has been included. The influence of surface ablation and absorption in the free stream have also been studied. Excellent discussions of these more recent developments can be found in two survey papers (refs. 13 and 14). The author is indebted to Professor H. W. Emmons for his guidance during the course of this study and to Mrs. J. T. Kemper who did most of the computer programming.

STAGNATION MODEL FOR A RADIATING SHOCK LAYER

Fundamental Equations of Radiation Gas Dynamics

Prior to setting up a particular flow model for the problem at hand, it is desirable to examine briefly the fundamental equations of radiation gas dynamics. An excellent discussion of these equations has been presented by Goulard (ref. 15), and the reader is referred to this work for a more detailed exposition.

The studies of this paper are limited to the steady flow of gases in local thermodynamic and chemical equilibrium. In addition, the effects of radiation pressure and radiation energy density are ignored. These effects are important only when the radiant energy flux is extremely large as it is deep in the interior of a stellar atmosphere. Finally, the presence of external forces, such as gravity and electromagnetic forces, are neglected. With these restrictions in mind, the conservation equations for a radiating gas can be written

$$\left(\rho u_i\right)_{,i} = 0 \qquad \text{(Continuity)} \tag{1}$$

$$\rho u_j u_{i,j} = p_{,i} + \tau_{ij,j} \qquad \text{(Momentum)} \tag{2}$$

$$\rho u_i h_{t,i} = -\left(u_j \tau_{ij}\right)_{,j} - q^c_{i,i} - q^R_{i,i} \qquad \text{(Energy)} \tag{3}$$

where the quantity h_t is the total specific enthalpy of the gas

$$h_t = h + \frac{1}{2} u_i u_i \tag{4}$$

The static specific enthalpy h includes the chemical energy of the gas in terms of the heats of formation of the various gaseous species.

The double subscript notation is employed wherein a subscript (i,j,k) denotes the (ith, jth, kth) component of a vector, a subscript preceded by a comma denotes differentiation of the subscripted quantity with respect to the (ith, jth, kth) direction, and any term which displays a repeated subscript represents the sum of terms over all possible values of the repeated subscript.

An expression relating the thermodynamic variables is needed to complete the set of equations. A convenient form is

$$h \equiv h(p,\rho) \tag{5}$$

The molecular transfer processes are represented by the classical expressions

$$\tau_{ij} = \mu\left(u_{i,j} + u_{j,i}\right) + \left(\mu' - \frac{2}{3}\mu\right)\delta_{ij} u_{k,k} \tag{6}$$

$$q^c_i = -k_{eff} T_{,i} \tag{7}$$

The quantity k_{eff} is an effective coefficient of heat conduction which includes the effects of energy transport by molecular collisions and by the diffusion of reacting species. These two processes can be lumped together like this only when the conditions of local thermodynamic and chemical equilibrium hold. (See ref. 16.)

The radiant-energy-flux vector q^R_i is defined in terms of the radiation intensity J_λ

$$\left.\begin{aligned} q^R_i &\equiv \int_0^\infty q^R_{\lambda i}\, d\lambda \\ q^R_{\lambda i} &\equiv \int_{4\pi} J_\lambda l_i\, d\omega \end{aligned}\right\} \tag{8}$$

and is the rate of flow of radiant energy per unit area across an element of area whose normal points in the ith direction. The quantity l_i is the direction cosine between the direction of a single beam of intensity J_λ and the ith direction. Then J_λ can be determined from the conservation equation of radiation transfer

$$\frac{dJ_\lambda}{ds} = -\rho\beta_\lambda\left(J_\lambda - \frac{j_\lambda}{\beta_\lambda}\right) \tag{9}$$

where β_λ is the mass extinction coefficient. It is composed of the mass absorption coefficient κ_λ and the mass scattering coefficient σ_λ

$$\beta_\lambda = \kappa_\lambda + \sigma_\lambda \tag{10}$$

The ratio of mass emission coefficient j_λ to the mass extinction coefficient β_λ is often called the source function $S_\lambda = j_\lambda/\beta_\lambda$.

For nonscattering media in a state of local thermodynamic equilibrium $(\sigma_\lambda = 0)$, the source function reduces to the Planck function

$$B_\lambda = \frac{2hc^2}{\lambda^5}\left(e^{hc/\lambda kT} - 1\right)^{-1} \tag{11}$$

provided that the mass absorption coefficient κ_λ includes the effects of induced emission. Here h and k are the Planck and Boltzmann constants, respectively, and c is the speed of light. Throughout the remainder of this paper, it is assumed that the gas in the shock layer is nonscattering. This assumption is reasonable as the number of large solid particles which might scatter radiation is expected to be negligible in the shock layer. A few such particles might exist in the cooler regions of the boundary layer adjacent to the body surface as a result of "spalling" of this surface. However, their presence might be accounted for, if necessary, by changing the effective reflectivity of the body surface.

At the extremely high shock-layer temperatures for which the gas is multiple ionized and free electrons are plentiful, Thomson scattering can become important. For example, Kivel and Mayer (ref. 17) show that scattering cannot be neglected when the temperature reaches 350 000° K at densities less than about 0.01 of the sea-level value.

For the nonscattering case the intensity of radiation at a point M in the direction $\vec{s}$ follows from a formal integration of equation (9)

$$J_\lambda^{(s)}(M) = \int_{P=Q}^{M} B_\lambda(P)\,\exp\left(-\tau_{\lambda,MP}\right)\,d\tau_{\lambda,MP} + J_\lambda^{(s)}(Q)\,\exp\left(-\tau_{\lambda,MQ}\right) \tag{12}$$

where

$$\tau_{\lambda,MP} = \int_P^M \rho\kappa_\lambda \, ds \tag{13}$$

is the "optical thickness" or "optical path length" along the beam between the points M and P and P is a "running" point on the beam between point M and the boundary point Q. (See sketch (a).) Although the terms optical thickness and optical path length, long established in astrophysical literature, seem to imply a dimension of length, the quantity $\tau_{\lambda,MP}$ is dimensionless and is indicative of the number of photon mean free path lengths in the physical distance between M and P.

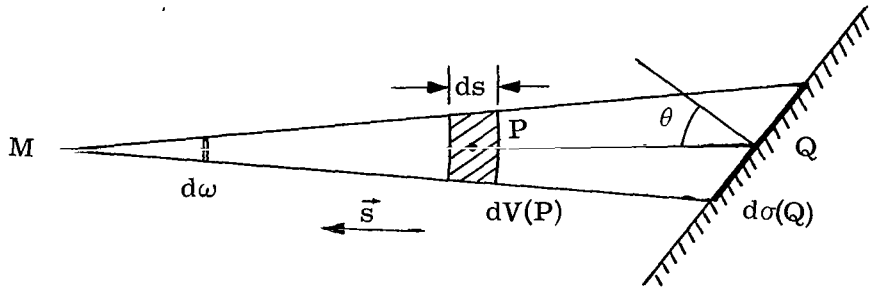

Sketch (a)

The quantity $J_\lambda^{(s)}(Q)$ represents the contribution to the intensity at point M from the boundary and, in general, includes emission from the surface, reflection from the boundary of radiation originating from within the region, and transmission through the boundary of radiation originating from without the region.

The integral term represents the summation of the contributions from all points P along the beam reduced by the attenuating factor $\exp\left(-\tau_{\lambda,MP}\right)$ which accounts for absorption by the intervening matter.

The divergence of the radiation flux vector can be found with the aid of solution (12) with the result

$$q_{i,i}^R = 4\left(\rho\kappa_P\right)_M \sigma T_M^4 - \int_0^\infty \left(\rho\kappa_\lambda\right)_M \int_V \left(\rho\kappa_\lambda B_\lambda\right)_P \frac{\exp\left(-\tau_{\lambda,MP}\right)}{\overline{MP}^2} \, dV(P) \, d\lambda$$

$$- \int_0^\infty \left(\rho\kappa_\lambda\right)_M \int_A J_\lambda^{(s)}(Q) \frac{\exp\left(-\tau_{\lambda,MQ}\right)}{\overline{MQ}^2} \cos\theta \, ds(Q) \, d\lambda \tag{14}$$

The integrations over the volume V of the gas and the area A of the bounding surface include only those portions of the volume and surface which are visible to an observer stationed at point M.

Stagnation Flow Model

The study of three-dimensional flow of compressible gas in the vicinity of the forward face of a blunt body cannot be reduced by transformation to the study of an equivalent one-dimensional system as can be done in the incompressible case. However, available numerical solutions (see, for example, refs. 18 to 20) indicate that for all practical purposes, a reduction from a three-dimensional to a nearly equivalent one-dimensional problem can be carried out in the stagnation region. The reason that this simplification can be applied is that the coupling between the momentum and energy equations is very weak. Also the various thermodynamic properties are nearly independent of the lateral or radial coordinate. Although the same arguments apply in the stagnation region of a radiating shock layer, it is not possible to postulate the existence (even approximately) of a one-dimensional solution solely on this basis. Some additional assumption is required regarding the effect of the far field on the radiant heat flux and its divergence. This effect, of course, cannot be obtained "a priori" as it depends on the solution to the entire flow field. Fortunately, the shock layer is thin and only a small part of the radiant energy emitted by gas removed from the stagnation region actually passes through the stagnation region. If absorption is small, only a small part of this energy is absorbed in the stagnation region. If, on the other hand, absorption is large, the beam is greatly attenuated when it reaches the stagnation region and thus only a small part of the energy which started the journey remains to be absorbed in the stagnation region. The divergence of the radiant flux is influenced only by the amount of energy absorbed and emitted. Consequently, the far-field effect on the divergence of the radiant flux is a result of that small part of radiant energy originating in the far field and absorbed in the stagnation region. In the transparent and optically thick limits, this effect of the far field vanishes.

It would appear from this discussion that a stagnation model for a radiating gas can be postulated as long as the assumptions concerning the far field are not grossly unrealistic. In what follows, a particular stagnation model is formulated and an estimate of the inaccuracy resulting from the assumption concerning the far field is obtained.

A schematic of the flow in the stagnation region of a blunt body is shown in sketch (b). At very high speeds, the ratio of the shock standoff distance Δ to the shock radius R_S is very much smaller than one (a typical value is 0.05). Under these conditions, the geometry of the stagnation region closely resembles a plane parallel gas slab. In addition, the enthalpy in the shock layer varies slowly with respect to r/Δ so that the stagnation region may be approximately represented by a gas slab in which the thermodynamics as well as the geometry is one dimensional.

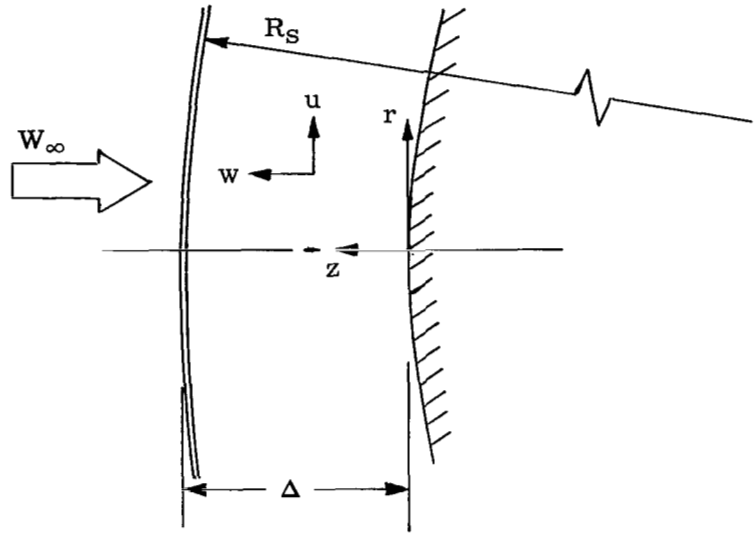

Sketch (b)

As a result of the above considerations, the model described below has been chosen to represent the flow of a radiating gas in the stagnation region of a blunt object. The model consists of an axially symmetric flow impinging upon an infinite flat plate normal to the stream direction. At a plane which is parallel to the plate and a distance Δ in front of it, the gas is suddenly raised to a total specific enthalpy of $\frac{1}{2} W_\infty^2$. The plate is held at a constant temperature T_w. Sketch (c) illustrates the geometry of the flow model.

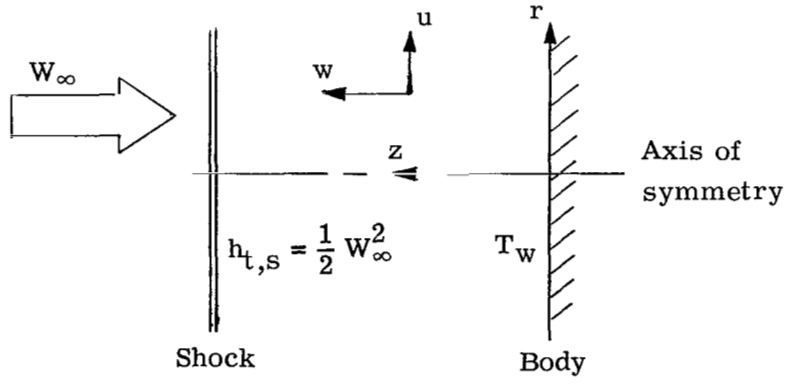

Sketch (c)

The general equations of motion (eqs. (1) and (3)) when specialized to the axisymmetric geometry become

$$\frac{\partial}{\partial r}(\rho u r) + \frac{\partial}{\partial z}(\rho w r) = 0 \tag{15}$$

$$\rho u \frac{\partial u}{\partial r} + \rho w \frac{\partial u}{\partial z} = -\frac{\partial p}{\partial r} + \frac{\partial \tau_{rr}}{\partial r} + \frac{\partial \tau_{rz}}{\partial z} + \frac{\tau_{rr} - \tau_{\theta\theta}}{r} \tag{16}$$

$$\rho u \frac{\partial w}{\partial r} + \rho w \frac{\partial w}{\partial z} = -\frac{\partial p}{\partial z} + \frac{\partial \tau_{zz}}{\partial z} + \frac{\partial \tau_{rz}}{\partial r} + \frac{\tau_{rz}}{r} \tag{17}$$

$$\rho u \frac{\partial h_t}{\partial r} + \rho w \frac{\partial h_t}{\partial z} = -\frac{\partial q_r}{\partial r} - \frac{q_r}{r} - \frac{\partial q_z}{\partial z} + \frac{\partial}{\partial r}\left(u\tau_{rr} + w\tau_{rz}\right) + \frac{1}{r}\left(u\tau_{rr} + w\tau_{rz}\right) + \frac{\partial}{\partial z}\left(u\tau_{rz} + w\tau_{zz}\right) \tag{18}$$

where q_r and q_z are the r- and z-components, respectively, of the heat flux vector which includes conduction, diffusion of reacting species, and radiation. The stress components are given by the expressions:

$$\tau_{rr} = 2\mu \frac{\partial u}{\partial r} + \left(\mu' - \frac{2}{3}\mu\right)\left(\frac{\partial u}{\partial r} + \frac{\partial w}{\partial z} + \frac{u}{r}\right) \tag{19}$$

$$\tau_{zz} = 2\mu \frac{\partial w}{\partial z} + \left(\mu' - \frac{2}{3}\mu\right)\left(\frac{\partial u}{\partial r} + \frac{\partial w}{\partial z} + \frac{u}{r}\right) \tag{20}$$

$$\tau_{\theta\theta} = 2\mu \frac{u}{r} + \left(\mu' - \frac{2}{3}\mu\right)\left(\frac{\partial u}{\partial r} + \frac{\partial w}{\partial z} + \frac{u}{r}\right) \tag{21}$$

$$\tau_{zr} = \mu\left(\frac{\partial w}{\partial r} + \frac{\partial u}{\partial z}\right) \tag{22}$$

The equation of state is

$$h \equiv h(p,\rho) \tag{23}$$

In order to specify the problem completely, a consistent set of boundary conditions must be provided. The kinematical conditions on the velocity are

$$w(r,0) = 0 \tag{24}$$

$$\rho(r,\Delta)\, w(r,\Delta) = -\rho_\infty W_\infty \tag{25}$$

The first of these conditions restricts the analysis to one for which there is no injection from the surface of the object. When gas injection is important, it is necessary to replace the zero on the right-hand side of equation (24) with w_w, the normal velocity of the gas at the wall. The second condition was obtained from continuity across the

normal shock at the stagnation point. A third kinematical condition is introduced here in order to relate the standoff distance Δ to the variation of the tangential velocity along the surface $z = \Delta$. This variation in velocity is taken to be equal to that behind the near-normal part of a spherical shock; that is,

$$u(r,\Delta) = W_\infty \cos \beta \approx W_\infty \frac{r}{R_S} \tag{26}$$

where β is the local inclination of the shock from the free-stream direction and R_S is the radius of the spherical shock.

The dynamical "no-slip" condition at the surface is

$$u(r,0) = 0 \tag{27}$$

The conditions on the enthalpy and pressure are

$$h_t(r,\Delta) = \frac{1}{2} W_\infty^2 \tag{28}$$

$$h_t(r,0) = h_w \tag{29}$$

$$p(r,\Delta) = \rho_\infty W_\infty^2 (1 - \chi)\left[1 - \left(\frac{r}{R_S}\right)^2\right] \tag{30}$$

where $\chi = \rho_\infty / \rho(0,\Delta)$ is the density ratio across the normal shock. Condition (28) comes from the conservation of energy across a strong normal shock and does not take into account absorption in the free stream of radiant energy emitted by the shock layer. Condition (29) restricts the analysis to those conditions at which a temperature "jump" or discontinuity is not present at the body surface. Such a "jump" can occur only when the molecular mean free path in the gas is not negligible in comparison with the characteristic length of the domain (in this case, the thickness of the thermal boundary layer). Condition (30) is the pressure distribution behind the near-normal part of a spherical shock of radius R_S.

In addition to the boundary conditions listed, boundary conditions on the radiant energy flux must be specified. These conditions are:

(1) The boundary at $z = \Delta$ (which corresponds to a bow shock) is transparent

(2) There is no radiant energy transfer from the free stream to the shock layer

(3) The boundary at $z = 0$ (which corresponds to the body surface) is cold and reflects diffusely and independently of wavelength a fraction r_w of the incident radiation.

The statement (contained in condition (3)) that the body surface is cold means that emission from the body surface has a negligible influence on the gas in the shock layer.

When the hot (temperatures in excess of 10 000° K) shock layer is optically thin, emission from the relatively cool (temperatures less than 4000° K) body surface may be comparable with emission from the shock-layer gas. However, because the shock layer is optically thin, very little of the radiant energy emitted at the body surface will be absorbed by the shock-layer gas. On the other hand, when absorption in the shock layer is important, the shock-layer gas emission will approach the black-body value corresponding to the high shock-layer temperature. Since black-body radiation is proportional to the fourth power of temperature, the gas emission from an optically thick layer will greatly exceed the emission from the body surface. Thus, whenever the body surface temperatures are small compared with the shock-layer gas temperatures, the influence of emission from the body surface on the shock-layer gas is unimportant.

It can be seen from the definition of the total enthalpy

$$h_t = h + \frac{1}{2}\left(u^2 + w^2\right)$$

and the boundary conditions (25) and (28) that the magnitude of the kinetic energy in the shock layer is of order χ^2 compared with the static specific enthalpy. For a strong shock, which is the only case of interest here, 0.05 is a typical value for χ, the density ratio across the shock. As a consequence of the small value of χ, the kinetic energy terms are neglected in the subsequent analysis. The viscous dissipation terms (the last three terms on the right-hand side of eq. (18)) are also neglected because only kinetic energy is dissipated through the action of the viscous forces.

It is desired that the solutions to the one-dimensional model represent, as closely as possible, the phenomena in the stagnation region of a blunt body. For simplicity, the blunt-body geometry, flow field, and thermodynamic properties are considered to be axially symmetric about the stagnation streamline. Expanding the solutions for the real blunt-body problem in terms of the radial coordinate r and arguing on physical grounds that $w(r,z)$, $p(r,z)$, $\rho(r,z)$, and $h(r,z)$ are even functions of r whereas $u(r,z)$ is odd, gives

$$\left.\begin{aligned} w &= w^{(0)}(z) + O(r^2) \\ u &= r u^{(1)}(z) + O(r^3) \\ p &= p^{(0)}(z) + O(r^2) \\ \rho &= \rho^{(0)}(z) + O(r^2) \\ h &= h^{(0)}(z) + O(r^2) \end{aligned}\right\} \tag{31}$$

In addition, the heat flux components will have the form

$$\left.\begin{aligned} q_z &= q_z^{(0)}(z) + O(r^2) \\ q_r &= r q_r^{(1)}(z) + O(r^3) \end{aligned}\right\} \tag{32}$$

Neglecting terms of order r^2 and higher restricts the solutions to the vicinity of the stagnation point. Since stagnation region solutions are desired, it is assumed that the solutions in the plane parallel model have the functional forms of equations (31) and (32) truncated after the linear term in r. For these assumed forms, the continuity equation (15) requires

$$\left.\begin{aligned} \rho u &= r g'(z) \\ \rho w &= -2g(z) \end{aligned}\right\} \tag{33}$$

That portion of the heat flux due to conduction and diffusion of reaction species is proportional to the enthalpy gradient; that is,

$$q_z^c \propto \frac{dh}{dz}$$

$$q_r^c \propto \frac{dh}{dr}$$

From conservation of energy across the near normal portion of a strong spherical shock

$$h \approx \frac{1}{2} W_\infty^2 \left[1 - \frac{1}{2}\left(\frac{r}{R_s}\right)^2\right]$$

Thus,

$$q_z^c \propto \frac{\frac{1}{2} W_\infty^2}{\Delta}$$

$$q_r^c \propto \frac{\frac{1}{2} W_\infty^2 \left(\frac{r}{R_s}\right)^2}{r}$$

By comparing terms that appear in the energy equation, it is found that

$$\frac{\frac{\partial q_r^c}{\partial r} + \frac{q_r^c}{r}}{\partial q_z^c / \partial z} \approx \left(\frac{\Delta}{R_s}\right)^2 << 1$$

Thus, the terms containing q_r^c can be neglected in the formation of the stagnation-flow model.

If the shock layer is optically thick, that is, the photon mean free path is very small compared with the shock standoff distance, the radiation flux terms take on the same form as the conduction term (according to the Rosseland or diffusion approximation) and $\partial q_r^R/\partial r + q_r^R/r$ may be neglected. On the other hand, if the gas is not optically thick, this simple order of magnitude analysis no longer suffices because the divergence of the radiant energy flux depends not only on local conditions, but on conditions throughout all the shock-heated gas which can be seen by an observer located at the point in question.

Calculations were made of the divergence of the radiant flux for a gray isothermal gas in a shock layer formed by two concentric spherical surfaces with a standoff distance to shock radius ratio of 0.05. A sketch showing the volume of gas which contributes to the radiant flux at a point on the stagnation streamline is shown in sketch (d).

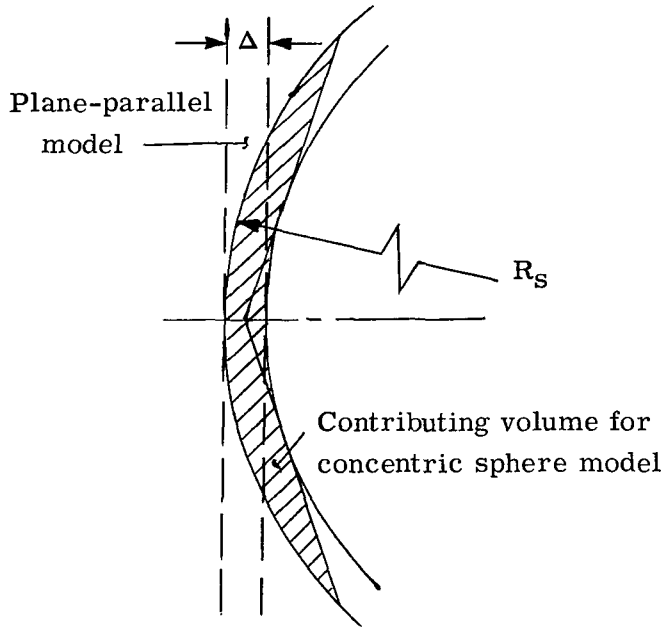

Sketch (d)

The largest difference between this result and the divergence of the radiant flux for a plane-parallel layer occurred adjacent to the wall for an optical thickness of about 0.13. The difference amounted to 2.2 percent of the value for the plane-parallel layer.

A second set of calculations was made to determine the effect of a nonuniform enthalpy distribution, in the lateral direction, on the magnitude of the divergence of the radiant flux. The enthalpy distribution was given by

$$h(r) = \begin{cases} h(0)\left[1 - \frac{1}{2}\left(\frac{\Delta}{R_S}\right)^2\left(\frac{r}{\Delta}\right)^2\right] & \left(r \leq \sqrt{2}R_S\right) \\ 0 & \left(r > \sqrt{2}R_S\right) \end{cases} \tag{34}$$

This expression approximately corresponds to the enthalpy distribution in the shock layer about a spherical body. The absorption coefficient was assumed to vary as the third power

of the enthalpy (this variation is consistent with the correlations of the optical properties of air to be discussed in a subsequent section) and the shock standoff distance to shock radius ratio Δ/R_S was chosen to be 0.05. A comparison of calculations for a plane-parallel layer in which the enthalpy was assumed to vary according to equation (34) and of calculations for a plane-parallel layer in which the lateral enthalpy distribution was uniform (that is, $h(r) = h(0)$) indicated that the largest difference in the magnitude of the divergence of the radiant flux occurred for a shock-layer optical thickness of about 0.1. This difference amounted to 2.8 percent of the value for the uniform distribution. These results are independent of the value of $h(0)$.

Since the errors in the divergence of the radiation flux for the one-dimensional shock layer due to the separate effects of geometry and nonuniform lateral distribution of enthalpy are small, their combined effect should be given approximately by the sum of the separate effects. That is, the maximum error due to the combined effects of geometry and nonuniform lateral distribution is probably not much greater than 5 percent for $\Delta/R_S = 0.05$. This statement, of course, does not imply that the final results for the enthalpy (for example) would be in error by 5 percent but only that one term in the energy equation is in error by 5 percent. In any event, the results of the calculations mentioned are considered to give sufficient justification for choosing the plane-parallel layer as a model for the stagnation region of a blunt body.

The expression for the radiant energy flux is more seriously affected by the plane-parallel layer assumption than is the divergence. For example, Koh (ref. 21) has computed the radiant flux at the wall for an isothermal shock layer formed by two concentric spheres. For a shock standoff distance to body nose radius ratio of 0.05 and a vanishingly small value of optical thickness, the result is about 17 percent less than that for a plane-parallel isothermal layer of equal optical thickness. This difference decreases with increasing optical thickness. Koh also computed the effect of nonuniform lateral enthalpy distribution by using an assumed enthalpy distribution similar to that given by equation (34). He found that the flux at the wall for the nonuniform distribution was about 1.5 percent less than that for an isothermal layer for a shock standoff distance to shock radius ratio $\Delta/R_S = 0.05$ and a vanishingly small optical thickness. As expected, the difference decreases as the optical thickness increases.

It is apparent from Koh's results, that an accurate estimate to the rate of radiant heat transfer to the stagnation point cannot be obtained through the use of the plane-parallel layer approximation unless some correction factor, which takes into account the actual geometry of the shock layer, is employed. However, because this investigation is concerned with obtaining a general understanding of the problem of radiating shock layers rather than with specific numerical results, such a correction factor will not be used herein.

At this point, it is convenient to introduce the variable transformation

$$\eta = \int_0^z \rho \, dz \tag{35}$$

The new variable η is often called the Dorodnitsyn variable. Under this transformation, the normal and tangential velocity components become

$$w = -2f(\eta)\frac{dz}{d\eta} \tag{36a}$$

$$u = rf'(\eta) \tag{36b}$$

The two momentum equations (eqs. (16) and (17)) take the form

$$\left[\rho f''(\eta)\right]' + 2f(\eta)\, f''(\eta) - \left[f'(\eta)\right]^2 = \frac{1}{\rho r}\frac{\partial p}{\partial r} \tag{37}$$

and

$$\rho\mu f''(\eta) - 2\rho\left[\mu\left(f'(\eta) - \frac{1}{\rho}\rho'(\eta)\, f(\eta)\right)\right]' + \rho\left[\left(\mu' - \frac{2}{3}\mu\right)\frac{1}{\rho}\rho'(\eta)\, f(\eta)\right]' - 2f(\eta)\, f'(\eta)$$

$$+ \frac{2}{\rho}\rho'(\eta)\left[f(\eta)\right]^2 = +\frac{1}{2}\rho p'(\eta) \tag{38}$$

An order of magnitude analysis of equation (38) indicates that $p'(\eta)$ is order χ or N_{Re}^{-1}, whichever is larger. Since both χ and N_{Re}^{-1} are very small compared with unity, equation (38) will be replaced by the simple approximate expression

$$p'(\eta) = 0 \tag{39}$$

Thus, the pressure is a function of r only. In particular, the strong shock relations for the near-normal portion of a spherical shock give

$$p(r) = \rho_\infty W_\infty^2(1 - \chi)\left[1 - \left(\frac{r}{R_S}\right)^2\right] + O(r^4) \tag{40}$$

To first-order in r

$$\frac{1}{r}\frac{\partial p}{\partial r} = -2\rho_\infty W_\infty^2(1 - \chi)\frac{1}{R_S^2}$$

so that equation (37) becomes

$$\left[\rho\mu f''(\eta)\right]' + 2f(\eta)\, f''(\eta) - \left[f'(\eta)\right]^2 = -\frac{2\rho_\infty W_\infty^2(1 - \chi)}{\rho R_S^2} \tag{41}$$

Under the foregoing assumptions and the coordinate transformation, the energy equation (18) becomes

$$-2f(\eta)\, h'(\eta) + q'(\eta) = 0 \tag{42}$$

The boundary conditions are

$$f(0) = 0 \tag{43}$$

$$f'(0) = 0 \tag{44}$$

$$f(\eta_\Delta) = \frac{1}{2}\rho_\infty W_\infty \tag{45}$$

$$f'(\eta_\Delta) = \frac{W_\infty}{R_S} \tag{46}$$

$$h(0) = h_W \tag{47}$$

$$h(\eta_\Delta) = \frac{1}{2} W_\infty^2 \tag{48}$$

where

$$\eta_\Delta = \int_0^\Delta \rho\, dz \tag{49}$$

The heat flux term $q(\eta)$ in the energy equation (42) is composed of a combined conduction and diffusion term

$$q^C(\eta) = -\rho k T'(\eta) = -\frac{\rho\mu}{N_{Pr}} h'(\eta) \tag{50}$$

and a radiation term

$$q^R(\eta) = -2\pi \int_0^\infty \left[\int_{\tau_\lambda}^{\tau_\lambda,\Delta} B_\lambda(t_\lambda)\, E_2(t_\lambda - \tau_\lambda)\, dt_\lambda - \int_0^{\tau_\lambda} B_\lambda(t_\lambda)\, E_2(\tau_\lambda - t_\lambda)\, dt_\lambda \right.$$

$$\left. - 2r_W E_3(\tau_\lambda) \int_0^{\tau_\lambda,\Delta} B_\lambda(t_\lambda)\, E_2(t_\lambda)\, dt_\lambda \right] d\lambda \tag{51}$$

This radiation term is representative of the case of a plane-parallel geometry with a transparent wall (shock) and a cold wall, which reflects diffusely and independently of wavelength a fraction r_W of the incident radiation, separated by a nonscattering nongray gas. The variable τ_λ is called the "optical path length" and is defined by the expression

$$\tau_\lambda = \int_0^z \rho\kappa_\lambda \, dz = \int_0^\eta \kappa_\lambda \, d\eta \tag{52}$$

Expression (51) was specialized from the more general expression of Goulard (ref. 22). Goulard derived the expression for the radiant flux in a plane-parallel geometry with arbitrary reflecting, absorbing, and emitting walls separated by a nonscattering, nongray gas. His expression was restricted to isotropically emitting and diffusely reflecting surfaces and hence, so is equation (51).

The first term in equation (51) represents the radiant energy flux passing through the plane τ_λ = Constant and which originated in the region between this plane and the shock at $\tau_\lambda = \tau_{\lambda,\Delta}$. This radiant flux has been attenuated by partial absorption in the intervening gas. The second term represents the radiant energy flux passing through the plane τ_λ = Constant and which originated in the region between this plane and the wall at $\tau_\lambda = 0$. This flux has also been attenuated by partial absorption in the intervening gas. The last term represents the radiant flux passing through the plane τ_λ = Constant and which was reflected from the wall and attenuated by the intervening absorbing gas.

Substituting the expressions for the energy flux equations (50) and (51) into the energy equation (42) gives

$$2f(\eta)\, h'(\eta) + \left[\frac{\rho\mu}{N_{Pr}} h'(\eta)\right]' + I[\eta] = 0 \tag{53}$$

where the divergence of the radiant flux is represented by the integral term

$$I[\eta] = -4\pi\kappa_P(\eta)\, B(\eta) + 2\pi \int_0^\infty \kappa_\lambda(\eta)\left[\int_0^{\eta_\Delta} \kappa_\lambda(\eta')\, B_\lambda(\eta')\, E_1\Big(\big|\tau_\lambda(\eta) - \tau_\lambda(\eta')\big|\Big)\, d\eta'\right.$$

$$\left. + 2r_w E_2\big(\tau_\lambda(\eta)\big) \int_0^{\eta_\Delta} \kappa_\lambda(\eta')\, B_\lambda(\eta')\, E_2\big(\tau_\lambda(\eta')\big)\, d\eta'\right] d\lambda \tag{54}$$

The final step in the derivation is to reduce the equation to nondimensional form. For this purpose, the following set of nondimensional quantities is introduced

$$\eta = \rho_s \Delta_A \bar{\eta}, \quad f(\eta) = \frac{1}{2}\rho_\infty W_\infty \bar{f}(\bar{\eta}), \quad h(\eta) = \frac{1}{2} W_\infty^2 \bar{h}(\bar{\eta})$$

$$\frac{\rho\mu}{N_{Pr}} = \left(\frac{\rho_s\mu_s}{N_{Pr,s}}\right)\mathcal{J}_1(\bar{h}), \quad \rho\mu = (\rho_s\mu_s)\mathcal{J}_2(\bar{h}), \quad \rho^{-1} = \rho_s^{-1}\mathcal{J}_3(\bar{h})$$

$$I[\eta] = 2\sigma T_s^4 \kappa_{P,s} \bar{I}[\bar{\eta}], \quad \kappa_\lambda(\eta) = \kappa_{P,s}\, \bar{\kappa}_\lambda(\bar{\eta}), \quad \tau_\lambda(\eta) = k_P\, \bar{\tau}_\lambda(\bar{\eta})$$

$\kappa_{P,s}$: cm²/gm

I think he means

$K_P \equiv$ Bouguer number

(Equations continued on next page)

$$B_\lambda(\eta) = \frac{\sigma T_s^4}{\pi} \bar{B}_\lambda(\bar{\eta}), \quad a^2 = 8\left(\frac{1-\chi}{\chi}\right)\left(\frac{\Delta_A}{R_s}\right)^2$$

$$N_{Pr,s} = \frac{\mu_s c_{p,s}}{k_s}, \quad N_{Re,s} = \frac{\rho_\infty W_\infty \Delta_A}{\mu_s}, \quad N_{Pe,s} = N_{Pr,s}\, N_{Re,s} \qquad (55)$$

$$N_{Bo} = \frac{\rho_\infty W_\infty^3}{4\sigma T_s^4}, \quad k_P = \rho_s \kappa_{P,s} \Delta_A, \quad \epsilon = \frac{k_P}{N_{Bo}}$$

The subscripts ∞ and s indicate conditions evaluated in the undisturbed free stream and immediately behind the shock, respectively. The quantity Δ_A is the shock-standoff distance for the nonradiating (or adiabatic) shock layer. The property variations represented by $\mathcal{J}_1$, $\mathcal{J}_2$, and $\mathcal{J}_3$ are functions of $\bar{h}$ only as the gas is in local thermodynamic and chemical equilibrium and the pressure has been assumed constant throughout the stagnation region. The quantities $N_{Pr,s}$, $N_{Re,s}$, and $N_{Pe,s}$ are the Prandtl, Reynolds, and Péclet numbers, respectively, based on conditions immediately behind the shock. The parameters N_{Bo}, k_P, and ϵ are the Boltzmann number, the Bouguer number, and the radiation cooling parameter, respectively. These parameters are fundamental to the study of radiation gas dynamics and have been discussed by a number of investigators. (See, for example, refs. 23 and 24.)

Substituting these nondimensional quantities into equations (41), (43) to (48), (53), and (54) yields the nondimensional system governing the flow in the stagnation region of a blunt body traveling at hypersonic speeds

$$\bar{f}(\bar{\eta})\, \bar{h}'(\bar{\eta}) + N_{Pe,s}^{-1}\left[\mathcal{J}_1(\bar{h})\, \bar{h}(\bar{\eta})\right]' + \epsilon \bar{I}[\bar{\eta}] = 0 \qquad (56)$$

$$2N_{Re,s}^{-1}\left[\mathcal{J}_2(\bar{h})\, \bar{f}''(\bar{\eta})\right]' + 2\bar{f}(\bar{\eta})\, \bar{f}''(\bar{\eta}) - \left[\bar{f}(\bar{\eta})\right]^2 + a^2 \mathcal{J}_3(\bar{h}) = 0 \qquad (57)$$

$$\bar{f}(0) = 0 \qquad (58)$$

$$\bar{f}'(0) = 0 \qquad (59)$$

$$\bar{f}(\eta_\Delta) = 1 \qquad (60)$$

$$\bar{f}'(\bar{\eta}_\Delta) = \frac{2}{\chi}\left(\frac{\Delta_A}{R_s}\right) = \frac{a}{\sqrt{2\chi(1-\chi)}} \qquad (61)$$

$$\bar{h}(0) = \bar{h}_w = \frac{h_w}{\frac{1}{2} W_\infty^2} \tag{62}$$

$$\bar{h}\left(\bar{\eta}_\Delta\right) = 1 \tag{63}$$

where $\bar{\eta}_\Delta$ is the value of the nondimensional Dorodnitsyn variable at the shock. This quantity is determined from the expression

$$\frac{\Delta}{\Delta_A} = \int_0^{\bar{\eta}_\Delta} \bar{h}(\bar{\eta})\, d\bar{\eta} \tag{64}$$

The integral term $\bar{I}\left[\bar{\eta}\right]$ is given by the expression

$$\bar{I}\left[\bar{\eta}\right] = -2\bar{\kappa}_P(\bar{\eta})\, \bar{B}(\bar{\eta}) + k_P \int_0^\infty \bar{\kappa}_\lambda(\bar{\eta}) \left[\int_0^{\bar{\eta}_\Delta} \bar{\kappa}_\lambda(\bar{\eta}')\, \bar{B}_\lambda(\bar{\eta}')\, E_1\left(k_P \left| \bar{\tau}_\lambda(\bar{\eta}') - \bar{\tau}_\lambda(\bar{\eta}) \right| \right) d\bar{\eta}' \right.$$

$$\left. + 2r_w E_2\left(k_P \bar{\tau}_\lambda(\bar{\eta})\right) \int_0^{\bar{\eta}_\Delta} \bar{\kappa}_\lambda(\bar{\eta}')\, \bar{B}_\lambda(\bar{\eta}')\, E_2\left(k_P \bar{\tau}_\lambda(\bar{\eta}')\right) d\bar{\eta}' \right] d\lambda \tag{65}$$

Later in this paper, it will be convenient to express the energy equation in terms of the optical path length as an independent variable. In both cases the optical properties of the gas are assumed to be independent of wavelength. In this event, the energy equation (less the thermal conductivity term) becomes

$$\bar{f}(\bar{\tau})\, \bar{h}'(\bar{\tau}) + \epsilon \bar{I}\left[\bar{\tau}\right] = 0 \tag{66}$$

where

$$\bar{I}\left[\bar{\tau}\right] = \frac{1}{\bar{\kappa}_P(\bar{\eta})} \bar{I}\left[\bar{\eta}\right] = -2\bar{B}(\bar{\tau}) + k_P \left[\int_0^{\bar{\tau}_\Delta} \bar{B}(\bar{t})\, E_1\left(k_P \left| \bar{\tau} - \bar{t} \right| \right) d\bar{t} \right.$$

$$\left. + 2r_w E_2\left(k_P \bar{\tau}\right) \int_0^{\bar{\tau}_\Delta} \bar{B}(\bar{t})\, E_2\left(k_P \bar{t}\right) d\bar{t} \right] \tag{67}$$

Throughout the remainder of this paper, the bars over the nondimensional variables are dropped. This procedure should not lead to any confusion because only the nondimensional form of the governing equations are employed.

Divergence of Radiant Flux

The nondimensional form of the divergence of the radiant flux is

$$\epsilon I[\eta] = -2\epsilon\kappa_P(\eta)\, B(\eta) + \epsilon k_P \int_0^\infty \kappa_\lambda(\eta) \left[\int_0^{\eta_\Delta} \kappa_\lambda(\eta')\, B_\lambda(\eta')\, E_1\Big(k_P \big| \tau_\lambda(\eta) - \tau_\lambda(\eta') \big| \Big)\, d\eta' \right.$$

$$\left. + 2r_w E_2\big(k_P \tau_\lambda(\eta)\big) \int_0^{\eta_\Delta} \kappa_\lambda(\eta')\, B_\lambda(\eta')\, E_2\big(\kappa_P \tau_\lambda(\eta')\big)\, d\eta' \right] d\lambda \qquad (68)$$

The first term on the right-hand side of this expression is the local emission term which represents the rate at which energy is emitted per unit volume of gas at the location η. The integration over all wavelengths λ has been performed for this term with the aid of the definition of the Planck mean-mass absorption coefficient. The second and third terms represent the rate at which radiant energy is absorbed per unit volume at the location η.

It is the presence of the second and third terms which so greatly complicate the radiation problem. These terms are integral expressions. In addition, their presence makes it impossible to define a wavelength averaged absorption coefficient by which the wavelength dependence might be eliminated. The importance of these terms is indicated by the magnitude of the Bouguer number k_P which is the ratio of the shock standoff distance for a nonradiating shock layer to the photon mean free path evaluated at conditions immediately behind the shock.

The radiation cooling parameter ϵ is a ratio of the rate of energy loss per unit area by radiation from both sides of a nonabsorbing isothermal layer of gas of thickness Δ_A to the rate at which kinetic energy enters the shock layer per unit area of shock surface. Alternatively, the parameter ϵ may be interpreted as the ratio of the radiationless standoff distance to the decay length where the decay length is the length required by an element of gas to lose all the energy it possessed upon emerging from the normal shock if it loses this energy by radiating (without reabsorbing) at a constant rate. This parameter modifies the entire radiation term and thus, acts as a measure of the relative efficiency of radiation compared with convection as energy transport mechanisms within the shock layer. In addition, the surface reflectivity r_w and the wavelength dependence of the absorption coefficient influence the character of the radiation terms and are considered as parameters in this study.

Most investigators who have studied problems in which a term similar to $I[\eta]$ appears have assumed that the gas and its surroundings are gray; that is, the optical properties are independent of wavelength. This assumption allows the integration over frequency to be performed analytically. Accurate results can be achieved in the two extreme cases of optically thin ($\tau_\Delta \ll 1$) and optically thick ($\tau_\Delta \gg 1$) gases. When the gas is optically thin at all wavelengths, the gray absorption coefficient is correctly given by the Planck mean mass absorption coefficient

$$\kappa_P = \int_0^\infty \kappa_\lambda B_\lambda \, d\lambda \quad , \text{Planck mean} \tag{69}$$

where κ_λ is the monochromatic mass absorption coefficient and the weighting function B_λ is the Planck black-body function. When the gas is optically thick at all wavelengths, the gray absorption coefficient, in the interior of the gas, is correctly given by the Rosseland mean mass absorption coefficient

$$\kappa_R = \frac{\int_0^\infty \frac{\partial B_\lambda}{\partial T} \, d\lambda}{\int_0^\infty \kappa_\lambda^{-1} \frac{\partial B_\lambda}{\partial T} \, d\lambda} \tag{70}$$

Near a radiation boundary or in regions of rapid (with respect to the optical path length) variations in thermodynamic properties the Rosseland mean is not valid. At intermediate values of optical depth, no single mean absorption coefficient, which depends only on local thermodynamic conditions can be defined. In fact, as has been pointed out by Krook (ref. 25), it would be necessary to define an infinite number of such mean coefficients. This restriction, of course, does not preclude the possibility of defining approximate mean coefficients under these conditions.

Stone (ref. 26) introduced a model in which the monochromatic absorption coefficient was a step function of frequency, the size of the steps being independent of the geometry or thermodynamics of the system. By means of this method, the integral over all wavelengths is reduced to a finite series. Carrier and Avrett (ref. 27) considered an absorption coefficient with only two steps, one of which was very much larger than the other. Both of these papers were concerned with Milne's problem of a stellar atmosphere in radiative equilibrium. Lick (ref. 11) and later Greif (ref. 12) studied the problem of one-dimensional energy transfer between two walls separated by a radiating and conducting gas. A picket fence model, which is a specialization of the step function model, for the absorption coefficient was used. Krook (ref. 28) derived expressions by means of the Poincaré-Lighthill-Kuo perturbation procedure for a slightly nongray gas. The solution represents a perturbation to the gray gas solution. Rhyming (ref. 29) considered wave propagation in a simple dissociating flow of a radiating gas where the absorption coefficient was given as a Gaussian function of the frequency.

However, even with these simple models for the absorption coefficient, the term $I[\eta]$ retains an integral character and the solution to the set of equations is still very difficult to obtain. Numerical procedures are extremely tedious. As a result of this difficulty, several approximate analytical methods have been derived in order to reduce this term to purely differential form. One such technique is the Milne-Eddington approximation (ref. 30), the derivation of which has been based on physical considerations, but

which may also be thought of as a substitute kernel approximation (ref. 31). The integral terms can then be eliminated by means of a double differentiation (for a gray gas only). Of course, this increases the order of the differential equation by two. This technique has been used by a number of authors in the study of the dynamics of radiating gases. (See, for example, refs. 32 and 33).[4] Barbier (ref. 30) introduced the method of expanding the source function in a Taylor series about the zero of the argument of the exponential integral kernel, $E_1\left(\left|\tau_\lambda(\eta) - \tau_\lambda(\eta')\right|\right)$. Because the kernel function has a logarithmic singularity at the zero of its argument, the integral over the first few terms of the series should provide a good approximation. The resulting integrals can then be evaluated analytically and the equation becomes purely differential in character. Yoshikawa and Chapman (ref. 8), Thomas (ref. 35), and Viskanta (ref. 36) all used the method of Barbier to different degrees of approximation. When more than the constant term in the Taylor series is retained, it may become necessary to introduce additional boundary conditions. In fact, it may not be enough merely to specify a new condition, it may be necessary to modify the existing conditions as well so that in the limit as the parameter $N = k\kappa_P/4\sigma T_0^3$ (for example) tends to zero, the solution will approach the proper pure radiation solution. This parameter, which appears in the literature concerning energy transport by radiation and conduction, represents the relative importance of conduction compared with radiation. When N tends to zero, radiation is the dominant mode of energy transport.

The diffusion approximation for optically thick gases has been used extensively in astrophysics and gas dynamics. Probstein (ref. 37) has shown how to extend the usefulness of this approximation to gas layers of finite optical thickness by means of radiation slip-boundary conditions. It is not at all clear, however, that these slip conditions can be used in the problem of this paper because of the presence of the convection term $\rho w\, dh/dz$.

The optically thin approximation of hot gases, in which absorption is neglected in comparison with emission has also been used extensively in gas dynamics. As Thomas (ref. 35) has pointed out, this approximation is not valid in those portions of the gas which are considerably cooler than the remainder of the gas.

In this paper, the integral term $I[\eta]$ is reduced to algebraic or differential form through the use of various approximations similar to those described. The manner in

---

[4]Traugott (ref. 34) has introduced a "method of moments" in order to reduce the integral term to differential form. This method may be taken to any degree of approximation desired (not without a considerable sacrifice in simplicity, however). The first approximation is identical to the Milne-Eddington approximation. Traugott's higher approximations can also be obtained by a substitute kernel method similar to that of Krook (ref. 31).

which this reduction is to be accomplished will depend on the order of magnitude of the parameters ϵ and k_P and is discussed in detail in the subsequent sections.

The Inviscid Shock Layer

As was pointed out in the Introduction, the studies of this paper will be concerned only with those cases for which the thicknesses of the wall boundary layers due to the presence of viscosity and thermal conductivity are very much less than the shock stand-off distance. For a nonradiating gas, the shock layer can be separated into an outer inviscid and nonheat-conducting region and an inner viscous and heat-conducting region or boundary layer. Considerable simplification will result if a similar separation can be achieved in the case of a radiating gas. As will be shown, such a separation can be obtained when the boundary is either optically thin or optically thick. Only the former situation is considered herein. The method of separation follows the procedures delineated by Van Dyke (ref. 38). Mathematical details are presented in appendix A.

It is shown in the appendix that the significant parameter which determines the extent of the boundary layer is the inverse square root of the Péclet number, $(N_{Pe})^{-1/2}$. The zero-order in $(N_{Pe})^{-1/2}$ system of equations which governs the flow in the inviscid region is

$$f_0(\eta)\, h_0'(\eta) + \epsilon I_0\left[\eta\right] = 0 \tag{71}$$

$$2f_0(\eta)\, f_0''(\eta) - \left[f_0'(\eta)\right]^2 + a^2 \mathfrak{F}_3(h) = 0 \tag{72}$$

$$f_0(0) = 0 \tag{73}$$

$$f_0(\eta_\Delta) = 1 \tag{74}$$

$$f_0'(\eta_\Delta) = \frac{2}{\chi}\frac{\Delta_A}{R_S} = \frac{a}{\sqrt{2\chi(1-\chi)}} \tag{75}$$

$$h_0(\eta_\Delta) = 1 \tag{76}$$

The dependent variables $f_0(\eta)$ and $h_0(\eta)$ are the asymptotic values of $f(\eta)$, the nondimensional stream function, and $h(\eta)$, the nondimensional enthalpy, respectively, as $(N_{Pe})^{-1/2}$ approaches zero.

In the boundary layer, the zero-order system of equations is

$$\left[\mathcal{F}_1(i_0)\, i_0'(\xi)\right]' + g_0(\xi)\, i_0'(\xi) + \epsilon J_0\left[\xi\right] = 0 \tag{77}$$

$$2N_{Pr,s}\left[\mathcal{F}_2(i_0)\, g_0''(\xi)\right]' + 2g_0(\xi)\, g_0''(\xi) - \left[g_0'(\xi)\right]^2 + a^2\mathcal{F}_3(i_0) = 0 \tag{78}$$

$$g_0(0) = 0 \tag{79}$$

$$g_0'(0) = 0 \tag{80}$$

$$\lim_{\xi\to\infty} g_0'(\xi) = f_0'(0) \tag{81}$$

$$i_0(0) = h_w \tag{82}$$

$$\lim_{\xi\to\infty} i_0(\xi) = h_0(0) \tag{83}$$

The independent variable ξ is the "stretched" boundary-layer coordinate defined by the relation

$$\xi = \left(N_{Pe}\right)^{1/2}\eta \tag{84}$$

The dependent variables $g(\xi)$ and $i(\xi)$ are defined by the expressions

$$i(\xi) = h(\eta) \tag{85}$$

$$g'(\xi) = f'(\eta) \tag{86}$$

in the boundary layer as $\left(N_{Pe}\right)^{-1/2}$ approaches zero.

The quantities $I_0\left[\eta\right]$ and $J_0\left[\xi\right]$ are terms of zero-order in the expansion of $I\left[\eta\right]$, the divergence of the radiant flux vector, for the inviscid and boundary-layer regions, respectively. The derivation of these quantities is presented in appendix A. The results are:

$$I_0[\eta] = -2\kappa_P[h_0(\eta)]\, B[h_0(\eta)]$$

$$+ k_P \int_0^\infty \kappa_\lambda[h_0(\eta)] \left\{ \int_0^{\eta_\Delta} \kappa_\lambda[h_0(\eta')]\, B_\lambda[h_0(\eta')]\, E_1\left(k_P|\tau_\lambda(\eta) - \tau_\lambda(\eta')|\right) d\eta' \right.$$

$$\left. + 2r_w E_2\left(k_P\tau_\lambda(\eta)\right) \int_0^{\eta_\Delta} \kappa_\lambda[h_0(\eta')]\, B_\lambda[h_0(\eta')]\, E_2\left(k_P\tau_\lambda(\eta')\right) d\eta' \right\} d\lambda \qquad (87)$$

and

$$J_0[\xi] = -2\kappa_P[i_0(\xi)]\, B[i_0(\xi)]$$

$$+ k_P \int_0^\infty \kappa_\lambda[i_0(\xi)] \left\{ \int_0^{\eta_\Delta} \kappa_\lambda[h_0(\eta')]\, B_\lambda[h_0(\eta')]\, E_1\left(k_P\tau_\lambda(\eta')\right) d\eta' \right.$$

$$\left. + 2r_w \int_0^{\eta_\Delta} \kappa_\lambda[h_0(\eta')]\, B_\lambda[h_0(\eta')]\, E_2\left(k_P\tau_\lambda(\eta')\right) d\eta' \right\} d\lambda \qquad (88)$$

The integrals which appear in the second of these expressions are definite integrals. Consequently, the system of equations governing the flow in the boundary layer is a purely differential system.

It must be realized that expressions (87) and (88) are restricted to the case of an optically thin boundary layer. It is only in this case, and the case for which the boundary layer is optically thick, that a complete separation between the inviscid region and the boundary layer can be achieved. At intermediate values of optical depth, the integral term $I_0[\eta]$ is a function of the enthalpy distribution in the boundary layer in addition to being a function of the enthalpy distribution in the inviscid region so that the equations in the inviscid region and the boundary layer are coupled. The influence on the inviscid region of radiation from an optically thick boundary layer cannot be neglected. However, most of this radiation originates at the outer edge of the boundary layer. The boundary-layer solution in this region is constrained by matching conditions to approach asymptotically the value of the inviscid solution at the wall. Hence, the radiation contribution to the inviscid region from the boundary layer can be obtained from the inviscid solution at the wall, and the inviscid solution remains uncoupled from the boundary-layer solution.

This restriction to an optically thin boundary layer is not so severe as it might first appear because the Planck mean optical thickness of a boundary layer in which the absorption coefficient is the same order of magnitude as it is for shock-heated air will not exceed about 0.1 at any altitude (above 20 km) and velocity (up to 15 km/sec) for a shock radius of 1 meter or less. In fact, the Planck mean optical thickness of the boundary layer will be less than 0.1 at that point of the trajectory of a Martian or lunar return vehicle with a shock radius of about 1 meter for which heating is a maximum even if the absorption coefficient in the boundary layer is 100 times that of shock-heated air. That the optical thickness should be small is not so difficult to see when it is realized that both the optical-path length and the boundary-layer thickness decrease rapidly with decreasing altitude. Thus, at low altitudes where the optical-path length is small and the shock layer may be optically thick, the boundary-layer thickness is very small. For larger objects, the boundary layer need not be optically thin at the lower altitudes because the boundary-layer thickness depends on the size of the object whereas the optical-path length does not.

These conclusions regarding the optical thickness of the boundary layer generally concur with the observations of Fay, Moffatt, and Probstein (ref. 10). Henceforth, the discussions of this paper will be limited to the case of an optically thin boundary layer, and radiation from this boundary layer will be considered to have no effect on the solution in the inviscid region of the shock layer.

If the inviscid system of equations (eqs. (71) to (76)) is solved for the nonradiating case ($\epsilon = 0$) along with condition of equation (64), the ratio of the shock standoff distance to the shock radius is given by the expression

$$\frac{\Delta_A}{R_S} = \frac{\chi}{1 + \sqrt{2\chi(1 - \chi)}} \tag{89}$$

Hayes (ref. 39) obtained the same result when the shock and body surfaces near the stagnation point are concentric spheres. When the shock and body surfaces are not concentric (that is, $R_S \neq R_N + \Delta$), condition (89) is still approximately true over a wide range of body shapes. (See, for example, refs. 40 and 41.) With this result

$$a = \frac{2\sqrt{2\chi(1 - \chi)}}{1 + \sqrt{2\chi(1 - \chi)}} \tag{90}$$

This value for a, the constant appearing in the momentum equation (72), will be used throughout the remainder of this investigation.

Thermodynamic and Optical Property Correlations

In order to achieve meaningful results, an attempt has been made in this paper to use simple yet physically reasonable approximations to the thermodynamic and optical

properties of high temperature gases. In particular, correlation formulas were derived from the existing store of information about equilibrium air. The thermodynamic properties were obtained from reference 42, for temperature up to 100 000° K and pressures from 10^{-3} to 10^{2} times atmospheric. The optical properties were obtained from a variety of sources which will be cited later.

It was noted from the data of reference 42, that both the density and temperature could be approximately represented by functions separable in the variables pressure and enthalpy; more specifically in the form $\left(p/p_0\right)^n f\left(h/RT_0\right)$. Plots of the functions $f\left(h/RT_0\right)$ for the density and temperature at various pressure levels are presented in figures 1 and 2, respectively. It is apparent from these plots that the density and temperature can adequately be represented by the expressions

$$\left(\frac{\rho}{\rho_0}\right) = 7.944\left(\frac{p}{p_0}\right)^{0.96}\left(\frac{h}{RT_0}\right)^{-1} \tag{91}$$

$$T = 308.8\left(\frac{p}{p_0}\right)^{0.09}\left(\frac{h}{RT_0}\right)^{0.55}, \ ^{o}K \tag{92}$$

A number of investigators (see, for example, refs. 43 to 47) have calculated the radiant properties of equilibrium air for temperatures up to 25 000° K and for densities from 10^{-6} to 10^{1} Amagats. Because of the extremely complex nature of these calculations, the many physical processes which produce radiation, and the uncertain knowledge of cross sections and transition probabilities the scatter among the various calculations is often quite large. Some of the results for the Planck mean mass absorption coefficients are presented in figure 3.

A correlation formula can be obtained from figure 3 by approximating the curves of the variation of $\log_{10} \rho\kappa_P$ with $\log_{10} T$ with straight lines. The resulting formula is

$$\rho\kappa_P = \left(7.94 \times 10^{-26}\right)\left(\frac{\rho}{\rho_0}\right)^{3.25} T^{6.0-0.5\log_{10}\left(\frac{\rho}{\rho_0}\right)}, \ cm^{-1} \tag{93}$$

This formula is not a particularly convenient form for use in the calculations of this paper. It is more desirable to express the Planck mean mass absorption coefficient κ_P in terms of the pressure and enthalpy. This expression was determined by crossplotting the logarithm of the absorption coefficient data shown in figure 3 against the logarithm of the temperature at constant pressure. Straight lines were then fitted to the resulting curves. Finally, the correlation formulas (eqs. (91) and (92)) for density and temperature were used to obtain the formula:

$$\kappa_P = \left(3.82 \times 10^{-9}\right)\left(\frac{p}{p_0}\right)^{+1.425-0.44 \log_{10}\left(\frac{p}{p_0}\right)}\left(\frac{h}{RT_0}\right)^{3.55-0.24 \log_{10}\left(\frac{p}{p_0}\right)}, \quad cm^2/gm \qquad (94)$$

This formula is valid for temperatures up to 20 000° K at the higher pressures $\left(p/p_0 = 10^{-1} \text{ to } 10^{1}\right)$ and to somewhat lower temperatures at the lower pressures (for example, when $p/p_0 = 10^{-3}$, the maximum temperature at which the formula is valid is 15 000° K).

At temperatures above about 20 000° K, the information about the radiative properties is not so comprehensive. Most of what exists consists of Planck and/or Rosseland mean absorption coefficients for continuum radiation. Line radiation is neglected. At these high temperatures, the radiation consists of spectral lines of the various ions which may be appreciably "Stark broadened" at high electron densities, and a continuum due to free bound and free-free transitions of electrons in collisions with the ions. Since the integrated line emission is proportional to the ion density whereas the continuum emission is proportional to the product of ion and electron densities, the ratio of the latter to the former increases with increasing density. Thus, at the higher density levels, the continuum calculations may be adequate.

The results of calculations of the Planck mean volume absorption coefficient for temperatures from 23 200° K to 100 000° K are presented in figure 3. These results were obtained from the paper by Armstrong et al. (ref. 45). A correlation formula was obtained from these results crossplotted in terms of constant density. The resulting formula was

$$\kappa_P = \left(2.95 \times 10^{19}\right)\left(\frac{p}{p_0}\right)^{-0.055+0.011 \log_{10}\left(\frac{p}{p_0}\right)}\left(\frac{h}{RT_0}\right)^{-1.217+0.065 \log_{10}\left(\frac{p}{p_0}\right)}, \quad cm^2/gm \qquad (95)$$

This formula can be used in the range of temperatures from 30 000° K to 100 000° K.

THE SMALL-PERTURBATION SOLUTION[5]

The Conventional Method

There is a flight regime of considerable importance in which the radiation cooling parameter ϵ is very much less than unity. In this regime, the energy transferred by

[5]The material in the corresponding section of the thesis has more recently appeared in reference 47 along with a considerable number of calculations for an improved nongray air absorption coefficient model. This report will present a summary of what is covered in the thesis and the reader is referred to reference 47 for details.

radiation is small compared with the influx of kinetic energy across the bow shock, and it would be reasonable to expect the flow properties to be only slightly perturbed from the radiationless case. Lunev and Murzinov (ref. 4) and Goulard (ref. 5) took advantage of this property and developed what amounted to first-order perturbation solutions of the temperature distribution in the inviscid region of a transparent, gray gas layer. In these papers, simplifying assumptions concerning the gas properties and flow model have been included.

In this section, the perturbation solutions are generalized to include nongray gases with arbitrary thermodynamic and optical properties. These solutions are not limited to shock layers of small optical thickness. Also, the solutions are extended to second order. As will be shown, the second-order solutions can be very important when the absorption coefficient varies rapidly with temperature.

The integro-differential system which governs the flow in the inviscid region of the shock layer is

$$f(\eta)\, h'(\eta) + \epsilon I\left[\eta\right] = 0 \tag{96}$$

$$2f(\eta)\, f''(\eta) - \left[f'(\eta)\right]^2 + a^2 h(\eta) = 0 \tag{97}$$

$$f(0) = 0 \tag{98}$$

$$f\left(\eta_\Delta\right) = 1 \tag{99}$$

$$h\left(\eta_\Delta\right) = 1 \tag{100}$$

$$f'\left(\eta_\Delta\right) = \frac{2}{\chi}\left(\frac{\Delta}{R_s}\right) = \frac{a}{\sqrt{2\chi(1-\chi)}} \tag{101}$$

Here $f(\eta)$ and $h(\eta)$ are the nondimensional stream function and enthalpy, respectively. The quantity η_Δ is the value of the Dorodnitsyn coordinate at the location of the shock. The constant a can be expressed in terms of χ, the density ratio across the shock, through expression (90). When the radiation cooling parameter ϵ is very small, the integral term in equation (96) becomes of only secondary significance throughout most of the domain of the problem with the obvious exception of the region $\eta \approx 0$ where $f(\eta) \approx 0$. (The difficulties presented by this exception are discussed later.) Neglecting the integral term $I\left[\eta\right]$ reduces the problem to one in which radiation does not play a part. If, as expected when ϵ is small, the presence of radiation only slightly influences the solution one can, to reasonable accuracy, evaluate $I\left[\eta\right]$ by using the radiationless solution for h so that equation (96) becomes purely differential. Thus, when the small-perturbation

procedure (which roughly proceeds in the manner outlined above) is applied to this problem, the integro-differential system is simplified to a purely differential system. In addition, as a result of the nature of the lowest order solution for the enthalpy distribution, the two differential equations become uncoupled and can be solved independently. Hence, it becomes possible to obtain analytic solutions to any order of approximation to the flow in the inviscid region of the shock layer. Details of the derivation of these solutions are presented in reference 47.

The zero-order, or radiationless, solution is simply

$$h_0(\eta) = 1 \tag{102}$$

$$f_0(\eta) = (1 - a)\eta^2 + a\eta \tag{103}$$

The first-order solution, which represents the effect of radiation when it is assumed that the emissive power of the gas is independent of temperature, is

$$h_1(\eta) = \int_\eta^1 \frac{I_0[x]\,dx}{(1 - a)x^2 + ax} \tag{104}$$

$$f_1(\eta) = -\frac{1}{2}\left\{\left[2(1 - a)\eta + a\right]\int_0^\eta \frac{\Phi_1(x)}{\left[(1 - a)x + a\right]^2}\,dx - \eta^2\int_\eta^1 \frac{2(1 - a)x + a}{x^2\left[(1 - a)x + a\right]^2}\,\Phi_1(x)\,dx\right\} \tag{105}$$

Here x is a dummy variable of integration. The quantity $I_0[\eta]$ is given by the formula

$$I_0[\eta] = -\int_0^\infty \kappa_\lambda B_\lambda\left\{E_2\left[k_\lambda(1 - \eta)\right] + \left(1 - r_{0,\lambda}\right)E_2\left[k_\lambda\eta\right]\right\}\,d\lambda \tag{106}$$

The notation has been simplified somewhat in this expression by omitting the argument h_0 in the terms κ_λ and B_λ and by introducing the quantities

$$k_\lambda = k_p\kappa_\lambda \tag{107}$$

$$r_{0,\lambda} = r_w\left[1 - 2E_3\left(k_\lambda\right)\right] \tag{108}$$

Also

$$\Phi_1(\eta) = -\frac{1}{2}a^2h_1(\eta) \tag{109}$$

The second-order solution takes into account the change in gas properties with changes in enthalpy. This solution is

$$h_2(\eta) = \eta_{\Delta,1} I_0[1] + \int_\eta^1 \left\{ \frac{I_1[x]}{f_0(x)} - \frac{f_1(x)\, I_0[x]}{f_0^2(x)} \right\} dx \tag{110}$$

$$f_2(\eta) = -(1-a)^2 \eta_{\Delta,1}^2 \eta^2 - \frac{1}{2}[2(1-a)\eta + a] \int_0^\eta \frac{\Phi_2(x)}{[(1-a)x + a]^2}\, dx$$

$$+ \frac{1}{2}\eta^2 \int_\eta^1 \frac{2(1-a)x + a}{x^2[(1-2)x + a]^2}\, \Phi_2(x)\, dx \tag{111}$$

where

$$I_1[x] = h_1(\eta) \int_0^\infty \left(\dot{\kappa}_\lambda B_\lambda \left\{ E_2[k_\lambda(1-\eta)] + (1 - r_{0,\lambda})\, E_2[k_\lambda \eta] \right\} - 2\kappa_\lambda \dot{B}_\lambda \right) d\lambda$$

$$+ \int_0^\infty k_\lambda \left(\kappa_\lambda \dot{B}_\lambda \int_0^1 h_1(x)\, E_1[k_\lambda | \eta - x|]\, dx + \dot{\kappa}_\lambda B_\lambda \left\{ E_1[k_\lambda(1-\eta)] \int_\eta^1 h_1(x)\, dx \right.\right.$$

$$\left.\left. + (1 - r_{0,\lambda})\, E_1[k_\lambda \eta] \int_0^\eta h_1(x)\, dx \right\} + r_{1,\lambda}\, E_2[k_\lambda \eta] \right) d\lambda \tag{112}$$

Here the argument h_0 is omitted in the terms $\dot{\kappa}_\lambda$ and $\dot{B}_\lambda$ and the quantity $r_{1,\lambda}$ is defined by the expression

$$r_{1,\lambda} = 2r_w \left[\kappa_\lambda \dot{B}_\lambda \int_0^1 h_1(x)\, E_2(k_\lambda x)\, dx + \dot{\kappa}_\lambda B_\lambda E_2(k_\lambda) \int_0^1 h_1(x)\, dx + \eta_{\Delta,1} \kappa_\lambda B_\lambda E_2(k_\lambda) \right] \tag{113}$$

Also

$$\Phi_2(\eta) = -f_1(\eta)\, f_1''(\eta) + \frac{1}{2}[f_1'(\eta)]^2 - \frac{1}{2} a^2 h_2(\eta) \tag{114}$$

The quantities $\eta_{\Delta,0}$, $\eta_{\Delta,1}$, and $\eta_{\Delta,2}$ are given by the formulas

$$\eta_{\Delta,0} = 1 \tag{115}$$

$$\eta_{\Delta,1} = \frac{1}{2} \int_0^1 \frac{\Phi_1(x)}{[(1-a)x + a]^2}\, dx \tag{116}$$

$$\eta_{\Delta,2} = (1 - a)\eta_{\Delta,1}^2 + \frac{1}{2}\int_0^1 \frac{\Phi_2(x)}{\left[(1 - a)x + a\right]^2}\,dx \tag{117}$$

It can be seen upon inspection of relation (112) that a large value of the rate of change of the Planck mean absorption coefficient with enthalpy will lead to large values of $I_1[\eta]$. Thus, at shock temperatures of less than about 30 000° K, for which the absorption coefficient does vary rapidly with enthalpy, the second-order solutions can become more important to the overall solution than their order in ϵ might at first indicate.

The Poincaré-Lighthill-Kuo Method

Inspection of the expressions (104) and (110) shows that the first-order solution for the enthalpy distribution has a logarithmic singularity at the point $\eta = 0$ and the second-order solution has a singularity of greater strength at this point. As a consequence, the assumed expansion diverges as the origin is approached and the small perturbation solution is not uniformly valid throughout the domain of the problem. This divergence can lead to serious errors in the calculation of the radiant heat flux to the wall because those regions close to the wall, in which the largest errors occur, are given the most weight in the calculation. This condition is particularly true for shock layers which are not optically thin. Additional difficulties are encountered when an attempt is made to specify the proper outer boundary conditions for the viscous boundary-layer equations. In classical boundary-layer theory, the outer boundary conditions are obtained from the values of the outer (or inviscid) solution at the wall ($\eta = 0$ in this problem). Because of the divergence of the outer solution, no finite value exists at $\eta = 0$.

In this section, the Poincaré-Lighthill-Kuo (P-L-K) perturbation of coordinate procedure[6] (ref. 48) is used to obtain a solution which is uniformly valid over the domain of the problem. The details of the application of this method to the problem of this paper are presented in reference 47. This method utilizes a coordinate transformation in the form of a perturbation expansion of the coordinate to remove the singularity (which caused the divergence of the conventional solution) from $\eta = 0$ to a small negative value of η which lies outside the domain of the problem. The P-L-K expansions are

$$\eta = x + \epsilon\eta_1^*(x) + \ldots \tag{118}$$

$$h(\eta;\epsilon) = h_0^*(x) + \epsilon h_1^*(x) + \ldots \tag{119}$$

$$f(\eta;\epsilon) = f_0^*(x) + \epsilon f_1^*(\eta) + \ldots \tag{120}$$

[6]Variously called the P-L-K method, the P-L method, Lighthill's technique, the method of strained coordinates, and the method of perturbation of coordinates.

where x is the coordinate in the transformed plane, and the asterisk superscript has been used to differentiate between the coefficients in the P-L-K expansion and the coefficients in the conventional expansion. Pritulo (ref. 49) has derived a general relation between the P-L-K and conventional coefficients. Adapted to this problem, the relationships become

$$h_0^*(x) = h_0(x) \tag{121}$$

$$h_1^*(x) = h_1(x) \tag{122}$$

$$f_0^*(x) = f_0(x) \tag{123}$$

$$f_1^*(x) = f_1(x) + \eta_1^*(x)\, f_0'(x) \tag{124}$$

$$\eta_1^*(x) = \frac{-h_2(x)}{h_1'(x)} \tag{125}$$

The second-order term $h_2(x)$ introduces the effects of variable thermodynamic and optical properties; thus it is apparent that these effects are contained in the first-order P-L-K solution.

A comparison of the P-L-K and conventional perturbation solutions for the enthalpy distribution for a constant-density transparent shock layer is presented in figure 4. The divergent character of the conventional solutions is apparent. Also shown in this figure is the exact analytic solution which can be obtained in this simple case. The formula for this exact solution is

$$h\left(\frac{\eta}{\eta_\Delta}\right) = \left\{1 + 4\epsilon(\gamma - 1)\log\left[\frac{1 + \frac{\eta}{\eta_\Delta}}{2\,\frac{\eta}{\eta_\Delta}}\right]\right\}^{-\frac{1}{\gamma-1}} \tag{126}$$

where γ (the exponent in the correlation formula $\kappa_P B = h^\gamma$) was taken to be 6 and the constant a (which appears in the momentum eq. (97)) was taken to be 0.5. The good agreement between the P-L-K solution and the exact solution indicates that the accuracy of the P-L-K solution is probably second order in the radiation cooling parameter ϵ throughout the domain except in the immediate neighborhood of the wall. It is clear that quantities such as the radiant heat flux at the wall, which depend upon an integration over the enthalpy distribution, will be considerably more accurate if the P-L-K solution rather than the conventional perturbation solution is used.

It should be noticed that the P-L-K solution does not lead to zero enthalpy at the wall as the exact transparent solution does. The reason for this disparity can be found

in the fact that the coordinate stretching displaces the boundary with regard to both the energy and momentum equations but not by a uniform amount. Thus, a physical interpretation of the first-order P-L-K solution is that the normal velocity of the flow at the boundary for the energy equation is not exactly zero, and a particle approaching this boundary will reach it in a finite time before losing all its energy by radiation.

It can be shown that since the expected error in the Dorodnitsyn coordinate η in terms of the stretched coordinate x is order ϵ^2 and since the gradients in $h_1(x)$ are very large in the vicinity of the wall, the difference between the P-L-K and exact solutions at the wall lies within expected limits. Convergence to the correct solution may be attained with the addition of higher order terms to the expansion of h and η.

Results and Discussion of Small-Perturbation Solution

The formulas derived in the preceding sections of this chapter were programed for numerical computation on the IBM 7094 electronic digital computer. The value of χ, the density ratio across the normal shock, was fixed at a constant value of 0.06 for the calculations reported in this and subsequent sections. This choice is justified because χ varies little with altitude and velocity and the effects of this variation on the stagnation solutions are slight. The value $\chi = 0.06$ is typical for hypervelocity flight in the atmosphere of the earth.

The numerical calculations indicate that the enthalpy is a double-valued function of the Dorodnitsyn coordinate η in the vicinity of the shock for large values of the Bouguer number. An examination of the governing equations failed to show the presence of any singularities which might adversely influence the solution in this region when k_P is large and ϵ small. On the other hand, the results of numerical calculations with varying mesh size seemed to rule out the possibility that the doubled-valued behavior can be attributed solely to numerical inaccuracies. Consequently, it is suspected that the difficulty results from truncation of the perturbation expansion and that inclusion of higher order terms would either eliminate the problem or increase the value of k_P at which it first appears. For truncation after the second order term, the condition for validity of the solution is $\epsilon k_P < 1$.

Gray gas results.- Shock-layer enthalpy distributions for a gray gas with differing values of the radiation cooling parameter ϵ, the Bouguer number k_P, the variation with enthalpy of the Planck mean mass absorption coefficient $\dot{\kappa}_P \left(= \partial \kappa_P / \partial h \text{ at } h = 1\right)$ and the reflectivity of the body surface r_w are presented in figures 5 to 7. Although the gray gas assumption may not be realistic for most gases of interest, its use is felt to be justified in the study of these parameters for two reasons. First, the highly complex and varied spectral structure of absorption coefficients makes a general parametric study of nongray gases impractical. Second, experience with nongray calculations indicates that

the qualitative dependence of the gray results on the various parameters will carry over to most nongray cases.

The decrease in enthalpy level with increasing ϵ is illustrated in figure 5. These results indicate that the loss of energy from the shock layer by radiation (that is, radiation cooling) can produce a noticeable drop in enthalpy for values of ϵ as small as 0.01. The dependence of the enthalpy distribution on the Bouguer number (hence, optical thickness) is also shown in these figures. As expected an increase in the Bouguer number (or optical thickness) inhibits shock-layer cooling and leads to higher values of enthalpy near the wall.

The variation of the enthalpy distribution with $\dot{\kappa}_P$ (the enthalpy variation of the Planck mean mass absorption coefficient) for several values of the Bouguer number k_P is shown in figure 6. These effects are most noticeable for optically thin shock layers $(k_P << 1.0)$ and tend to vanish as the optical thickness increases. In a transparent layer, the rate of emission of radiant energy is proportional to the Planck mean mass absorption coefficient κ_P. Thus, gases with small values of $\dot{\kappa}_P$ (which mean larger values of κ_P when the nondimensional enthalpy is less than 1) will be cooled more than gases with large values of $\dot{\kappa}_P$. As the optical thickness increases, smaller $\dot{\kappa}_P$ values still imply greater emission rates but they also mean greater absorption and more radiant energy available for absorption. The process of absorption tends to counteract the differences in emission rates due to differences in $\dot{\kappa}_P$. Finally, when radiation equilibrium is reached (this state is achieved in the interior of optically thick regions), the energy of the particle is independent of its optical properties. Of course, in those regions optically close to the shock and the wall, the amount of radiant energy available for absorption is not so great as in the interior of the shock layer and particles in these regions cannot approach the state of radiation equilibrium (except in a region optically close to a perfectly reflecting surface). Thus, the enthalpy distribution remains dependent on the value of $\dot{\kappa}_P$ near the shock and the wall. This dependence of $\dot{\kappa}_P$ is suppressed near the shock where h is almost 1 because the values of κ_P are nearly the same despite the differences in $\dot{\kappa}_P$.

The effect of surface reflectivity r_W on the shock-layer enthalpy distribution is shown in figure 7. If the shock-layer gas is transparent (that is, the gas does not absorb), surface reflectivity has no effect on the enthalpy distribution because all photons emitted by the layer escape. Whether a photon is absorbed or reflected by the wall is of no consequence. As the optical thickness of the layer increases, the chance of capture of a photon by absorption in the layer is increased. If the surface reflectivity is increased also, the probability of capture is increased still further because many photons which might otherwise have escaped into the wall are reflected back into the layer and are once

again subject to capture there. Consequently, the enthalpy level is higher near a reflecting wall than it would be near a nonreflecting wall.

It can be concluded from these statements that use of a reflecting surface will not reduce the radiant heat-transfer rate from the gas to the wall by the factor $1 - r_w$ (unless, of course, the gas is transparent) but will reduce it by some smaller fraction. This condition exists because the radiant heat flux incident on the wall is larger when the wall is reflecting as a result of the higher enthalpy level. In addition, the rate of heat transferred to the wall by conduction will be greater, also because of the higher enthalpy level. Of course, increasing the surface reflectivity always decreases the total heat-transfer rate to the wall because the higher enthalpy level must lead to an increased loss of energy by radiation through the shock in the upstream direction and by convection in a lateral direction away from the stagnation point. If the energy balance is to be maintained, the rate of heat transferred to the wall must be reduced.

The effects of variations in the parameters ϵ, k_P, $\dot{\kappa}_P$, and r_w on the rate of radiant heat transfer to the wall q_w^R $\left(\text{normalized by the energy influx to the shock layer, } \frac{1}{2}\rho_\infty W_\infty^3\right)$ are shown in figures 8 to 10. The rate of radiant heat transfer to the stagnation point was calculated with the formula

$$q_w^R = \epsilon(1 - r_w)\int_0^{\eta_\Delta} \kappa_P(\eta)\, B(\eta)\, E_2\left(k_P\tau(\eta)\right) d\eta \tag{127}$$

where the optical thickness $k_P\tau$ is given by

$$k_P\tau(\eta) = k_P \int_0^{\eta} \kappa_P(\eta)\, d\eta \tag{128}$$

The dashed curves in figure 8 indicate the "no decay limits" for various values of the Bouguer number. These limiting curves were computed by assuming the shock layer to be isenthalpic so that $\kappa_P(\eta) = B(\eta) = 1$. Thus, the no-decay-limit curves are given by the formula

$$q_w^R = \epsilon(1 - r_w)\frac{1 - 2E_3(k_P)}{2k_P} \tag{129}$$

where $E_3(k_P)$ is the exponential integral function of third order. This no-decay approximation is often used to predict the rate of radiant heat transfer when radiation effects are small. Use of this approximation always gives an upper bound to the true value of q_w^R. A study of figure 8 indicates that the no-decay limit curve is least accurate in predicting the rate of radiant heat transfer in the transparent case $k_P = 0$. This result is expected because the enthalpy distribution for the transparent case is the most perturbed from an isenthalpic state. Results presented in this figure also indicate the importance of

absorption (as characterized by the Bouguer number k_P) in reducing the rate of radiant heat transfer from the shock layer to the wall.

The results presented in figure 9 indicate the differences in $\dot{\kappa}_P$, the enthalpy variation of the Planck mean mass absorption coefficient, are most important when the optical thickness of the shock layer is small.

Here the radiant heat transfer to the wall is greatest for the smallest value of $\dot{\kappa}_P$. This result, of course, supplements the observation (from fig. 6(a)) that radiation cooling is greatest for gases in which $\dot{\kappa}_P$ is least. The differences in radiant heat transfer to the wall brought about by differences in the value of $\dot{\kappa}_P$ tend to vanish as the optical thickness of the layer increases.

The reduction in radiant heat transfer to the wall due to surface reflectivity is shown in figure 10. When the shock layer is transparent, the rate of radiant heat transferred q_w^R is in the ratio $1 - r_w$. However, as the optical thickness of the shock layer increases, the ratio becomes somewhat greater than $1 - r_w$ as predicted in an earlier discussion of this section.

The effect of the parameters ϵ, k_P, and r_w on the shock standoff distance is shown in figures 11 and 12. The quantity $\overline{\Delta}$ is the ratio of the shock standoff distance in a radiating shock layer to that in a nonradiating (or adiabatic) shock layer at the same flight conditions and was computed with the formula

$$\overline{\Delta} = \int_0^{\eta_\Delta} h(\eta)\, d\eta \tag{130}$$

The results shown in figures 11 and 12 indicate, as expected, that a decrease in enthalpy level (with the consequent increase in density level) in a shock layer leads to a reduction in shock standoff distance.

Nongray results.- The absorption coefficient of high temperature air and other gases depends strongly on wavelength. Consequently, the assumption that the gas is gray (that is, that the optical properties of the gas are independent of wavelength) is poor indeed, and has been resorted to so frequently in the literature only because of the resulting relative simplicity. Fortunately, the small perturbation solution derived in this chapter overcomes these difficulties by reducing the absorption integrals in the divergence of the radiant flux to a form amenable to direct evaluation. Thus, one need only perform an integration over a known, albeit complicated, function of wavelength. In view of the current uncertainties, with regard to spectral distributions of gaseous absorption coefficients, it was decided to use a simplified model for the absorption coefficient of air. Consequently, the step function model shown in figure 13 was chosen for use in the calculations. The height and width of the steps were chosen so that the simple step function model provides an adequate representation of the absorption coefficient of air at a temperature of

about 15 000° K as predicted by Nardone et al. (ref. 50) and so that the Planck mean absorption coefficients of both distributions are equal. The relative heights of the nine steps located at wavelengths less than 0.113 micrometer were chosen to be independent of enthalpy whereas the tenth step which covers the wavelength interval (0.113,∞) was chosen to vary as the 1.28 power of the enthalpy. The relative heights shown in figure 13 are for $h = 1$, where h is the nondimensional enthalpy. The enthalpy variation of the step heights listed is consistent with the condition that the Planck mean mass absorption coefficient is proportional to the fourth power of the enthalpy.

Shock-layer enthalpy distributions were calculated by using the nongray absorption coefficient model for various values of the Bouguer number k_P. A comparison of the results of these calculations with gray calculations by using the Planck mean mass absorption coefficient is presented in figure 14.

The maximum monochromatic Bouguer number for the nongray shock layers is 1.86 times the Planck mean Bouguer number. When the Planck mean Bouguer number k_P is less than about 0.001 (this case is not shown), the shock layer is optically thin at all wavelengths and no perceptible difference between the nongray and the gray calculations for the enthalpy distribution can be found. When $k_P = 0.01$, the monochromatic Bouguer numbers for several of the steps are of an order of magnitude of unity and absorption becomes important in the nongray model whereas absorption is still negligible in the gray model. As a consequence, the enthalpy distribution for the nongray model lies above that for the gray model. When k_P is increased to 0.1, the disparity between the two solutions is increased still further. In this case, absorption is very important in those regions of the spectrum for the nongray model in which much of the energy is emitted. Absorption is still of minor significance in the gray model. When $k_P = 1.0$, absorption becomes important in the gray model but still not to the extent that it is in the nongray case.

Obviously, and not unexpectedly, a gray model which uses the Planck mean mass absorption coefficient will not provide an acceptable estimate of the shock-layer enthalpy distribution for a nongray gas unless that gas is optically thin at all wavelengths in which a significant amount of radiation is transported. Nevertheless, it is very interesting, and encouraging to note that enthalpy distributions computed for the nongray models do not differ significantly in their general shape from those that can be computed for gray models. Thus, it appears that there is some wavelength-averaged absorption coefficient (other than the Planck mean when absorption is important but tending toward it in the transparent limit) which will provide a good approximation to the enthalpy distribution in a nongray gas.

The rate of radiant heat transfer to the stagnation point has been calculated for nongray shock layers. The results are compared in figure 15 with the results of gray calculations using the Planck mean absorption coefficient. The gray approximation provides

a considerable overestimate of the radiant heating even for values of the Planck mean Bouguer number as small as 10^{-3}. It is apparent from this result that the tallest steps play a very important role in the transfer of energy by radiation. This result is not surprising when one considers that nearly 40 percent of the energy emitted by a particle in the shock layer is transmitted in the wavelength intervals occupied by the three tallest steps.

It can be concluded from the foregoing discussion that the effective optical thickness (or Bouguer number) of a nongray shock layer is greater than that predicted by a gray analysis using the Planck mean absorption coefficient.

OPTICALLY THIN SHOCK LAYERS

The Transparent Approximation

Under certain conditions, the Bouguer number, which is indicative of the optical depth of the shock layer, is very small compared with unity. When these conditions are met, absorption is unimportant and the absorption integrals which are modified by the Bouguer number can be dropped from the expression for the divergence of the radiant flux vector. (See eq. (87).) This procedure leads to considerable simplification because only the local emission rate of radiant energy needs to be considered. All this radiant energy is assumed to escape the shock layer and it matters not, insofar as the gas is concerned, what path it takes. Consequently, surface reflectivity will have no influence on the enthalpy distribution in the shock layer. Since only the total rate of radiant energy emitted locally is of interest, the details of its spectral distribution can be ignored.

The results of the simplification is the "transparent" form of the divergence of the radiant flux vector

$$I[\eta] = -2\kappa_P(\eta)\, B(\eta) \tag{131}$$

The shock layer is termed transparent because the gas is transparent to its own radiation. Use of the transparent approximation reduces the governing equations from integro-differential to a purely differential form. Several investigators (see, for example, refs. 4 to 7) have taken advantage of this simplicity to obtain approximate analytic solutions.

The Optically Thin Approximation

In this paper, a distinction shall be made between the terms "transparent" and "optically thin." A layer of gas will be called transparent if none of the radiation emitted by the gas in the layer is reabsorbed. An optically thin layer is one in which a small amount of absorption does occur and the optical depth of the layer is small but not zero. In the literature, "optically thin" is often used synonymously with "transparent" as defined above.

P. D. Thomas (ref. 29) expressed concern about the validity of the transparent approximation, particularly in the highly cooled region adjacent to the cold wall. The transparent approximation is based on the assumption that emission is much greater than absorption throughout the shock layer. In regions of small enthalpy, emission no longer dominates absorption, and when radiation cooling effects are large, these regions may extend over a significant portion of the shock layer. Even when radiation cooling effects are small, the value of enthalpy adjacent to the wall tends to vanish[7] and absorption must become important compared with the local rate of emission. Of course, for this case, the region of nonvalidity is very small and has no appreciable effect on overall properties such as the radiant energy flux to the wall and the shock standoff distance.

Thomas sought to modify the transparent equations in order to take into account this small amount of reabsorption. He did so by expanding the Planck function $B_\lambda(t)$ which appears in the integrand of the divergence of the radiant flux vector in a Taylor series about the zero of the argument of the displacement kernel $E_1\left(k_p\left|\tau_\lambda - t_\lambda\right|\right)$. The expansion is then arbitrarily truncated after the linear term. Strictly speaking, this procedure can be used only when the Planck function varies slowly within a photon mean free path length. Obviously, this criterion is not met when the shock layer is optically thin (particularly close to the wall, the region of greatest interest, where the enthalpy and hence, the Planck function varies rapidly) and some doubt must be cast on the validity of Thomas' analysis.

It would appear that the effects of small absorption could better be discovered through a straightforward expansion of the equations in terms of the Bouguer number k_p. Such a solution, up to first order in k_p, is presented here. In order to simplify the analysis, the exponential integral functions $E_2(x)$ and $E_3(x)$ which appear in the expression for the radiant flux are replaced by the exponential functions e^{-2x} and $(1/2)e^{-2x}$, respectively. The particular form of the exponential functions was chosen so that the area under the curve of $E_2(x)$ and the approximating exponential are equal for the interval $\left(0,x_\Delta\right)$, for $x_\Delta \ll 1$; thus the value for the radiant flux reduces to the proper value in the transparent limit. This substitute kernel approximation has been used with considerable success in a variety of problems of radiant transfer. (See, for example, refs. 11, 32, 33, and 51.)

Use of the substitute kernel approximation reduces the expression for the radiant flux to the form

[7]An element of gas approaching the wall requires an infinite time to reach its destination. Because of this time required and the fact that the rate of energy lost by radiation is proportional to a positive power of the enthalpy, the enthalpy of a transparent gas must approach zero as the particle approaches the wall.

$$q^R(\eta) = \epsilon \int_0^\infty \left\{ \int_0^{\eta_\Delta} \kappa_\lambda(\xi)\, B_\lambda(\xi)\, \mathrm{sign}\left[\tau_\lambda(\eta) - \tau_\lambda(\xi)\right] e^{-2k_P\left|\tau_\lambda(\eta)-\tau_\lambda(\xi)\right|}\, d\xi \right.$$

$$\left. + r_w e^{-2k_P\tau_\lambda(\eta)} \int_0^{\eta_\Delta} \kappa_\lambda(\xi)\, B_\lambda(\xi)\, e^{-2k_P\tau_\lambda(\xi)}\, d\xi \right\} d\lambda \qquad (132)$$

The divergence of the radiant flux vector is

$$I[\eta] = 2\kappa_P(\eta)\, B(\eta) - 2k_P \int_0^\infty \kappa_\lambda(\eta) \left\{ \int_0^{\eta_\Delta} \kappa_\lambda(\xi)\, B_\lambda(\xi)\, e^{-2k_P\left|\tau_\lambda(\eta)-\tau_\lambda(\xi)\right|}\, d\xi \right.$$

$$\left. + r_w e^{-2k_P\tau_\lambda(\eta)} \int_0^{\eta_\Delta} \kappa_\lambda(\xi)\, B_\lambda(\xi)\, e^{-2k_P\tau_\lambda(\xi)}\, d\xi \right\} d\lambda \qquad (133)$$

Here the monochromatic optical depth is

$$\tau_\lambda(\eta) = \int_0^\eta \kappa_\lambda(\eta)\, d\eta \qquad (134)$$

It was seen in the section "The Small-Perturbation Solution" that an expansion of the governing equations in terms of the small parameter ϵ led to a fortuitous uncoupling of the energy and momentum equations. Unfortunately, the same is not accomplished when the expansion is performed in terms of k_P. It is frequently pointed out in the literature (for example, refs. 4 and 6) that the coupling is very weak. The solution to the momentum equation depends on the solution to the energy equation through the term $a^2\mathcal{F}_3(\eta)$ (see eq. (72)) where a^2 is order of magnitude χ. An analysis of equation (72) indicates that the contribution of this term to $f(\eta)$ is order $\sqrt{\chi}$. Since χ is very small (typically 0.06), the effect of the solution of the energy equation to $f(\eta)$ is order 0.25. Advantage can be taken of this situation by replacing $\mathcal{F}_3(\eta) = h(\eta)$ which appears in the momentum equation (72) with $\bar{h}$, the integrated average of $h(\eta)$ over the interval $(0,\eta_\Delta)$; that is,

$$\bar{h} = \frac{1}{\eta_\Delta} \int_0^{\eta_\Delta} h(\eta)\, d\eta \qquad (135)$$

(This replacement is tantamount to solving the momentum equation by the integral method with $f(\eta)$ assumed to be a quadratic function.) This approximation has the twin virtues of retaining the coupling, albeit in approximate form, and greatly simplifying the solution to the energy equation.

Now the governing system of equations takes the approximate form:

$$f(\eta)\, h'(\eta) + \epsilon I\left[\eta\right] = 0 \tag{136}$$

$$2f(\eta)\, f''(\eta) - \left[f'(\eta)\right]^2 + a^2\bar{h} = 0 \tag{137}$$

$$f(0) = 0 \tag{138}$$

$$f\left(\eta_\Delta\right) = 1 \tag{139}$$

$$f'\left(\eta_\Delta\right) = \frac{a}{\sqrt{2\chi(1 - \chi)}} \tag{140}$$

$$h\left(\eta_\Delta\right) = 1 \tag{141}$$

where $I\left[\eta\right]$ is given by equation (133). When the Bouguer number is very small, the absorption integrals in equation (133) assume a secondary significance throughout the domain of the problem. Neglecting these absorption integrals reduces the system to a purely differential form. If, as expected, when the Bouguer number k_P is small, the presence of absorption only slightly influences the solution, one can, to reasonable accuracy, evaluate the absorption integrals by using the transparent solution for h. The perturbation expansion scheme used herein follows the general outline discussed above. Mathematical details are presented in appendix B.

The zero-order, or transparent, solution is

$$\int_{h_0}^{1} \frac{dh_0}{\kappa_P\left(h_0\right) B\left(h_0\right)} = \frac{2\epsilon\eta_{\Delta,0}}{a^*} \log_e \frac{\left(1 - a^*\right)x + a^*}{x} \tag{142}$$

$$f_0(x) = \left(1 - a^*\right)x + a^*x \tag{143}$$

where

$$x = \frac{\eta}{\eta_{\Delta,0}} \tag{144}$$

$$a^* = a\sqrt{\bar{h}_0}\eta_{\Delta,0} \tag{145}$$

$$\eta_{\Delta,0} = \frac{1 + \sqrt{2\chi(1 - \chi)}}{1 + \sqrt{2\bar{h}_0\chi(1 - \chi)}} \tag{146}$$

$$\bar{h}_0 = \int_0^1 h_0(x)\, dx \tag{147}$$

It has been shown that the Planck mean mass absorption coefficient normalized by its value immediately behind the shock can be adequately represented by

$$\kappa_P(h) = \begin{cases} h^{\gamma_2} & (h \geqq h^*) \\ Ch^{\gamma_1} & (h < h^*) \end{cases} \tag{148}$$

where $\frac{1}{2} W_\infty^2 h^*$ is the value of the enthalpy (depending on the pressure, of course) at which the value of the exponent of h changes. The constant C is obtained by equating the two expressions for $\kappa_P(h)$ at $h = h^*$ with the result

$$C = (h^*)^{\gamma_2 - \gamma_1} \tag{149}$$

It also has been shown that the nondimensional Planck function $B(h)$ is approximately given by the expression

$$B(h) = h^{2.2} \tag{150}$$

When the correlation formulas (148) and (150) are introduced into equation (142), the integration on the left-hand side can be carried out, and the solution for $h_0(x)$ given by the explicit formula

$$h_0(x) = \left\{ 1 + \frac{2\epsilon(\gamma_2 + 1.2)\eta_{\Delta,0}}{a^*} \log_e \frac{(1 - a^*)x + a^*}{x} \right\}^{-\frac{1}{\gamma_2 + 1.2}} \tag{151a}$$

for $h_0(x) \geqq h^*$, and

$$h_0(x) = \left\{ (h^*)^{-(\gamma_2 + 1.2)} - \left(\frac{\gamma_1 + 1.2}{\gamma_2 + 1.2} \right) C \left[(h^*)^{-(\gamma_1 + 1.2)} - 1 \right] + \frac{2\epsilon(\gamma_1 + 1.2) C \eta_{\Delta,0}}{a^*} \log_e \frac{(1 - a^*)x + a^*}{x} \right\}^{-\frac{1}{\gamma_1 + 1.2}} \tag{151b}$$

for $h_0(x) < h^*$.

The first-order solutions which include the effects of absorption, surface reflectivity, and nongray radiation are:

$$h_1(x) = -2\epsilon\kappa_{P,0}(x)\, B_0(x)\left\{\eta_{\Delta,1} + \left(\frac{\eta_{\Delta,0}\,\bar{h}_1}{2\bar{h}_0}\right)\left[\left(1 - a^* + \frac{a^{*2}}{2}\right)\right.\right.$$

$$\left.\left. \times \frac{(1 - x)}{(1 - a^*)x + a^*} - \frac{1}{a^*}\log_e \frac{(1 - a^*)x + a^*}{x}\right]\right\}$$

$$+ (1 + r_w)\kappa_{P,0}(x)\, B_0(x)\, \eta_{\Delta,0} \int_0^\infty \left\{\left[\int_0^1 \kappa_{\lambda,0}(\xi)\, B_{\lambda,0}(\xi)\, d\xi\right] \int_{h_0}^1 \frac{\kappa_\lambda(h)}{\left[\kappa_P(h)\, B(h)\right]^2}\, dh\right\} d\lambda \tag{152}$$

$$f_1(x) = -\frac{\eta_{\Delta,1}}{\eta_{\Delta,0}}\, x(2 - a^*x) \tag{153}$$

where

$$\eta_{\Delta,1} = -\frac{a^*\,\bar{h}_1}{4\bar{h}_0}\,\eta_{\Delta,0} \tag{154}$$

$$\bar{h}_1 = \frac{\bar{h}_0 \int_0^1 h_1(x)\, dx}{h_0 + \frac{a^*}{4}(1 - h_0)} \tag{155}$$

The Poincaré-Lighthill-Kuo Solution

Careful inspection of the last term on the right-hand side of equation (152) reveals that the first-order term $h_1(x)$ displays a singular behavior near $\eta = 0$ (where h_0 approaches zero). By way of illustration, consider the case of a gray gas with $\kappa_P(h) = h^\gamma$ and $B(h) = h^{2.2}$. In this case the term in question is proportional to the quantity

$$h_0^{\gamma+2.2} \int_{h_0}^1 \frac{dh}{h^{\gamma+4.4}} = \frac{h_0^{\gamma+2.2}}{\gamma + 3.4}\left[h_0^{-(\gamma+3.4)} - 1\right] \tag{156}$$

Near the wall, h_0 approaches zero and equation (156) approaches $\dfrac{h_0^{-1.2}}{\gamma + 3.4}$ which increases without limit. This seemingly anomalous behavior can be explained as follows:

The first-order solution represents a gas which absorbs radiation at a rate determined by the absorption coefficient for the zero-order solution (the magnitude of the incident radiation is independent of the amount absorbed) while it emits energy at a rate proportional to the derivative with respect to h_0 of the emission rate for the zero-order solution. Both the absorption and emission rates tend to zero as an element of gas approaches the wall. However, the emission rate tends to zero much more rapidly than the absorption rate. The difference in the limiting behavior of these rates coupled with the infinite residence time for an element of gas in the stagnation region allows the gas element to absorb an infinite amount of energy and thus the enthalpy of the gas adjacent to the wall becomes infinite.

The difficulty which has arisen as the result of the singularity can be avoided through the use of the P-L-K perturbation of coordinates procedure which transforms the coordinate in such a way that the singularity is removed from the boundary (at $x = 0$) to a point outside the domain of the problem (a slightly negative value of x). Mathematical details of the application of this method are described in appendix B. The P-L-K solutions to first order in k_P are

$$x = y + k_P x_1^*(y) \tag{157}$$

$$h\left(x;k_P\right) = h_0^*(y) \tag{158}$$

$$f\left(x;k_P\right) = f_0^*(y) + k_P\, f_1^*(y) \tag{159}$$

where the starred coefficients in the P-L-K expansions are related to the unstarred coefficients in the regular perturbation expansions. (See ref. 49.)

$$h_0^*(y) = h_0(y) \tag{160}$$

$$f_0^*(y) = f_0(y) \tag{161}$$

$$f_1^*(y) = f_1(y) + x_1^*(y)\, f_0'(y) \tag{162}$$

$$x_1^*(y) = \frac{-h_1(y)}{h_0'(y)} \tag{163}$$

Results and Discussion of Solution for Optically Thin Shock Layers

In order to obtain some indication of the accuracy of the optically thin shock-layer approximation, the results computed for a typical case are compared in figure 16 with the results computed by means of the small-perturbation method and the results of a

numerical calculation performed by Howe and Viegas (ref. 9). The agreement the three solutions is excellent. However, a word of caution should be interject in order to avoid the implication that the numerical results of Howe and Viegas r sent the "exact" solution to the inviscid, plane-parallel geometry, stagnation flow . The results of Howe and Viegas include viscosity, heat conductivity, and body curva ture. The effects of curvature are expected to be very small. The flight conditions (W_∞ = 9.75 km/sec; p_s = 10 atm) were chosen to insure that the boundary layer was very thin so that "displacement" effects on the inviscid region were minimized. Finally, the thermodynamic and optical properties used by Howe and Viegas were obtained from their own correlations while the optically thin and small perturbation methods were computed by using the correlations presented herein. Thus, the comparisons between the results from the methods of this paper and the numerical results of Howe and Viegas are as much, or more, checks on the validity of using the inviscid approach and checks on the similarity of two different sets of correlations as they are checks on the accuracy of the analytical methods of this paper. It is conceivable that errors due to the various factors mentioned tend to cancel in this example. Nevertheless, the individual errors due to the omission of viscosity, heat conductivity, and curvature and due to the difference in correlation functions are expected to be very small so that the excellent agreement can still be interpreted as an indication of the accuracy of the small perturbation and optically thin methods.

The optically thin solution was used to study the effects of the radiation cooling parameter ϵ, the Bouguer number k_p, the surface reflectivity r_w, and the enthalpy dependence of the absorption coefficient on the shock-layer enthalpy distribution, the rate of radiant heat transfer to the stagnation point, and the shock standoff distance. As in the previous section, the density ratio χ across the near-normal section of the shock was fixed at a value of 0.06. In addition, all the results are limited to the case of a gray gas.

The effect of absorption on the enthalpy distribution is indicated by the curves of figure 17. The solid curves represent the enthalpy distributions in a transparent shock layer for ϵ = 0.01, 1.0, and 100. The dashed curves represent the enthalpy distributions in optically thin shock layers for the same values of the radiation cooling parameter ϵ. Values of the optical thicknesses are shown in the figure. These results show the expected trend, the enthalpy level falling as the radiation cooling parameter ϵ increases. Absorption tends to increase the enthalpy particularly in the cooler regions of the flow. Absorption also affects the location of the shock and reduces the value of η_Δ (the location of the shock in terms of the Dorodnitsyn coordinate) because of the decreased density level. Although the value of η_Δ decreases, the shock standoff distance Δ increases with increasing optical depth.

The effect of the enthalpy dependence of the absorption coefficient on the enthalpy distribution in transparent shock layers $(k_P = 0)$ is shown in figure 18. In figure 18(a) the absorption coefficient was given by the relation $\kappa_P = h^\gamma$, where γ takes on the values[8] 3, 4, and 5. The value of γ determines how the rate of energy emission varies with enthalpy across the shock layer. The rate of energy loss by radiation will decrease more rapidly as the enthalpy falls if γ is large than if it is small. Consequently, the enthalpy distribution for a large value of γ lies above that for a smaller value. This trend, of course, is the same trend exhibited by the small-perturbation solutions of the preceding section. In figure 18(b) the absorption coefficient is given by the relation $\kappa_P = Ch^\gamma$ where $C = (h^*)^{\gamma_2 - \gamma_1}$ and $\gamma = \gamma_1 = 4$ for $h < h^*$, and $C = 1$ and $\gamma = \gamma_2 = -1$ for $h > h^*$. This model should be used when the shock-layer temperatures are in excess of about 20 000° K since at moderate altitudes h^* (the enthalpy at which the exponent γ changes value) corresponds to temperatures of approximately this value. The effects of varying h^* are shown in figure 18(b). A decrease in h^* produces a decrease in the enthalpy level because γ takes on the smaller value (-1) throughout a greater portion of the shock layer.

The effect of surface reflectivity r_w on the enthalpy distribution is shown in figure 19. Of course, this effect vanishes in a truly transparent layer. With a small amount of absorption an increase in reflectivity brings about an increase in enthalpy level, the greatest increases occurring adjacent to the wall. These results corroborate the findings obtained with the small-perturbation solution.

The variation with the radiation cooling parameter ϵ of the rate of radiant heat transfer to the wall for various values of the Bouguer number is presented in figure 20. Also shown in this figure are two limit curves. One of these curves is labeled the "no decay limit" and was computed by assuming that the shock layer was isenthalpic and transparent. The second limit curve is labeled the "available energy limit" because it represents an upper bound to the radiant flux on the basis of energy balance. The amount of energy entering the shock layer per unit time per unit area of the shock surface has been normalized to unity. If all this energy is radiated out of a transparent shock layer, only one-half will be incident on the wall.

The curve labeled $k_P = 0$ shows the effect of radiation decay or cooling in reducing the rate of radiant heat transfer to the wall. The remaining curves indicate the important effect of absorption (as characterized here by the Bouguer number k_P) in reducing the rate of radiant heat transfer to the wall. Although values of k_P presented in figure 20 are as large as 3, the corresponding shock layers are all optically thin $(k_P \tau_\Delta << 1)$.

---

[8]These values of γ are typical for air at temperatures less than about 20 000° K. (See, for example, eq. (94).)

The effect of the enthalpy dependence of the absorption coefficient on the rate of radiant heat transfer to the wall in a transparent shock layer $(k_P = 0)$ is shown in figure 21. It is apparent that an increase in the exponent γ (which appears in the correlation formula $\kappa_P = h^\gamma$) magnifies the effect of decay on the rate of radiant heat transfer.

The effect of the radiation cooling parameter ϵ on the shock standoff distance for various values of the Bouguer number k_P and γ is shown in figure 22. As expected, an increase in ϵ reduces the value of $\overline{\Delta}$ (the ratio of shock standoff distances with and without radiation) for given k_P and γ because the cooling by radiation tends to increase the density level in the shock layer. Increases in k_P and γ for fixed ϵ inhibits the effect of decay on $\overline{\Delta}$ whereas these increases magnified the effects of decay on the rate of radiant heat transfer.

The variation of shock-layer optical thickness $k_P\tau_\Delta$ with the radiation cooling parameter ϵ and the Bouguer number k_P is shown in figure 23. When the absorption coefficient varies as a positive power of the enthalpy, the shock-layer optical thickness may be very much less than one even if the Bouguer number is order of magnitude one or greater provided that ϵ is sufficiently large.

The criterion for the validity of the analysis presented in this chapter is that the optical depth of the shock layer be much smaller than one for those wavelength regions in which a significant amount of radiant energy is transported. It has been shown herein, for the case of a gray gas for which the absorption coefficient is proportional to a positive power of the enthalpy, that this condition is always less restrictive than the condition that the Bouguer number k_P is very much less than one. However, for the more realistic case of a nongray gas, the criterion stated is generally more restrictive than the condition $k_P \ll 1$. In mathematical terms the criterion implies the inequality

$$2(1 + r_w)k_P \int_0^\infty \kappa_\lambda(\eta) \left\{ \int_0^{\eta_\Delta} \kappa_\lambda(\xi)\, B_\lambda(\xi)\, d\xi \right\} d\lambda \ll 1 \tag{164}$$

The quantity on the left-hand side of the inequality is the first-order term in the expansion of $I[\eta]$, the divergence of the radiant flux vector, in terms of the Bouguer number k_P. When both κ_λ and B_λ are proportional to a positive power of the enthalpy, an upper bound to the aforementioned quantity can be obtained by replacing $\kappa_\lambda(\eta)$, $\kappa_\lambda(\xi)$, and $B_\lambda(\xi)$ by their values at $\eta = \eta_\Delta$, immediately behind the shock. The result is

$$2(1 + r_w)k_P\eta_\Delta \int_0^\infty \kappa_\lambda^2(\eta_\Delta)\, B_\lambda(\eta_\Delta)\, d\lambda \ll 1 \tag{165}$$

If the same substitution is used for a gray gas, the result is simply

$$2(1 + r_w)k_P\eta_\Delta \ll 1 \tag{166}$$

because $\kappa_\lambda(\eta_\Delta)$ and $\int_0^\infty B_\lambda(\eta_\Delta)\,d\lambda$ are both identically equal to 1. When the nongray step function model for the absorption coefficient of air, which was used in the small perturbation solution (see fig. 13), is used to evaluate the quantity (165), the result is about 60 times greater than the corresponding gray quantity given by equation (166). Thus, the criterion for the validity of the optically thin analysis, in this nongray example, is

$$60k_P << 1$$

for small values of the radiation cooling parameter ϵ. For larger values the criterion could probably be relaxed somewhat (for example, $60k_P\tau_\Delta << 1$). As a result of this criterion, the practical applicability of the optically thin analysis (and consequently of all transparent analyses) is seriously restricted.

THE OPTICALLY THICK SHOCK LAYER

The Optically Thick Approximation

A qualitative description of the optically thick shock layer has been given by Goulard (ref. 5). He pointed out that this layer is characterized by an isothermal region between two thin boundary layers adjacent to the shock and the wall. The boundary layer immediately behind the shock is a result of the cooling of the hot gas by radiation through the transparent shock. Because radiation travels only a short distance before being absorbed in an optically thick layer, this energy loss is restricted to a narrow region which extends approximately a photon mean free path. Once this initial adjustment in energy has occurred, the gas particle is carried into the interior of the shock layer by the flow where convection is the dominant mode of energy transport. In this region, the enthalpy of the gas is essentially constant. As the particle nears the cold wall, moving ever more slowly as it does so, convection becomes of decreasing importance and energy transfer by radiation begins to assume the major role. Finally, in the immediate vicinity of the wall, all the energy transport proceeds by means of radiation. When the emissive power in the interior (or isothermal portion) of the shock layer is large, the "take-over" by radiation occurs at greater distances from the wall than if the emissive power is small. Thus, the thickness of the wall boundary layer depends not only on the optical thickness of the shock layer but also on the emissive power of the gas.

Although the shock layer is optically thick, the thermal boundary layer immediately behind the shock is not and thus the Rosseland or diffusion approximation so commonly used in the study of optically thick gases cannot be applied in this region. The Rosseland approximation is valid only in regions of an opaque gas which are at great optical distances from all radiation boundaries (a perfectly reflecting barrier is not a radiation boundary)

and in which the thermodynamic and optical properties do not vary greatly within a photon mean free path. Neither of these conditions are met in the shock boundary layer.

The conditions of validity for the Rosseland approximation might hold throughout much of the wall boundary layer if the emissive power of the gas is sufficiently large. However, the approximation must break down optically close to the wall. The use of a temperature jump boundary condition as suggested by several investigators (refs. 27, 52, and 53) has proven successful in problems of radiant and combined radiant and conductive energy transport. Whether this concept can be applied with equal success to problems of combined radiant and convective energy transport has not, as yet, been demonstrated. In a region optically close to a radiation boundary, the temperature predicted through the use of the Rosseland approximation and a slip boundary condition represents not the temperature of the molecules of the gas, but a sort of average photon temperature. The convective heat flux depends on the molecular temperature. Thus, it is not clear that the slip boundary condition can be used in a problem of combined radiant and convective energy transport. There is a basis for optimism when considering the problem of this chapter, however, in that the convective flux may be negligible compared with the radiant flux optically close to the wall.

In order to arrive at a solution to the problem of the optically thick shock layer, the substitute kernel approximation, introduced earlier is used. It is shown that in the interior of the shock layer and close to the wall but not in the shock boundary layer, this method is equivalent to using the Rosseland approximation with slip-boundary conditions. The use of this approximation will restrict the analysis to gray gases. This restriction is not a condition for application of these approximations, but has been invoked here to avoid the considerable additional complication that relaxation of this restriction would incur.

The Substitute Kernel Approximation

In this and the subsequent section, it will be convenient to rewrite the energy equation (eq. (71)) with the optical path length τ as the independent variable; that is,

$$f(\tau)\, h'(\tau) + \epsilon I\left[\tau\right] = 0 \tag{167}$$

Here, f is the nondimensional stream function; h, the nondimensional enthalpy; and ϵ, the radiation cooling parameter. The divergence of the radiant flux vector $I\left[\tau\right]$ is given by the expression

$$I\left[\tau\right] = \frac{1}{\kappa(\eta)} I\left[\eta\right] = -2B(\tau)\, E_2(0) + k_P \int_0^{\tau_\Delta} B(t)\, E_1\left(k_P\left|\tau - t\right|\right) dt + 2k_P r_w E_2\left(k_P\tau\right) \int_0^{\tau_\Delta} B(t)\, E_2\left(k_P t\right) dt \tag{168}$$

τ is the nondimensional absorption coefficient; B, the nondimensional Planck body function; k_P, the Bouguer number; r_w, the reflectivity of the wall (at $\tau = 0$); value of the optical path length at the shock; and E_1 and E_2, the exponential integral functions of first and second order, respectively.

In order to simplify the analysis, the substitute kernel approximation is used. For the optically thick shock layer, the appropriate substitution for $E_2(x)$ is found to be $(3/4)e^{-(3/2)x}$. This substitution satisfies the conditions that the areas under the two functions over the domain $0 \leqq x \leqq \infty$ are equal and that the expressions for the radiant flux approach the Rosseland expression as x increases without limit.

If the expression for the radiation flux is differentiated twice with respect to τ, the integral terms can be eliminated with the result

$$I''[\tau] - \frac{9}{4} k_P^2 I[\tau] = -\frac{3}{2} B''(\tau) \tag{169}$$

The energy equation (167) can then be used to eliminate $I[\tau]$

$$[f(\tau)\, h'(\tau)]'' - \frac{9}{4} k_P^2 f(\tau)\, h'(\tau) = \frac{3}{2} \epsilon B''(\tau) \tag{170}$$

This alternate form of the energy equation is a third-order nonlinear ordinary differential equation, the solution of which must satisfy the condition $h(1) = 1$. Two additional constants of integration are introduced by the solution of equation (170). These constants are determined by satisfying appropriate physical conditions or by satisfying the original integro-differential equation (eq. (167)).

An expression for the flux of radiant energy which enters the wall can be obtained very simply. The expression for the flux incident on the wall is

$$\frac{q_w^R}{1 - r_w} = \frac{3}{4} \epsilon \int_0^{\tau_\Delta} B(t)\, e^{-\frac{3}{2} k_P t}\, dt$$

When the integro-differential form of the energy equation (eq. (167)) is evaluated at $\tau = 0$, it becomes (since $f(0) = 0$ is a boundary condition)

$$B(0) - \frac{3}{4} k_P (1 + r_w) \int_0^{\tau_\Delta} B(t)\, e^{-\frac{3}{2} k_P t}\, dt = 0$$

Thus, the flux entering the wall can be written in terms of the value of the black-body emissive power of the gas adjacent to the wall; that is,

$$q_w^R = \frac{1 - r_w}{1 + r_w} \frac{\epsilon}{k_P} B(0) \tag{171}$$

Boundary-Layer Analysis

In terms of the substitute kernel approximation, the complete differential system governing the flow in the stagnation region of a radiating shock layer is

$$\left[f(\tau)\, h'(\tau)\right]'' - \frac{3}{2}\epsilon B''(\tau) - \frac{9}{4} k_P^2 f(\tau)\, h'(\tau) = 0 \tag{172}$$

$$2f(\eta)\, f''(\eta) - \left[f'(\eta)\right]^2 + a^2 h(\eta) = 0 \tag{173}$$

$$f(0) = 0 \tag{174}$$

$$f\left(\eta_\Delta\right) = 1 \tag{175}$$

$$f'\left(\eta_\Delta\right) = \frac{a}{\sqrt{2\chi(1-\chi)}} \tag{176}$$

$$h\left(\tau_\Delta\right) = 1 \tag{177}$$

$$f(\tau)\, h'(\tau) + \epsilon\left\{\frac{9}{8} k_P \int_0^{\tau_\Delta} B(t)\, e^{-\frac{3}{2}|t-\tau|k_P}\, dt - \frac{3}{2} B(\tau)\right.$$

$$\left. + \frac{9}{8} k_P r_w e^{-\frac{3}{2}k_P \tau} \int_0^{\tau_\Delta} B(t)\, e^{-\frac{3}{2}k_P t}\right\} dt = 0 \tag{178}$$

When the optical thickness of the shock layer is such that $k_P^2 \gg 1$ and $k_P^2 \gg \epsilon$, equation (172) becomes asymptotic to the equation

$$f(\tau)\, h'(\tau) = 0 \tag{179}$$

Thus, the enthalpy approaches a constant. It can be shown by attempting to satisfy equation (178) as a condition, that this solution is valid only at large optical distances from both the shock and the wall (unless it is a perfectly reflecting wall). It also becomes clear that the value of this constant, hereafter denoted h_2, cannot be determined without knowledge of the shock boundary layer.

If the enthalpy throughout most of the shock layer is constant with a value h_2, the density will be constant also with a value ρ_2. In this case, the momentum equation may be easily solved with the result that

$$f(\eta) = \left(1 - a\eta_\Delta \sqrt{\frac{\rho_2}{\rho_s}}\right)\left(\frac{\eta}{\eta_\Delta}\right)^2 + a\eta_\Delta \sqrt{\frac{\rho_2}{\rho_s}}\left(\frac{\eta}{\eta_\Delta}\right) \tag{180}$$

The first approximation to the shock standoff distance is

$$\frac{\Delta}{R_s} = \frac{(\rho_s/\rho_2)\chi}{1 + \sqrt{2(\rho_s/\rho_2)\chi(1 - \chi)}} = \frac{h_2\chi}{1 + \sqrt{2h_2\chi(1 - \chi)}} \tag{181}$$

In addition to the region of constant enthalpy in the interior of the layer, there are two thermal boundary layers, one immediately behind the shock and the other adjacent to the wall.

The forms that the energy equation assumes in these boundary layers can be determined by means of conventional boundary-layer techniques. In the vicinity of the shock the "stretched" coordinate

$$\xi = (\tau_\Delta - \tau)k_P \tag{182}$$

is introduced. Close to the shock the quantity $f(\tau)$ is slowly varying and may be adequately represented by the first term in the Taylor expansion about $\xi = 0$; that is,

$$f(\xi) \approx f(\eta_\Delta) = 1 \tag{183}$$

Substitution of equation (182) and equation (183) into the energy equation (172) gives the shock boundary-layer equation

$$h''(\xi) + \frac{3}{2}\frac{\epsilon}{k_P}B'(\xi) - \frac{9}{4}h(\xi) = \text{Constant} \tag{184}$$

Solution of this equation is complicated by the nonlinear term $\frac{3}{2}\frac{\epsilon}{k_P}B'(\xi)$. If ϵ is at least an order of magnitude less than k_P, this term can be neglected and the solution to equation (184) is easily found. This solution is

$$h(\xi) = (1 - h_2)e^{-\frac{3}{2}\xi} + h_2 \tag{185}$$

The constant h_2 can be determined by writing an energy balance across the shock boundary layer. This energy balance is

$$1 = h_2 + \frac{3}{4}\frac{\epsilon}{k_P}\int_0^\infty B(\xi)\, e^{-\frac{3}{2}\xi}\, d\xi \tag{186}$$

When $\epsilon \ll k_P$, condition (186) reduces to

$$h_2 \approx 1 - \frac{1}{2}\frac{\epsilon}{k_P}$$

and it is apparent that h_2 approaches one and the boundary layer ceases to exist. Thus, there cannot be a shock boundary layer with a thickness characterized solely by the optical path length in the gas.

An approximate solution to the boundary-layer equation (eq. (184)) can be obtained if the nonlinear term $\frac{3}{2}\frac{\epsilon}{k_P}B'(\xi)$ is replaced by an appropriate linear term; for example,

$$\frac{3}{2}\frac{\epsilon}{k_P}B'(\xi) \approx \frac{3}{2}\frac{\epsilon}{k_P}\frac{d}{d\xi}\left[\overline{B} + \dot{\overline{B}}h(\xi)\right] = \frac{3}{2}\frac{\epsilon}{k_P}\dot{\overline{B}}h'(\xi)$$

where the constant $\overline{B}$ is arbitrary and represents a mean value of the black-body emissive power B and the constant $\dot{\overline{B}}$ is arbitrary and represents a mean variation of B with h over the range of values of h encountered in the shock boundary layer. The linearized version of equation (184) has the simple solution

$$h(\xi) = \left(1 - h_2\right)e^{-\omega_1\xi} + h_2 \tag{187}$$

where

$$\omega_1 = \frac{3}{4}\frac{\epsilon}{k_P}\dot{\overline{B}}\left[1 + \sqrt{1 + \frac{4}{\left(\frac{\epsilon}{k_P}\dot{\overline{B}}\right)^2}}\right] \tag{188}$$

Where ϵ/k_P is very much less than unity, this solution reduces to equation (185). When ϵ/k_P is very much larger than unity, the solution takes the form

$$h(\xi) = \left(1 - h_2\right)e^{-\frac{3\epsilon}{2k_P}\dot{\overline{B}}\xi} + h_2 \tag{189}$$

and, in this limit, the thickness of the shock boundary layer is determined by the parameter ϵ^{-1} instead of simply k_P^{-1}. Thus, the shock boundary layer can be very much thinner than a photon mean free path if the black-body radiative power behind the shock is large. This effect was shown by Heaslet and Baldwin (ref. 33) in their study of radiation-resisted shock waves. Simply stated it means that a particle starting immediately behind the shock loses energy at such a rapid rate by means of radiation that it is substantially cooled in the time that it takes to travel only a small section of a photon mean free path.

A value for the constant $\dot{\overline{B}}$ can be obtained from the condition

$$\omega_1^2 - \frac{3}{2}\frac{\epsilon}{k_P}\left(1 + h_2\right)\omega_1 - \frac{9}{4} = 0 \tag{190}$$

This condition was derived by integration of the nonlinear energy equation (eq. (184)) between the limits zero and infinity and substitution into the result of the linearized solution (eq. (187)). In addition, the correlation formula $B = h^{\delta}$ was used. It was shown earlier that $\delta \approx 2.2$. However, the ensuing analysis will be greatly simplified, without any significant loss in accuracy, by setting $\delta = 2$. The value of $\dot{\overline{B}}$ so obtained is

$$\dot{\overline{B}} = 1 + h_2 \tag{191}$$

A second condition is required to determine uniquely the enthalpy distribution in the shock layer. The energy balance relation (eq. (186)) evaluated with the aid of the linearized solution provides this condition, which is

$$\frac{8}{9}\left[h_2^2 - 2\frac{k_P}{\epsilon}(1 - h_2)\right]\omega_1^2 + \left[\frac{2}{3}(1 + 2h_2) - 4\frac{k_P}{\epsilon}(1 - h_2)\right]\omega_1 + \left[1 - 2\frac{k_P}{\epsilon}(1 - h_2)\right] = 0 \qquad (192)$$

The quantity ω_1 can be eliminated between the conditions (190) and (191) to obtain an expression for h_2, the enthalpy level in the interior of the shock layer, as a function of ϵ/k_P. The result of this calculation is presented in figure 24.

The thickness of the shock boundary layer (in terms of optical path length) is characterized by the parameter $(\omega_1 k_P)^{-1}$. A plot of ω_1 as a function of ϵ/k_P is presented in figure 25.

As has been indicated previously, there is also a thermal boundary layer due to radiation adjacent to the wall. If this boundary layer is thin, which shall be assumed, herein, the dimensionless stream function $f(\tau)$ may be represented by the first two terms of its MacLaurin expansion

$$f(\tau) \approx f(0) + \tau f'(0)$$

By employing the kinematic boundary condition (174) and the asymptotic solution for $f(\eta)$ (eq. (180)), one finds

$$f(\tau) \approx \frac{a}{\kappa(0)\sqrt{h_2}}\tau = b\tau \qquad (193)$$

Of the several approximations introduced in the analysis of this section, this approximation is perhaps the poorest because the requirement that the wall boundary layer be thin with respect to the optical path length τ does not necessarily imply that it is thin with respect to either the Dorodnitsyn coordinate η or the geometric coordinate z.

Substituting this expression into the energy equation (eq. (172)), introducing the "stretched" coordinate

$$\zeta = \tau k_P^{1/2} \qquad (194)$$

and neglecting terms of order k_P^{-1} yields the boundary-layer equation

$$B''(\zeta) + \frac{3}{2}\frac{k_P}{\epsilon} b\zeta\, h'(\zeta) = 0 \qquad (195)$$

In general, equation (195) is nonlinear and does not possess an analytic solution. A simple approximate analytic solution can be obtained by replacing the quantity $h'(\zeta)$ with $\dot{h}B'(\zeta)$, where $\dot{h}$ is an as yet undetermined constant. This substitution reduces equation (195) to the linearized form

$$B''(\zeta) + 2\omega_2 \zeta B'(\zeta) = 0 \tag{196}$$

where

$$\omega_2 = \frac{3}{4} \frac{k_P}{\epsilon} b\dot{h} \tag{197}$$

The solution to equation (196) is easily found with the result

$$B(\zeta) = B_w + \left(B_2 - B_w\right) \operatorname{erf}\left(\sqrt{\omega_2}\, \zeta\right) \tag{198}$$

The quantities B_w, the nondimensional black-body emissive power of the gas adjacent to the wall, and ω_2 (because it contains the arbitrary constant $\dot{h}$) are still unknown. One condition for evaluating these quantities can be obtained by integrating the nonlinear boundary-layer equation (195) with respect to ζ between the limits zero and infinity. In performing this integration, it is convenient to eliminate the term $B''(\zeta)$ in equation (195) with equation (196). Then it is found that

$$\dot{h} = \frac{h_2 - h_w}{B_2 - B_w} = \frac{1}{h_2 + h_w} \tag{199}$$

Here B_2 is the nondimensional black-body emissive power of the gas in the interior of the shock layer and h_w is the nondimensional enthalpy of the gas adjacent to the wall. The last equality in expression (199) holds because it has been assumed that $B = h^2$.

The second condition is obtained by evaluating the integral condition (eq. (178)) at $\tau = 0$. When written in terms of the boundary-layer coordinate ζ, this condition becomes

$$B_w = \frac{3}{4} k_P^{1/2} \left(1 + r_w\right) \int_0^\infty B(\zeta)\, e^{-\frac{3}{2} k_P^{1/2} \zeta}\, d\zeta \tag{200}$$

Substitution of the linearized solution for $B(\zeta)$ into equation (200) and integration yields

$$B_w = \frac{\left(1 + r_w\right) e^{\frac{9k_P}{16\omega_2}} \operatorname{erfc}\sqrt{\frac{9k_P}{16\omega_2}}}{\left(1 - r_w\right) + \left(1 + r_w\right) e^{\frac{9k_P}{16\omega_2}} \operatorname{erfc}\sqrt{\frac{9k_P}{16\omega_2}}} B_2 \tag{201}$$

Equations (197) and (199) can be used to eliminate ω_2 from equation (201) to yield a transcendental equation for the value of the black-body emissive power at the wall B_w.

The variation of B_w as a function of the radiation cooling parameter to Bouguer number ratio ϵ/k_P for various values of k_P and the exponent γ (from the correlation

formula $\kappa = h^{\gamma}$) is shown in figure 26. This curve has particular significance because the ratio of radiant heat transfer to the cold wall is directly related to B_w through expression (171). The variation of the quantity ω_2 (eq. (197)) with these same parameters is presented in figure 27.

The Rosseland Approximation

The Rosseland or diffusion approximation is frequently used in the study of problems in which the medium is optically thick. As was pointed out earlier, this approximation is not valid in regions optically close to a radiation boundary or in regions in which the optical and thermodynamic properties vary significantly within an optical path length. Some investigators have attempted to correct the former deficiency through the use of temperature-jump boundary conditions and have achieved considerable success in problems of pure radiant or combined radiant and conductive energy transport.

In this section, an attempt is made to use the Rosseland approximation and temperature-jump boundary conditions to analyze the optically thick shock layer. It is hoped that this exercise will provide some insight into the attributes and limitations of this approximation in problems of combined radiant and convective energy transport.

With the Rosseland approximation for the divergence of the radiant flux, the energy equation becomes

$$B''(\tau) + \frac{3}{2}\frac{k_P^2}{\epsilon} f(\tau)\, h'(\tau) = 0 \tag{202}$$

This equation is the same as equation (172) except for the omission of the third-order differential term $\left[f(\tau)\, h'(\tau)\right]''$.

In the interior of the optically thick shock layer, equation (202) reduces to

$$f(\tau)\, h'(\tau) = 0$$

provided $k_P >> \epsilon/k_P$. This result is identical to the result obtained by means of the substitute kernel approximation. This agreement is not surprising because the diffusion approximation is known to be valid in this region. Of course, the value of the constant enthalpy in the interior of the shock layer cannot be determined until something is known about the shock boundary layer.

If the usual type of boundary-layer analysis is applied to the energy equation in the Rosseland approximation (202) for the neighborhood of the wall, the result is

$$B''(\zeta) + \frac{3}{2}\frac{k_P}{\epsilon} b\zeta h'(\zeta) = 0$$

This equation is identical to the wall boundary-layer equation in the substitute kernel analysis. Two boundary conditions are required to determine the solution to this equation completely. One of these conditions is

$$\lim_{\zeta \to \infty} B(\zeta) = B_2$$

Here B_2 is the black-body emissive power of the gas in the interior of the shock layer. The second is the jump boundary condition, written in terms of the black-body emissive power B rather than the temperature

$$B_w = CB'(0) = \frac{3}{2}\left(\frac{k_P^2}{\epsilon}\right) C q_w^R \tag{203}$$

The second equality follows from the expression for the radiant flux in the Rosseland approximation. The constant C is usually evaluated by requiring the flux to be correct in the black-body limit. (See, for example, ref. 37.) However, it is noted that condition (203) is identical to the condition used in the substitute kernel approximation (that is, eq. (200)) if C is chosen to be

$$C = \frac{2}{3k_P} \frac{1 + r_w}{1 - r_w} \tag{204}$$

Thus, the results obtained in the wall boundary layer by the two methods are identical if C is chosen to satisfy equation (204). It has been shown that the two methods also give identical results when applied to the problem of combined radiative and conductive energy transport between two infinite parallel plates separated by a radiating and conducting gas. (See ref. 37.)

If the usual boundary-layer analysis is used to obtain the boundary-layer form of the energy equation in the Rosseland approximation for the neighborhood of the shock, the result is

$$B'(\xi) - \frac{3}{2}\left(\frac{k_P}{\epsilon}\right) h(\xi) = \text{Constant} \tag{205}$$

This equation is not identical with the shock boundary-layer equation in the substitute kernel approximation because of the omission of the third-order differential term. Inspection of equation (205) indicates that any solution other than the trivial solution $h(\xi) \equiv h_2$ will not tend to a constant h_2 as ξ becomes very large. Thus equation (205) cannot be forced to satisfy simultaneously the conditions $h(0) = 1$ and $\lim_{\xi \to \infty} h(\xi) = h_2$. Apparently then, the jump boundary condition at the shock must be $h(0) = h_2$, but this result leads nowhere as there is insufficient information to determine h_2 accurately.

It must be concluded then that the Rosseland approximation with slip-boundary conditions is not sufficient by itself to be used in the analysis of the complete shock layer.

It can be used in the combined radiation and conduction problem because the two separate energy fluxes are represented by similar mathematical models and may be treated as an equivalent radiation-alone or conduction-alone problem. Even in this case, it is not possible to obtain a temperature distribution nor to determine separately the radiant and conductive fluxes optically close to a boundary. This inability to determine a temperature distribution optically close to a boundary (such as a transparent shock) presents a serious obstacle to the solution of the combined radiation and convection problem because the convective flux depends on the temperature distribution.

Results and Discussion of Solution for Optically Thick Shock Layers

The analysis presented in this section applies only when the two enthalpy boundary layers are thin compared with the shock standoff distance with these distances expressed in terms of the Dorodnitsyn variable η. When ϵ/k_P, the ratio of the radiation cooling parameter and the Bouguer number, is much less than one, the thickness of the shock boundary layer is characterized by the inverse of the Bouguer number k_P^{-1}; whereas when ϵ/k_P is large, the shock boundary-layer thickness is characterized by the inverse of the radiation cooling parameter ϵ^{-1}. The thickness of the wall boundary layer is characterized by the parameter $\left(\epsilon/k_P^2\right)^{1/2}$. Thus, the most restrictive conditions on the applicability of the optically thick analysis are that $k_P \gg 1$ for ϵ small and $k_P \gg \epsilon^{1/2}$ for ϵ large.

Several enthalpy distributions were calculated with the formulas developed in the preceding section. The results are presented in figure 28. The previous discussion of the effects of the parameters on the thicknesses of the boundary layers is substantiated by these results. The effect of the Bouguer number k_P and the ratio of radiation cooling parameter to Bouguer number ϵ/k_P on the shock-layer optical thickness $k_P\tau_\Delta$ is also shown. The effect of ϵ/k_P depends on the enthalpy variation of the absorption coefficient. In the cases shown, the absorption coefficient is proportional to the fourth power of the enthalpy and an increase in ϵ/k_P brings about a reduction in the shock-layer optical depth. The nondimensional value of the enthalpy of the gas adjacent to the wall (which is related to the rate of radiant heat transfer to the wall through eq. (171) and the correlation formula $B = h^2$) decreases with increasing ϵ/k_P and/or k_P.

The effect of γ (where γ is the exponent in the correlation formula $\kappa = h^\gamma$) and the surface reflectivity r_W on the character of the wall boundary layer has not been shown but can be readily deduced from the curves of figures 26 and 27. Increasing γ tends to reduce the optical thickness of the wall boundary layer and increase the value of the enthalpy of the gas adjacent to the wall. It can be shown that the wall boundary-layer thickness expressed in terms of the Dorodnitsyn coordinate η is only slightly affected by a change in γ. Increasing the surface reflectivity r_W tends to increase the optical

thickness of the wall boundary layer and increase the value of the enthalpy of the gas adjacent to the wall. When expressed in terms of the Dorodnitsyn coordinate η, the boundary-layer thickness decreases with increasing r_w. These results are consistent with the results obtained with the small-perturbation solution.

The manner in which the rate of radiant heat transfer to the wall q_w^R depends on the radiation cooling parameter to Bouguer number ratio ϵ/k_p, the Bouguer number k_p, the variation with enthalpy of the absorption coefficient (through the exponent γ of the correlation formula $\kappa = h^\gamma$), and the surface reflectivity r_w is indicated in figure 26. For fixed values of k_p, γ, and r_w, the rate of radiant heat transfer to the wall q_w^R increases with increasing ϵ/k_p. It appears that q_w^R would become asymptotic to the available energy limit of 1/2 as ϵ/k_p increased without limit. As the Bouguer number k_p increases (hence, the shock-layer optical thickness is increased), all other parameters remaining fixed, the value of q_w^R decreases and becomes asymptotic to zero. This trend is the same trend exhibited in the problem of radiant-energy transfer between two plane parallel walls separated by an absorbing and emitting, but motionless and non-heat-conducting gas. (See, for example, ref. 11.) Increasing γ while the other parameters are held fixed results in an increase in q_w^R. This trend is the reverse of that for a transparent shock layer. (See fig. 21.) The results of the small-perturbation analysis (see fig. 9) show that this reversal occurs at intermediate values of the Bouguer number k_p. Finally, it is apparent from figure 26 that an increase in surface reflectivity r_w for fixed values of the other parameters results in a decrease in q_w^R. The change in q_w^R with r_w satisfies the inequality

$$q_w^R \geqq (1 - r_w)\left(q_w^R\right)_{r_w=0}$$

which agrees with the physical argument presented in the discussion of the small-perturbation solution.

RADIATION-DEPLETED SHOCK LAYER

The Strong Radiation Approximation

When the radiation cooling parameter ϵ is very much greater than both one and k_p^2, the Bouguer number squared, a particle leaving the shock with an initial enthalpy of $\frac{1}{2} W_\infty^2$ will emit radiation at such a rapid rate that it will lose a significant amount of its energy before traveling the distance of a photon mean free path. Because this energy is emitted in a region of small optical thickness adjacent to the transparent shock, most of it will escape from the shock layer, and the enthalpy level within the shock layer will be very small in comparison with the value at the shock. In fact, as will be shown subsequently, the zero-order solution for the enthalpy in the interior of the shock layer is

identically zero. It is for this reason that the term "radiation-depleted shock layer" has been coined. Of course, the narrow region adjacent to the shock in which the large change in enthalpy occurs can be described as a boundary layer and boundary-layer techniques can be applied to obtain solutions in it.

The conditions which must hold in order that there be a radiation-depleted shock layer $\left(\text{that is, } \epsilon \text{ very large and } k_P^2 \text{ not too large}\right)$ occur at high altitudes for rather large objects (shock radius greater than 1 meter) entering at extremely high speeds (entry speeds close to 70 km/sec). It is not at all clear that the requirement for chemical equilibrium can be satisfied under these conditions, particularly in view of the existence of a shock boundary layer in which large changes occur over a short distance, and hence, a short time. Despite this objection, the solutions for the radiation-depleted shock layer represent an interesting limiting case which should lead to an increased understanding of the radiating shock layer and provide a firm base for extension into areas of more practical concern.

Analysis

Once again, as was the case for the optically thin and optically thick shock layers, analysis can be facilitated through the use of the substitute kernel approximation. In this case, the energy equation, written in terms of the optical path length, is

$$\left[f(\tau)\, h'(\tau)\right]' - \frac{3}{2}\,\epsilon B''(\tau) - \frac{9}{4}\,k_P^2 f(\tau)\, h'(\tau) = 0 \tag{206}$$

Here f is the nondimensional stream function, h the nondimensional enthalpy, B the nondimensional blackbody emissive power, ϵ the radiation cooling parameter, k_P the Bouguer number, and τ the optical path length. It should be remembered that use of this equation restricts the analysis to gray gases only. The boundary conditions on the enthalpy are as before

$$h\left(\tau_\Delta\right) = 1 \tag{207}$$

and the integral condition

$$f(\tau)\, h'(\tau) - \frac{3}{2}\,\epsilon\left[B(\tau) - \frac{3}{4}\,k_P \int_0^{\tau_\Delta} B(t)\, e^{-\frac{3}{2}k_P|t-\tau|}\, dt\right.$$

$$\left. - \frac{3}{4}\,k_P r_w e^{-\frac{3}{2}k_P\tau} \int_0^{\tau_\Delta} B(t)\, e^{-\frac{3}{2}k_P t}\, dt\right] = 0 \tag{208}$$

The particular form of the substitute kernel employed here, that is, $E_2\left(k_P\tau\right) \approx \frac{3}{4}\, e^{-\frac{3}{2}k_P\tau}$, was chosen for simplicity. Somewhat greater accuracy might be achieved by letting the

constants depend on the optical depth $k_P\tau_\Delta$. However, it was not felt that this procedure would lead to a better understanding of the radiation-depleted shock layer.

The momentum equation, in terms of the Dorodnitsyn coordinate, and the boundary conditions on the nondimensional stream function are

$$2f(\eta)\, f''(\eta) - \left[f'(\eta)\right]^2 + a^2 h = 0 \tag{209}$$

$$f(0) = 0 \tag{210}$$

$$f\left(\eta_\Delta\right) = 1 \tag{211}$$

$$f'\left(\eta_\Delta\right) = \frac{2}{\chi}\left(\frac{\Delta}{R_s}\right) = \frac{a}{\sqrt{2\chi(1 - \chi)}} \tag{212}$$

When the radiation cooling parameter ϵ is very much greater than one and very much greater than k_P^2, the energy equation (eq. (206)) admits the asymptotic solution

$$B(\tau) = C_1 + C_2\tau \tag{213}$$

Substitution into the asymptotic form of the integral condition (208) reveals that each of the two constants must be identically zero. Thus, in the interior of the shock layer $B(\tau)$ and $h(\tau)$ are zero. In this case, the density is infinite and the momentum equation can be readily solved for $f(\eta)$ with the result that

$$f(\eta) = \left(\frac{\eta}{\eta_\Delta}\right)^2 \tag{214}$$

and, of course, the shock standoff distance tends to zero.

In order to investigate the shock boundary layer, it is convenient to introduce the "stretched" coordinates

$$\xi = \left(\tau_\Delta - \tau\right)\epsilon^n \tag{215}$$

and

$$\zeta = \left(\eta_\Delta - \eta\right)\epsilon^n \tag{216}$$

into the energy and momentum equations, respectively. Performing the usual manipulations (details are presented in appendix C) shows that the boundary layer is characterized by the parameter ϵ^{-1} and it would seem proper to expand both the boundary-layer and asymptotic solutions in power series of this small parameter. However, $f_a(\eta)$ (where the subscript a indicates the asymptotic solution valid far from the shock) is not analytic

in ϵ^{-1} near $\epsilon^{-1} = 0$, but is analytic in $\epsilon^{-1/2}$. Consequently, the solutions must be expanded as power series in $\epsilon^{-1/2}$.

The lowest order form of the energy equation in the boundary layer is

$$\frac{dh}{dB_{b,0}} B'_{b,0}(\xi) + \frac{3}{2} B_{b,0}(\xi) = C_1 + C_2\xi \tag{217}$$

The subscript b,0 has been used to denote the zero-order boundary-layer solutions. This equation must satisfy the boundary conditions that both $B_{b,0}(\xi)$ and $B'_{b,0}(\xi)$ vanish as ξ increases without limit. Thus, the constants C_1 and C_2 are both identically zero. The third condition to be satisfied is

$$B_{b,0}(0) = 1 \tag{218}$$

The solution to equation (217) subject to the boundary conditions is

$$\xi = \frac{2}{3}\int_{B_{b,0}}^{1} \left(\frac{dh}{dB}\right)\frac{dB}{B} \tag{219}$$

Solution of the momentum equation in the boundary layer gives the zero-order form of the nondimensional stream function

$$f_{b,0}(\zeta) = 1 \tag{220}$$

These zero-order solutions can be used to generate solutions of higher order. Mathematical details are presented in appendix C. In general, the analysis follows the procedure outlined by Van Dyke. (See ref. 38.)

A complete listing of these solutions up to second order in the parameter $\epsilon^{-1/2}$ is presented.

Zero-order solutions.- The zero-order solutions are:

$$B_{a,0}(\tau) = 0 \tag{221}$$

$$f_{a,0}(\eta) = \left(\frac{\eta}{\eta_\Delta}\right)^2 \tag{222}$$

$$\xi = \frac{2}{3}\int_{B_{b,0}}^{1} \left(\frac{dh}{dB}\right)\frac{dB}{B} \tag{223}$$

$$f_{b,0}(\zeta) = 1 \tag{224}$$

$$\eta_{\Delta,0} = \frac{2\sqrt{2\chi(1 - \chi)}}{a} = 1 + \sqrt{2\chi(1 - \chi)} \tag{225}$$

$$\tau_{\Delta,0} = \frac{\eta_{\Delta,0}}{\kappa_P^{-1}(0)} \tag{226}$$

First-order solutions.- The first-order solutions are:

$$B_{a,1}(\tau) = 0 \tag{227}$$

$$f_{a,1}(\eta) = a\eta_{\Delta,0}\sqrt{\dot{h}(0)\ B_{a,2}(0)}\left(\frac{\eta}{\eta_{\Delta,0}}\right)\left[1 - \left(\frac{\eta}{\eta_{\Delta,0}}\right)\right] \tag{228}$$

$$B_{b,1}(\xi) = 0 \tag{229}$$

$$f_{b,1}(\zeta) = 0 \tag{230}$$

$$\eta_{\Delta,1} = \frac{1}{2}\, a\eta_{\Delta,0}^2\sqrt{\dot{h}(0)\ B_{a,2}(0)} \tag{231}$$

$$\tau_{\Delta,1} = \frac{\eta_{\Delta,1}}{\kappa_P^{-1}(0)} \tag{232}$$

Second-order solutions.- The second-order solutions are:

$$B_{a,2}(\tau) = \frac{k_P\left(1 + r_w\right)\left[1 + \frac{3}{2}\, k_P\tau\right]}{2\left[1 + \frac{3}{4}(1 - r_w)k_P\tau_{\Delta,0}\right]} \tag{233}$$

$$f_{a,2}(\eta) = \left[\left(\frac{\eta_{\Delta,1}}{\eta_{\Delta,0}}\right)^2 - 2\left(\frac{\eta_{\Delta,2}}{\eta_{\Delta,0}}\right) - A\log_e \eta_{\Delta,0}\right]\left(\frac{\eta}{\eta_{\Delta,0}}\right)^2 + \left[A\log_e \eta_{\Delta,0}\right]\left(\frac{\eta}{\eta_{\Delta,0}}\right) + A\left(\frac{\eta}{\eta_{\Delta,0}}\right)\log_e\left(\frac{\eta}{\eta_{\Delta,0}}\right) \tag{234}$$

where

$$A = 3\left(\frac{\eta_{\Delta,1}}{\eta_{\Delta,0}}\right)^2 k_P\tau_{\Delta,0} \tag{235}$$

$$\eta_{\Delta,2} = -\eta_{\Delta,0}\left(\frac{\eta_{\Delta,1}}{\eta_{\Delta,0}}\right)^2\left[1 + \frac{3}{2}k_P\tau_{\Delta,0}\left(1 - \log_e \eta_{\Delta,0}\right)\right] \tag{236}$$

$$\tau_{\Delta,2} = \frac{\eta_{\Delta,2}}{\kappa_P^{-1}(0)} + \eta_{\Delta,0}\frac{\left[\dot{\kappa}_P^{-1}(0)\right]}{\left[\kappa_P^{-1}(0)\right]^2}B_{a,2}(0)\left[1 + \frac{3}{4}k_P\tau_{\Delta,0}\right]$$

$$+ \int_0^{\epsilon\tau_{\Delta,0}+\epsilon^{1/2}\tau_{\Delta,1}+\tau_{\Delta,2}}\left[\frac{k_P^{-1}\left(B_{b,0}(\xi)\right)}{\kappa_P^{-1}(0)} - 1\right]d\xi \tag{237}$$

Radiant heat flux and standoff distance.- The total radiant heat flux to the wall q_w^R and the ratio of the shock standoff distance to the shock standoff distance for radiationless flow $\overline{\Delta}$ are given by the following expressions:

$$\frac{q_w^R}{1 - r_w} = \frac{1}{2\left[1 + \frac{3}{4}\left(1 - r_w\right)k_P\tau_{\Delta,0}\right]} \tag{238}$$

$$\overline{\Delta} = \epsilon^{-1}\left\{\eta_{\Delta,0}\left[\dot{h}(0) + h(0)\frac{\left(\dot{\kappa}_P^{-1}(0)\right)}{\kappa_P^{-1}(0)}\right]B_{a,2}(0)\left[1 + \frac{3}{4}k_P\tau_{\Delta,0}\right]\right.$$

$$\left. + \int_0^{\epsilon\tau_{\Delta,0}+\epsilon^{1/2}\tau_{\Delta,1}+\tau_{\Delta,2}} h\left(B_{b,0}(\xi)\right)\kappa_P^{-1}\left(B_{b,0}(\xi)\right)\,d\xi\right\} \tag{239}$$

Results and Discussion of Solution for Radiation-Depleted Shock Layers

In the analysis of the preceding section, it was convenient to use the black-body emissive power B rather than the enthalpy h as the dependent variable. This choice necessitated the assumption that the thermodynamic and optical properties (in particular h and κ_P^{-1}) be analytic functions of B in the interval (0,1). Unfortunately, this condition does not hold for the correlations of the section "Stagnation Model for a Radiating Shock Layer" when written in terms of B in the limit as B approaches zero.

This difficulty can be circumvented through the use of analytic approximations to the correlating functions. For example, the enthalpy might be approximated by the function

$$h = (B + B^*)^{1/2} \tag{240}$$

where B^* is a very small positive number. Use of formula (240) in the expression (223) results in the following solution for $B_{b,0}(\xi)$:

$$B_{b,0}(\xi) = B^*\left[\left(\frac{1 + Ce^{-3\sqrt{B^*}\,\xi}}{1 - Ce^{-3\sqrt{B^*}\,\xi}}\right)^2 - 1\right] \tag{241}$$

where

$$C = \frac{\sqrt{1 + B^*} - \sqrt{B^*}}{\sqrt{1 + B^*} + \sqrt{B^*}} \tag{242}$$

For large values of ξ, that is,

$$\xi >> \frac{1}{3}\sqrt{B^*}$$

the value of $B_{b,0}(\xi)$ is directly proportional to B^*. It is clear then that B^* should be chosen sufficiently small to insure that $B_{b,0}(\xi)$ is nearly independent of B^* for values of $B_{b,0}$ as small as $\epsilon^{-1}B_{a,2}(0)$.

Because of the unlikelihood of establishing local thermodynamic and chemical equilibrium in a physical shock layer under those conditions for which this model analysis is supposed to apply, it would be somewhat superfluous to present the results of detailed calculations for the enthalpy distribution and shock standoff distance. It is sufficient to say that the shock layer is characterized by an enthalpy boundary layer immediately behind the shock the thickness of which (in terms of the Dorodnitsyn variable η) is characterized by the inverse of the radiation cooling parameter ϵ^{-1}. It should also be pointed out that the shock boundary layer is always very much less than a photon mean free path and hence is always optically thin. The enthalpy level in the interior of the shock layer is of order of magnitude k_P/ϵ. The ratio of the shock standoff distance to the shock standoff distance for radiationless flow is of order of magnitude ϵ^{-1}.

Curves representing the magnitude of the radiant heat flux which is absorbed by the wall q_w^R are presented in figure 29. In the optically thin limit $\left(k_P\tau_{\Delta,0} << 1\right)$, the radiant heat flux approaches the "available energy limit" of $(1 - r_w)/2$. As the optical thickness of the wall increases and absorption becomes more important, less of the energy emitted from the gas in the shock boundary layer in the direction of the wall is able to penetrate the shock layer and reach the wall before being absorbed. Part of what is absorbed is

then reradiated in the forward direction and escapes from the shock layer through the transparent shock. Finally, as $k_p \tau_{\Delta,0}$ tends to infinity, none of the energy emitted in the shock boundary layer reaches the wall and the radiant flux incident on the wall vanishes.

RADIATING SHOCK LAYERS

Discussion of the Approximate Solutions

Four different approximate stagnation-point solutions for an inviscid, radiating shock layer have been obtained. Each one represents a limiting case for some combination of the radiation cooling parameter ϵ and the Bouguer number k_p. The regions of validity of the approximate solutions are depicted in figure 30. The boundaries as drawn pertain only to a gray gas with constant absorption coefficient. It would be necessary to redraw the boundaries for each nongray gas and for every change in the enthalpy dependence of the absorption coefficient. As was pointed out in the section "Optically Thin Shock Layers," the criterion for validity of the optically thin solution is that the gas layer be optically thin in all wavelength intervals in which a significant amount of energy is transported by radiation. For a gray gas, this criterion means $k_p \tau_\Delta \ll 1$. Thus, the boundary is not specified completely by k_p but varies with ϵ as well (since $k_p \tau_\Delta$, the shock-layer optical thickness depends on ϵ as well as k_p when the absorption coefficient is a function of the enthalpy). When applied to a nongray gas, the criterion for validity of the optically thin solution is always more restrictive than the condition that the Planck mean optical depth be small. Thus, the boundaries for all nongray gases are displaced to the left of the boundary for the "Planck-equivalent" gray gas. A "Planck-equivalent" gray gas is one in which the wavelength-independent absorption coefficient is equal to the Planck mean absorption coefficient in the nongray gas.

The location of the boundary for the small-perturbation approximation depends on the radiation cooling parameter ϵ and the enthalpy variation of the absorption coefficient. The value of ϵ for which the solution will yield results of a given accuracy is reduced with an increase in γ (where γ is the exponent in the correlation formula $\kappa_p = h^\gamma$), because of the reduced accuracy of the truncated expansion for κ_p. Since the small-perturbation solution was shown to be correct to second order throughout most of the domain of the problem, the condition for establishing the boundary is $\epsilon^2 \ll 1$. (This condition holds when $\gamma = 0$. When $\gamma = 4$, the proper condition becomes $10\epsilon^2 \ll 1$.) The location of the boundary does not depend on the wavelength dependence of the absorption coefficient.

The most restrictive condition limiting the validity of the optically thick analysis for moderate values of the radiation cooling parameter ϵ is the thickness of the enthalpy

layer adjacent to the shock. This thickness is characterized by the inverse of the Bouguer number $1/k_p$. Thus, the criterion for validity is $k_p \gg 1$. For larger values of ϵ, the condition $\left(\epsilon/k_p^2\right)^{1/2} \ll 1$ becomes more restrictive and must be used to establish the boundary. This latter condition insures that the enthalpy boundary layer adjacent to the wall is thin compared with the shock standoff distance. The optically thick analysis is restricted to the case of a gray gas but could be extended rather simply to the case of an absorption coefficient with a step-function dependence on wavelength for which the step heights are either $\alpha(h)\ \kappa_p(h)$ or zero. There is no restriction to the number or width of the steps. The only changes that would appear in the formulas would be the substitution of $\alpha(h)\ \kappa_p(h)$ for $\kappa_p(\kappa)$ and $B(h)/\alpha(h)$ for $B(h)$. The boundary to the region of validity of the optically thick shock-layer analysis would be displaced to the left for this particular class of nongray gases.

The region of validity of the radiation-depleted shock-layer analysis is restricted by the conditions $\epsilon \gg 1$ and $\epsilon \gg k_p^2$. The first condition insures that the thickness of the enthalpy boundary layer adjacent to the shock is small compared with the shock standoff distance, whereas the second condition insures that radiation is the preponderant mode of energy transport within the shock layer. Like the optically thick analysis, the radiation-depleted shock-layer analysis is restricted to gray gases but can be extended to the nongray model absorption coefficient with multiple steps of uniform height. Use of such a nongray model would cause a leftward shift in the boundaries to the region of validity.

In order to relate the radiation shock-layer regimes to the problem of entry into the atmosphere of the earth, several trajectories are indicated on the $\epsilon - k_p$ map presented in figure 31. The arrows indicate the direction of increasing time. Trajectories 1 and 2 represent iron spheres of radius 1 meter and 1 centimeter, respectively, entering vertically with an initial velocity of 70 km/sec. (No account has been taken of mass loss of these spheres due to ablation.) Trajectories for all other objects of the same size and lesser or equal initial velocities must lie below them in the $\epsilon - k_p$ space. The third and fourth trajectories correspond to the entry of round-trip Martian probes of different nose radius which would encounter some of the more severe heating conditions of the currently envisioned class of manmade objects. It is apparent that the small-perturbation approximation has considerable utility for the analysis of radiation effects on the entry of manmade objects. (See ref. 47.) It also appears that the optically thin shock-layer analysis might enjoy wide applicability. However, in the more realistic case of a nongray gas the boundary would be shifted to the left one or two orders of magnitude in the Bouguer number k_p, and would thereby considerably reduce the practical usefulness of the optically thin approximation. The optically thick and radiation-depleted shock-layer analysis would seem to be nearly devoid of direct practical usefulness, both because of the inaccessibility of the proper magnitudes of the parameters ϵ and k_p to objects

of interest and because of the restriction of these analyses to the gray case (and the simple nongray model absorption coefficient with multiple steps of uniform height).

A Model Earth-Entry Environment

The four approximate solutions can be used to compute the radiant heat transfer to the stagnation point over a wide range of the radiation cooling parameter ϵ and the Bouguer number k_P. The results depend on the particular gas, the surface reflectivity, and the size of the object and must be recomputed for every change in these variables. Actually, the size of the object is important only if the exponent γ (which appears in the correlation formula $\kappa_P = h^\gamma$) varies throughout the ϵ - k_P space. In this event, the value of h at which a change in γ occurs depends on the parameter $k_P = \rho_s \kappa_{P,s} \Delta_A$ which is influenced by the body size through the radiationless shock standoff distance Δ_A.

Contours of constant values of T_s (the temperature immediately behind the shock), $\rho_s \kappa_{P,s}$ (the Planck mean volume absorption coefficient immediately behind the shock), ϵ/k_P, and χ (the ratio of free-stream density to the density immediately behind the shock) on plots of ambient density ratio ρ_∞/ρ_0 as a function of free-stream velocity W_∞ up to 70 km/sec are presented in figure 32 for a model earth-entry environment. This entry environment was obtained by combining the thermodynamic and optical property correlations presented earlier with the strong normal-shock relations. The resulting formulas are:

$$T_s = \left(1.038 \times 10^3\right)\left(\frac{\rho_\infty}{\rho_0}\right)^{0.09} W_\infty^{1.28}, \quad {}^\circ K \qquad C \qquad (243)$$

$$\chi = \left(\frac{\rho_s}{\rho_\infty}\right)^{-1} = \left(6.95 \times 10^{-2}\right)\left(\frac{\rho_\infty}{\rho_0}\right)^{0.04} W_\infty^{0.08} \qquad C \qquad (244)$$

$$\frac{\epsilon}{k_P} = \left(1.852 \times 10^{-16}\right) T_s^4 \left(\frac{\rho_\infty}{\rho_0}\right)^{-1} W_\infty^{-3} \qquad (245)$$

$$\rho_s \kappa_{P,s} = \left(7.94 \times 10^{-26}\right)\left(\chi^{-1} \frac{\rho_\infty}{\rho_0}\right)^{3.25} T_s^{6.0-0.5 \log_{10}\left(\chi^{-1} \frac{\rho_\infty}{\rho_0}\right)}, \quad cm^{-1} \qquad (246a)$$

for the lower temperatures (less than about 20 000° K) and

$$\rho_s \kappa_{P,s} = \left(9.33 \times 10^2\right)\left(\chi^{-1} \frac{\rho_\infty}{\rho_0}\right)^{0.507} T_s^{-0.39+0.21 \log_{10}\left(\chi^{-1} \frac{\rho_\infty}{\rho_0}\right)}, \quad cm^{-1} \qquad (246b)$$

for the higher temperatures.

The values of χ and γ (the exponent in the correlation formula vary greatly over a rather extensive range of ambient densities and velo quently, it was decided to fix these quantities at the constant values, $\chi = 0$ $\gamma = 4.0$, for the discussions which follow.

Radiant Heat Transfer

The rate of radiant heat transfer to the stagnation point of a blunt object q_w was calculated by the four approximate methods for a wide range of the radiation cooling parameter ϵ and the Bouguer number k_P. The results are presented in figure 33 as a plot of q_w^R against k_P for various values of the ratio ϵ/k_P. This ratio, sometimes known as the inverse of the Boltzmann number, was used because it is what might be termed an "environmental parameter," that is, a parameter dependent only on free-stream conditions (ambient density and velocity) and not on body geometry. The Bouguer number k_P, on the other hand, is directly proportional to the body nose radius for a given set of free-stream conditions. Thus, each curve in figure 33 can be thought of as representing the effect of body nose radius on radiant heat transfer at a given trajectory point.

For the purpose of calculating the results presented in figure 33, the shock-layer gas was assumed to have a gray mass absorption coefficient which varies as the fourth power of the enthalpy. The surface of the object was considered to be nonreflecting. The dashed portions of the curves do not represent computed data, but rather represent arbitrary connections across regions in which the various approximate solutions are invalid.

The radiation cooling parameter ϵ is equal to the radiant flux which leaves each side of a transparent, isenthalpic gas slab in which the nondimensional enthalpy takes the value one. Hence, this product represents an upper bound to the rate of radiant heat transfer to the stagnation point (or wall) q_w^R. When this product is small, the rate of energy loss through radiation is small, and the average intensity is only slightly perturbed from the isenthalpic value. However, as ϵ increases (the Bouguer number k_P remaining very much less than one), the increased energy lost by radiation results in decreased levels of enthalpy and average intensity. Hence, q_w^R becomes a decreasing fraction of ϵ. Finally, as ϵ becomes very large (k_P still small), nearly all the energy is removed from the shock layer by radiation and q_w^R which represents the rate at which radiant energy leaves one side of the transparent layer approaches the physical maximum of 1/2.

As k_P increases toward and beyond unity, absorption becomes important and this mechanism, which tends to inhibit radiant energy transfer, halts the increasing trend of q_w^R with k_P. As k_P continues to increase, the trend is reversed and q_w^R decreases and becomes asymptotic to zero. Consequently, the curves of rate of radiant heat transfer

to the stagnation point q_w^R against Bouguer number k_P for constant values of the ratio ϵ/k_P have maximums the locations and heights of which depend on ϵ/k_P. It can be inferred from this statement that for every altitude and velocity in this simple model atmosphere, there is a finite value of nose radius for which the rate of radiant heat transfer to the stagnation point will be a maximum. It should be kept in mind that this analysis assumes a gray gas and that absorption in the free stream ahead of the shock has been neglected.

In order to obtain some understanding of the effects of radiation cooling, gray absorption, and spectral absorption on the rate of radiant heat transfer to the stagnation point, a series of calculations utilizing various approximations were performed. The results of these calculations corresponding to a free-stream velocity of 14.2 km/sec and an altitude of 32.4 km are plotted against body nose radius R_N in meters in figure 34. The curve labeled 1 was computed by assuming that the shock layer was both isenthalpic and nonabsorbing. In this case the rate of radiant heat transfer to the stagnation point is given by the simple expression $q_w^R = \epsilon$. This approximation was used in the early estimates of radiant heating. (See refs. 1 and 2.) Curve 2 was computed by assuming that the shock layer was isenthalpic and contained a gray, absorbing gas. The effect of gray absorption is seen to be small (under the conditions of this example) for a nose radius as large as 0.1 m. The third curve was obtained using the transparent approximation discussed in the section "Optically Thin Shock Layers." This assumption of a nonabsorbing but radiation-cooled shock layer is frequently employed in the literature. (See, for example, refs. 3 to 7.) For this example, at least, the effect of radiation cooling is more important than the effect of gray absorption for nose radii of 0.1 m or less. Curve 4 contains the effects of both radiation cooling and gray absorption. These combined effects are included in the numerical solutions of Howe and Veigas (ref. 9). It can be seen that for small nose radii (less than about 0.1 m), gray absorption has little effect. However, gray absorption plays an increasingly important role as the radius increases. The final curve, curve 5, includes the combined effects of radiation cooling and nongray absorption. The absorption coefficient used in these calculations was the step function model introduced in the section on the small-perturbation solution. (See fig. 13.) The curve is limited to small values of nose radius because of the restricted region of validity of the small-perturbation method with which this curve was computed. It is very apparent from these results that nongray effects cannot be ignored if one wishes to obtain a realistic evaluation of the radiant heating of objects during entry at hyperbolic velocities.

The analysis of this paper has been restricted to a shock layer with plane-parallel geometry. The largest effect of this assumption is felt in the calculation of the rate of radiant heat transfer. Koh (ref. 21) has shown that the plane-parallel geometry assumption can lead to an overestimation of q_w^R by no more than 15 percent when the gas is

transparent to its own radiation and when the shock standoff distance to shock radius ratio is no greater than 0.05. As the Bouguer number k_p increases, the size of the error decreases and vanishes when the shock layer becomes optically thick. Because the effective optical thickness of a nongray shock layer is greater than that for a Planck equivalent gray gas, the error due to geometry will be smaller for a given Bouguer number in the more realistic nongray case.

Convective Heat Transfer

Even though the analysis of this investigation is based on the assumption that the gas in the shock layer is inviscid and nonheat conducting, it is possible to draw some conclusions regarding the coupling between radiant heat transfer and convection heating. The convective heating rate (sometimes referred to as the aerodynamic heating rate) is, in the case of a laminar boundary layer, the rate at which heat energy is transferred to the body surface by means of conduction.

To first order in the boundary-layer parameter $(N_{Pe})^{-1/2}$, the convective heating rate is proportional to the enthalpy difference across the conduction boundary layer. If the wall is cold (as has been assumed throughout this investigation), the enthalpy of the wall can be neglected and the convective heating rate becomes proportional to the enthalpy at the outer edge of the boundary layer. The location of the outer edge depends upon the Péclet number. Since it has been assumed throughout this investigation that the viscous boundary layer is thin (in terms of both the Dorodnitsyn coordinate and the optical path length), the location of the edge of the viscous boundary layer is arbitrarily specified as $\eta/\eta_\Delta = 0.05$ for both the small-perturbation and the transparent solutions. The rapid change in enthalpy near the wall, particularly for the transparent approximation which gives a value of zero for the enthalpy of the gas adjacent to the wall, necessitates choosing an edge location other than zero. For the optically thick and radiation-depleted shock layers, it is more convenient to specify the edge of the viscous boundary layer in terms of the normalized optical path length τ. The variation of enthalpy near the wall is very small in the case of the radiation-depleted shock layer. Consequently, the edge of the viscous boundary layer can be considered to be located at $\tau = 0$ for this case. A wall boundary layer due to radiation has been shown to exist in the optically thick shock layer. This wall boundary layer is always thicker than a photon mean free path and, of course, is very much thicker than the optically thin viscous boundary layer. Therefore, $\tau = 0$ can be considered as the edge of the viscous boundary layer for this case also. Values of the enthalpy h_e at the outer edge of the viscous boundary layer have been determined from the four approximate solutions for a wide range of the ratio of the radiation cooling parameter to the Bouguer number ϵ/k_p and the Bouguer number k_p. The results are shown in figure 35. The dashed portions of the curves represent arbitrary connections across regions of nonvalidity.

The quantity h_e is a rough approximation to the ratio of the convective heating rate for a radiating shock layer to that for a nonradiating shock layer. When radiant energy transport is important, the convective heating is reduced from the radiationless value $(h_e = 1)$. The effect becomes larger as both ϵ/k_P and k_P increase. It is interesting to note that the convective heating continues to decrease for increasing k_P even when the shock layer is optically thick and the rate of radiant heat transfer is decreasing as a result of absorption. Even though the total heating rate (radiant plus convective) cannot be deduced from an inviscid analysis, it is apparent that the total heating rate decreases with increasing shock-layer optical thickness for all values of k_P at least as large as the value for maximum rate of radiant heat transfer to the stagnation point q_w^R.

Of course, the results of figure 35 only give an order-of-magnitude estimate of the radiation-convection heating coupling. Not included are the effects of variable transport properties, enthalpy gradient at the edge of the boundary layer, and differences in the characteristic Reynolds and Prandtl numbers between the radiating and nonradiating cases. Also no account has been taken of the effect of radiation in the boundary layer. In the cooled region of the boundary layer adjacent to the wall, the gas will absorb more radiant energy than it will emit. This condition will tend to increase the slope of the enthalpy distribution adjacent to the wall and thereby increase somewhat the convective heat transfer.

The effects of radiation cooling, gray absorption, and spectral absorption on the ratio of convective heating rate for a radiating shock layer to that for a nonradiating shock layer h_e is shown in figure 36. It is apparent that radiation cooling plays the major role whereas absorption (both gray and nongray) tends to reduce the effectiveness of radiation cooling. The calculations for curves 1 and 2 ignored cooling. Consequently, no reduction in the calculated value of the convective heating rate was obtained. Curve 3 includes radiation cooling and ignores absorption. Thus the reduction in the calculated value of the convective heating rate is maximized in this approximation. Finally, curves 4 and 5 indicate that absorption inhibits the effectiveness of radiation cooling, and since absorption is more important in a nongray gas than it is in a Planck equivalent gray gas, the rate of convective heating will be greater in the nongray case.

The Role of the Radiation Cooling Parameter and the Bouguer Number

The radiation cooling parameter ϵ admits of several physical interpretations which are useful in the understanding of the radiating shock layer. Of these interpretations, one of the most useful is the following:

$$\epsilon = \frac{\left(\begin{array}{l}\text{Rate of emission from element of} \\ \text{volume of gas emerging from shock}\end{array}\right)\left(\begin{array}{l}\text{Time required by element of volume} \\ \text{to traverse distance } \Delta_A \text{ at rate of} \\ \text{emergence from shock}\end{array}\right)}{2(\text{Energy of element of volume upon emergence from shock})}$$

Here Δ_A is the shock standoff distance in a nonradiating (or adiabatic) flow.

It can be seen from this interpretation that the radiation cooling parameter is indicative of the slope of the enthalpy distribution immediately behind the shock. In fact, in the transparent limit there is a direct relation between ϵ and the initial slope; that is,

$$\frac{dh}{d\left(\eta/\eta_\Delta\right)} = 2\epsilon$$

(See, for example, fig. 17.)

In the case of an optically thick shock layer, the initial enthalpy gradient is reduced by absorption. However, a lower bound to the gradient is the value ϵ (one-half the transparent value) because the emergent elementary volume will emit at least twice as much energy as it absorbs; it emits energy at a rate proportional to the Planck function at the equilibrium shock temperature T_S in both the upstream and downstream directions while it absorbs energy at a rate at most proportional (by the same factor; the monochromatic volume absorption coefficient) to the Planck function at temperature T_S from only the downstream side.

A physical interpretation of the Bouguer number is:

$$k_P = \frac{\text{Radiationless shock standoff distance, } \Delta_A}{\text{Planck average photon mean free path in gas emerging from shock}}$$

Only when conditions do not vary greatly across the shock layer will the Bouguer number be indicative of the Planck mean optical thickness and only when the gas is nearly gray will the Planck mean optical thickness be indicative of the various important monochromatic optical thicknesses. Consequently, critical values of the Bouguer number are subject to a number of influences; among them, the enthalpy and spectral variation of the absorption coefficient and the value of the radiation cooling parameter. For example, the value of k_P for which absorption first becomes important is about 0.1, when the radiation cooling parameter is very much less than one and the absorption coefficient is independent of wavelength. When the absorption coefficient varies spectrally as shown in figure 13, and when ϵ is very small, absorption begins to become important for Bouguer numbers as small as 0.001. With ϵ about 10 for a gray gas, absorption is important for values of the Bouguer number greater than about three. Despite these drawbacks, the Bouguer number as defined in this investigation is about the best "a priori" indicator of the importance of absorption that can be obtained.

When the radiation cooling parameter ϵ is very much less than one, an elementary volume of gas will lose very little of its energy by radiant emission in the time required to traverse most of the shock layer. (Of course, it takes an elementary volume of gas traveling along the stagnation streamline an infinite time to reach the wall.) Hence, radiation cooling of the shock layer will be slight. When the radiation cooling parameter is very much greater than one, an elementary volume of gas will emit energy at such a rapid rate that the energy of the volume will be reduced a significant amount before it leaves the vicinity of the shock. This is true whether the shock layer is optically thick or optically thin (that is, regardless of the size of the Bouguer number). This physical argument is used to establish the existence of the thermal boundary layer behind the shock in the radiation-depleted shock layer. If the shock layer is optically thick, the reduction in enthalpy will continue only so long as the elementary volume is within about a photon mean free path of the shock. Beyond this point, the elementary gas volume receives radiation from all sides and begins to establish a condition of radiative equilibrium with its surroundings. The energy lost during the time required by the elementary volume to travel a single photon mean free path is characterized by the ratio of the radiation cooling parameter to the Bouguer number ϵ/k_P. (It was shown earlier that the enthalpy level in the interior of an optically thick shock layer was characterized solely by the parameter ϵ/k_P.)

Within the interior of an optically thick shock layer, radiation heat transfer can be treated in a manner analogous to conductive heat transfer. Thus, one would expect that a parameter analogous to the Péclet number could be constructed which would suggest the nature of the enthalpy boundary layer adjacent to the wall. Such a parameter, which is a ratio representing the relative importance of convective to radiative heat transfer is given by the grouping k_P^2/ϵ.[9] Since the thickness of the enthalpy boundary layer is characterized by $(N_{Pe})^{-1/2}$ in the conduction problem, one expects, by analogy, the thickness of the enthalpy boundary layer adjacent to the wall in an optically thick radiating shock layer to be characterized by $\epsilon^{1/2}/k_P$. The importance of this parameter (in a somewhat different form) and its analogy with the Péclet number was pointed out previously by Goulard. (See ref. 23.)

The importance of the surface reflectivity r_W depends on the importance of absorption in the shock layer. When absorption is negligible, the effects of surface reflectivity are negligible because all photons originating within the shock layer will escape the layer and it matters not whether some of these photons are absorbed by the cold wall or

[9]In the optically thick shock-layer analysis, the gas was assumed to be gray. Thus, the fact that the Bouguer number was based on a Planck mean absorption coefficient was of no consequence. However, in the case of a nongray gas, it would probably be more correct to use a Bouguer number based on a Rosseland mean absorption coefficient.

reflected by the wall into the free stream. However, when absorption is important, the reflected photons have a large probability of being recaptured in the shock layer. Thus, an increase in surface reflectivity tends to raise the enthalpy level of an absorbing gas in the vicinity of the wall.

In this section it was shown that both the radiation cooling parameter ϵ and the Bouguer number k_p play prominent and interrelated roles in determining the character of the radiating shock layer. Further, it was shown that the spectral variation of the absorption coefficient greatly influences the role of the Bouguer number. In general, then, one cannot ignore either of the processes of radiation cooling and nongray absorption.

CONCLUDING REMARKS

A mathematical model for the stagnation region of a radiating shock layer was derived in this investigation subject to the following conditions: (1) the gas in the shock layer is in local thermodynamic and chemical equilibrium, (2) the body geometry is axisymmetric, (3) there is no mass addition to the flow from the body surface, (4) the thicknesses of the shock and the viscous boundary layer are small in comparison with the shock standoff distance, and (5) absorption in the free stream ahead of the body is negligible. The divergence of the radiant flux vector, which appears in the energy equation, was formulated to include a wavelength-varying absorption coefficient. The body surface was considered to be cold and to reflect diffusely and independently of wavelength a fraction equal to the surface reflectivity r_w of the incident radiation. The results of a boundary-layer analysis indicate that the equations for the flow in the inviscid region are independent of the boundary-layer equations only when the boundary layer is optically thin or optically thick. It has been assumed throughout this study that the boundary layer is optically thin. Simple correlation formulas for the thermodynamic and optical properties of high-temperature equilibrium air were developed and used herein.

The general form of the governing system of equations was found to be integro-differential in character. The solution of this system is extremely difficult to find even with numerical techniques and high-speed electronic computing machines. The approach of this investigation was to take advantage of the simplified form to which the governing equations were reduced when the radiation cooling parameter ϵ and the Bouguer number k_p took on limiting values and obtain approximate analytic solutions if available. It was found that the general problem reduced to a singular perturbation problem in each of the four cases studied. A small-perturbation solution valid when the energy lost to the shock layer by radiation is small (that is, when the radiation cooling parameter is small) was derived. The Poincaré-Lighthill-Kuo (P-L-K) perturbation of coordinate method

was used to obtain a uniformly valid solution. This solution was used to study radiation cooling, absorption, effects of surface reflectivity, and effects of nongray optical properties.

An optically thin shock-layer method of solution utilizes an expansion in terms of the Bouguer number k_P to reduce the governing system to purely differential form. Again it was necessary to resort to the P-L-K method to obtain a uniformly valid solution. This solution was used to study radiation cooling, absorption, and the effects of surface reflectivity.

The optically thick approximation, valid when the optical thickness of the shock layer is very large (that is, the Bouguer number very much greater than 1) was used. The governing equations were reduced to differential form through the use of a substitute kernel approximation. Two thermal boundary layers were seen to exist; one adjacent to the shock and the other adjacent to the wall. It was noted that the Rosseland approximation together with a properly specified temperature-jump or slip condition at the wall reduces the governing equations to the same form as the substitute kernel approximation in the interior or isenthalpic portion of the shock layer and in the wall boundary layer. However, the Rosseland approximation with slip conditions was found to be inadequate for analyzing the shock boundary layer. The optically thick solutions were restricted to gray gases but were used to study radiation cooling, absorption, and the effects of surface reflectivity.

A radiation-depleted shock layer was analyzed. This approximation is valid when the rate at which energy is radiated away from the shock layer is nearly equal to the rate at which energy enters the shock layer (that is, the radiation cooling parameter is very large) so that the enthalpy level is very much less than the radiationless value. The substitute kernel approximation was used to reduce the governing system of equations to differential form. The method of matching of inner and outer expansions was used to obtain solutions valid in the thermal boundary layer adjacent to the shock and in the interior of the shock layer. These solutions were restricted to gray gases but were used to study radiation cooling, absorption, and the effects of surface reflectivity.

It is apparent from the results that radiation cooling first becomes important when the rate of energy lost by radiation from the shock layer is only about 1 percent of the rate with which energy enters the shock layer. Absorption in a gray gas begins to become important for shock layer optical thicknesses greater than about one-tenth. An increase in the surface reflectivity r_w from zero reduces the radiant heat transfer by a factor of roughly $1 - r_w$ and increases the heat-transfer rate to the wall by conduction because of an increase in enthalpy level near the wall.

The results of some nongray calculations obtained with the small-perturbation solution are presented. The Planck mean absorption coefficient can be used to compute the

enthalpy distribution and the radiation heat-transfer rate to the wall as long as the optical depth of the shock layer is very much less than one in all wavelength regions in which a significant amount of radiant energy is emitted. For larger optical thicknesses nongray effects are very important.

The various approximate solutions were used to compute the rate of radiant heat transfer to the stagnation point of blunt objects traversing an optically gray model earth atmosphere. The results of this computation indicate that at every altitude and velocity, there is a finite value of body nose radius for which the rate of radiant heat transfer to the stagnation point is a maximum. (This result is contrary to the earlier results, based on the assumptions of an isenthalpic and transparent shock layer, which indicated that the heating rate was directly proportional to nose radius.) A significant reduction in the computed value of the radiant heating resulted upon taking the nongray character of air into account. This result served to emphasize that the nongray character of gases plays a very real and important part in problems of radiation gas dynamics.

In general, the coupling between radiant and convective heat transfer is such that increases in the rate of radiant heat transfer result in decreases in the rate of convective heat transfer to the body surface. Of course, the amount by which the total heating rate is affected cannot be determined from this inviscid analysis.

Langley Research Center,
National Aeronautics and Space Administration,
Langley Station, Hampton, Va., February 18, 1970.

APPENDIX A

THE VISCOUS BOUNDARY LAYER

In this appendix, a boundary-layer analysis will be performed on the integro-differential system (52) to (59) to determine the form of the equations in the inviscid region and the viscous boundary layer and to determine under what conditions such a separation can be achieved. For convenience, the system will be rewritten here

$$f(\eta)\, h'(\eta) + \lambda^2\left[\mathcal{J}_1(h)\, h'(\eta)\right]' + \epsilon I[\eta] = 0 \tag{A1}$$

$$2\lambda^2\left[N_{Pr}\mathcal{J}_2(h)\, f''(\eta)\right]' + 2f(\eta)\, f''(\eta) - \left[f(\eta)\right]^2 + a^2 h(\eta) = 0 \tag{A2}$$

$$f(0) = 0 \tag{A3}$$

$$f'(0) = 0 \tag{A4}$$

$$f(\eta_\Delta) = 1 \tag{A5}$$

$$f'(\eta_\Delta) = \frac{a}{\sqrt{2\chi(1-\chi)}} \tag{A6}$$

$$h(0) = h_w \tag{A7}$$

$$h(\eta_\Delta) = 1 \tag{A8}$$

where

$$\epsilon = \rho_s \kappa_{P,s} \Delta_A \frac{4\sigma T_s^4}{\rho_\infty W_\infty^3} \tag{A9}$$

and λ, introduced here for convenience of notation, is the inverse square root of the Péclet number.

When the parameter λ is very much less than one, a perturbation type solution can be attempted. However, the energy and momentum equations each lose the most highly differentiated term as λ vanishes. As a result, neither the zero-order (in the small parameter λ) solution for $f(\eta)$ nor that for $h(\eta)$ can satisfy all the boundary conditions. In particular, the conditions $f'(0) = 0$ and $h(0) = 0$ must be relaxed, and

the perturbation solution will not be valid as η approaches zero. Thus, this problem is a singular perturbation problem of the "boundary layer" type. (See refs. 38 and 54.)

In order to obtain the boundary-layer form of the equations, the "stretched" coordinate $\xi = \lambda^{-\alpha}\eta$ is introduced where α is an as yet undetermined constant. It is also convenient, to avoid confusion, to introduce the change in notation

$$i(\xi) = h(\eta) \tag{A10}$$

$$g'(\xi) = f'(\eta) \tag{A11}$$

$$J[\xi] = I[\eta] \tag{A12}$$

Equation (A11) is written in this particular form because it is $f'(\eta)$ and not $f(\eta)$ which fails to satisfy the boundary condition at $\eta = 0$.

When the stretched coordinate ξ and the definitions (A10) to (A12) are introduced into system of equations (A1) to (A8), the only choice for α which will retain the most highly differentiated terms without loss of the most significant terms in the "unstretched" problem is $\alpha = 1$. Thus, λ and not λ^2 is the significant small parameter and the stretched coordinate is

$$\xi = \lambda^{-1}\eta \tag{A13}$$

Perturbation solutions are now sought in the forms:

$$i(\xi,\lambda) = \sum_{n=0}^{\infty} \lambda^n i_n(\xi) \tag{A14}$$

$$g(\xi,\lambda) = \sum_{n=0}^{\infty} \lambda^n g_n(\xi) \tag{A15}$$

in the boundary layer, and

$$h(\eta,\lambda) = \sum_{n=0}^{\infty} \lambda^n h_n(\eta) \tag{A16}$$

$$f(\eta,\lambda) = \sum_{n=0}^{\infty} \lambda^n f_n(\eta) \tag{A17}$$

in the inviscid region.

It shall be assumed that all functions of h (and i) are analytic about the value h_0 (and i_0) so that they may be expanded in Taylor series about $h = h_0$ and $i = i_0$ in the following manner:

$$F(h) \equiv F\left(h_0 + \lambda h_1 + \lambda^2 h_2 + \ldots\right) = F\left(h_0\right) + \lambda \dot{F}\left(h_0\right) h_1 + \lambda^2 \left[\dot{F}\left(h_0\right) h_2 + \frac{1}{2} \ddot{F}\left(h_0\right) h_1^2\right] + \ldots \tag{A18}$$

The existence of the expansions

$$I\left[\eta,\lambda\right] = \sum_{n=0}^{\infty} \lambda^n I_n\left[\eta\right] \tag{A19}$$

$$J\left[\xi,\lambda\right] = \sum_{n=0}^{\infty} \lambda^n J_n\left[\xi\right] \tag{A20}$$

$$a = \sum_{n=0}^{\infty} \lambda^n a_n \tag{A21}$$

$$\eta_\Delta = \sum_{n=0}^{\infty} \lambda^n \eta_{\Delta,n} \tag{A22}$$

is also assumed without, for the present, specifying details of the terms $I_n\left[\eta\right]$ and $J_n\left[\xi\right]$.

Furthermore, to insure compatibility of the boundary layer and inviscid solutions, it is necessary that the inner boundary condition on the outer solution be written in the form

$$f(\delta) = 0 \tag{A23}$$

where δ (the displacement distance) is specified by the matching condition

$$\lim_{\xi \to \infty} g(\xi) = \lambda^{-1} f(\eta) \tag{A24}$$

The quantity δ depends on λ and must be written in expanded form

$$\delta = \sum_{n=1}^{\infty} \lambda^n \delta_n \tag{A25}$$

The term δ_0 was chosen to be zero because δ is of order λ.

The system which describes the solutions valid in the inviscid region can be obtained by substituting expansions (A16) to (A22), and (A25) into system equations (A1) to (A8). The result is an infinite power series in λ the sum of which is zero for all values of λ. The only such series is one for which the coefficient of each of the λ^n terms is identically zero. These coefficients yield a set of recursive integro-differential systems. The system of zero order is

$$f_0(\eta)\, h_0'(\eta) + \epsilon I_0\left[\eta\right] = 0 \tag{A26}$$

$$2f_0(\eta)\, f_0''(\eta) - \left[f_0'(\eta)\right]^2 + a_0^2 h_0(\eta) = 0 \tag{A27}$$

$$f_0(0) = 0 \tag{A28}$$

$$f_0\left(\eta_{\Delta,0}\right) = 1 \tag{A29}$$

$$f_0'\left(\eta_{\Delta,0}\right) = \frac{a_0}{\sqrt{2\chi(1-\chi)}} \tag{A30}$$

$$h_0\left(\eta_{\Delta,0}\right) = 1 \tag{A31}$$

The system which describes the solutions valid in the boundary layer can be obtained by substituting expansions (A14), (A15), and (A18) to (A22) into system (A1) to (A8). As for the inviscid case, this procedure results in a set of differential systems. The zero-order system is

$$\left[\mathcal{F}_1\left(i_0\right)\, i_0'(\xi)\right]' + g_0(\xi)\, i_0'(\xi) + \epsilon J_0\left[\xi\right] = 0 \tag{A32}$$

$$2\left[\mathcal{F}_2^*\left(i_0\right)\, g_0''(\xi)\right]' + 2g_0(\xi)\, g_0''(\xi) - \left[g_0'(\xi)\right]^2 + a_0^2 i_0(\xi) = 0 \tag{A33}$$

$$g_0(0) = 0 \tag{A34}$$

$$g_0'(0) = 0 \tag{A35}$$

$$\lim_{\xi \to \infty} g_0'(\xi) = f_0'(0) \tag{A36}$$

$$i_0(0) = h_w \tag{A37}$$

$$\lim_{\xi \to \infty} i_0(\xi) = h_0(0) \tag{A38}$$

The first-order term of the displacement distance δ_1 is found from the matching condition

$$\lim_{\xi \to \infty} g_0(\xi) = \left(\xi - \delta_1\right) f_0'(0) \tag{A39}$$

It is apparent that the zero-order solution for the boundary-layer equations depends only on the inviscid enthalpy level in the vicinity of the wall and not the enthalpy gradient. The enthalpy gradient will, of course, have an effect on the first-order boundary-layer solution. Thus, if the enthalpy gradient is very large, as it can be for a radiating shock layer, the boundary-layer solutions must be carried out to first order in λ. When absorption is neglected, the enthalpy gradient at the body surface can be infinite and the analysis presented herein will not be valid. Burggraf (ref. 55) has shown how to overcome this difficulty.

The divergence of the radiation flux (see eq. (64)) includes integrals which extend over the whole domain of the problem. It is convenient to separate each of these integrals into two integrals as follows:

$$\int_0^{\tau_\lambda,\Delta} B_\lambda\left(t_\lambda\right) E_1\left(k_P\left|\tau_\lambda - t_\lambda\right|\right) dt_\lambda = \int_{\tau_\lambda^*}^{\tau_\lambda,\Delta} B_\lambda\left[h\left(t_\lambda\right)\right] E_1\left(k_P\left|\tau_\lambda - t_\lambda\right|\right) dt_\lambda + \int_0^{\sigma_\lambda^*} B_\lambda\left[i\left(s_\lambda\right)\right] E_1\left(k_P\left|\tau_\lambda - \lambda s_\lambda\right|\right) ds_\lambda \tag{A40}$$

and

$$\int_0^{\tau_\lambda,\Delta} B_\lambda\left(t_\lambda\right) E_2\left(k_P t_\lambda\right) dt_\lambda = \int_{\tau_\lambda^*}^{\tau_\lambda,\Delta} B_\lambda\left[h\left(t_\lambda\right)\right] E_2\left(k_P t_\lambda\right) dt_\lambda + \lambda \int_0^{\sigma_\lambda^*} B_\lambda\left[i\left(s_\lambda\right)\right] E_2\left(k_P \lambda s_\lambda\right) ds_\lambda \tag{A41}$$

where

$$\tau_\lambda^* = \lambda \sigma_\lambda^* = \lambda \int_0^{\xi^*} \kappa_\lambda(i)\, d\xi \tag{A42}$$

is the monochromatic optical thickness of the boundary layer and ξ^* is the thickness of the boundary layer in terms of the stretched Dorodnitsyn variable ξ.

It is convenient to redefine the monochromatic optical path length as

$$\tau_\lambda = \lambda\int_0^\xi \kappa_\lambda(i)\, d\xi \qquad \left(\tau_\lambda \leqq \tau_\lambda^*\right) \tag{A43}$$

$$\tau_\lambda = \int_{\lambda\xi^*}^\eta \kappa_\lambda(h)\, d\eta + \tau_\lambda^* \qquad \left(\tau_\lambda > \tau_\lambda^*\right) \tag{A44}$$

In order to expand equation (64) as a power series in λ, it is necessary to expand the exponential integral functions and all functions of h (and i) as well. Expanding the optical thickness yields, for $\tau_\lambda \leqq \tau_\lambda^*$

$$\tau_\lambda = \lambda\sigma_\lambda = \lambda\int_0^\xi \kappa_\lambda\left(i_0\right) d\xi + \lambda^2\int_0^\xi i_1(\xi)\, \dot{\kappa}_\lambda\left(i_0\right) d\xi + \ldots \tag{A45}$$

and for $\tau_\lambda > \tau_\lambda^*$

$$\tau_\lambda = \int_0^\eta \kappa_\lambda\left(h_0\right) d\eta + \lambda\left\{\int_0^\eta h_1(\eta)\, \dot{\kappa}_\lambda\left(h_0\right) d\eta - \int_0^\infty\left[\kappa_\lambda\left(h_0(0)\right) - \kappa_\lambda\left(i_0\right)\right] d\xi\right\} + \ldots \tag{A46}$$

The exponential integral functions can be expanded in the Taylor series

$$E_n(x - y) \equiv E_n\left[\left(x_0 - y_0\right) + \lambda\left(x_1 - y_1\right) + \ldots\right] \equiv E_n\left(x_0 - y_0\right) - \lambda\left(x_1 - y_1\right)E_{n-1}\left(x_0 - y_0\right) + \ldots \tag{A47}$$

If the argument is of order λ,

$$E_n(\lambda x) = E_n(0) - \lambda_1 x E_{n-1}(0) + \ldots + (-1)^{n-2}\lambda^{n-2}\frac{x^{n-2}}{(n-2)!}E_2(0)$$
$$- (-1)^{n-1}\left(\lambda^{n-1}\log_e\lambda\right)\frac{x^{n-1}}{(n-1)!} - (-1)^{n-1}\lambda^{n-1}\frac{x^{n-1}}{(n-1)!}\left[\gamma + \log_e x\right] + \ldots \tag{A48}$$

where γ is Euler's constant ($\gamma = 0.577216$). Use of this expansion, while it avoids any dependence of the terms $I_n[\xi]$ on λ, introduces terms of order $\lambda \log_e \lambda$ into the boundary-layer solutions.

Incorporating the various expansions into equation (64) and separating the result into powers of λ and $\lambda \log_e \lambda$ yields the zero-order expressions:

$$I_0[\eta] = -2\kappa_P[h_0(\eta)]\, B[h_0(\eta)] + k_P\int_0^\infty \kappa_\lambda[h_0(\eta)]\left\{\int_0^{\eta_\Delta} \kappa_\lambda[h_0(\eta')]\, B_\lambda[h_0(\eta')]\, E_1\left(k_P\left|\tau_\lambda(\eta) - \tau_\lambda(\eta')\right|\right) d\eta' + 2r_w E_2\left(k_P\tau_\lambda(\eta)\right)\int_0^{\eta_\Delta} \kappa_\lambda[h_0(\eta')]\, B_\lambda[h_0(\eta')]\, E_2\left(k_P\tau_\lambda(\eta')\right) d\eta'\right\} d\lambda \tag{A49}$$

and

$$J_0[\xi] = -2\kappa_P[i_0(\xi)]\, B[i_0(\xi)] + k_P\int_0^\infty \kappa_\lambda[i_0(\xi)]\left\{\int_0^{\eta_\Delta} \kappa_\lambda[h_0(\eta')]\, B_\lambda[h_0(\eta')]\, E_1\left(k_P\tau_\lambda(\eta')\right) d\eta' + 2r_w\int_0^{\eta_\Delta} \kappa_\lambda[h_0(\eta')]\, B_\lambda[h_0(\eta')]\, E_2\left(k_P\tau_\lambda(\eta')\right) d\eta'\right\} d\lambda \tag{A50}$$

The second of these expressions, which contains only definite integrals, is valid only when expansion (A47) holds. But equation (A47) converges in the first few terms only if the argument λx (or in the terms of this problem $\lambda k_P \sigma$) is small compared with 1. Thus, expressions (A48) and (A49) can be used only when the boundary layer is optically thin; that is,

$$\lambda k_P \sigma^* = k_P \tau^* << 1.0 \tag{A51}$$

APPENDIX B

MATHEMATICAL DEVELOPMENT FOR OPTICALLY THIN SHOCK LAYERS

With the substitute kernel approximation, the divergence of the radiant flux vector can be written

$$I\left[\eta\right] = 2\kappa_P(\eta)\, B(\eta) - 2k_P\int_0^\infty \kappa_\lambda(\eta)\left\{\int_0^{\eta_\Delta} \kappa_\lambda(\xi)\, B_\lambda(\xi)\, e^{-2k_P\left|\tau_\lambda(\eta)-\tau_\lambda(\xi)\right|}\, d\xi + r_w e^{-2k_P\tau_\lambda(\eta)}\int_0^{\eta_\Delta} \kappa_\lambda(\xi)\, B_\lambda(\xi) e^{-2k_P\tau_\lambda(\xi)}\, d\xi\right\} d\lambda \tag{B1}$$

The monochromatic optical path length $k_P\tau_\lambda(\eta)$ is given by the expression

$$k_P\tau_\lambda(\eta) = k_P\int_0^{\eta} \kappa_\lambda(\xi)\, d\xi \tag{B2}$$

where k_P is the Bouguer number

$$k_P = \rho_s\kappa_{P,s}\Delta_A \tag{B3}$$

The approximate governing system presented in the section "Optically Thin Shock Layers" is

$$f(\eta)\, h'(\eta) + \epsilon I\left[\eta\right] = 0 \tag{B4}$$

$$2f(\eta)\, f''(\eta) - \left[f'(\eta)\right]^2 + a^2\bar{h} = 0 \tag{B5}$$

$$f(0) = 0 \tag{B6}$$

$$f\left(\eta_\Delta\right) = 1 \tag{B7}$$

$$f'\left(\eta_\Delta\right) = \frac{2}{1 + \sqrt{2\chi(1 - \chi)}} \tag{B8}$$

$$h\left(\eta_\Delta\right) = 1 \tag{B9}$$

The quantity $\bar{h}$ is defined by the expression:

$$\bar{h} = \frac{1}{\eta_\Delta} \int_0^{\eta_\Delta} h(\xi)\, d\xi \tag{B10}$$

The Conventional Perturbation Procedure

If the functions $h(\eta;k_P)$ and $f(\eta;k_P)$ are analytic in the vicinity of $k_P = 0$ (it is assumed herein that such is the case), they may be written in the expanded form:

$$h(\eta;k_P) = \sum_{n=0}^{\infty} k_P^n h_n(\eta) \tag{B11}$$

$$f(\eta;k_P) = \sum_{n=0}^{\infty} k_P^n h_n(\eta) \tag{B12}$$

It is anticipated that the first few terms of these expansions will provide an accurate estimate of the solution to the system equations (B4) to (B10) when k_P is small compared with unity.

In addition, all quantities which depend on the parameter k_P either directly or indirectly must be expanded in terms of k_P. For example, a function $\mathcal{F}[h(\eta)]$ becomes

$$\mathcal{F}[h(\eta)] \equiv \mathcal{F}[h_0(\eta) + k_P h_1(\eta) + \ldots] = \mathcal{F}[h_0(\eta)] + k_P \dot{\mathcal{F}}[h_0(\eta)]\, h_1(\eta) + \ldots \tag{B13}$$

$$\mathcal{F}[h(\eta)] = \mathcal{F}_0(\eta) + k_P \dot{\mathcal{F}}_0(\eta)\, h_1(\eta) + \ldots \tag{B14}$$

The quantities $\mathcal{F}_0(\eta)$ and $\dot{\mathcal{F}}_0(\eta)$ have been introduced to simplify the notation. The constant η_Δ is given by the expansion:

$$\eta_\Delta = \eta_{\Delta,0} + k_P \eta_{\Delta,1} + \ldots \tag{B15}$$

Substituting the expansions (B11) to (B15) into system equations (B4) to (B10) yields

$$\left[f_0(\eta)\, h_0'(\eta) - 2\epsilon\kappa_{P,0}(\eta)\, B_0(\eta)\right] + k_P\left\{f_0(\eta)\, h_1'(\eta) + f_1(\eta)\, h_0'(\eta) - 2\epsilon\left[\dot{\kappa}_{P,0}(\eta)\, B_0(\eta) + \kappa_{P,0}(\eta)\, \dot{B}_0(\eta)\right] h_1(\eta) + 2\epsilon(1 + r_w)\int_0^{\infty}\left[\kappa_{\lambda,0}(\eta)\int_0^{\eta_{\Delta,0}} \kappa_{\lambda,0}(\xi)\, B_{\lambda,0}(\xi)\, d\xi\right] d\lambda\right\} + \ldots = 0 \tag{B16}$$

$$\left\{2f_0(\eta)\, f_0''(\eta) - \left[f_0'(\eta)\right]^2 + a^2\bar{h}_0\right\} + k_P\left\{2f_0(\eta)\, f_1''(\eta) - 2f_0'(\eta)\, f_1'(\eta) + 2f_0''(\eta)\, f_1(\eta) + a^2\bar{h}_1\right\} + \ldots = 0 \tag{B17}$$

$$f_0(0) + k_P f_1(0) + \ldots = 0 \tag{B18}$$

$$f_0\left(\eta_{\Delta,0}\right) + k_P\left[f_1\left(\eta_{\Delta,0}\right) + \eta_{\Delta,1} f_0'\left(\eta_{\Delta,0}\right)\right] + \ldots = 1 \tag{B19}$$

$$f_0'\left(\eta_{\Delta,0}\right) + k_P\left[f_1'\left(\eta_{\Delta,0}\right) + \eta_{\Delta,1} f_0''\left(\eta_{\Delta,0}\right)\right] + \ldots = \frac{2}{1 + \sqrt{2\chi(1-\chi)}} \tag{B20}$$

$$h_0\left(\eta_{\Delta,0}\right) + k_P\left[h_1\left(\eta_{\Delta,0}\right) + \eta_{\Delta,1} h_0'\left(\eta_{\Delta,0}\right)\right] + \ldots = 1 \tag{B21}$$

where

$$\bar{h}_0 + k_P\bar{h}_1 + \ldots = \frac{1}{\eta_{\Delta,0}}\int_0^{\eta_{\Delta,0}} h_0(\xi)\, d\xi + k_P\left\{\frac{1}{\eta_{\Delta,0}}\int_0^{\eta_{\Delta,0}} h_1(\xi)\, d\xi - \frac{\eta_{\Delta,1}}{\eta_{\Delta,0}^2}\int_0^{\eta_{\Delta,0}} h_0(\xi)\, d\xi + \frac{\eta_{\Delta,1}}{\eta_{\Delta,0}}\right\} + \ldots \tag{B22}$$

Since the small parameter is arbitrary, equation system (B16) to (B21) can be satisfied only if each coefficient of each term is identically zero. This condition leads to a recursive set of purely differential systems. The zero-order system is

$$f_0(\eta)\, h_0'(\eta) - 2\epsilon\kappa_{P,0}(\eta)\, B_0(\eta) = 0 \tag{B23}$$

$$2f_0(\eta)\, f_0''(\eta) - \left[f_0'(\eta)\right]^2 + a^2\bar{h}_0 = 0 \tag{B24}$$

$$f_0(0) = 0 \tag{B25}$$

$$f_0\left(\eta_{\Delta,0}\right) = 1 \tag{B26}$$

$$f_0'\left(\eta_{\Delta,0}\right) = \frac{2}{1 + \sqrt{2\chi(1-\chi)}} \tag{B27}$$

$$h_0\left(\eta_{\Delta,0}\right) = 1 \tag{B28}$$

$$\bar{h}_0 = \frac{1}{\eta_{\Delta,0}} \int_0^{\eta_{\Delta,0}} h_0(\xi)\, d\xi \tag{B29}$$

The solutions to this system are

$$\int_{h_0}^{1} \frac{dh}{\kappa_P(h)\, B(h)} = \frac{2\epsilon\eta_{\Delta,0}}{a^*} \log_e \frac{(1 - a^*)x + a^*}{x} \tag{B30}$$

$$f_0(\eta) = \left(1 - a\sqrt{\bar{h}_0}\eta_{\Delta,0}\right)\left(\frac{\eta}{\eta_{\Delta,0}}\right)^2 + a\sqrt{\bar{h}_0}\eta_{\Delta,0}\left(\frac{\eta}{\eta_{\Delta,0}}\right) \tag{B31a}$$

$$f_0(\eta) = (1 - a^*)x^2 + a^*x \tag{B31b}$$

$$\eta_{\Delta,0} = \frac{1 + \sqrt{2\chi(1 - \chi)}}{1 + \sqrt{2\bar{h}_0\chi(1 - \chi)}} \tag{B32}$$

$$\bar{h}_0 = \int_0^1 h_0(x)\, dx \tag{B33}$$

where the definitions

$$a^* = a\sqrt{\bar{h}_0}\eta_{\Delta,0} \tag{B34}$$

$$x = \frac{\eta}{\eta_{\Delta,0}} \tag{B35}$$

have been added to simplify the notation.

The first-order system is

$$\begin{aligned} &f_0(\eta)\, h_1'(\eta) - 2\epsilon\left[\dot{\kappa}_{P,0}(\eta)\, B_0(\eta) + \kappa_{P,0}(\eta)\, \dot{B}_0(\eta)\right] h_1(\eta) \\ &\quad = -f_1(\eta)\, h_0'(\eta) - 2\epsilon\left(1 + r_w\right)\int_0^{\infty}\left[\kappa_{\lambda,0}(\eta)\int_0^{\eta_{\Delta,0}} \kappa_{\lambda,0}(\xi)\, B_{\lambda,0}(\xi)\, d\xi\right] d\lambda \end{aligned} \tag{B36}$$

$$f_0(\eta)\, f_1''(\eta) - f_0'(\eta)\, f_1'(\eta) + f_0''(\eta)\, f_1(\eta) + \frac{1}{2}\, a^2 \bar{h}_1 = 0 \tag{B37}$$

$$f_1(0) = 0 \tag{B38}$$

$$f_1\left(\eta_{\Delta,0}\right) = -\eta_{\Delta,1} f_0'\left(\eta_{\Delta,0}\right) = -\frac{2\eta_{\Delta,1}}{1 + \sqrt{2\chi(1-\chi)}} \tag{B39}$$

$$f_1'\left(\eta_{\Delta,0}\right) = -\eta_{\Delta,1} f_0''\left(\eta_{\Delta,0}\right) = -\frac{2(1-a^*)\eta_{\Delta,1}}{\eta_{\Delta,0}^2} \tag{B40}$$

$$h_1\left(\eta_{\Delta,0}\right) = -\eta_{\Delta,1} h_0'\left(\eta_{\Delta,0}\right) = -2\epsilon\eta_{\Delta,1} \tag{B41}$$

The solutions to this system are

$$h_1(\eta) = -2\epsilon\kappa_{P,0}(x)\, B_0(x)\left\{\eta_{\Delta,1} + \left(\frac{\eta_{\Delta,0}\bar{h}_1}{2\bar{h}_0}\right)\left[\left(1 - a^* + \frac{a^{*2}}{2}\right)\frac{(1-x)}{(1-a^*)x + a^*} - \frac{1}{a^*}\log_e\frac{(1-a^*)x + a^*}{x}\right]\right\}$$
$$+ 2\epsilon\left(1 + r_w\right)\kappa_{P,0}(x)\, B_0(x)\eta_{\Delta,0}^2\int_x^1 \frac{\int_0^\infty\left[\kappa_{\lambda,0}(\xi)\int_0^1 \kappa_{\lambda,0}(\xi')\, B_{\lambda,0}(\xi')\, d\xi'\right] d\lambda}{f_0(\xi)\,\kappa_{P,0}(\xi)\, B_0(\xi)}\, d\xi \tag{B42}$$

$$f_1(x) = -\frac{\eta_{\Delta,1}}{\eta_{\Delta,0}}\, x(2 - a^* x) \tag{B43}$$

$$\eta_{\Delta,1} = -\frac{a^*\bar{h}_1}{4\bar{h}_0}\,\eta_{\Delta,0} \tag{B44}$$

$$\bar{h}_1 = \frac{\bar{h}_0\int_0^1 h_1(x)\, dx}{\left[\bar{h}_0 + \frac{a^*}{4}\left(1 - \bar{h}_0\right)\right]} \tag{B45}$$

The expression for $h_1(\eta)$ (eq. (B42)) can be simplified somewhat by transforming the integral over ξ into an integral over h_0 through the use of equation (B23). The result of this transformation is

$$h_1(x) = -2\epsilon\kappa_{P,0}(x)\, B_0(x)\left\{\eta_{\Delta,1} + \left(\frac{\eta_{\Delta,0}\bar{h}_1}{2\bar{h}_0}\right)\left[\left(1 - a^* + \frac{a^{*2}}{2}\right)\frac{(1-x)}{(1-a^*)x + a^*} - \frac{1}{a^*}\log_e\frac{(1-a^*)x + a^*}{x}\right]\right\}$$

$$+ \left(1 + r_w\right)\kappa_{P,0}(x)\, B_0(x)\, \eta_{\Delta,0}\int_0^\infty\left\{\left[\int_0^1 \kappa_{\lambda,0}(\xi')\, B_{\lambda,0}(\xi')\, d\xi'\right]\int_{h_0}^1 \frac{\kappa_\lambda(h)\, dh}{\left[\kappa_P(h)\, B(h)\right]^2}\right\} d\lambda \tag{B46}$$

The Poincaré-Lighthill-Kuo Solution

It can be seen on careful inspection of equation (B46) that the first-order term $h_1(x)$ displays a singular behavior in the vicinity of the wall ($x = 0$). Consequently, the assumed expansion for $h\left(x;k_P\right)$ diverges as the origin is approached and the perturbation solution is not uniformly valid. However, if the coordinate x is perturbed, the solution can be made uniformly valid. Thus, according to the P-L-K method,

$$x = y + k_P x_1^*(y) + \ldots \tag{B47}$$

where y is the transformed variable. The enthalpy when expanded in terms of k_P with coefficients as functions of y, not x, becomes

$$h\left(x;k_P\right) = h_0^*(y) + k_P h_1^*(y) + \ldots \tag{B48}$$

and the nondimensional stream function

$$f\left(x;k_P\right) = f_0^*(y) + k_P f_1^*(y) + \ldots \tag{B49}$$

According to Pritulo (ref. 49), the coefficients in the P-L-K expansions can be related to the coefficients in regular expansions in the following manner:

$$h_0^*(y) = h_0(y) \tag{B50}$$

$$h_1^*(y) = h_1(y) + x_1^*(y)\, h_0'(y) \tag{B51}$$

$$f_0^*(y) = f_0(y) \tag{B52}$$

$$f_1^*(y) = f_1(y) + x_1^*(y)\, f_0'(y) \tag{B53}$$

The arbitrary quantity $x_1^*(y)$ should be chosen to eliminate the singularity in $h_1^*(y)$. An obvious choice is

$$x_1(y) = \frac{-h_1(y)}{h_0'(y)} \tag{B54}$$

The transformation of the independent variable by means of formula (B47) removes the singularity from the domain of the problem, because y takes on some small positive value when x is zero. Hence, the first-order term $h_1^*(y)$ is nonsingular throughout the domain of the problem $0 \leqq x \leqq x_\Delta$.

APPENDIX C

MATHEMATICAL DEVELOPMENT FOR THE RADIATION-DEPLETED SHOCK LAYER

The system of equations governing the flow in the stagnation region of a radiating shock layer is derived in the text by use of the substitute kernel approximation. This system is

$$\left[f(\tau)\, h'(\tau)\right]'' - \frac{3}{2}\epsilon B''(\tau) - \frac{9}{4} k_P^2 f(\tau)\, h'(\tau) = 0 \tag{C1}$$

$$2f(\eta)\, f''(\eta) - \left[f'(\eta)\right]^2 + a^2 h(\eta) = 0 \tag{C2}$$

$$f(0) = 0 \tag{C3}$$

$$f\left(\eta_\Delta\right) = 1 \tag{C4}$$

$$f'\left(\eta_\Delta\right) = \frac{a}{\sqrt{2\chi(1-\chi)}} = \frac{2}{\chi\left(\frac{\Delta}{R_s}\right)} \tag{C5}$$

$$h\left(\tau_\Delta\right) = 1 \tag{C6}$$

This set of equations is subject to the additional condition

$$f(\tau)\, h'(\tau) + \epsilon\left[\frac{9}{8} k_P \int_0^{\tau_\Delta} B(t)\, e^{-\frac{3}{2}k_P|t-\tau|}\, dt - \frac{3}{2} B(\tau) + \frac{9}{8} r e^{-\frac{3}{2}k_P\tau}\right] \tag{C7}$$

where

$$r = r_w k_P \int_0^{\tau_\Delta} B(t)\, e^{-\frac{3}{2}k_P\tau}\, dt \tag{C8}$$

When the parameter ϵ is very much larger than unity and k_P^2, the asymptotic solution to the energy equation (C1) is simply $B(\tau) = C_1 + C_2\tau$. Substitution of this solution into the asymptotic form of the integral condition (C7) gives $C_1 = C_2 = 0$. This solution obviously does not satisfy the boundary condition $h\left(\tau_\Delta\right) = 1$, which indicates that the asymptotic solution is not valid in the vicinity of the boundary (shock) at $\tau = \tau_\Delta$. This result is not surprising when it is recalled that the existence of a thermal boundary layer has been established on physical grounds in the text.

In order to determine the form of the "boundary layer" equation valid near the shock, the stretched coordinate

$$\xi = \left(\tau_\Delta - \tau\right)\epsilon^n \tag{C9}$$

and the functions

$$B_b(\xi) = B(\tau) \tag{C10}$$

$$f_b(\xi) = f(\tau) \tag{C11}$$

are introduced. The subscript b indicates that these functions are valid only in the boundary layer.

When rewritten in terms of the boundary-layer variables, equation (C1) becomes

$$-\epsilon^{3n-1}\left[f_b(\xi)\, h_b'(\xi)\right]'' + \epsilon^{n-1}\frac{9}{4}k_P^2 f_b(\xi)\, h_b'(\xi) - \epsilon^{2n}\frac{3}{2}B_b''(\xi) = 0$$

If n is set equal to 1 and ϵ is allowed to grow without limit, the most highly differentiated term will be retained without losing the significant term of the unstretched problem. The resulting differential equation is

$$\left[f_b(\xi)\, h_b'(\xi)\right]'' + \frac{3}{2}B_b''(\xi) = \epsilon^{-2}\frac{9}{4}k_P^2 f_b(\xi)\, h_b'(\xi) \tag{C12}$$

The momentum equation, when written in terms of the stretched coordinate $\zeta = \left(\eta_\Delta - \eta\right)\epsilon$, becomes

$$2f_b(\zeta)\, f_b''(\zeta) - \left[f_b'(\zeta)\right]^2 = -\epsilon^{-2}a^2 h_b(\zeta) \tag{C13}$$

It has been shown that the boundary layer is characterized by the parameter ϵ^{-1} and it would seem proper to expand both the boundary layer and asymptotic solutions as power series in ϵ^{-1}. However, $f_a(\eta)$ (where the subscript a indicates the asymptotic solution valid far from the shock) is not analytic in ϵ^{-1} near $\epsilon^{-1} = 0$, but is analytic in $\epsilon^{-1/2}$. Consequently, the solutions will be expanded as power series in $\epsilon^{-1/2}$; that is,

$$B_a(\tau) = \sum_{n=0}^{\infty} \epsilon^{-n/2} B_{a,n}(\tau) \tag{C14}$$

$$f_a(\eta) = \sum_{n=0}^{\infty} \epsilon^{-n/2} f_{a,n}(\eta) \tag{C15}$$

$$B_b(\xi) = \sum_{n=0}^{\infty} \epsilon^{-n/2} B_{b,n}(\xi) \tag{C16}$$

$$f_b(\xi) = \sum_{n=0}^{\infty} \epsilon^{-n/2} f_{b,n}(\xi) \tag{C17}$$

In addition, it will be assumed that the enthalpy h is an analytic function of B throughout the interval $0 \leqq B \leqq 1$, and from physical considerations it will be assumed that $h = 0$ when $B = 0$. Then

$$h(B) = h\left(B_0\right) + \epsilon^{-1/2} B_1 \dot{h}\left(B_0\right) + \epsilon^{-1}\left[B_2 \dot{h}\left(B_0\right) + -B_1^2 \ddot{h}\left(B_0\right)\right] + \ldots \tag{C18}$$

where the dot ($\dot{}$) indicates differentiation with respect to the variable B_0. Substitution of expansions (C14), (C15), and (C18) into systems (C1) to (C7) gives

$$\frac{3}{2} B''_{a,0}(\tau) + \epsilon^{-1/2} \frac{3}{2} B''_{a,1}(\tau) + \epsilon^{-1}\left\{\frac{3}{2} B''_{a,2}(\tau) - \left[f_{a,0}(\tau)\, \dot{h}\left(B_{a,0}\right) B'_{a,0}(\tau)\right]''\right.$$

$$\left. + \frac{9}{4} k_P^2 f_{a,0}(\tau)\, \dot{h}\left(B_{a,0}\right) B'_{a,0}(\tau)\right\} + \ldots = 0 \tag{C19}$$

$$\left\{2 f_{a,0}(\eta)\, f''_{a,0}(\eta) - \left[f'_{a,0}(\eta)\right]^2 + a^2 h\left(B_{a,0}\right)\right\} + \epsilon^{-1/2}\left\{2 f_{a,0}(\eta)\, f''_{a,1}(\eta)\right.$$

$$\left. - 2 f'_{a,0}(\eta)\, f'_{a,1}(\eta) + 2 f''_{a,0}(\eta)\, f_{a,1}(\eta) + a^2 \dot{h}\left(B_{a,0}\right) B_{a,1}(\eta)\right\} + \ldots = 0 \tag{C20}$$

$$f_{a,0}(0) + \epsilon^{-1/2} f_{a,1}(0) + \epsilon^{-1} f_{a,2}(0) + \ldots = 0 \tag{C21}$$

$$\left\{f_{a,0}\left(\eta_{\Delta,0}\right) - 1\right\} + \epsilon^{-1/2}\left\{f_{a,1}\left(\eta_{\Delta,0}\right) + \eta_{\Delta,1} f'_{a,0}\left(\eta_{\Delta,0}\right)\right\} + \epsilon^{-1}\left\{f_{a,2}\left(\eta_{\Delta,0}\right) + \eta_{\Delta,1} f'_{a,1}\left(\eta_{\Delta,0}\right)\right.$$

$$\left. + \eta_{\Delta,2} f'_{a,0}\left(\eta_{\Delta,0}\right) + \frac{1}{2} \eta_{\Delta,1}^2 f''_{a,0}\left(\eta_{\Delta,0}\right)\right\} + \ldots = 0 \tag{C22}$$

$$\left\{f'_{a,0}\left(\eta_{\Delta,0}\right) - \frac{a}{\sqrt{2\chi(1-\chi)}}\right\} + \epsilon^{-1/2}\left\{f'_{a,1}\left(\eta_{\Delta,0}\right) + \eta_{\Delta,1}f''_{a,0}\left(\eta_{\Delta,0}\right)\right\} \epsilon^{-1}\left\{f'_{a,2}\left(\eta_{\Delta,0}\right)\right.$$

$$\left. + \eta_{\Delta,1}f''_{a,1}\left(\eta_{\Delta,0}\right) + \eta_{\Delta,2}f''_{a,0}\left(\eta_{\Delta,0}\right) + \frac{1}{2}\eta^2_{\Delta,1}f'''_{a,0}\left(\eta_{\Delta,0}\right)\right\} + \ldots = 0 \tag{C23}$$

$$\left\{\frac{9}{8}k_P\int_0^{\tau_{\Delta,0}} B_{a,0}(t)\, e^{-\frac{3}{2}k_P|\tau-t|}\, dt - \frac{3}{2}B_{a,0}(\tau) + \frac{9}{8}r_0 e^{-\frac{3}{2}k_P\tau}\right\} + \epsilon^{-1/2}\left\{\frac{9}{8}k_P\int_0^{\tau_{\Delta,0}} B_{a,1}(t)\, e^{-\frac{3}{2}k_P|\tau-t|}\, dt + \frac{9}{8}k_P\tau_{\Delta,1}B_{a,0}\left(\tau_{\Delta,0}\right) -\right.$$

$$\left. - \frac{3}{2}B_{a,1}(\tau) + \frac{9}{8}r_1 e^{-\frac{3}{2}k_P\tau}\right\} + \epsilon^{-1}\left\{\frac{9}{8}k_P\int_0^{\tau_{\Delta,0}} B_{a,2}(t)\, e^{-\frac{3}{2}k_P|\tau-t|}\, dt + \frac{9}{8}k_P\tau_{\Delta,1}B_{a,1}\left(\tau_{\Delta,0}\right) + \frac{9}{8}k_P\tau_{\Delta,2}B_{a,0}\left(\tau_{\Delta,0}\right) - \frac{3}{2}B_{a,2}(\tau)\right.$$

$$\left. + \frac{9}{8}r_2 e^{-\frac{3}{2}k_P\tau} + f_{a,0}(\tau)\,\dot{h}\left(B_{a,0}\right)B'_{a,0}(\tau) + \frac{9}{8}k_P e^{-\frac{3}{2}k_P\left(\tau_{\Delta,0}-\tau\right)}\int_0^{\epsilon\tau_\Delta}\left[B_{b,0}(\xi) - B_{a,0}\left(\tau_{\Delta,0}\right)\right] d\xi\right\} + \ldots = 0 \tag{C24}$$

where

$$r_0 = r_w k_P\int_0^{\tau_{\Delta,0}} B_{a,0}(t)\, e^{-\frac{3}{2}k_P t}\, dt \tag{C25}$$

$$r_1 = r_w k_P\int_0^{\tau_{\Delta,0}} B_{a,1}(t)\, e^{-\frac{3}{2}k_P t}\, dt + r_w k_P\tau_{\Delta,1}B_{a,0}\left(\tau_{\Delta,0}\right) \tag{C26}$$

$$r_2 = r_w k_P\int_0^{\tau_{\Delta,0}} B_{a,2}(t)\, e^{-\frac{3}{2}k_P t}\, dt + r_w k_P\tau_{\Delta,2}B_{a,2}\left(\tau_{\Delta,0}\right) + r_w k_P\tau_{\Delta,1}B_{a,1}\left(\tau_{\Delta,0}\right)$$

$$+ r_w k_P e^{-\frac{3}{2}k_P\tau_{\Delta,0}}\int_0^{\epsilon\tau_\Delta}\left[B_{b,0}(\xi) - B_{a,0}\left(\tau_{\Delta,0}\right)\right] d\xi \tag{C27}$$

The shock-layer optical thickness is determined from the condition

$$\left\{\eta_{\Delta,0} - \int_0^{\tau_{\Delta,0}} \kappa_P^{-1}\left(B_{a,0}\right) dt\right\} + \epsilon^{-1/2}\left\{\eta_{\Delta,1} - \tau_{\Delta,1}\kappa_P^{-1}\left[B_{a,0}\left(\tau_{\Delta,0}\right)\right] - \int_0^{\tau_{\Delta,0}}\left(\kappa_P^{-1}\left(B_{a,0}\right)\right) B_{a,1}(t)\, dt\right\} + \epsilon^{-1}\left\{\eta_{\Delta,2} - \tau_{\Delta,2}\kappa_P^{-1}\left[B_{a,0}\left(\tau_{\Delta,0}\right)\right]\right.$$

$$\left. - \tau_{\Delta,1}\left(\kappa_P^{-1}\left[B_{a,0}\left(\tau_{\Delta,0}\right)\right]\right) B_{a,1}\left(\tau_{\Delta,0}\right) - \int_0^{\tau_{\Delta,0}}\left(\kappa_P^{-1}\left(B_{a,0}\right)\right) B_{a,2}(t)\, dt - \frac{1}{2}\int_0^{\tau_{\Delta,0}}\left(\kappa_P^{-1}\left(B_{a,0}\right)\right)^{\cdot\cdot} B^2_{a,1}(t)\, dt - \int_0^{\epsilon\tau_\Delta}\left[\kappa_P^{-1}\left(B_{b,0}(\xi)\right)\right.\right.$$

$$\left.\left. - \kappa_P^{-1}\left(B_{a,0}\left(\tau_{\Delta,0}\right)\right)\right] d\xi\right\} + \ldots = 0 \tag{C28}$$

The corresponding boundary-layer equations are obtained by substituting the expansions for B_b and f_b into equations (C12) and (C13) with the result

$$\left[f_{b,0}(\xi)\,\dot{h}\left(B_{b,0}\right)B'_{b,0}(\xi)+\frac{3}{2}B_{b,0}(\xi)\right]''+\epsilon^{-1/2}\left[f_{b,0}(\xi)\,\dot{h}\left(B_{b,0}\right)B'_{b,1}(\xi)\right.$$

$$+f_{b,0}(\xi)\,\ddot{h}\left(B_{b,0}\right)B'_{b,0}(\xi)\,B_{b,1}(\xi)+f_{b,1}(\xi)\,\dot{h}\left(B_{b,0}\right)B'_{b,0}(\xi)$$

$$\left.+\frac{3}{2}B_{b,1}(\xi)\right]''+\epsilon^{-1}\left[f_{b,0}(\xi)\,\dot{h}\left(B_{b,0}\right)B'_{b,2}(\xi)+\ldots\right]''+\ldots=0 \tag{C29}$$

$$\left\{2f_{b,0}(\zeta)\,f''_{b,0}(\zeta)-\left[f'_{b,0}(\zeta)\right]^2\right\}+\epsilon^{-1/2}\left\{2f_{b,0}(\zeta)\,f''_{b,1}(\zeta)-2f'_{b,0}(\zeta)\,f'_{b,1}(\zeta)\right.$$

$$\left.+2f''_{b,0}(\zeta)\,f_{b,1}(\zeta)\right\}+\epsilon^{-1}\left\{2f_{b,0}(\zeta)\,f''_{b,2}(\zeta)+\ldots\right\}+\ldots=0 \tag{C30}$$

$$f_b(0)+\epsilon^{-1/2}f_{b,1}(0)+\epsilon^{-1}f_{b,2}(0)+\ldots=0 \tag{C31}$$

$$\left\{\lim_{\zeta\to\infty}f_{b,0}(\zeta)-1\right\}+\epsilon^{-1/2}\left\{\lim_{\zeta\to\infty}f_{b,1}(\zeta)\right\}+\epsilon^{-1}\left\{\lim_{\zeta\to\infty}f_{b,2}(\zeta)+\frac{a\zeta}{\sqrt{2\chi(1-\chi)}}\right\}+\ldots=0 \tag{C32}$$

$$B_{b,0}(0)+\epsilon^{-1/2}B_{b,1}(0)+\epsilon^{-1}B_{b,2}(0)+\ldots=1 \tag{C33}$$

$$\left\{\lim_{\zeta\to\infty}B_{b,0}(\xi)-B_{a,0}\left(\tau_{\Delta,0}\right)\right\}+\epsilon^{-1/2}\left\{\lim_{\zeta\to\infty}B_{b,1}(\xi)-B_{a,1}\left(\tau_{\Delta,0}\right)-\tau_{\Delta,1}B'_{a,0}\left(\tau_{\Delta,0}\right)\right\}$$

$$+\epsilon^{-1}\left\{\lim_{\zeta\to\infty}B_{b,2}(\xi)-B_{a,2}\left(\tau_{\Delta,0}\right)-\tau_{\Delta,1}B'_{a,1}\left(\tau_{\Delta,0}\right)-\tau_{\Delta,2}B'_{a,0}\left(\tau_{\Delta,0}\right)\right.$$

$$\left.-\xi B'_{a,0}\left(\tau_{\Delta,0}\right)-\frac{1}{2}\tau^2_{\Delta,1}B''_{a,0}\left(\tau_{\Delta,0}\right)\right\}+\ldots=0 \tag{C34}$$

$$\left\{\lim_{\xi\to\infty}B'_{b,0}(\xi)\right\}+\epsilon^{-1/2}\left\{\lim_{\xi\to\infty}B'_{b,1}(\xi)\right\}+\epsilon^{-1}\left\{\lim_{\xi\to\infty}B'_{b,2}(\xi)-B'_{a,0}\left(\tau_{\Delta,0}\right)\right\}+\ldots=0 \tag{C35}$$

Systems (C19) to (C24) and (C29) to (C35) lead to a set of recursive systems for the solution of $B_{a,i}$, $f_{a,i}$, $B_{b,i}$, and $f_{b,i}$.

Zero-Order Solutions

The differential system which describes the asymptotic solutions to zero order in the small parameter $\epsilon^{-1/2}$ is

$$B''_{a,0}(\tau) = 0 \tag{C36}$$

$$2f_{a,0}(\eta)\, f''_{a,0}(\eta) - \left[f'_{a,0}(\eta)\right]^2 + a^2 h\left(B_{a,0}\right) = 0 \tag{C37}$$

$$f_{a,0}(0) = 0 \tag{C38}$$

$$f_{a,0}\left(\eta_{\Delta,0}\right) = 1 \tag{C39}$$

$$f'_{a,0}\left(\eta_{\Delta,0}\right) = \frac{a}{\sqrt{2\chi(1-\chi)}} \tag{C40}$$

$$\frac{3}{2} k_P \int_0^{\tau_\Delta} B_{a,0}(t)\, e^{-\frac{3}{2}k_P|t-\tau|}\, dt - 2B_{a,0}(\tau) - \frac{3}{2} r_0 e^{-\frac{3}{2}k_P\tau} = 0 \tag{C41}$$

The solution is

$$B_{a,0}(\tau) = 0 \tag{C42}$$

$$f_{a,0}(\eta) = \left(\frac{\eta}{\eta_{\Delta,0}}\right)^2 \tag{C43}$$

$$\eta_{\Delta,0} = \frac{2\sqrt{2\chi(1-\chi)}}{a} = 1 + \sqrt{2\chi(1-\chi)} \tag{C44}$$

$$\tau_{\Delta,0} = \frac{\eta_{\Delta,0}}{\kappa^{-1}(0)} \tag{C45}$$

The zero-order boundary-layer system is

$$f_{b,0}(\xi)\, \dot{h}\left(B_{b,0}\right) B'_{b,0}(\xi) + \frac{3}{2} B_{b,0}(\xi) = C_1^{(0)} + C_2^{(0)} \xi \tag{C46}$$

$$2f_{b,0}(\zeta)\, f''_{b,0}(\zeta) - \left[f'_{b,0}(\zeta)\right]^2 = 0 \tag{C47}$$

$$f_{b,0}(0) = 1 \tag{C48}$$

$$\lim_{\xi \to \infty} f_{b,0}(\xi) = 1 \tag{C49}$$

$$B_{b,0}(0) = 1 \tag{C50}$$

$$\lim_{\xi \to \infty} B_{b,0}(\xi) = 0 \tag{C51}$$

$$\lim_{\xi \to \infty} B'_{b,0}(\xi) = 0 \tag{C52}$$

The solution to this system is

$$\xi = \frac{2}{3}\int_{B_{b,0}}^{1} \dot{h}(B)\frac{dB}{B} \tag{C53}$$

$$f_{b,0}(\zeta) = 1 \tag{C54}$$

First-Order Solutions

The differential system which describes the asymptotic solutions to first order in $\epsilon^{-1/2}$ is

$$B''_{a,1}(\tau) = 0 \tag{C55}$$

$$2\eta^2 f'''_{a,1}(\eta) - 4\eta f'_{a,1}(\eta) + 4f_{a,1}(\eta) + 8\chi(1-\chi)\,\dot{h}(0)\, B_{a,1}(\eta) = 0 \tag{C56}$$

$$f_{a,1}(0) = 0 \tag{C57}$$

$$f_{a,1}\left(\eta_{\Delta,0}\right) = -2\left(\frac{\eta_{\Delta,1}}{\eta_{\Delta,0}}\right) \tag{C58}$$

$$f'_{a,1}\left(\eta_{\Delta,0}\right) = -2\left(\frac{\eta_{\Delta,1}}{\eta^2_{\Delta,0}}\right) \tag{C59}$$

$$\frac{3}{2} k_P \int_0^{\tau_{\Delta,0}} B_{a,1}(t)\, e^{-\frac{3}{2}|t-\tau|k_P}\, dt - 2B_{a,1}(\tau) + \frac{3}{2} r_1 e^{-\frac{3}{2}k_P\tau} + \frac{3}{2} k_P \tau_{\Delta,1} B_{a,0}\left(\tau_{\Delta,0}\right) = 0 \tag{C60}$$

The system for determining $B_{a,1}(\tau)$ is identical to the system for obtaining $B_{a,0}(\tau)$. Therefore,

$$B_{a,1}(\tau) = 0 \tag{C61}$$

and equation (C56) becomes

$$2\eta^2 f''_{a,1}(\eta) - 4\eta f'_{a,1}(\eta) + 4 f_{a,1}(\eta) = 0$$

subject to the boundary conditions (C57) and (C58). Inspection of the preceding equation indicates that condition (C57) is satisfied automatically, so that another independent condition or equation must be specified in order to obtain a nonarbitrary solution for $f_{a,1}(\eta)$. This condition can be obtained from the differential system for terms of second order.

The system which determines the first-order boundary-layer solutions is

$$\dot{h}\left(B_{b,0}\right) B'_{b,1}(\xi) + \ddot{h}\left(B_{b,0}\right) B'_{b,0}(\xi)\, B_{b,1}(\xi) + \frac{3}{2} B_{b,1}(\xi) = C_1^{(1)} + C_2^{(2)}\xi \tag{C62}$$

$$f''_{b,1}(\xi) = 0 \tag{C63}$$

$$f_{b,1}(0) = 0 \tag{C64}$$

$$\lim_{\xi\to\infty} f_{b,1}(\xi) = 0 \tag{C65}$$

$$B_{b,1}(0) = 0 \tag{C66}$$

$$\lim_{\xi\to\infty} B_{b,1}(\xi) = 0 \tag{C67}$$

$$\lim_{\xi\to\infty} B'_{b,1}(\xi) = 0 \tag{C68}$$

The solution to this trivial system is, of course,

$$B_{b,1}(\xi) = 0 \tag{C69}$$

$$f_{b,1}(\xi) = 0 \tag{C70}$$

Second-Order Solutions

The differential system which determines the second-order asymptotic solution is

$$B''_{a,2}(\tau) = 0 \tag{C71}$$

$$2\eta^2 f''_{a,2}(\eta) - 4\eta f'_{a,2}(\eta) + 4f_{a,2}(\eta) = -\eta^2_{\Delta,0}\left[2f_{a,1}(\eta)\, f''_{a,1}(\eta) - \left[f'_{a,1}(\eta)\right]^2 + a^2\dot{h}(0)\, B_{a,2}(\eta)\right] \tag{C72}$$

$$f_{a,2}(0) = 0 \tag{C73}$$

$$f_{a,2}\left(\eta_{\Delta,0}\right) = -\eta_{\Delta,1} f'_{a,1}\left(\eta_{\Delta,0}\right) - 2\left(\frac{\eta_{\Delta,2}}{\eta_{\Delta,0}}\right) - \left(\frac{\eta_{\Delta,1}}{\eta_{\Delta,0}}\right)^2 \tag{C74}$$

$$f'_{a,2}\left(\eta_{\Delta,0}\right) = -\eta_{\Delta,1} f''_{a,1}\left(\eta_{\Delta,0}\right) - 2\,\frac{\eta_{\Delta,2}}{\eta^2_{\Delta,0}} \tag{C75}$$

$$\frac{3}{2}\, k_P \int_0^{\tau_{\Delta,0}} B_{a,2}(t)\, e^{-\frac{3}{2}k_P|t-\tau|}\, dt - 2B_{a,2}(\tau) + \frac{3}{2}\, r_2 e^{-\frac{3}{2}k_P\tau} + \frac{3}{2}\, k_P \tau_{\Delta,1} B_{a,1}\left(\tau_{\Delta,0}\right)$$

$$+ \frac{3}{2}\, k_P \tau_{\Delta,2} B_{a,0}\left(\tau_{\Delta,0}\right) + \frac{3}{2}\, k_P e^{-\frac{3}{2}k_P\left(\tau_{\Delta,0}-\tau\right)} \int_0^{\epsilon\tau_\Delta} \left[B_{b,0}(\xi) - B_{a,0}\left(\tau_{\Delta,0}\right)\right] d\xi = 0 \tag{C76}$$

The solution to this system is

$$B_{a,2}(\tau) = \frac{k_P\left(1 + r_w\right)\left(1 + \frac{3}{2}\, k_P\tau\right)}{2\left[1 + \frac{3}{4}\left(1 - r_w\right)k_P\tau_{\Delta,0}\right]} \tag{C77}$$

The second condition for the quantity $f_{a,1}(\eta)$ can be obtained by evaluating equation (C72) at $\eta = 0$, which gives

$$f'_{a,1}(0) = a\sqrt{\dot{h}(0)\, B_{a,2}(0)} \tag{C78}$$

With this condition, the solution for $f_{a,1}(\eta)$ can be completely specified with the result

$$f_{a,1}(\eta) = a\sqrt{\dot{h}(0)\, B_{a,2}(0)}\, \frac{\eta}{\eta_{\Delta,0}}\left(1 - \frac{\eta}{\eta_{\Delta,0}}\right)\eta_{\Delta,0} \tag{C79}$$

In addition,

$$\eta_{\Delta,1} = -a\eta_{\Delta,0}^2\sqrt{\dot{h}(0)\, B_{a,2}(0)} \tag{C80}$$

and

$$\tau_{\Delta,1} = \frac{\eta_{\Delta,1}}{\kappa_P^{-1}(0)} \tag{C81}$$

As before, it is necessary to look to the next higher order system in order to obtain a second independent condition or equation for $f_{a,2}(\eta)$. This condition is

$$f'_{a,2}(0) = 0 \tag{C82}$$

In order to solve equation (C72) for $f_{a,2}(\eta)$, it is necessary to express the optical path length τ as a function of η. This relationship can be made with aid of the definitions of τ and η. The result is

$$\tau = \tau_{\Delta,0}\, \frac{\eta}{\eta_{\Delta,0}} + O\left(\epsilon^{-1}\right) \tag{C83}$$

Now, equation (C72) can be written in the form

$$2\eta^2 f''_{a,2}(\eta) - 4\eta f'_{a,2}(\eta) + 4f_{a,2}(\eta) = -a^2\eta_{\Delta,0}\dot{h}(0)\frac{3\left(1 + r_w\right)k_P^2\tau_{\Delta,0}}{4\left[1 + \frac{3}{4}\left(1 - r_w\right)k_P\tau_{\Delta,0}\right]}\,\eta$$

The solution to this equation is

$$f_{a,2}(\eta) = \left[\left(\frac{\eta_{\Delta,1}}{\eta_{\Delta,0}}\right)^2 - 2\,\frac{\eta_{\Delta,2}}{\eta_{\Delta,0}} - A\,\log_e \eta_{\Delta,0}\right]\left(\frac{\eta}{\eta_{\Delta,0}}\right)^2 + \left[A\,\log_e \eta_{\Delta,0}\right]\frac{\eta}{\eta_{\Delta,0}} + A\,\frac{\eta}{\eta_{\Delta,0}}\,\log_e \frac{\eta}{\eta_{\Delta,0}} \tag{C84}$$

where

$$A = a^2\eta_{\Delta,0}^2\dot{h}(0)\frac{3\left(1 + r_w\right)k_P^2\tau_{\Delta,0}}{8\left[1 + \frac{3}{4}\left(1 - r_w\right)k_P\tau_{\Delta,0}\right]} = 3\left(\frac{\eta_{\Delta,1}}{\eta_{\Delta,0}}\right)^2 k_P\tau_{\Delta,0}$$

Also,

$$\eta_{\Delta,2} = -\eta_{\Delta,0}\left(\frac{\eta_{\Delta,1}}{\eta_{\Delta,0}}\right)^2\left[1 + \frac{3}{2}\,k_P\tau_{\Delta,0}\left(1 - \log_e \eta_{\Delta,0}\right)\right] \tag{C85}$$

and

$$\tau_{\Delta,2} = \frac{\eta_{\Delta,2}}{\kappa_P^{-1}(0)} + \eta_{\Delta,0}\frac{\left[\dot{\kappa_P^{-1}}(0)\right]}{\left[\kappa_P^{-1}(0)\right]^2}\,B_{a,2}(0)\left(1 + \frac{3}{4}\,k_P\tau_{\Delta,0}\right)$$

$$+ \int_0^{\epsilon\tau_{\Delta,0}+\epsilon^{1/2}\tau_{\Delta,1}+\tau_{\Delta,2}}\left[\frac{\kappa_P^{-1}\left(B_{b,0}(\xi)\right)}{\kappa_P^{-1}(0)} - 1\right]d\xi \tag{C86}$$

Radiative Flux and Standoff Distance

In the section "The Optically Thick Shock Layer," it was shown that with the substitute kernel approximation, the radiant flux passing into the cold wall can be expressed in terms of the black-body emissive power of the gas adjacent to the wall. Substituting the solution for $B_a(0)$ into the expression (171) gives

$$\frac{q_w^R}{1 - r_w} = \frac{1}{2\left[1 + \frac{3}{4}\left(1 - r_w\right)k_P\tau_{\Delta,0}\right]} \tag{C87}$$

The ratio of the shock standoff distance to the shock standoff distance for radiationless flow is given by the condition

$$\bar{\Delta} = \int_0^{\tau_\Delta} h(B)\,\kappa_P^{-1}(B)\,dt \tag{C88}$$

Expanding this expression in powers of $\epsilon^{-1/2}$ gives

$$\overline{\Delta} = \epsilon^{-1}\left\{\eta_{\Delta,0}\left[\dot{h}(0) + h(0)\frac{\left(\kappa_P^{-1}(0)\right)^{\cdot}}{\kappa_P^{-1}(0)}\right] B_{a,2}(0)\left(1 + \frac{3}{4}\, k_P \tau_{\Delta,0}\right)\right.$$

$$\left. + \int_0^{\epsilon\tau_{\Delta,0}+\epsilon^{1/2}\tau_{\Delta,1}+\tau_{\Delta,2}} h\left(B_{b,0}(\xi)\right)\, \kappa_P^{-1}\left(B_{b,0}(\xi)\right)\, d\xi\right\} \qquad \text{(C89)}$$

APPENDIX D

SYMBOLS

a constant defined by equation (55)

a_n nth-order coefficient in perturbation expansion of constant a

a^* constant defined by equation (145)

B black-body emissive power, nondimensional except in section "Stagnation Model for a Radiating Shock Layer" where it is $\frac{\sigma}{\pi} T^4$, erg/cm^2-ster-sec

B_λ Planck function, nondimensional except in section "Stagnation Model for a Radiating Shock Layer" where it is defined by equation (11), erg/cm^3-ster-sec

$\overline{B}$ nondimensional black-body emissive power in section "Stagnation Model for a Radiating Shock Layer"

$\overline{B}_\lambda$ nondimensional Planck function in section "Stagnation Model for a Radiating Shock Layer"

$B_0( ) = B\left[h_0( )\right]$

$B_{\lambda,0}( ) = B_\lambda\left[h_0( )\right]$

B_2 value of nondimensional black-body emissive power in interior of an optically thick shock layer

B_w value of nondimensional black-body emissive power in gas adjacent to wall in an optically thick shock layer

$\overline{B}, \dot{\overline{B}}$ constants defined in section "The Optically Thick Shock Layer"

B_a nondimensional black-body emissive power in interior of a radiation-depleted shock layer

$B_{a,n}$ nth-order coefficient in perturbation expansion of B_a

B_b nondimensional black-body emissive power in shock boundary layer in a radiation-depleted shock layer

$B_{b,n}$ nth-order coefficient in perturbation expansion of B_b

B^* constant in formula (240)

b constant defined by equation (193)

C constant defined by equation (149)

$C_1^{(0)}, C_1^{(1)}$
$C_2^{(0)}, C_2^{(1)}, C_2^{(2)}$
C_1, C_2
} constants of integration

c velocity of light, cm/sec

E_n exponential integral function of order n

$\mathfrak{I}_1, \mathfrak{I}_2, \mathfrak{I}_3$ functions of h defined by equation (55)

f nondimensional stream function defined by equation (36a)

f_n nth-order coefficient in perturbation expansion of f

f_n^* nth-order coefficient in P-L-K expansion of f

f_a nondimensional stream function in interior of a radiation-depleted shock

$f_{a,n}$ nth-order coefficient in perturbation expansion of f_a

f_b nondimensional stream function in shock boundary layer in a radiation-depleted shock layer

$f_{b,n}$ nth-order coefficient in perturbation expansion of f_b

g stream function; used in section "Stagnation Model for a Radiating Shock Layer," g/cm^2-sec

g nondimensional stream function in viscous boundary layer; defined by equation (86)

g_n nth-order coefficient in perturbation expansion of g

h enthalpy, nondimensional except in section "Stagnation Model for a Radiating Shock Layer" where it is the static specific enthalpy, erg/g; also Planck's constant, erg/sec

h_n nth-order coefficient in perturbation expansion of h, the nondimensional enthalpy

h_n^* nth-order coefficient in P-L-K expansion of h, nondimensional enthalpy

$h^{(n)}$ nth-order coefficient in expansion of h, the static specific enthalpy, erg/g

$\bar{h}$ average value of nondimensional enthalpy h (eq. (135)); also nondimensional enthalpy in section "Stagnation Model for a Radiating Shock Layer"

$\bar{h}_n$ nth-order coefficient in perturbation expansion of $\bar{h}$

h^* value of h for which γ $\left(\text{exponent in correlation formula } \kappa_p(h) = Ch^{\gamma}\right)$ changes

h_t total enthalpy in section "Stagnation Model for a Radiating Shock Layer," erg/g

h_2 value of nondimensional enthalpy in interior of an optically thick shock layer

h_w enthalpy in gas adjacent to wall, nondimensional except in section "Stagnation Model for a Radiating Shock Layer" where it is the static specific enthalpy in gas at wall conditions, erg/g

h_e value of nondimensional enthalpy at outer edge of viscous boundary layer

I divergence of radiant flux vector, nondimensional except in section "Stagnation Model for a Radiating Shock Layer" where it has the dimensions, erg/cm^3-sec

I_n nth-order coefficient in perturbation expansion of nondimensional divergence of radiant flux vector, I

i nondimensional enthalpy in viscous boundary layer; defined by equation (85)

i_n nth-order coefficient in perturbation expansion of i

J nondimensional divergence of radiant flux vector in viscous boundary layer

J_n nth-order coefficient in the perturbation expansion of J

$J_\lambda^{(s)}$ specific intensity of radiation, erg/cm^3-ster-sec

j_λ mass emission coefficient, erg/g-cm-ster-sec

k Boltzmann's constant, erg/^oK

k_{eff} effective coefficient of heat conduction including energy transport by molecular collisions and by diffusion of reacting species, erg/cm-sec-^oK

k_P Bouguer number $\rho_s \kappa_{P,s} \Delta_A$

k_λ quantity defined in equation (107)

l_i direction cosine between direction of a beam of intensity J_λ and ith direction

N_{Bo} Boltzmann number

N_{Pe} Péclet number

N_{Pr} Prandtl number

N_{Re} Reynolds number

p pressure, dyne/cm^2

p_0 standard pressure of air, 1.013×10^6 dyne/cm^2

$p^{(n)}$	nth-order coefficient in expansion p, dyne/cm^2
q_i	ith component of combined radiant and conductive heat fluxes, erg/cm^2-sec
$q_i^{(n)}$	nth-order coefficient in expansion of q_i, erg/cm^2-sec
q^c	component of conductive heat flux vector in η-direction, erg/cm^2-sec
q_i^c	component of conductive heat flux vector in ith direction, erg/cm^2-sec
q^R	component of radiant heat flux vector in η-direction, erg/cm^2-sec
q_i^R	component of radiant heat flux vector in ith direction, erg/cm^2-sec
$q_{\lambda,i}^R$	component of monochromatic radiant heat flux vector in ith direction, erg/cm^2-sec
q_w^R	nondimensional rate of radiant heat transfer to wall
R	gas constant for air, 2.882×10^6, cm^2/sec^2-^{o}K
R_N	body nose radius, cm
R_S	shock radius in vicinity of stagnation streamline, cm
r	position coordinate, cm
$r_{0,\lambda}$	defined by equation (108)
$r_{1,\lambda}$	defined by equation (113)
r_w	reflectivity of wall
S_λ	radiation source function, erg/cm^3-ster-sec
s	position coordinate, cm
s_λ	nondimensional variable of integration

T	temperature, ^{o}K
T_0	standard temperature, 273.16^{o} K
T_w	temperature of wall, ^{o}K
$\bar{t}$	dummy variable of integration
t_λ	nondimensional variable of integration
u	component of gas velocity in r-direction, cm/sec
$u^{(n)}$	nth-order coefficient in expansion of u, cm/sec
u_i	component of gas velocity in ith direction, cm/sec
V	volume, cm^3
W_∞	free-stream velocity, cm/sec
w	component of gas velocity in z-direction, cm/sec
$w^{(n)}$	nth-order coefficient in expansion of w, cm/sec
x	coordinate in transformed plane; also normalized Dorodnitsyn coordinate, $\eta/\eta_{\Delta,0}$
x_n^*	nth-order coefficient of P-L-K expansion of x
x_0	value of transformed coordinate for which $\eta = 0$
y	coordinate in transformed plane
z	position coordinate, cm
α	magnitude of step in step function model of absorption coefficient
β	local angle of inclination of bow shock from stream direction

β_λ mass extinction coefficient, cm^2/g

γ Euler's constant, $\gamma = 0.577216\ldots$

γ exponent in correlation formula, $\kappa_P = h^\gamma$

γ_1, γ_2 exponents in correlation formula for κ_P (eq. (148))

Δ shock standoff distance, cm

Δ_A shock standoff distance for nonradiating shock layer, cm

$\overline{\Delta}$ ratio of shock standoff distance for radiating and nonradiating shock layer, Δ/Δ_A

δ displacement distance for viscous boundary layer, cm; also exponent in correlation formula $B = h^\delta$

δ_n nth-order coefficient in perturbation expansion of displacement distance, δ, cm

ϵ radiation cooling parameter, $4\sigma T_s^4 k_P / \rho_\infty W_\infty^3$

ζ transformed nondimensional Dorodnitsyn coordinate in radiation-depleted shock layer

ζ transformed optical path length in optically thick shock layer

η Dorodnitsyn coordinate, nondimensional except in section "Stagnation Model for a Radiating Shock Layer" where it is defined by equation (35), g/cm^2

$\overline{\eta}$ nondimensional Dorodnitsyn coordinate in section "Stagnation Model for a Radiating Shock Layer"

η' variable of integration

η_Δ location of shock in terms of Dorodnitsyn coordinate, nondimensional except in section "Stagnation Model for a Radiating Shock Layer" where it has dimensions, g/cm^2

$\overline{\eta}_{\Delta}$ nondimensional location of shock in terms of Dorodnitsyn coordinate in section "Stagnation Model for a Radiating Shock Layer"

$\eta_{\Delta,n}$ nth-order coefficient in perturbation expansion of η_{Δ}

η_n^* nth-order coefficient in P-L-K expansion of η

θ angle defined in sketch (a)

κ_{λ} mass absorption coefficient, nondimensional except in section "Stagnation Model for a Radiating Shock Layer" where it has dimensions, cm^2/g

$\overline{\kappa}_{\lambda}$ nondimensional mass absorption coefficient in section "Stagnation Model for a Radiating Shock Layer"

κ_P Planck mean mass absorption coefficient, nondimensional except in section "Stagnation Model for a Radiating Shock Layer" where it has dimensions, cm^2/g

$\overline{\kappa}_P$ nondimensional Planck mean mass absorption coefficient in section "Stagnation Model for a Radiating Shock Layer"

$\dot{\kappa}_P = \frac{\partial \kappa_P}{\partial h}$ evaluated at $h = 1$

$\kappa_{P,n}$ nth-order coefficient in perturbation expansion of κ_P

κ_R Rosseland mean mass absorption coefficient, cm^2/g

λ wavelength, cm; also boundary-layer parameter, $\left(N_{Pe}\right)^{-1/2}$

μ coefficient of viscosity, dyne-sec/cm^2

μ' second coefficient of viscosity, dyne-sec/cm^2

ξ transformed nondimensional Dorodnitsyn coordinate in viscous boundary layer

ξ^* thickness of viscous boundary layer in terms of ξ

ρ	density, g/cm^3
ρ_0	standard density, 1.288×10^{-3} g/cm^3
ρ_2	density in interior of an optically thick shock layer, g/cm^3
$\rho^{(n)}$	nth-order coefficient in expansion of ρ, g/cm^3
σ	Stefan-Boltzmann constant, 5.669×10^{-5} $erg/cm^2\text{-}sec\text{-}^oK^4$
σ	area, cm^2
σ_λ	mass scattering coefficient, cm^2/g
σ_λ	transformed monochromatic optical path length in viscous boundary layer
σ_λ^*	thickness of viscous boundary layer in terms of σ_λ
τ	optical path length in a gray gas, normalized except in section "Stagnation Model for a Radiating Shock Layer"
$\overline{\tau}$	normalized optical path length in a gray gas in section "Stagnation Model for a Radiating Shock Layer"
τ_λ	monochromatic optical path length, normalized except in section "Stagnation Model for a Radiating Shock Layer"
$\overline{\tau}_\lambda$	normalized monochromatic optical path length in section "Stagnation Model for a Radiating Shock Layer"
$\tau_\lambda^{(s)}$	monochromatic optical path length in s-direction
τ_λ^*	thickness of viscous boundary layer in terms of τ_λ
τ_Δ	shock location in terms of τ
$\tau_{\Delta,n}$	nth-order coefficient in perturbation expansion of τ_Δ
$\tau_{\lambda,\Delta}$	shock location in terms of τ_λ

τ_{ij} component of viscous stress tensor, dyne/cm^2

Φ_n functions of η defined by equations (109) and (114)

χ density ratio across normal shock, ρ_∞/ρ_s

ω solid angle

ω_1 constant defined by equation (188)

ω_2 constant defined by equation (197)

Subscripts:

b shock boundary layer in radiation-depleted solution

s indicates value of dimensional quantity at normal-shock equilibrium conditions

∞ indicates value of dimensional quantity in the free stream

0,1 order of perturbation

Primed symbols denote differentiation with respect to the argument. An arrow over a symbol denotes a vector. Bars over symbols denote nondimensional quantities in section "Stagnation Model for a Radiating Shock Layer."

1.258×10^{-3} g/cm

REFERENCES

1. Kivel, Bennett: Radiation From Hot Air and Its Effect on Stagnation-Point Heating. J. Aerospace Sci., vol. 28, no. 2, Feb. 1961, pp. 96-102.

2. Yoshikawa, Kenneth K.; and Wick, Bradford H.: Radiative Heat Transfer During Atmosphere Entry at Parabolic Velocity. NASA TN D-1074, 1961.

3. Goulard, R.: The Coupling of Radiation and Convection in Detached Shock Layers. J. Quant. Spectrosc. Radiat. Transfer, vol. I, Pergamon Press Ltd., 1961, pp. 249-257.

4. Lunev, V. V.; and Murzinov, I. N.: The Effect of Radiation on the Flow in the Neighborhood of the Stagnation Point of a Blunt Body. Zh. Prikl. Mekhan. i Tekhn. Fiz., vol. 1, no. 2, Mar.-Apr. 1961, pp. 26-30.

5. Goulard, Robert: Preliminary Estimates of Radiative Transfer Effects on Detached Shock Layers. AIAA J., vol. 2, no. 3, Mar. 1964, pp. 494-502.

6. Hanley, G. M.; and Korkan, K. D.: Approximate Inviscid, Nonadiabatic Stagnation Region Flow Field Solution. AIAA J. (Tech. Notes), vol. 3, no. 8, Aug. 1965, pp. 1537-1538.

7. Wilson, K. H.; and Hoshizaki, H.: Inviscid, Nonadiabatic Flow About Blunt Bodies. AIAA J., vol. 3, no. 1, Jan. 1965, pp. 67-74.

8. Yoshikawa, Kenneth K.; and Chapman, Dean R.: Radiative Heat Transfer and Absorption Behind a Hypersonic Normal Shock Wave. NASA TN D-1424, 1962.

9. Howe, John T.; and Viegas, John R.: Solutions of the Ionized Radiating Shock Layer, Including Reabsorption and Foreign Species Effects, and Stagnation Region Heat Transfer. NASA TR R-159, 1963.

10. Fay, James A.; Moffatt, W. Craig; and Probstein, Ronald F.: An Analytical Study of Meteor Entry. AIAA J., vol. 2, no. 5, May 1964, pp. 845-854.

11. Lick, Wilbert: Energy Transfer by Radiation and Conduction. Proceedings of the 1963 Heat Transfer and Fluid Mechanics Institute, Anatol Roshko, Bradford Sturtevant, and D. R. Bartz, eds., Stanford Univ. Press, 1963, pp. 14-26.

12. Greif, Ralph: Energy Transfer by Radiation and Conduction With Variable Gas Properties. Int. J. Heat Mass Transfer, vol. 7, no. 8, Aug. 1964, pp. 891-900.

13. Goulard, R.; Boughner, R. E.; Burns, R. K.; and Nelson, H. F.: Radiating Flows During Entry Into Planetary Atmospheres. IAF Paper RE70, Amer. Inst. Aeron. Astronaut., Oct. 1968.

14. Anderson, John D., Jr.: An Engineering Survey of Radiating Shock Layers. AIAA J., vol. 7, no. 9, Sept. 1969, pp. 1665-1675.

15. Goulard, R.: Fundamental Equations of Radiation Gas Dynamics. The High Temperature Aspects of Hypersonic Flow, Wilbur C. Nelson, ed., Pergamon Press Inc., c.1964, pp. 529-554.

16. Cohen, Nathaniel B.: Correlation Formulas and Tables of Density and Some Transport Properties of Equilibrium Dissociating Air for Use in Solutions of the Boundary-Layer Equations. NASA TN D-194, 1960.

17. Kivel, B.; and Mayer, H.: Opacity of Highly Ionized Air. J. Quant. Spectrosc. Radiat. Transfer, vol. 5, no. 1, Jan.-Feb. 1965, pp. 13-38.

18. Vaglio-Laurin, Roberto; and Ferri, Antonio: Theoretical Investigation of the Flow Field About Blunt-Nosed Bodies in Supersonic Flight. J. Aero/Space Sci., vol. 25, no. 12, Dec. 1958, pp. 761-770.

19. Gravalos, F. G.; Edelfelt, I. H.; and Emmons, H. W.: The Supersonic Flow About a Blunt Body of Revolution for Gases at Chemical Equilibrium. IXth International Astronautical Congress, F. Hecht, ed., Springer-Verlag, 1959, pp. 312-332.

20. Hayes, Wallace D.; and Probstein, Ronald F.: Hypersonic Flow Theory. Academic Press, Inc., 1959.

21. Koh, J. C. Y.: Radiation From Nonisothermal Gases to the Stagnation Point of a Hypersonic Blunt Body. ARS J., vol. 32, no. 9, Sept. 1962, pp. 1374-1377.

22. Goulard, R. and M.: One-Dimensional Energy Transfer in Radiant Media. Int. J. Heat Mass Transfer, vol. 1, no. 1, June 1960, pp. 81-91.

23. Goulard, R.: Similarity Parameters in Radiation Gas-Dynamics, High Temperature in Aeronautics, C. Ferrari, ed., Pergamon Press, Inc., c.1964, pp. 181-210.

24. Penner, S. S.; Thomas, M.; and Adomeit, G.: Similarity Parameters for Radiative Energy Transfer in Isothermal and Nonisothermal Gas Mixtures. Supersonic Flow Chemical Processes and Radiative Transfer, D. B. Olfe and V. Zakkay, eds., Pergamon Press Inc., c.1964, pp. 279-305.

25. Krook, Max: Structure of Stellar Atmospheres. II. Astrophys. J., vol. 129, no. 3, May 1959, pp. 724-733.

26. Stone, Peter H.: Approximate Integral Equations for the Temperature in Non-Gray Model Atmospheres. Astrophys. J., vol. 137, no. 2, Feb. 15, 1963, pp. 628-640.

27. Carrier, G. F.; and Avrett, E. H.: A Non-Gray Radiative-Transfer Problem. Astrophys. J., vol. 134, no. 2, Sept. 1961, pp. 469-481.

28. Krook, Max: A Perturbation Method for Non-Gray Stellar Atmospheres. Astrophys. J., vol. 137, no. 3, Apr. 1, 1963, pp. 863-873.

29. Ryhming, Inge L.: Effects of Non-Grey Radiation on Wave Propagation in a Simple Dissociating Gas. SSD-TDR-63-355, U.S. Air Force, Jan. 13, 1964. (Available from DDC as AD 430 650.)

30. Kourganoff, V.: Basic Methods in Transfer Problems – Radiative Equilibrium and Neutron Diffusion. Dover Publ., Inc., c.1963.

31. Krook, Max: On the Solution of Equations of Transfer. I. Astrophys. J., vol. 122, no. 3, Nov. 1955, pp. 488-497.

32. Clarke, John F.: Radiation-Resisted Shock Waves. Phys. Fluids, vol. 5, no. 11, Nov. 1962, pp. 1347-1361.

33. Heaslet, Max A.; and Baldwin, Barrett S.: Predictions of the Structure of Radiation-Resisted Shock Waves. Phys. Fluids, vol. 6, no. 6, June 1963, pp. 781-791.

34. Traugott, S. C.: A Differential Approximation for Radiative Transfer With Application to Normal Shock Structure. Proceedings of the 1963 Heat Transfer and Fluid Mechanics Institute, Anatol Roshko, Bradford Sturtevant, and D. R. Bartz, eds., Stanford Univ. Press, 1963, pp. 1-13.

35. Thomas, P. D.: Transparency Assumption in Hypersonic Radiative Gasdynamics. AIAA J., vol. 3, no. 8, Aug. 1965, pp. 1401-1407.

36. Viskanta, R.: Interaction of Heat Transfer by Conduction, Convection, and Radiation in a Radiating Fluid. Trans. ASME, Ser. C: J. Heat Transfer, vol. 85, no. 4, Nov. 1963, pp. 318-328.

37. Probstein, Ronald F.: Radiation Slip. AIAA J., vol. 1, no. 5, May 1963, pp. 1202-1204.

38. Van Dyke, Milton: Perturbation Methods in Fluid Mechanics. Academic Press, 1964.

39. Hayes, Wallace D.: Some Aspects of Hypersonic Flow. The Ramo-Wooldridge Corp., Jan. 4, 1955.

40. Li, Ting-Yi; and Geiger, Richard E.: Stagnation Point of a Blunt Body in Hypersonic Flow. J. Aeronaut. Sci., vol. 24, no. 1, Jan. 1957, pp. 25-32.

41. Kaatari, George E.: Predicted Shock Envelopes About Two Types of Vehicles at Large Angles of Attack. NASA TN D-860, 1961.

42. Anon.: The Thermodynamic Properties of High Temperature Air. Rep. No. RE-IR-14, Chance Vought Res. Center, June 28, 1961.

43. Kivel, B.; and Bailey, K.: Tables of Radiation From High Temperature Air. Res. Rep. 21 (Contracts AF 04(645)-18 and AF 49(638)-61), AVCO Res. Lab., Dec. 1957.

44. Gilmore, F. R.: Approximate Radiation Properties of Air Between 2000 and 8000° K. RM-3997-ARPA, The Rand Corp., Mar. 1964.

45. Armstrong, B. H.; Sokoloff, J.; Nicholls, R. W.; Holland, D. H.; and Meyerott, R. E.: Radiative Properties of High Temperature Air. J. Quant. Spectry. Radiative Transfer, vol. 1, no. 2, Nov. 1961, pp. 143-162.

46. Sewell, K. G.: The Radiative Properties of Air in Thermodynamic Equilibrium. Rep. No. 0-71000/2R-26, LTV Res. Center, July 1962.

47. Olstad, Walter B.: Blunt-Body Stagnation-Region Flow With Nongray Radiation Heat Transfer – A Singular Perturbation Solution. NASA TR R-295, 1968.

48. Tsien, H. S.: The Poincaré-Lighthill-Kuo Method. Vol. IV of Advances in Applied Mechanics, H. L. Dryden and Th. von Kármán, eds., Academic Press, Inc., 1956, pp. 281-349.

49. Pritulo, M. F.: On the Determination of the Uniformly Accurate Solutions to Differential Equations by the Method of the Perturbation of Coordinates. J. Appl. Math. Mech., vol. 26, no. 3, 1962, pp. 661-667.

50. Nardone, M. C.; Breene, R. G.; Zeldin, S. S.; and Riethof, T. R.: Radiance of Species in High Temperature Air. Tech. Inform. Ser. R63SD3 (Contract AF 04(694)-222), Missile and Space Div., Gen. Elec. Co., June 1963. (Available from DDC as AD No. 408564.)

51. Pearson, Walter E.: On the Direct Solution of the Governing Equation for Radiation-Resisted Shock Waves. NASA TN D-2128, 1964.

52. Deissler, R. G.: Diffusion Approximation for Thermal Radiation in Gases With Jump Boundary Condition. Trans. ASME, ser. C: J. Heat Transfer, vol. 86, no. 2, May 1964, pp. 240-246.

53. Adrianov, V. N.; and Polyak, G. L.: Differential Methods for Studying Radiant Heat Transfer. Int. J. Heat Mass Transfer, vol. 6, no. 5, May 1963, pp. 355-362.

54. Carrier, G. F.: Boundary Layer Problems in Applied Mechanics. Vol III of Advances in Applied Mechanics, Richard von Mises and Theodore von Kármán, eds., Academic Press, Inc., 1953, pp. 1-19.

55. Burggraf, Odus R.: Asymptotic Solution for the Viscous Radiating Shock Layer. AIAA J., vol. 4, no. 10, Oct. 1966, pp. 1725-1734.

Figure 1.- Density correlation. $\rho/\rho_0 = (p/p_0)^{0.960} f_1(h/RT_0)$.

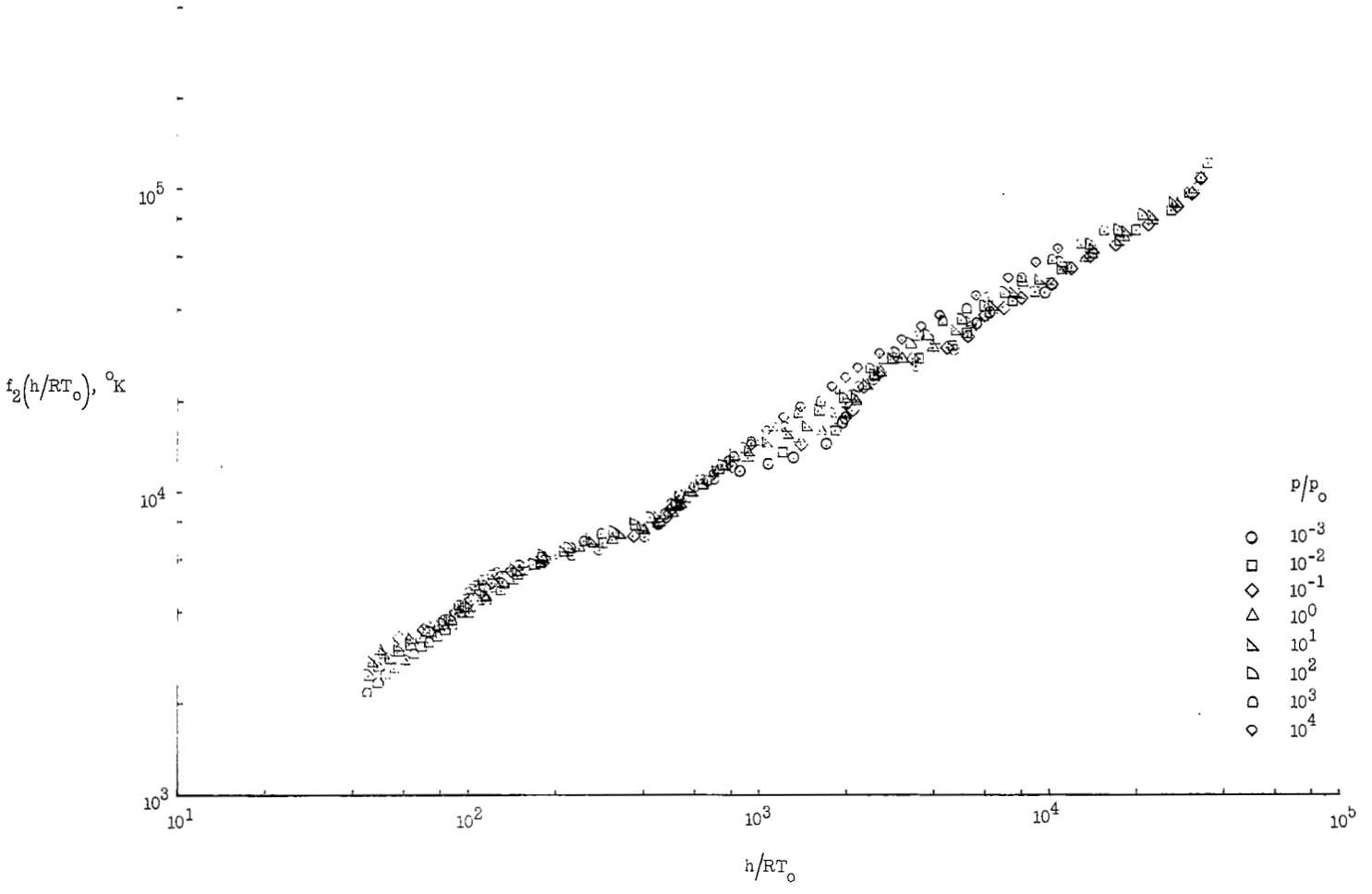

Figure 2.- Temperature correlation. $T = (p/p_0)^{0.09} f_2(h/RT_0)$, °K.

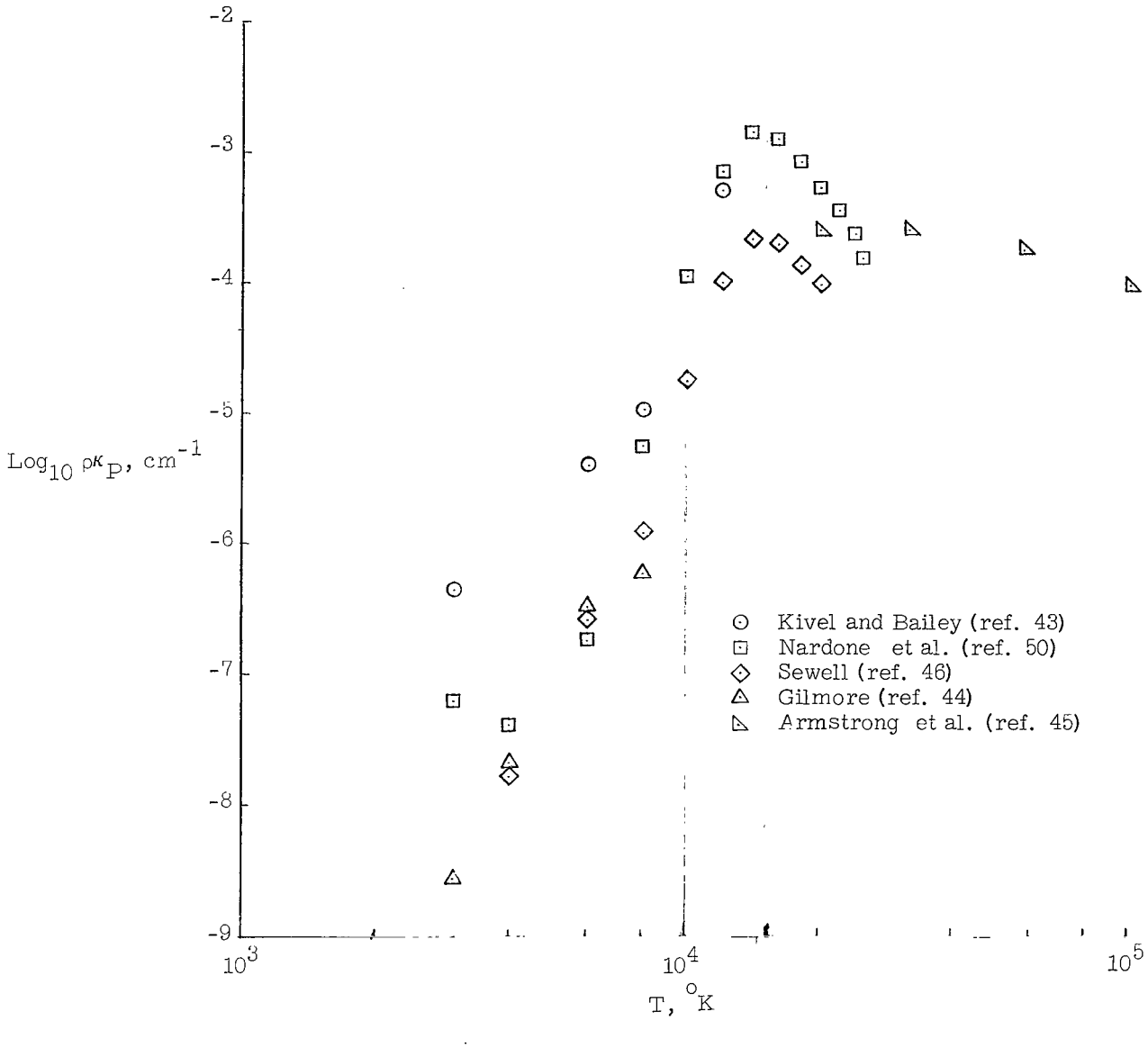

(a) $\rho/\rho_0 = 10^{-3}$.

Figure 3.- Planck mean mass absorption coefficient correlation.

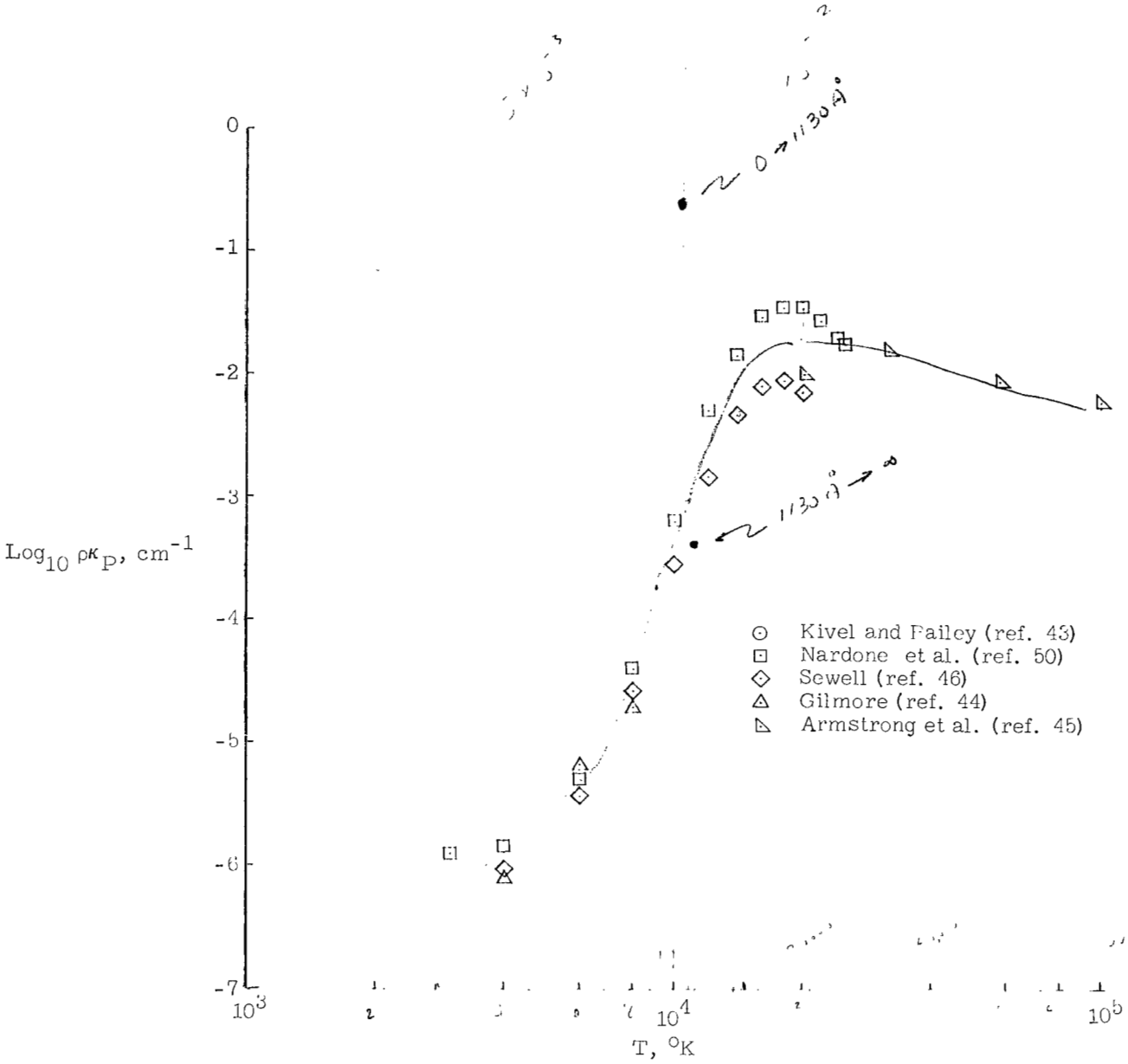

(b) $\rho/\rho_0 = 10^{-2}$.

Figure 3.- Continued.

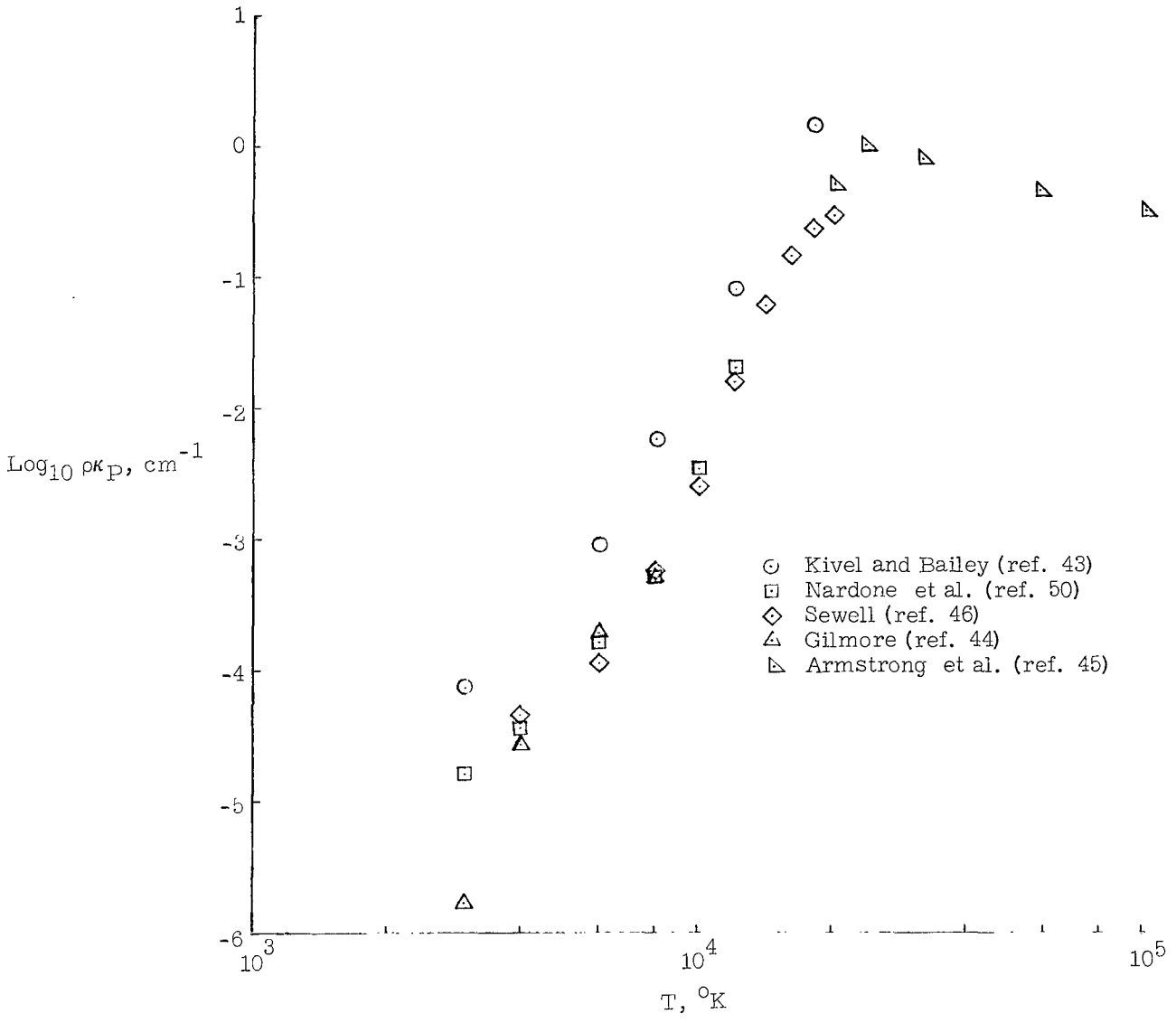

(c) $\rho/\rho_0 = 10^{-1}$.

Figure 3.- Continued.

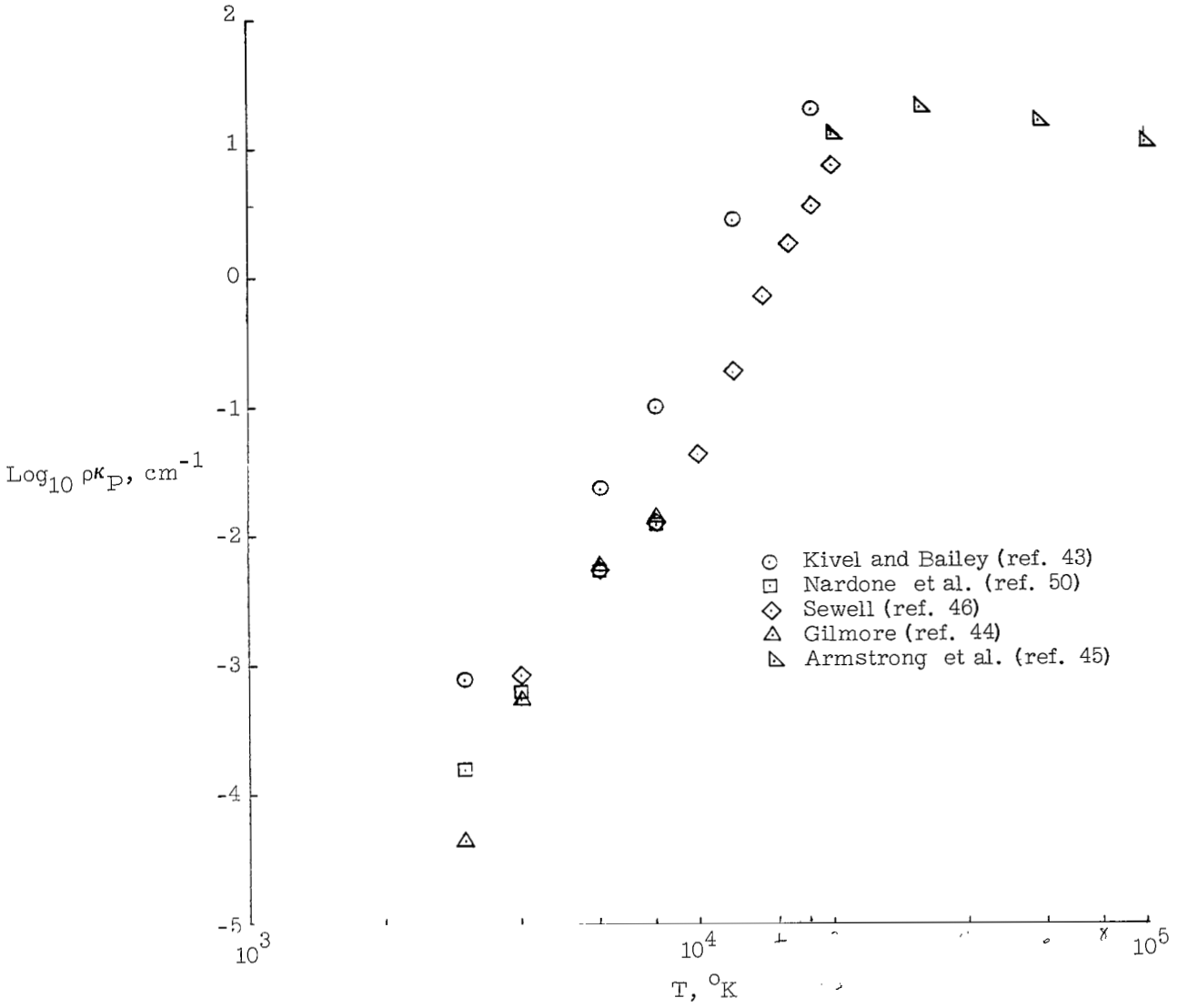

(d) $\rho/\rho_0 = 10^0$.

Figure 3.- Continued.

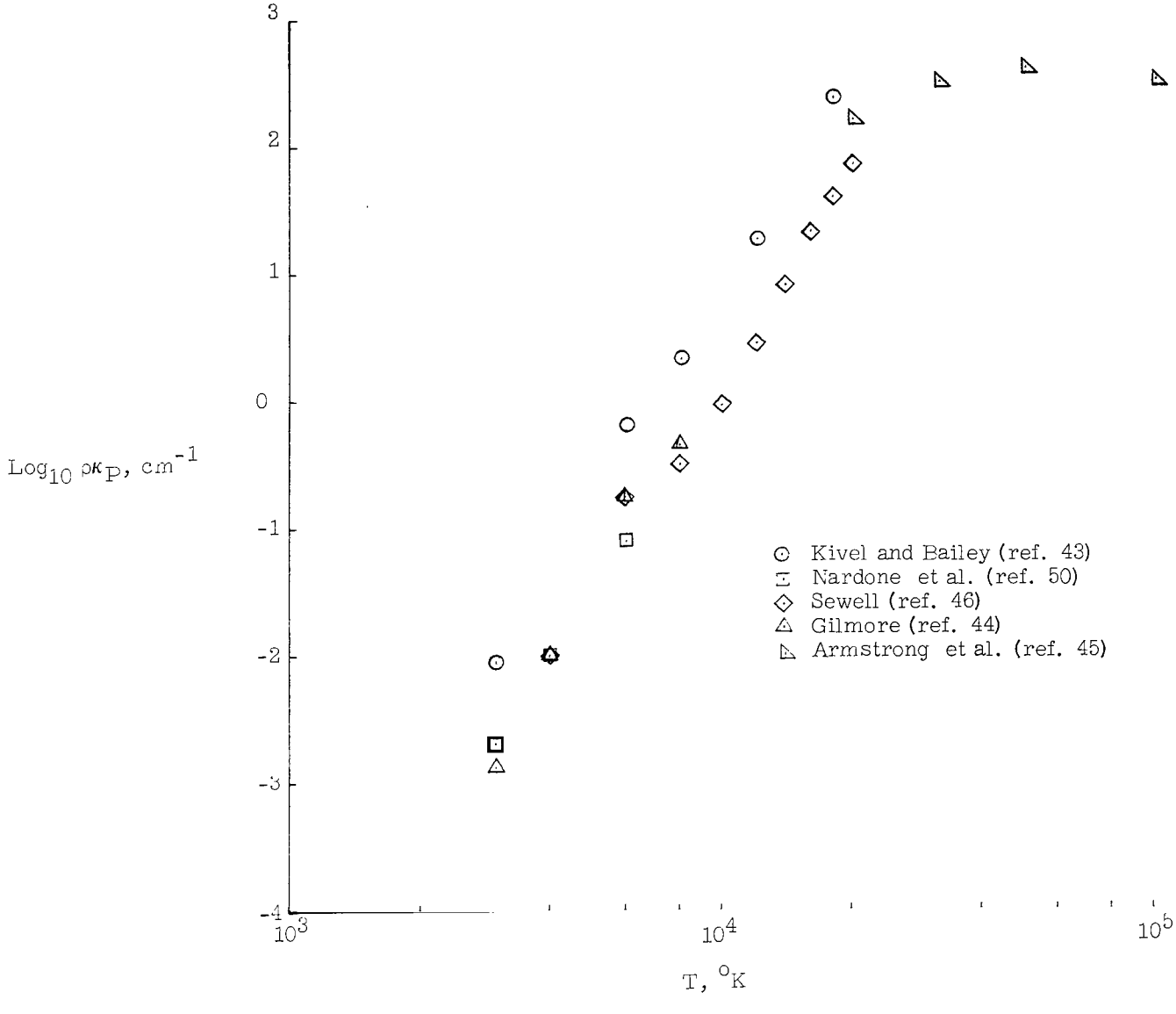

(e) $\rho/\rho_0 = 10^1$.

Figure 3.- Concluded.

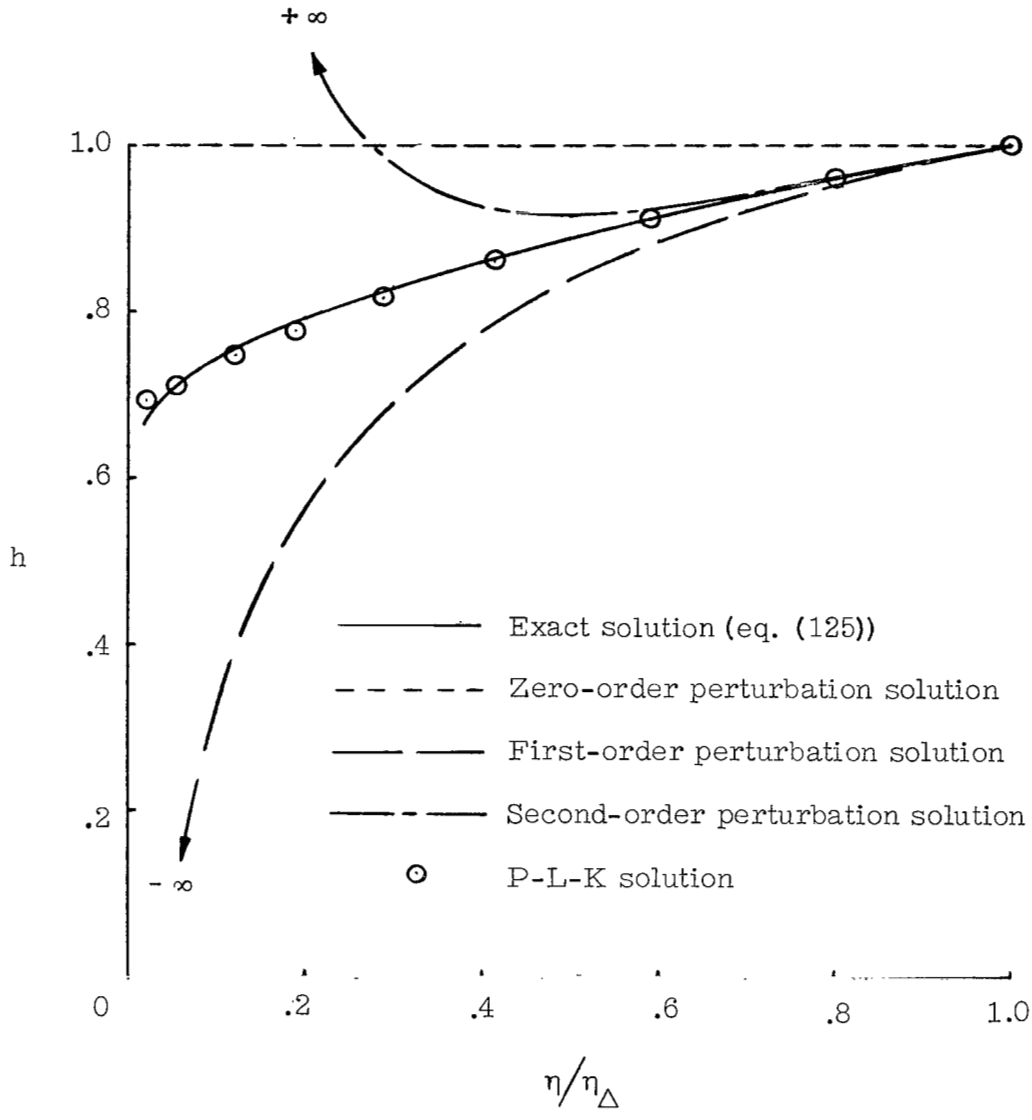

Figure 4.- Comparison of the Poincaré-Lighthill-Kuo (P-L-K), conventional perturbation, and exact solutions. $\varepsilon = 0.1$, $k_\rho = 0$, ρ = Constant, $\kappa_\rho B = h^6$.

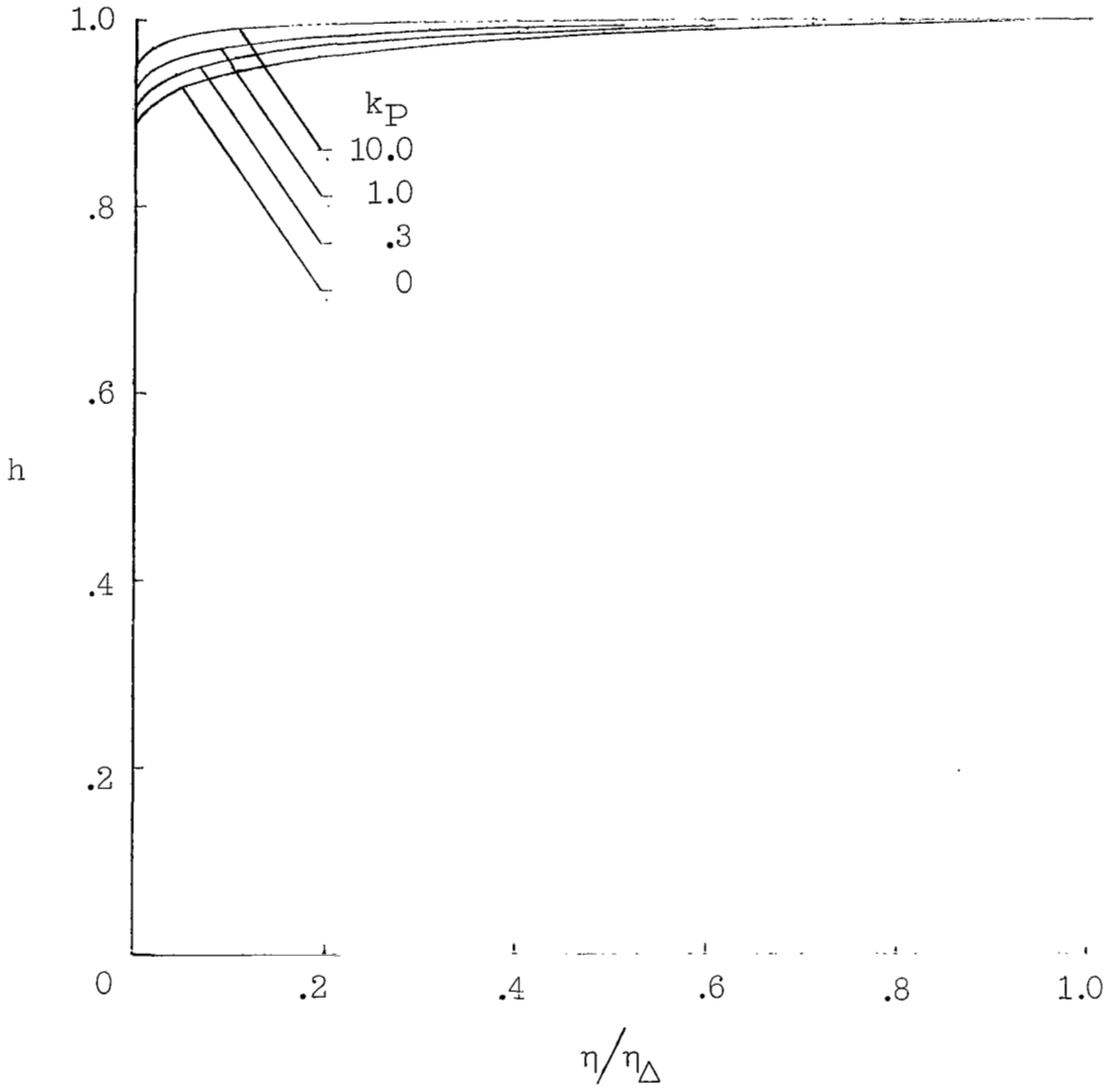

(a) $\varepsilon = 0.01$.

Figure 5.- Effect of the parameters ε and k_P on the shock-layer enthalpy distribution. $\dot{\kappa}_P = 4.0$.

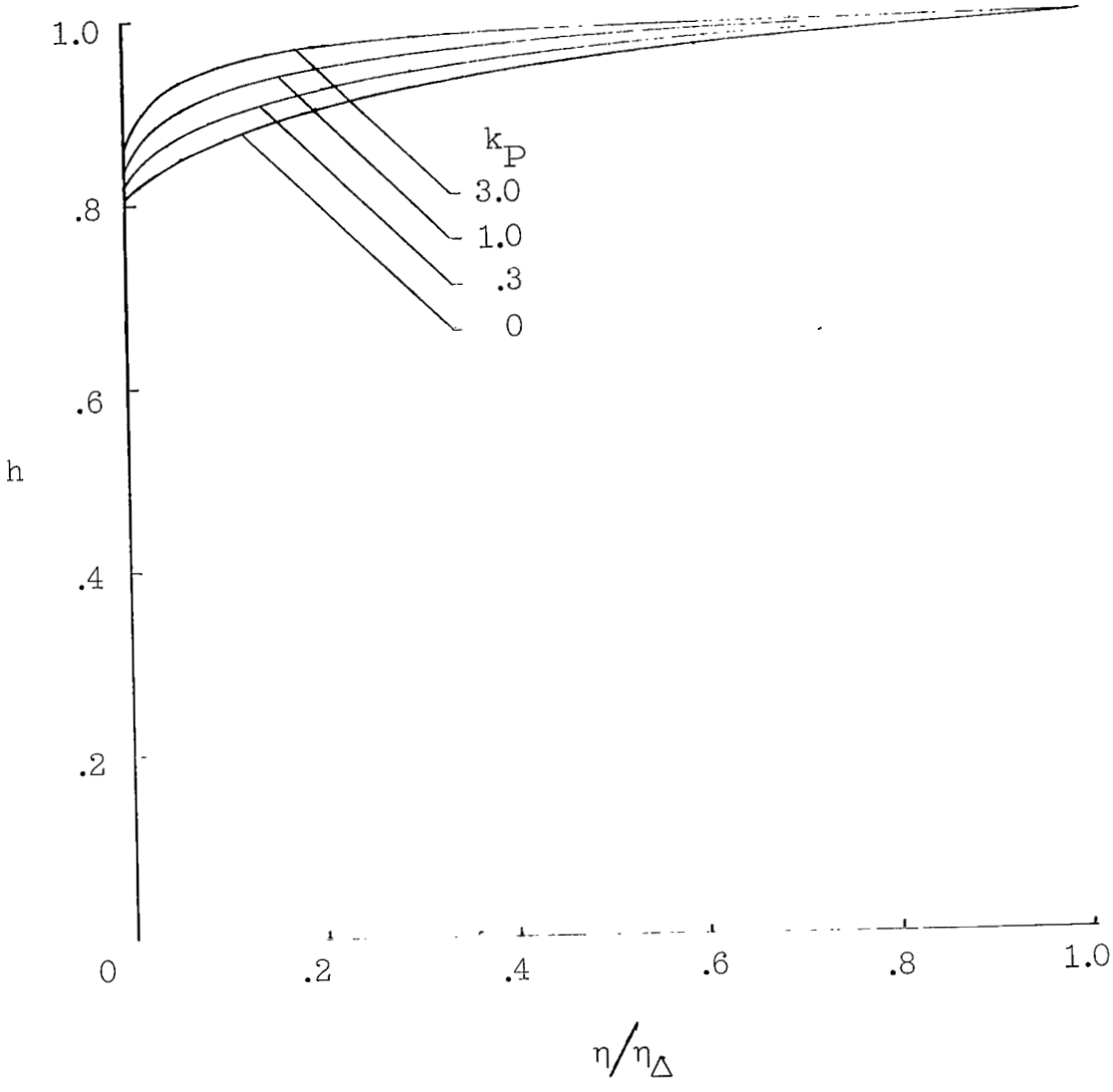

(b) $\varepsilon = 0.03$.

Figure 5.- Continued.

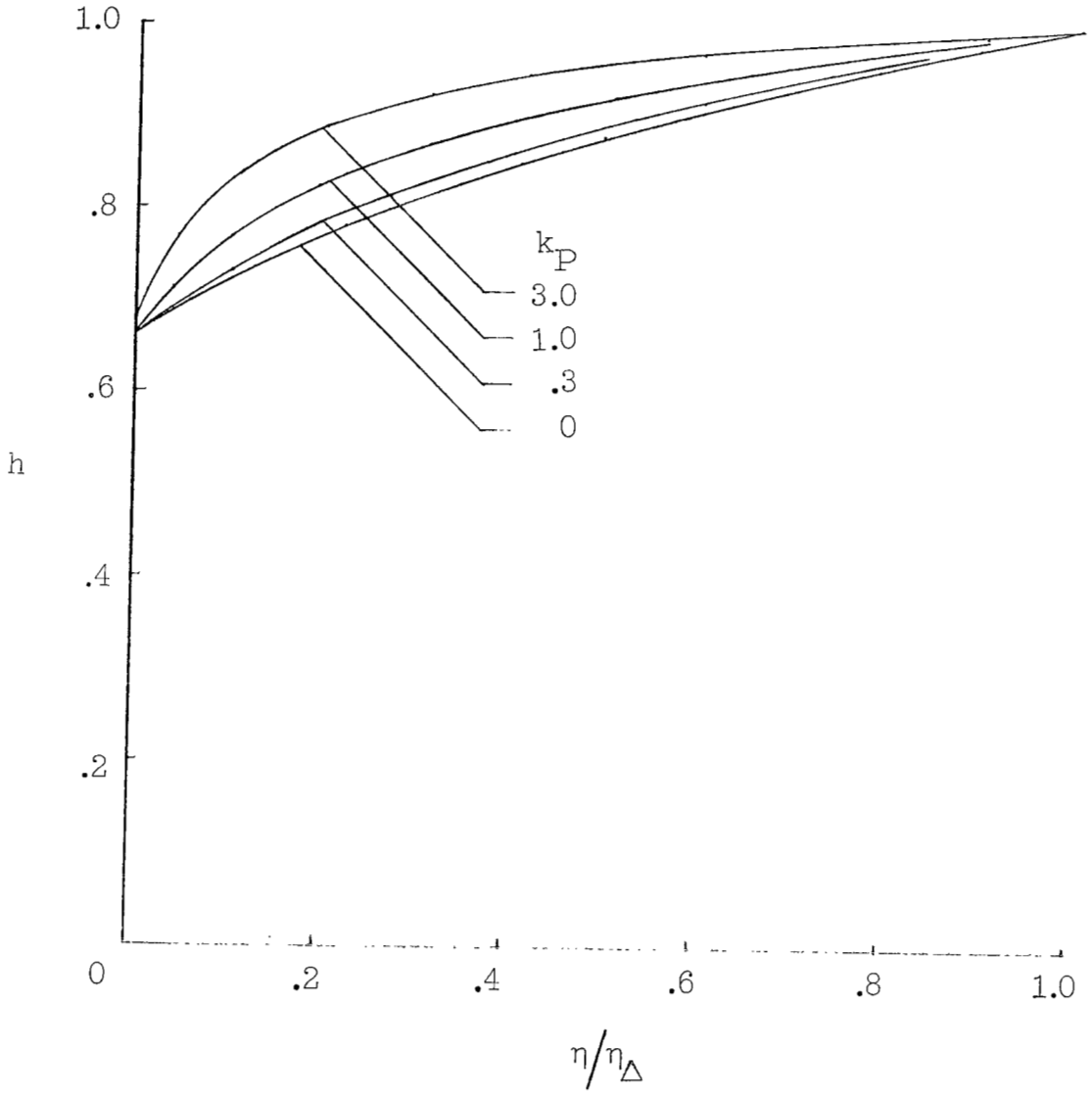

(c) $\varepsilon = 0.10$.

Figure 5.- Concluded.

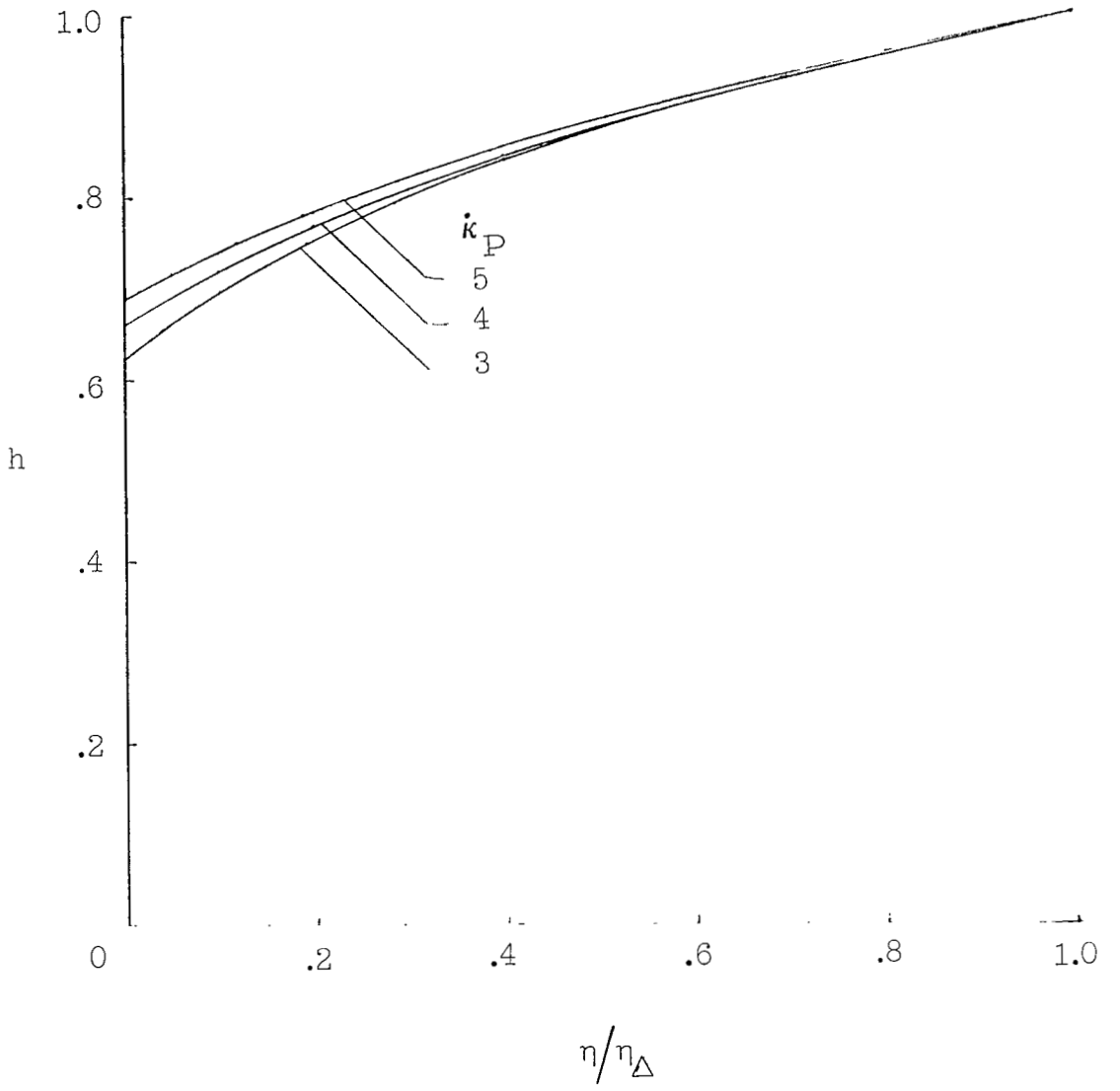

(a) $k_P = 0$.

Figure 6.- Effect of the enthalpy variation of the absorption coefficient on the shock-layer enthalpy distribution. $\varepsilon = 0.1$; $r_w = 0$.

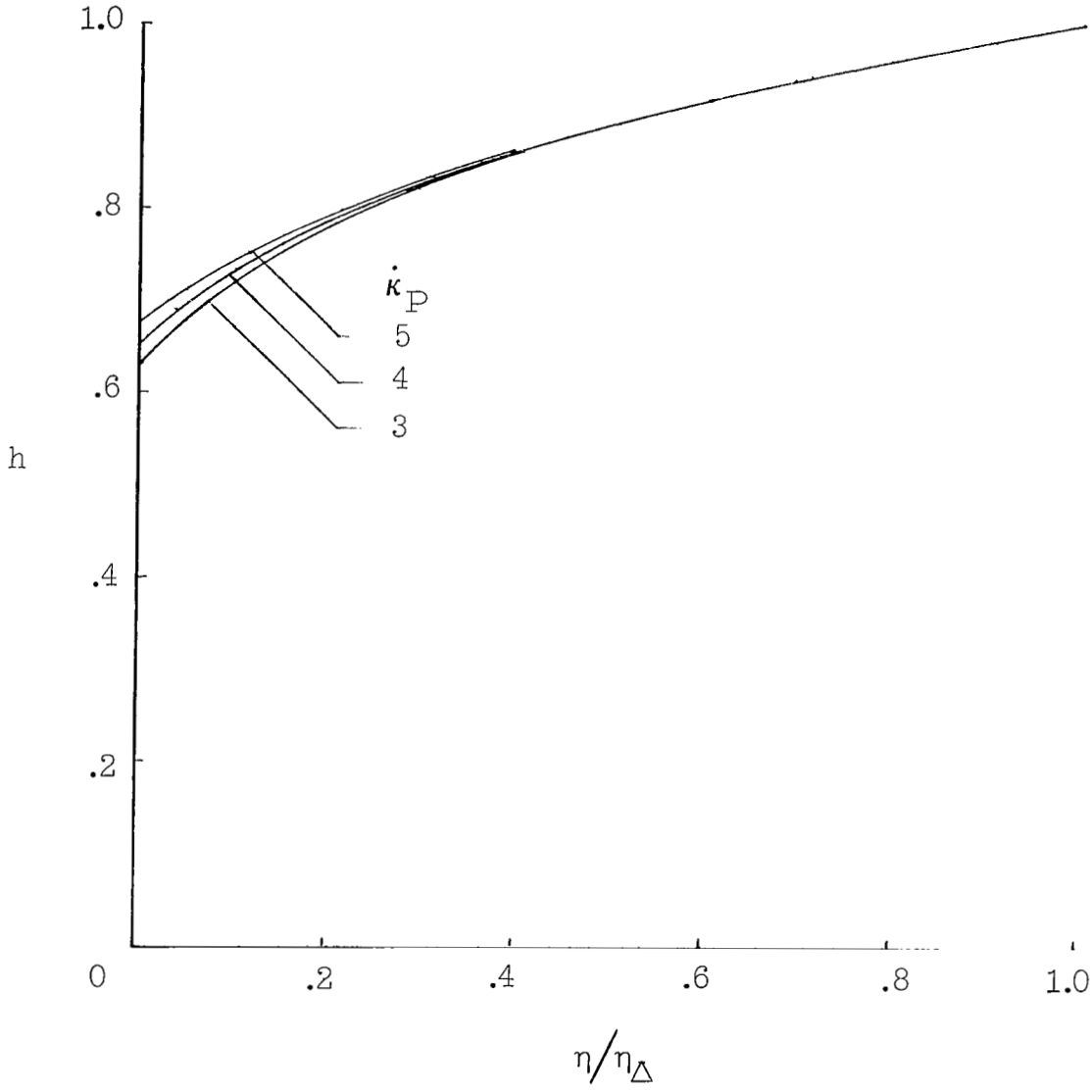

(b) $k_P = 0.3$.

Figure 6.- Continued.

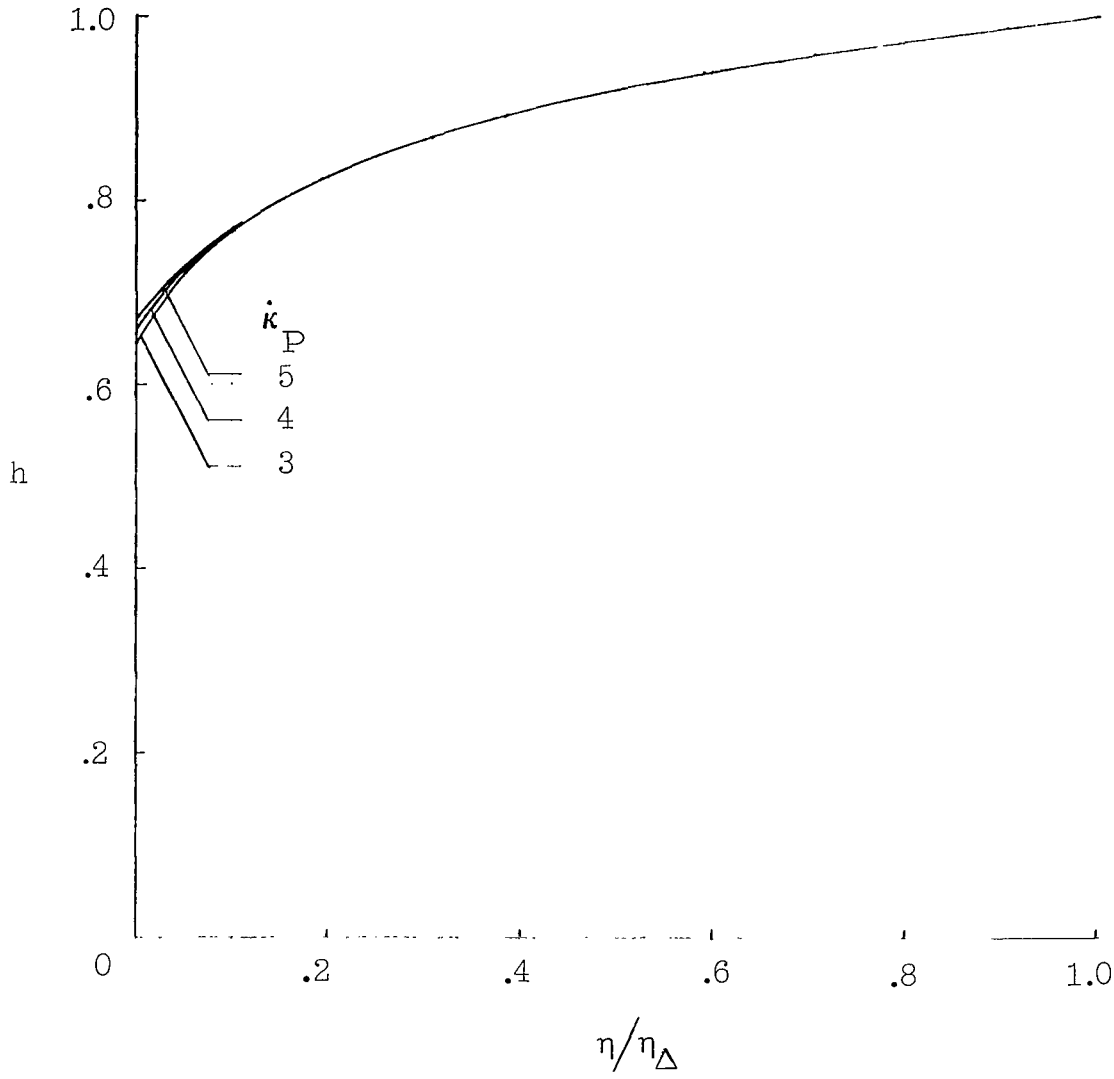

(c) $k_P = 1.0$.

Figure 6.- Concluded.

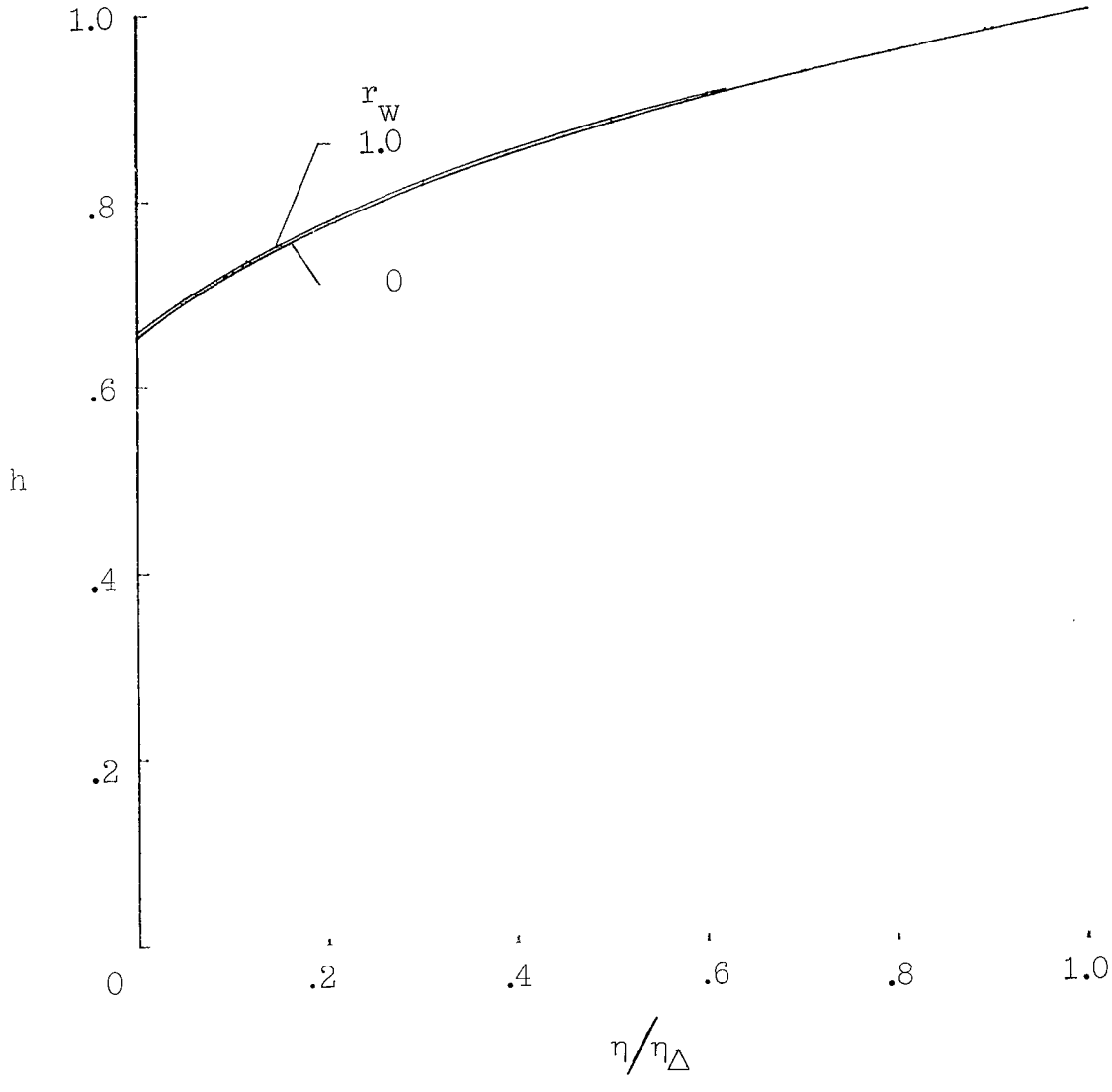

(a) $k_P = 0.1$.

Figure 7.- Effect of surface reflectivity on the shock-layer enthalpy distribution. $\varepsilon = 0.1$; $\dot{\kappa}_P = 4.0$.

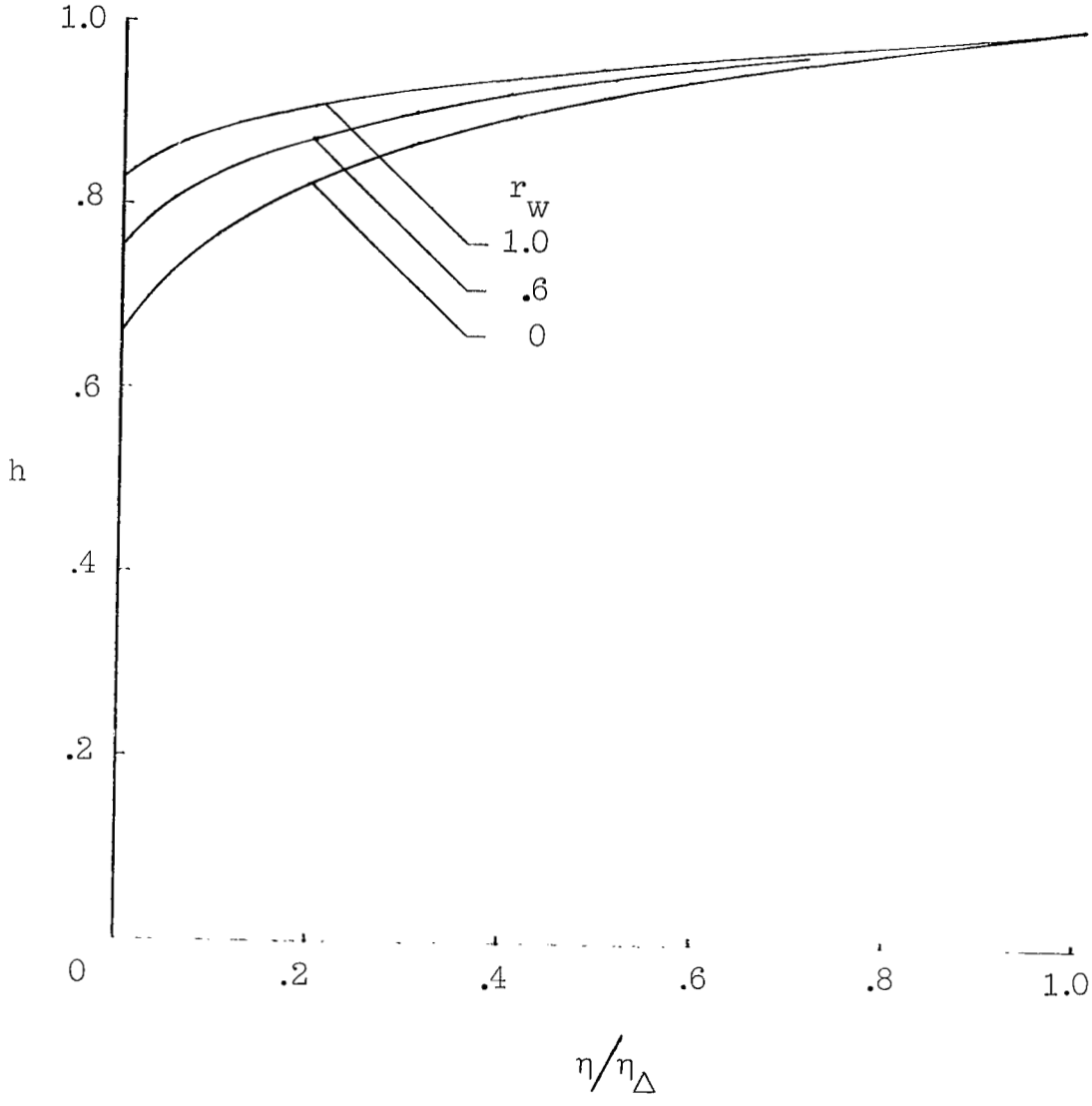

(b) $k_P = 1.0$.

Figure 7.- Continued.

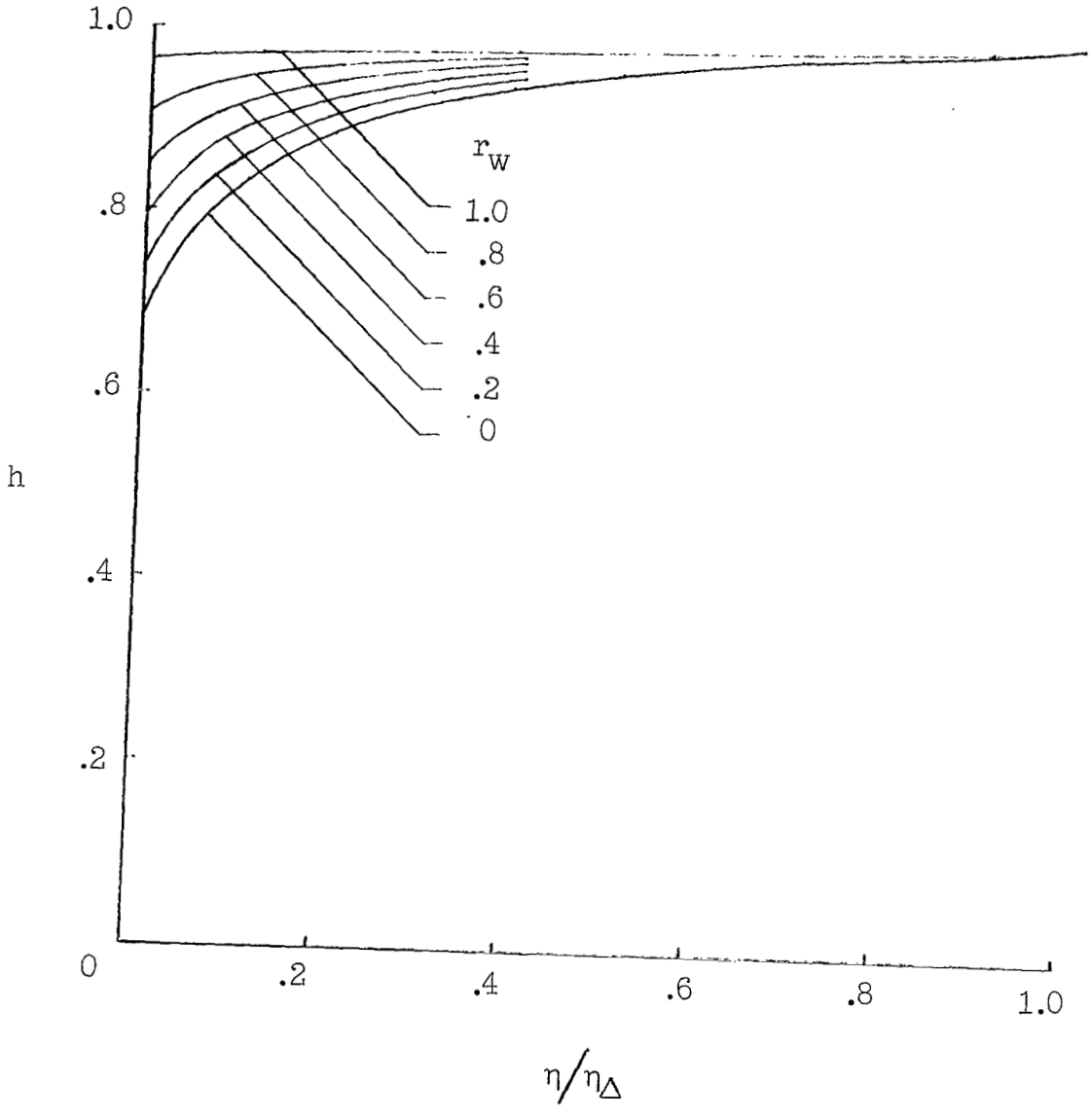

(c) $k_P = 3.0$.

Figure 7.- Concluded.

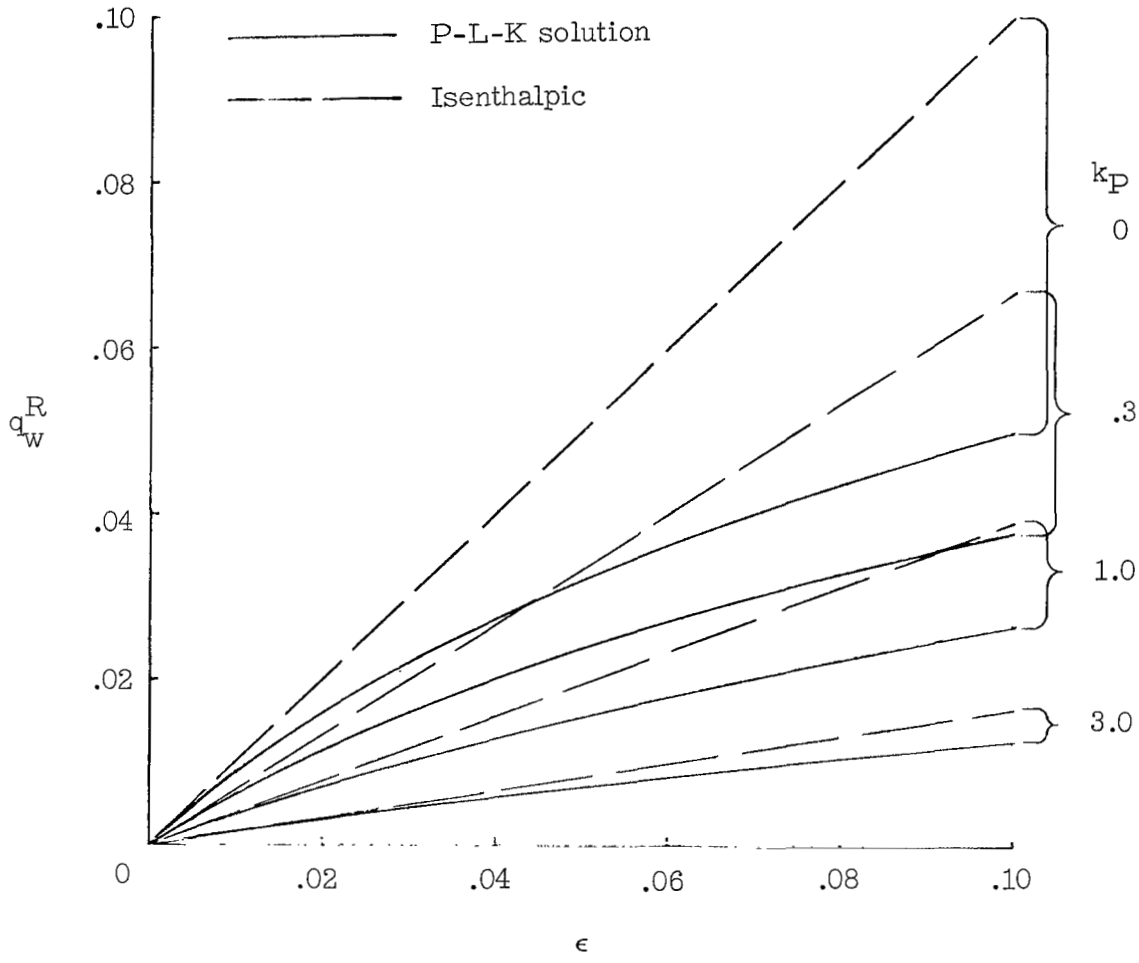

Figure 8.- Effect of ε and k_P on the rate of radiant heat transfer to the stagnation point. $\dot{\kappa}_P = 4.0$; $r_w = 0$.

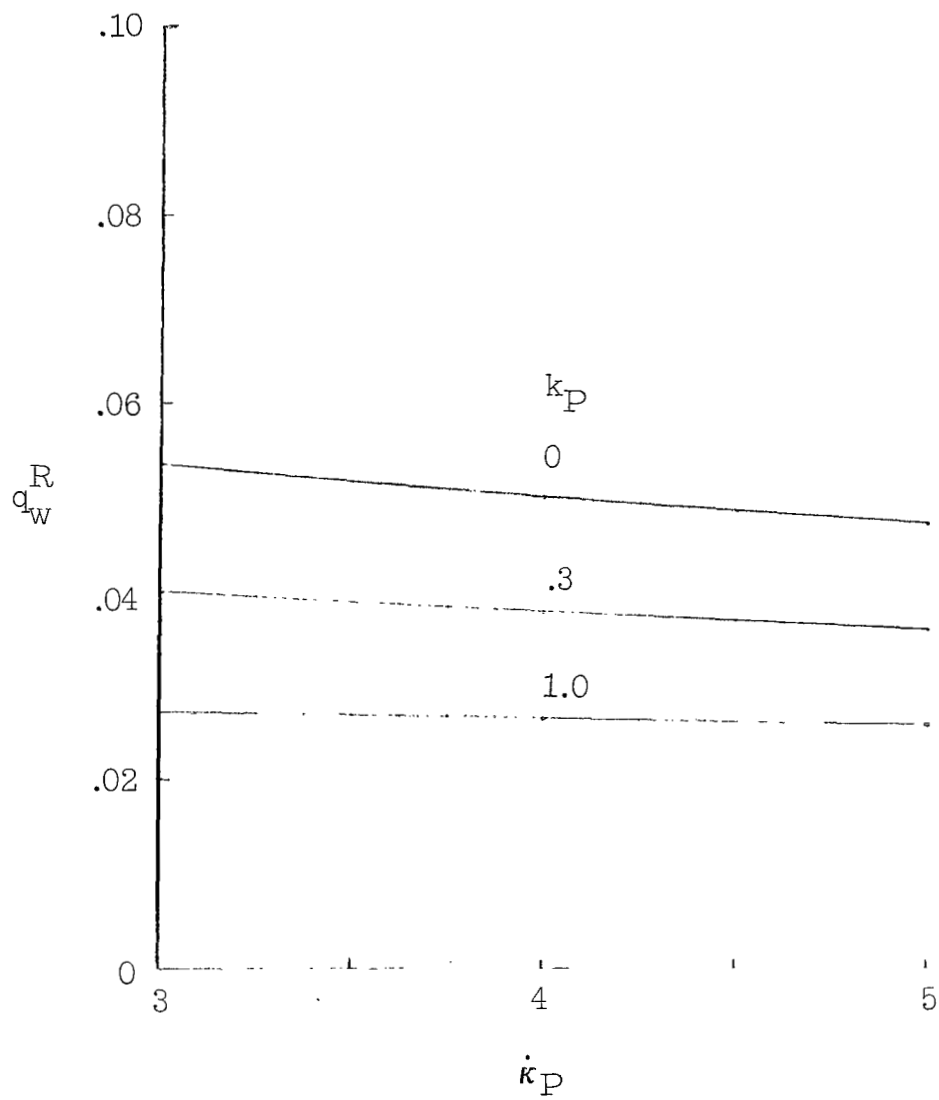

Figure 9.- Effect of the enthalpy variation of the absorption coefficient on the rate of radiant heat transfer to the stagnation point. $\epsilon = 0.1$; $r_w = 0$.

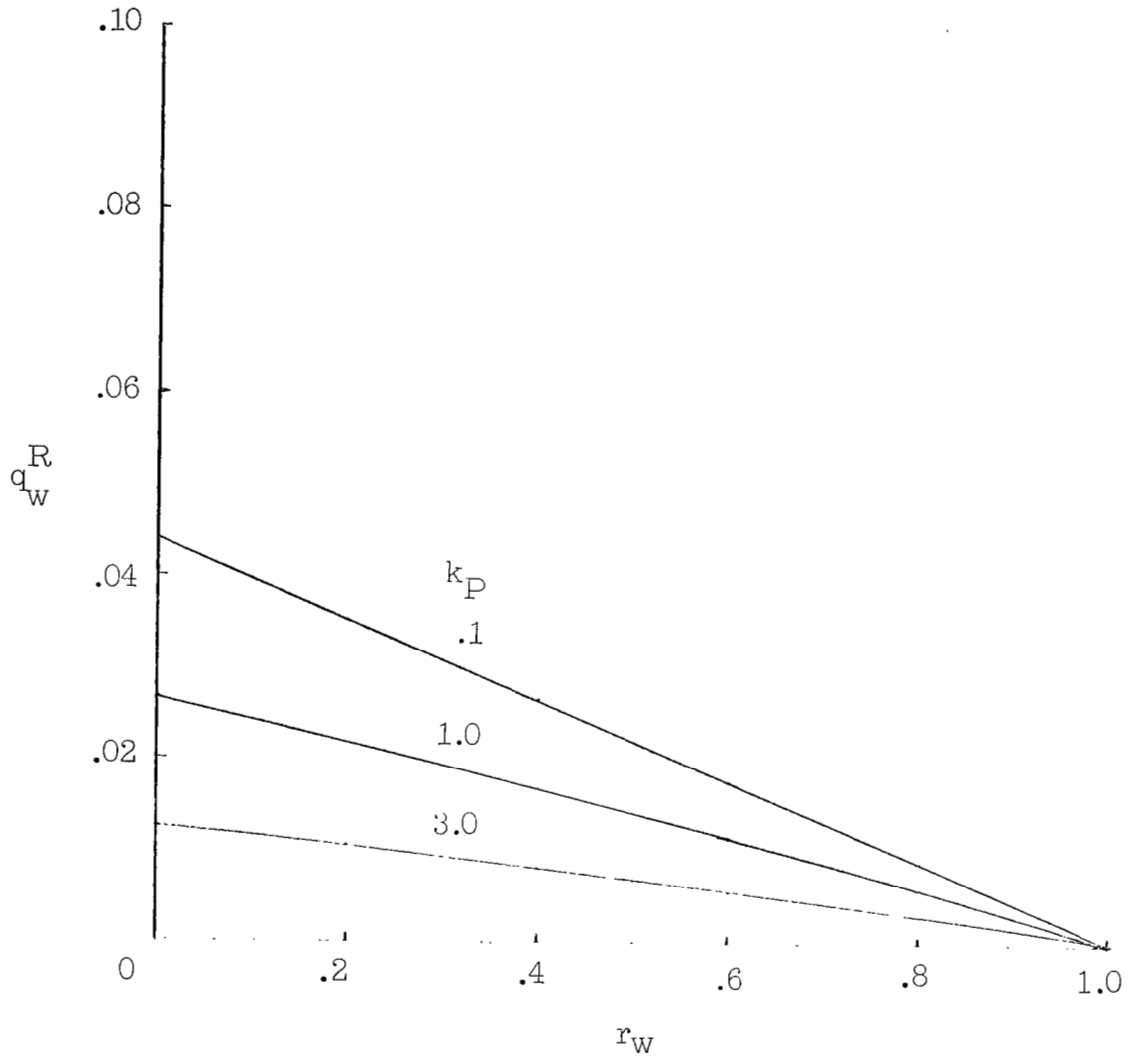

Figure 10.- Effect of surface reflectivity on the rate of radiant heat transfer to the stagnation point. $\epsilon = 0.1$; $\dot{\kappa}_P = 4.0$.

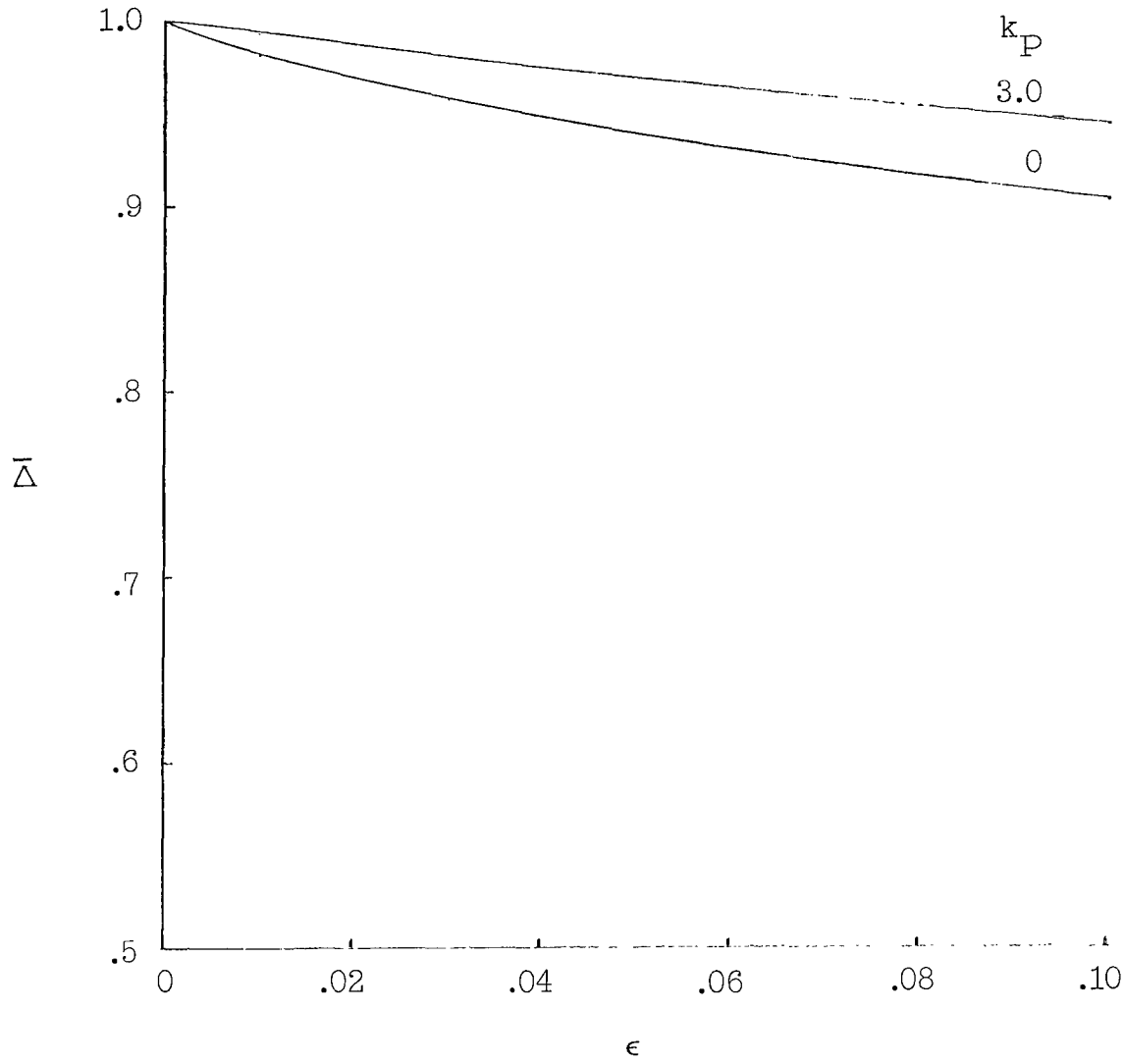

Figure 11.- Effect of ϵ and k_P on the shock standoff distance. $\dot{\kappa}_P = 4.0$; $r_W = 0$.

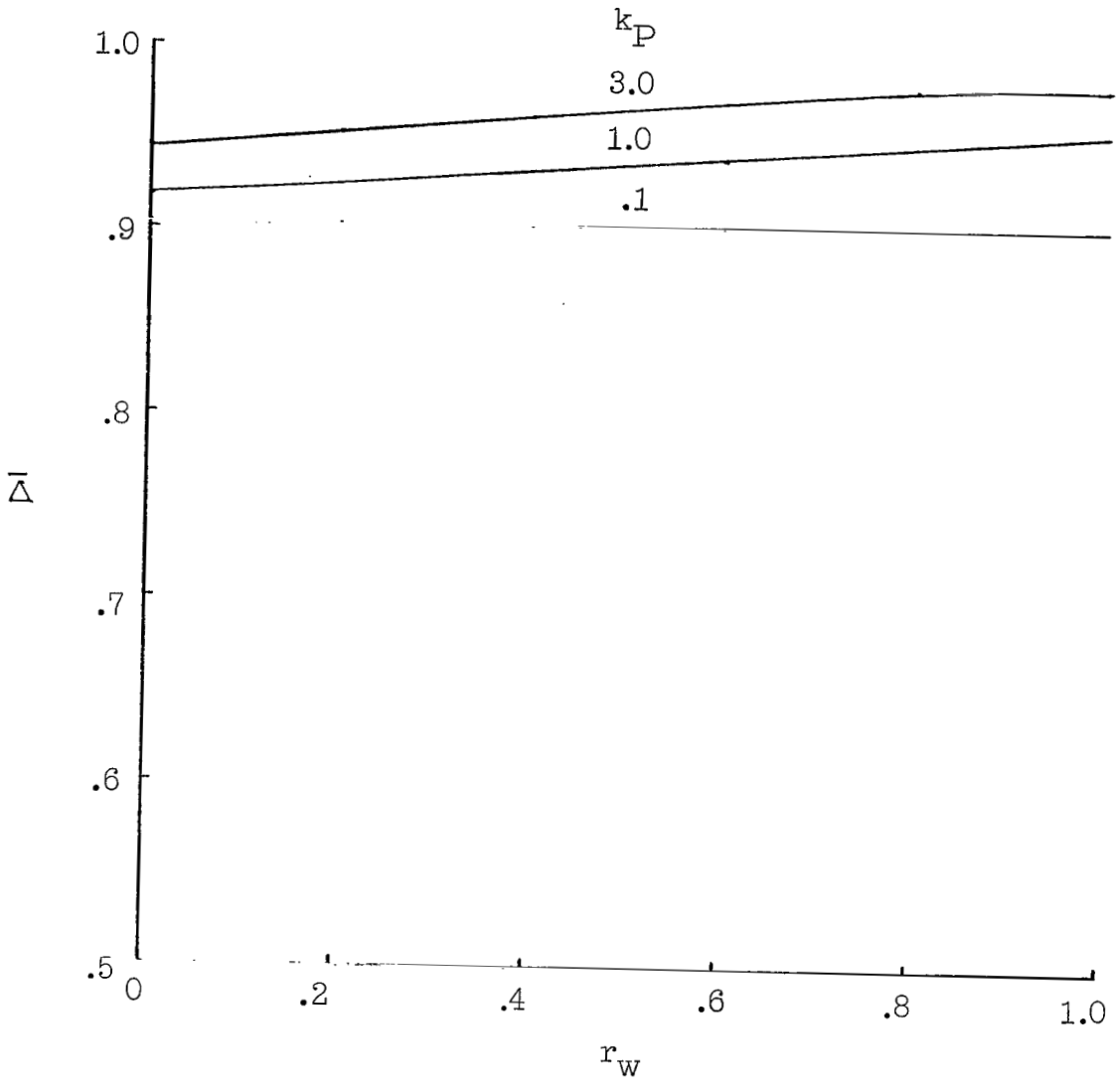

Figure 12.- Effect of surface reflectivity on the shock standoff distance. $\varepsilon = 0.1$; $\kappa_P = 4.0$.

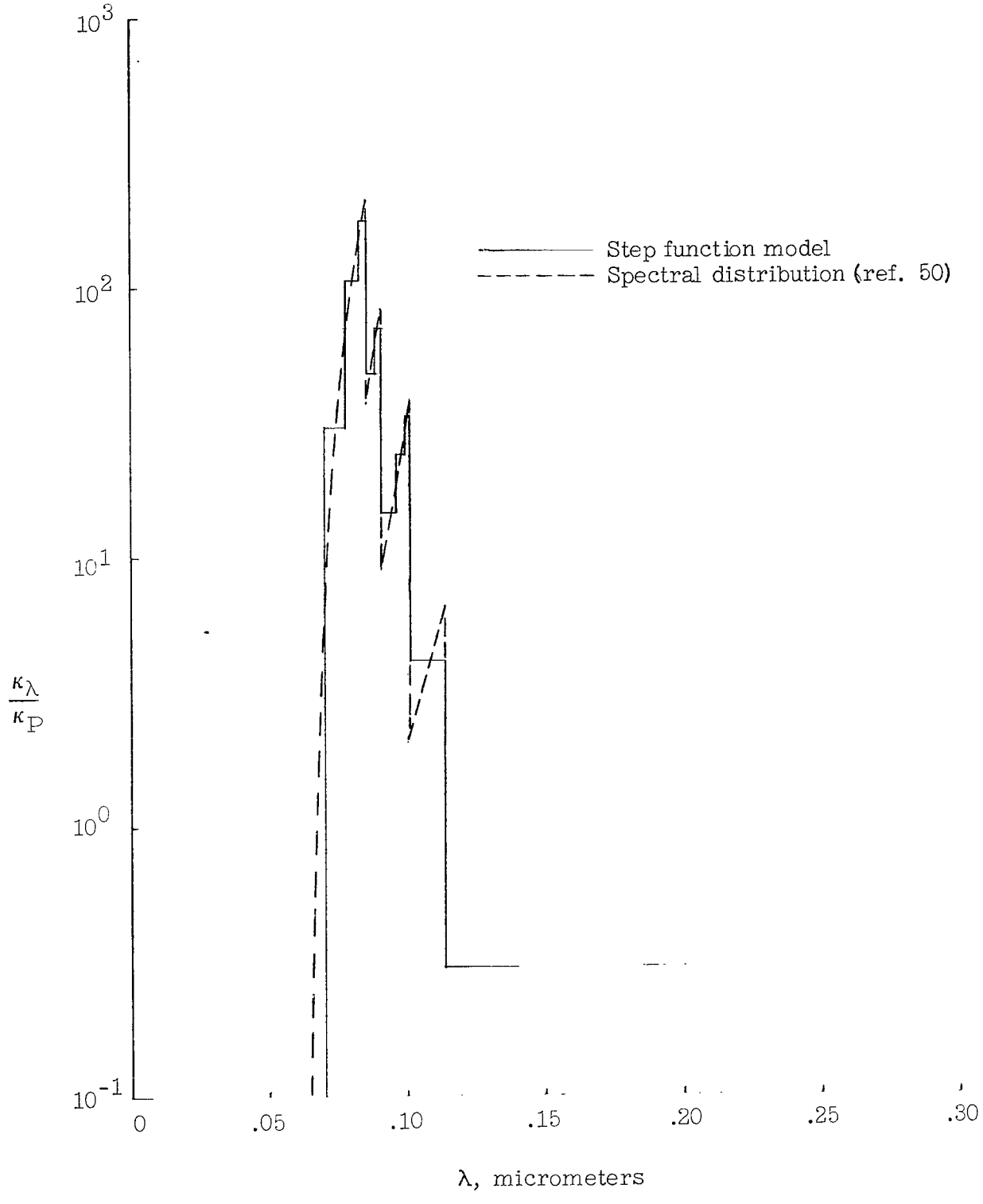

Figure 13.- Step function model of the mass absorption coefficient of high temperature air.

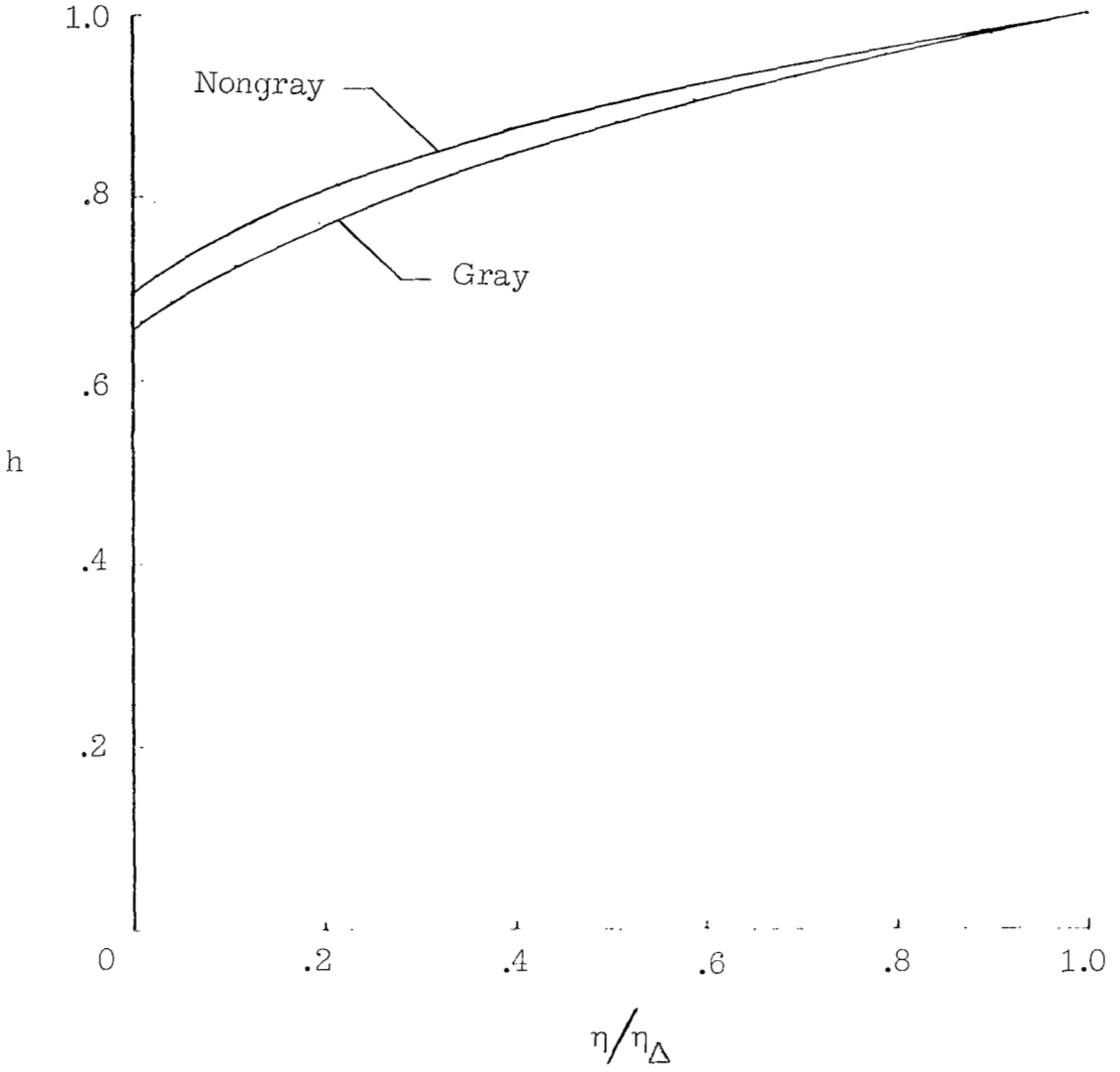

(a) $k_P = 0.01$.

Figure 14.- Shock-layer enthalpy distribution for a nongray absorption coefficient. $\epsilon = 0.1$; $\dot{\kappa}_P = 4.0$; $r_W = 0$.

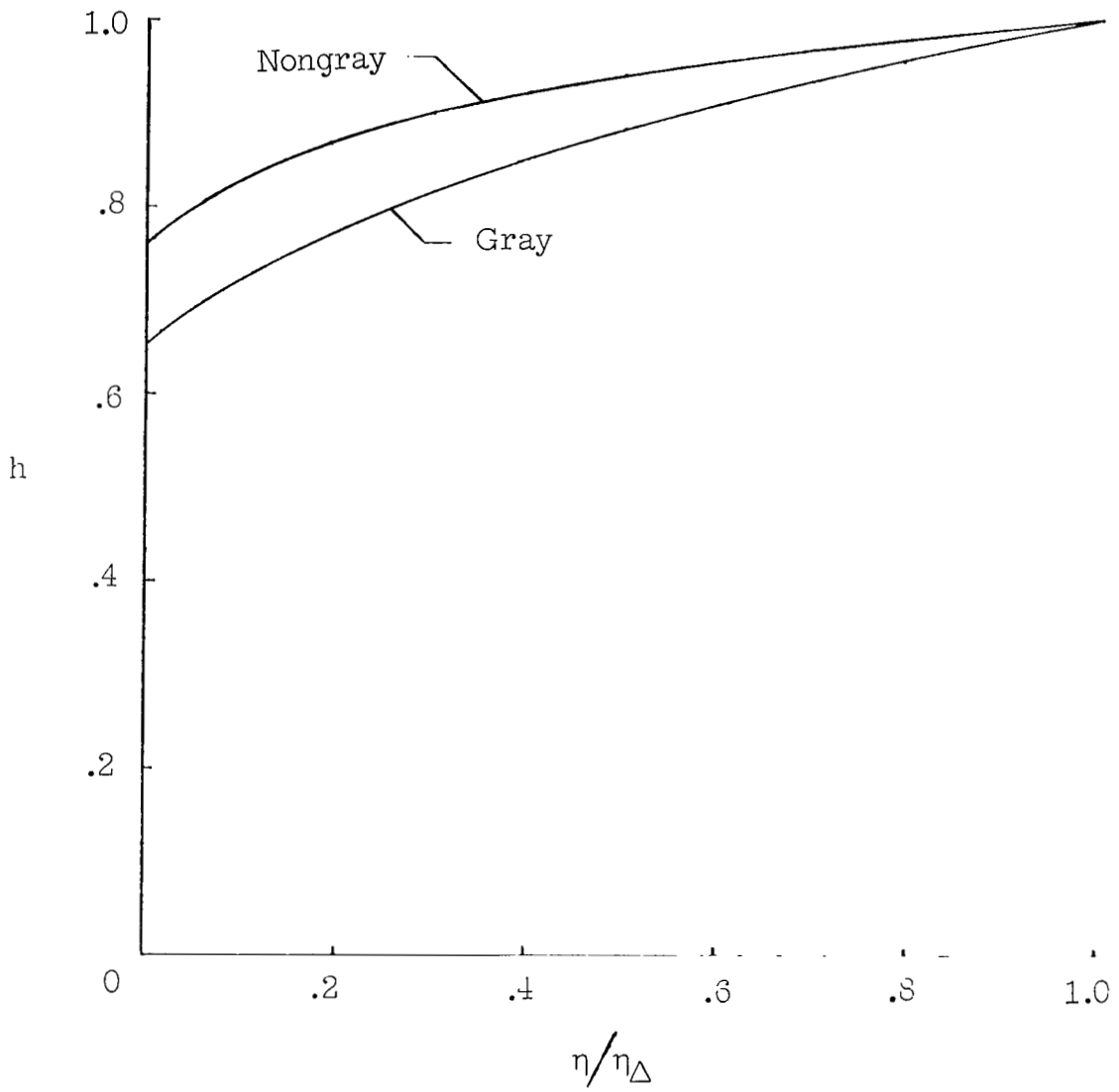

(b) $k_P = 0.1$.

Figure 14.- Continued.

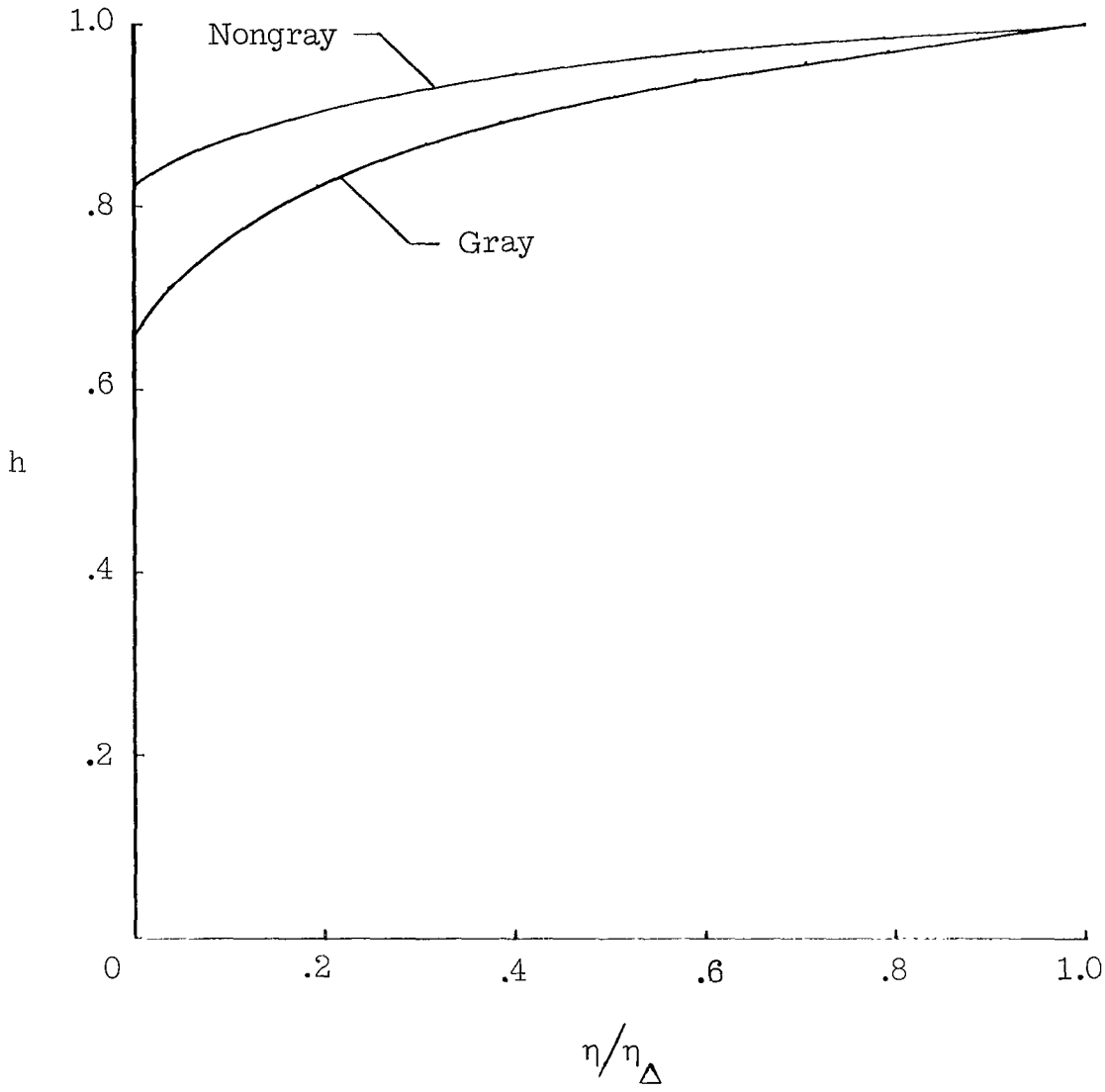

(c) $k_P = 1.0$.

Figure 14.- Concluded.

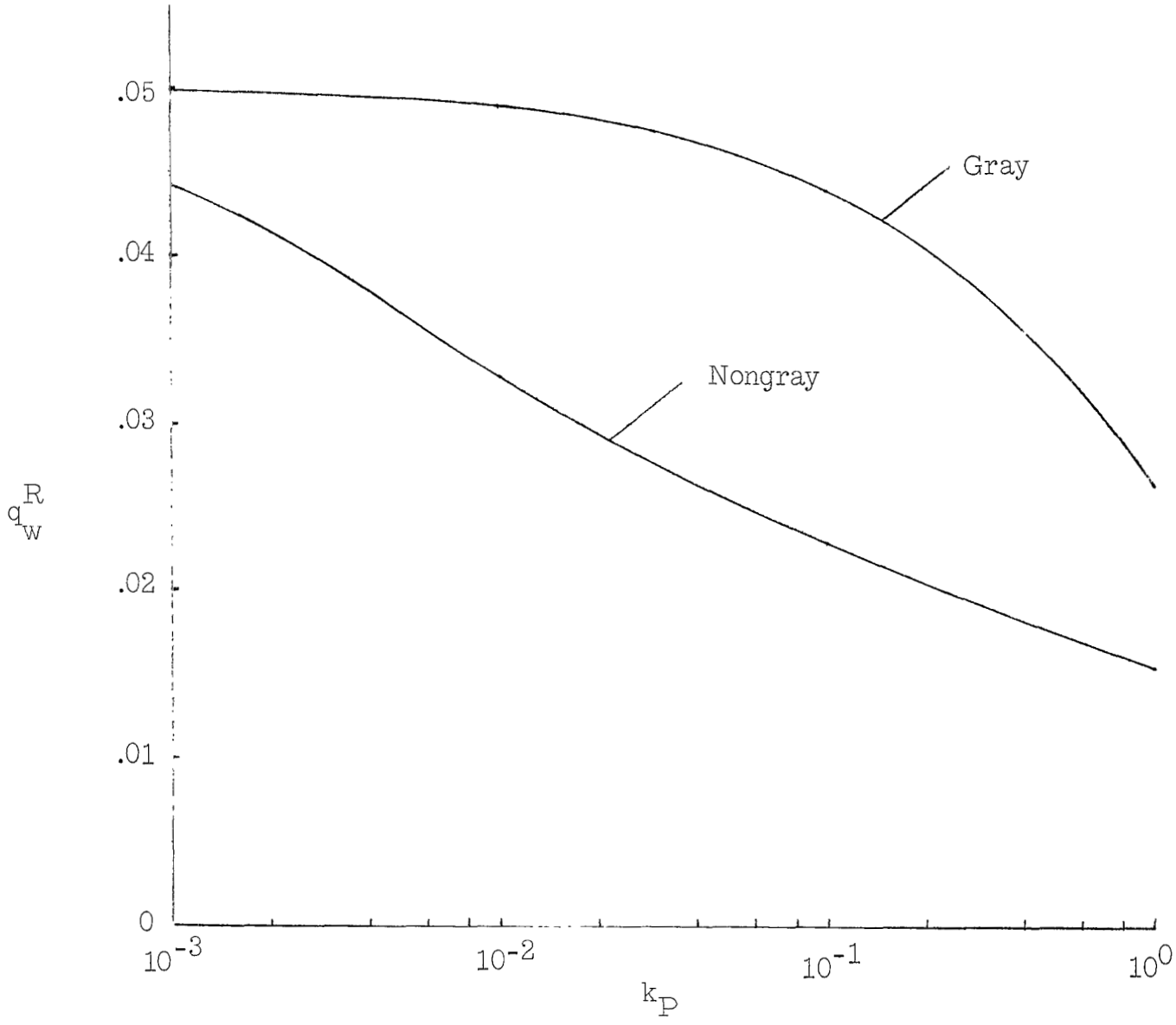

Figure 15.- Rate of radiant heat transfer to the stagnation point in a nongray gas. $\epsilon = 0.1$; $\dot{\kappa}_P = 4.0$; $r_w = 0$.

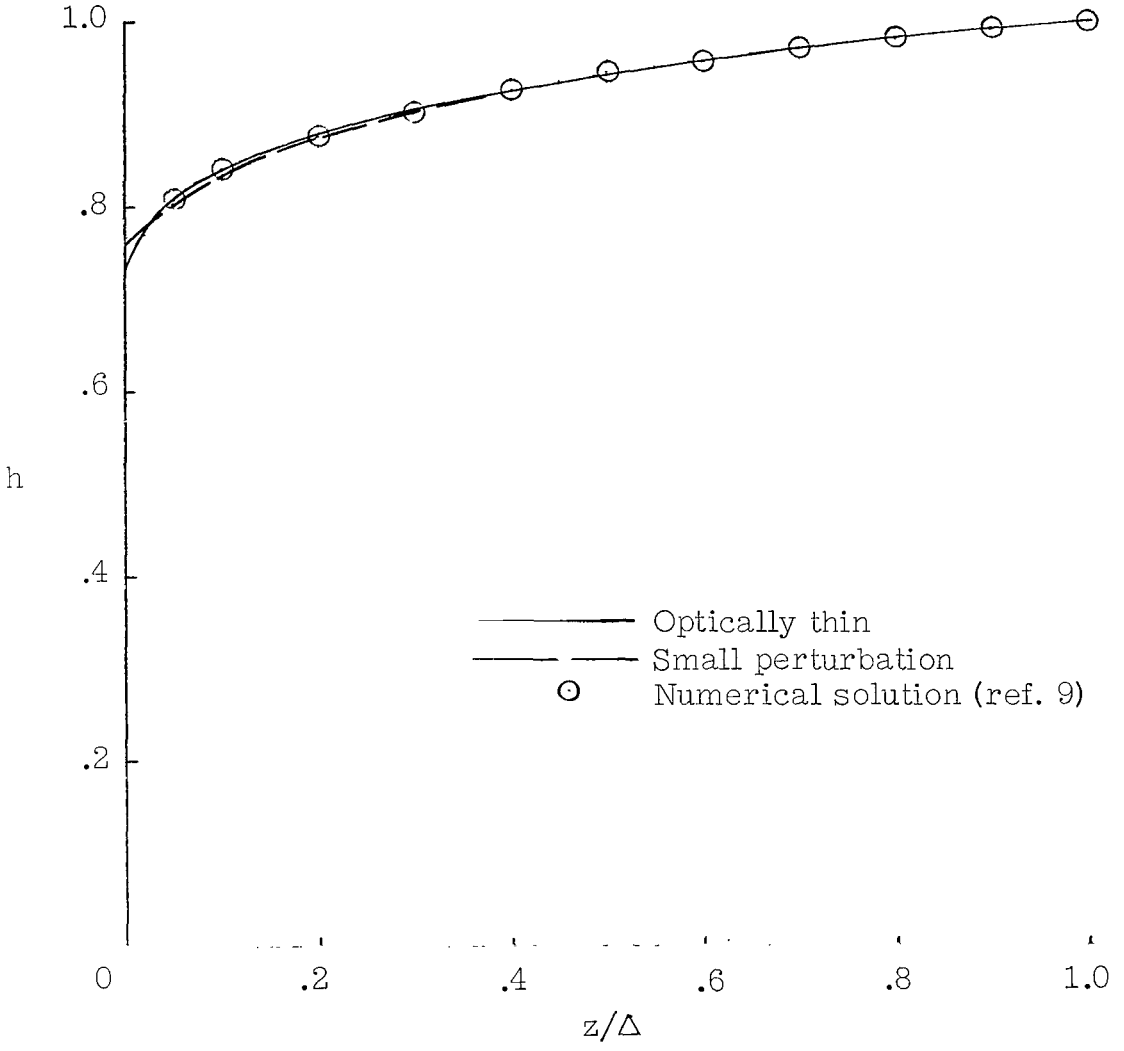

Figure 16.- Comparison of the optically thin and small perturbation solutions with numerical results of reference 9. W_∞ = 9.75 km/sec; p_s = 10 atm; R_s = 1.525 m.

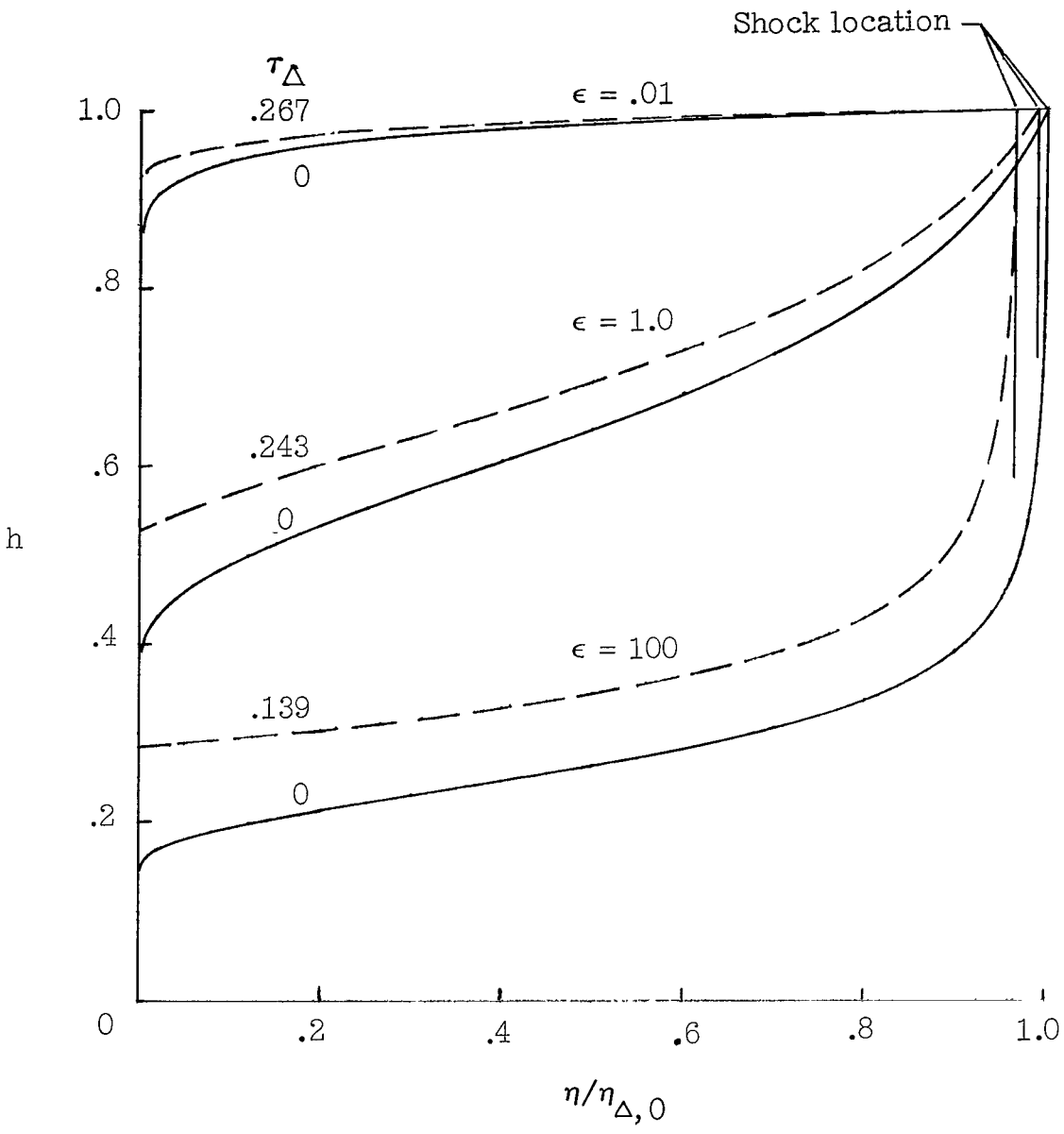

Figure 17.- Effect of absorption on the enthalpy distribution in an optically thin shock layer.

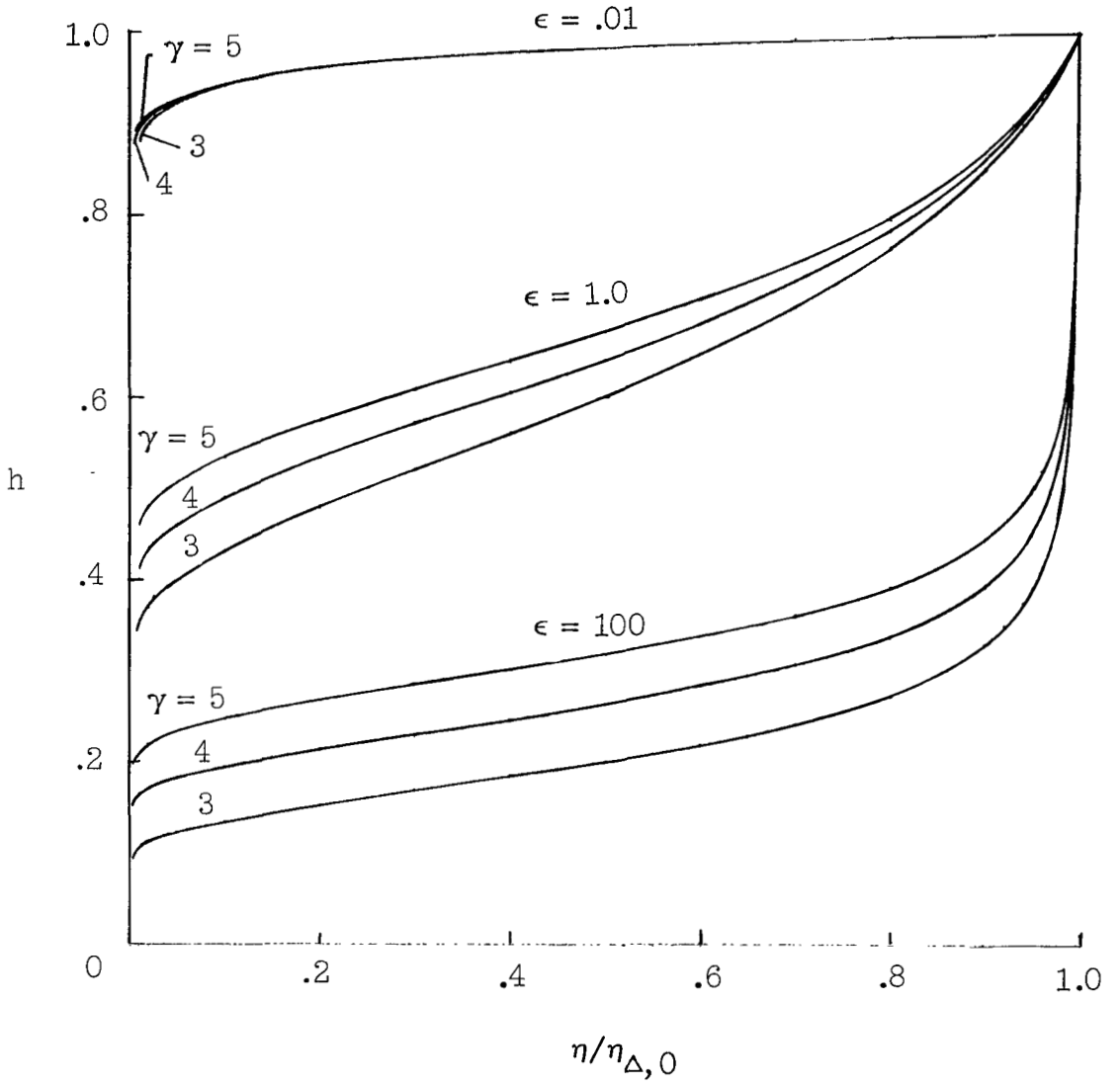

(a) Effect of γ.

Figure 18.- Effect of the enthalpy dependence of the absorption coefficient on the enthalpy distribution in a transparent shock layer.

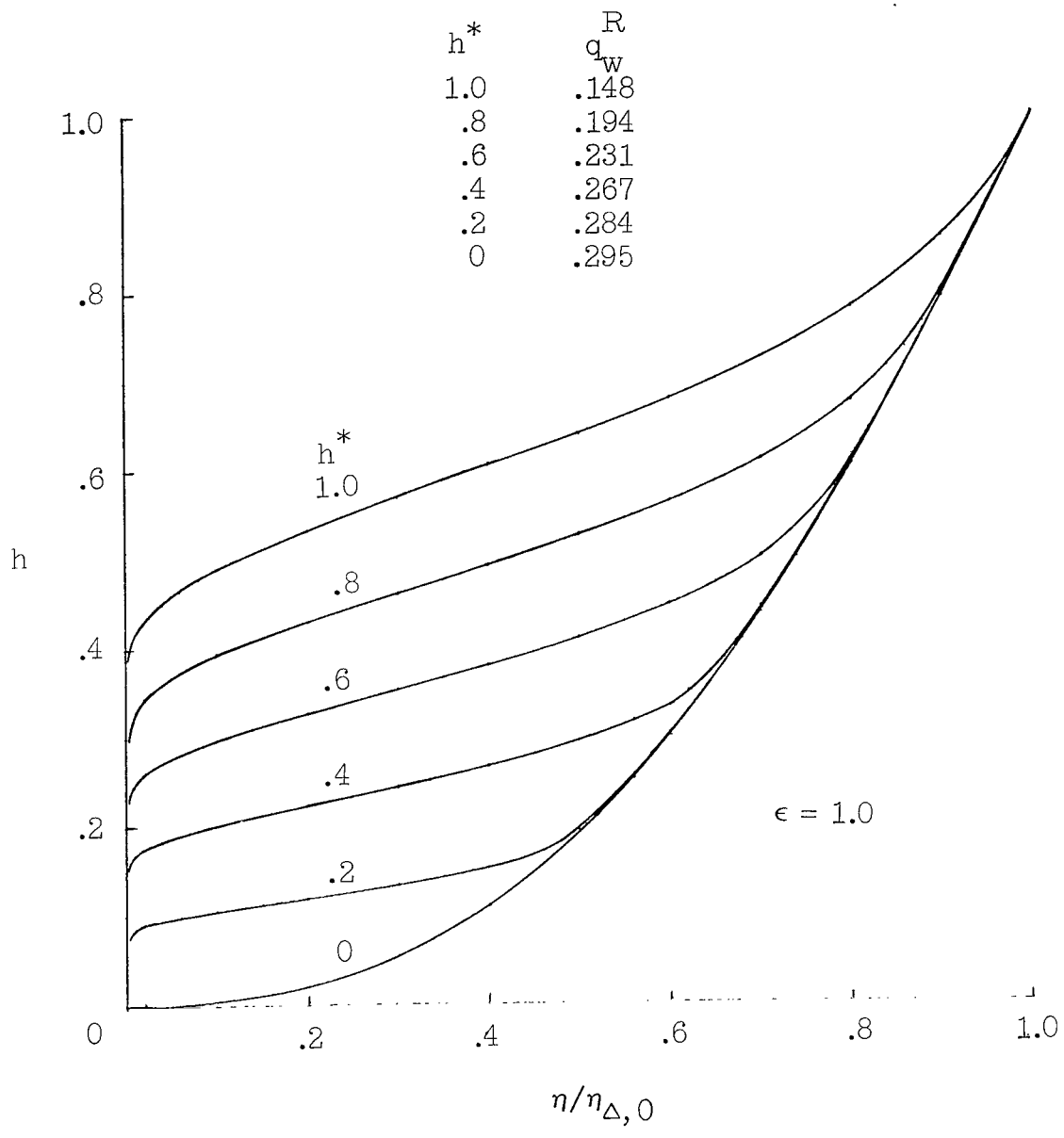

(b) Effect of h^*.

Figure 18.- Concluded.

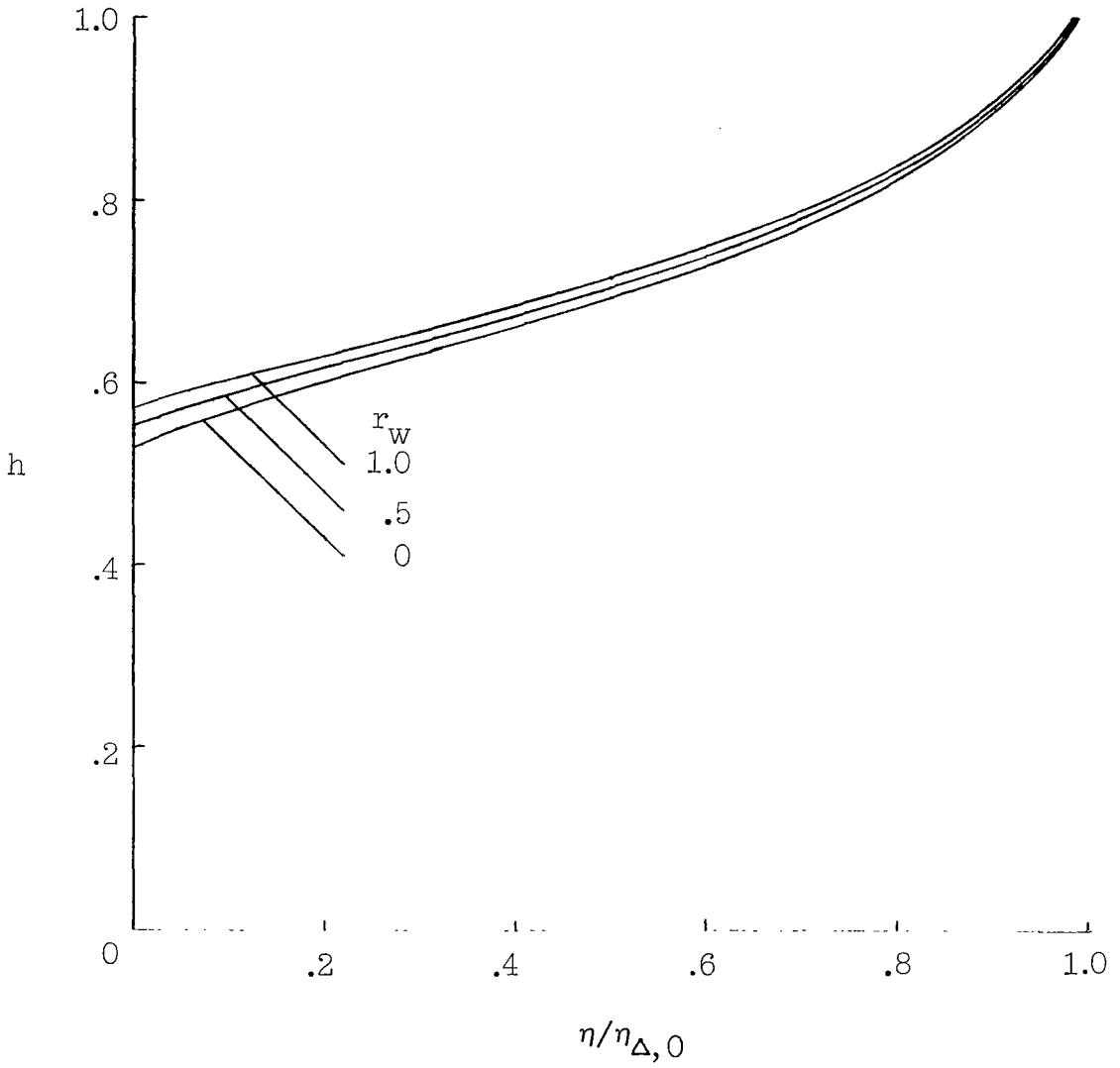

Figure 19.- Effect of surface reflectivity on the enthalpy distribution in an optically thin shock layer. $\epsilon = 1.0$; $k_p = 1.0$.

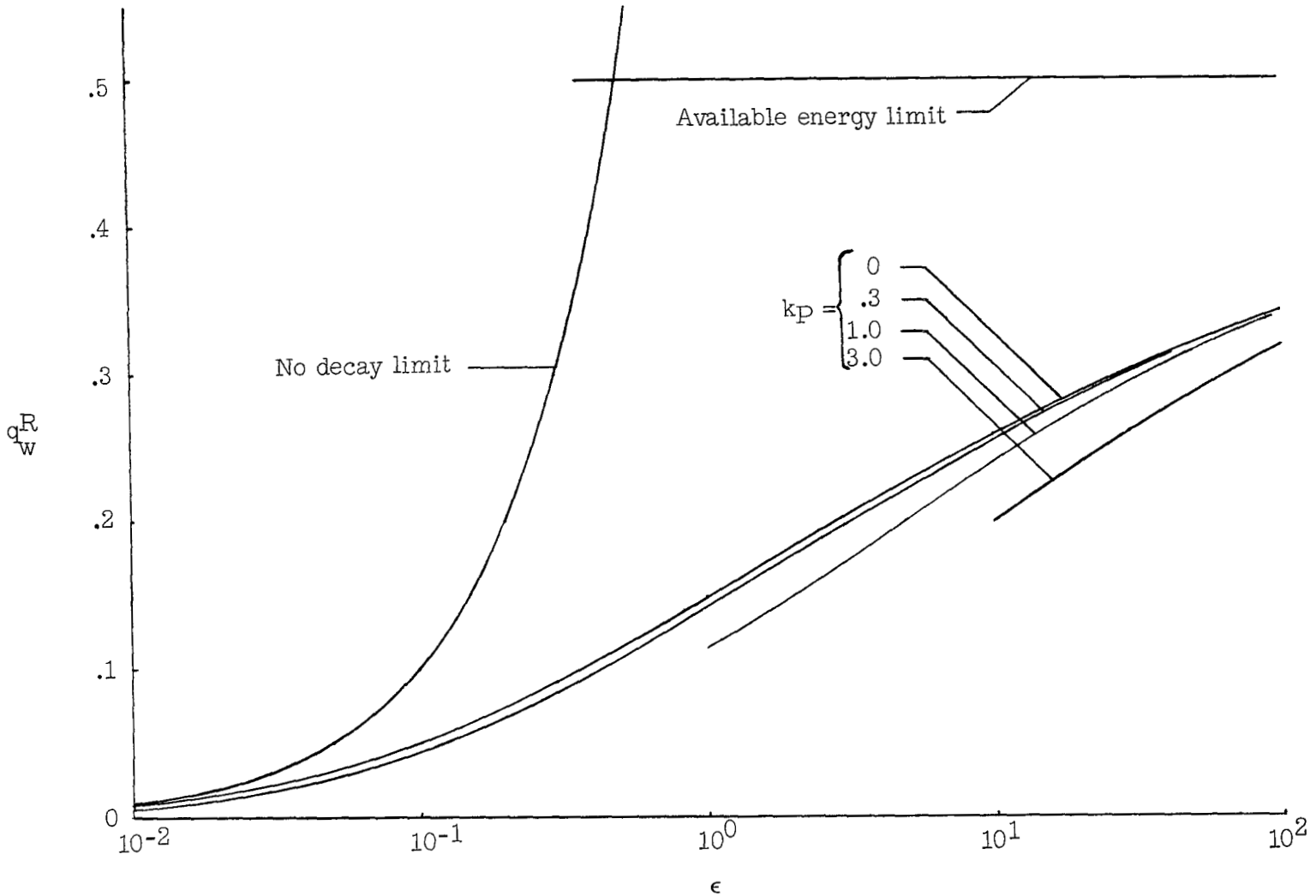

Figure 20.- Effect of the Bouguer number on the rate of radiation heat transfer to the stagnation point. $\gamma = 4.0$.

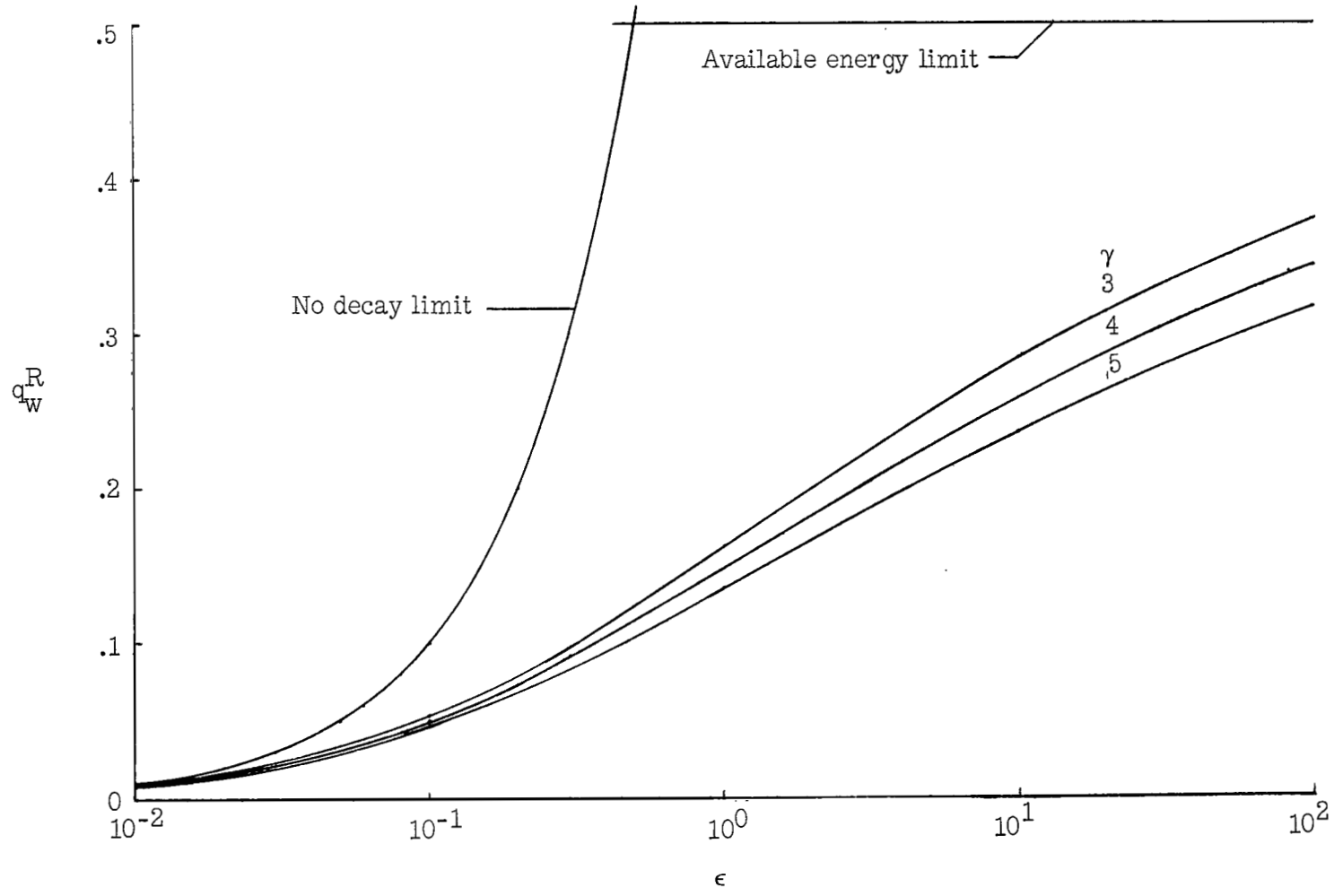

Figure 21.- Effect of the enthalpy dependence of the absorption coefficient on the rate of radiant heat transfer to the stagnation point. $k_P = 0$.

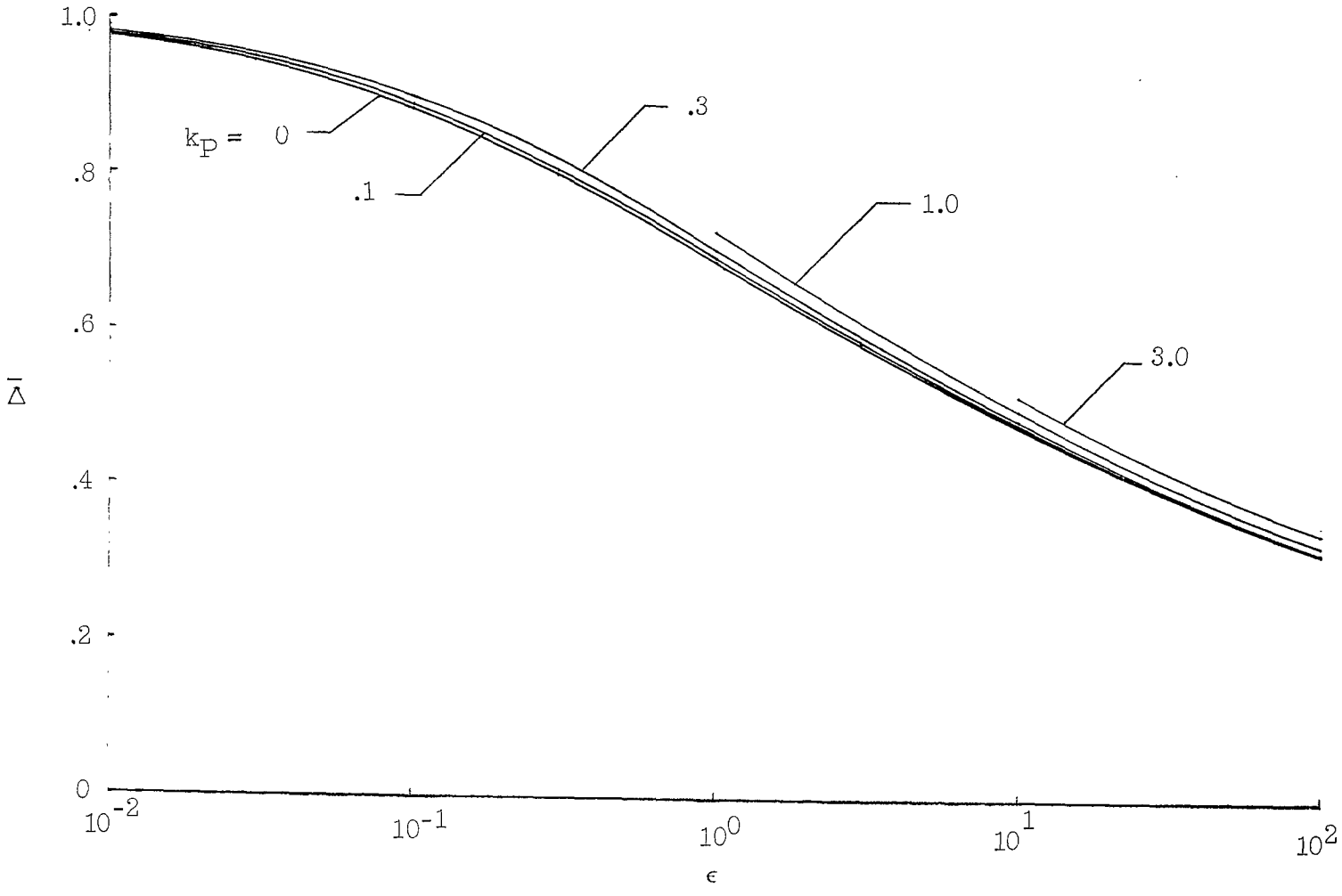

(a) Effect of k_p.

Figure 22.- Variation of the shock standoff distance with the radiation cooling parameter ϵ.

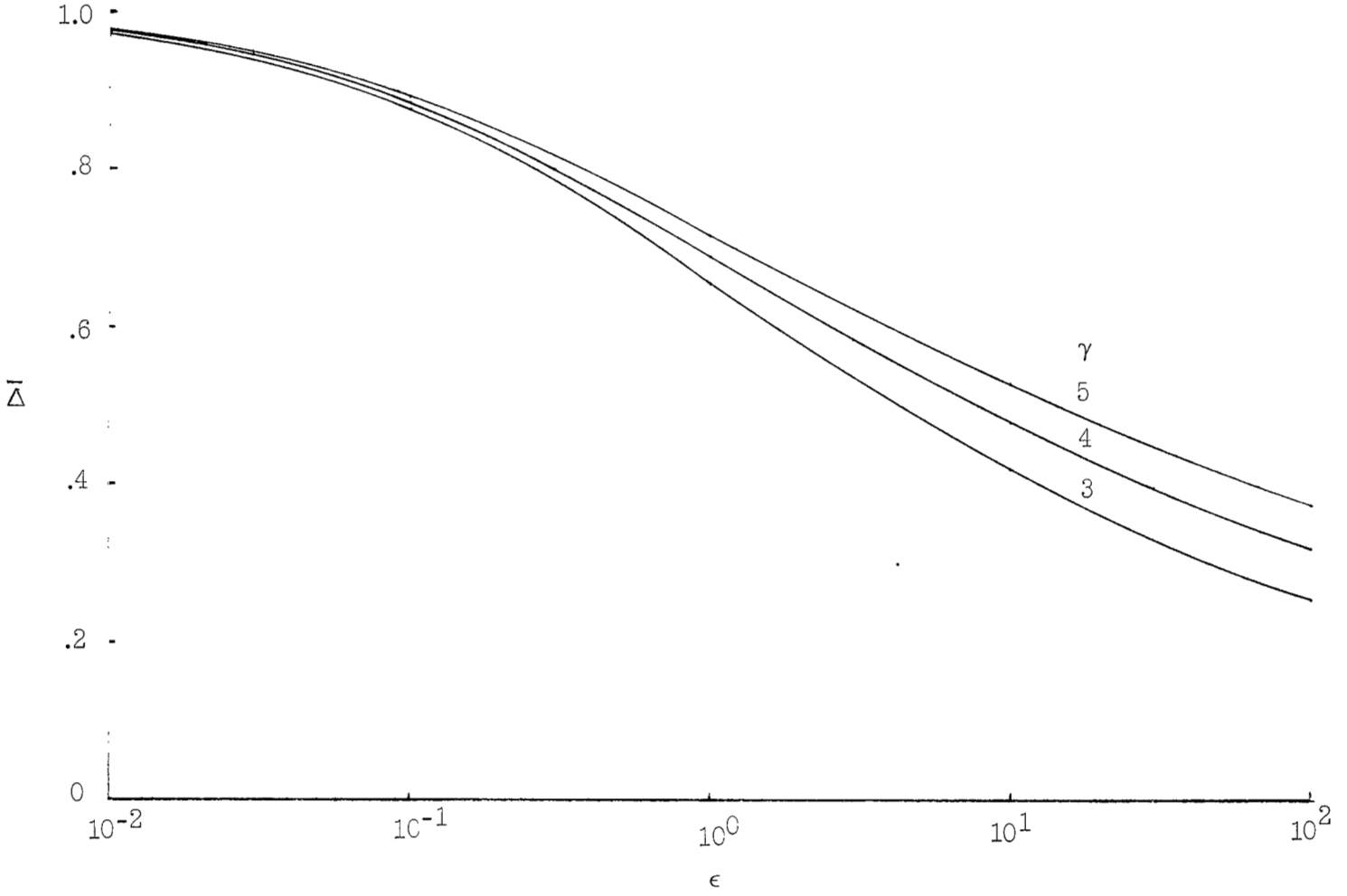

(b) Effect of γ.

Figure 22.- Concluded.

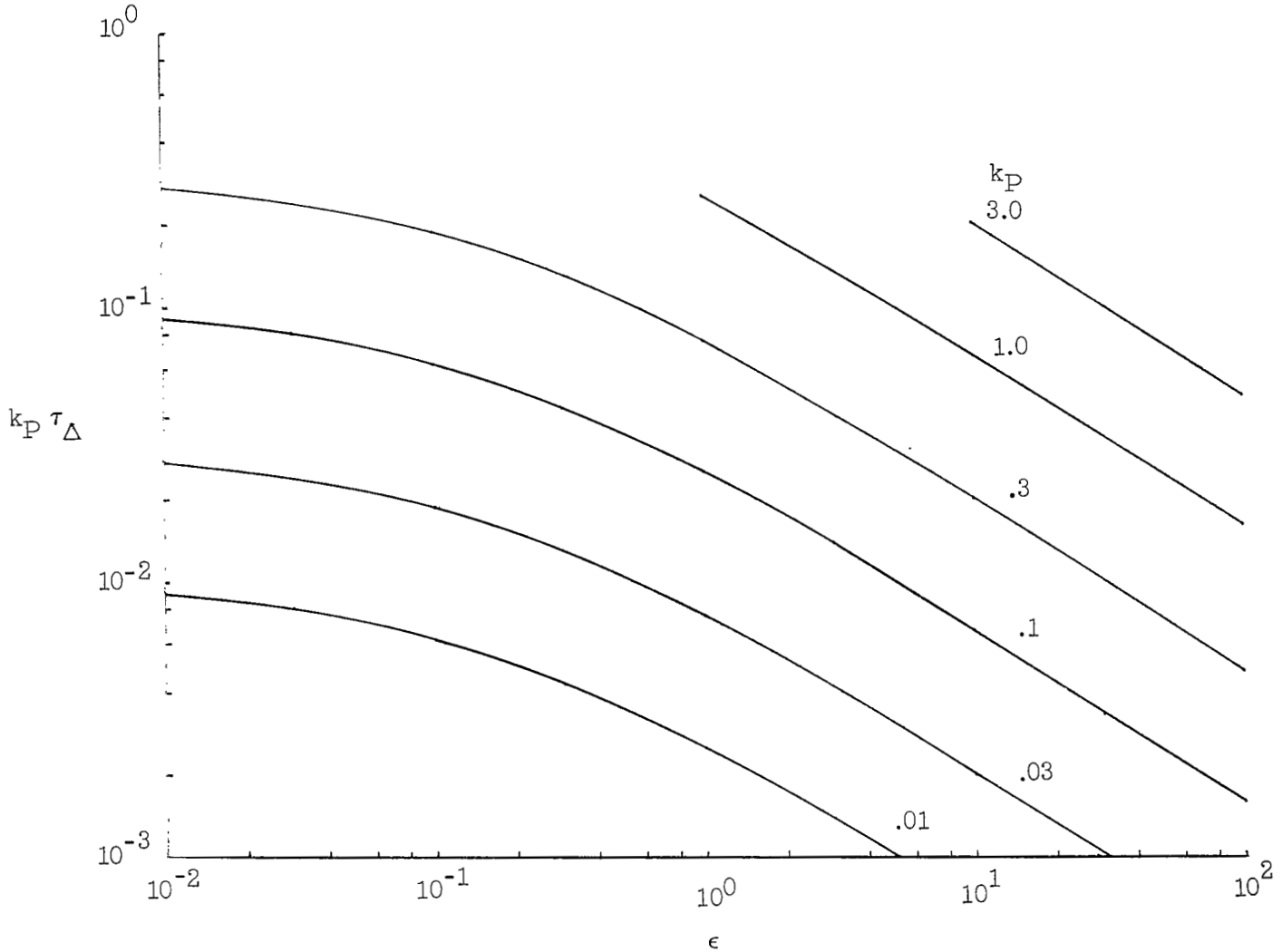

Figure 23.- Effect of Bouguer number on the optical thickness of an optically thin shock layer. $\gamma = 4.0$.

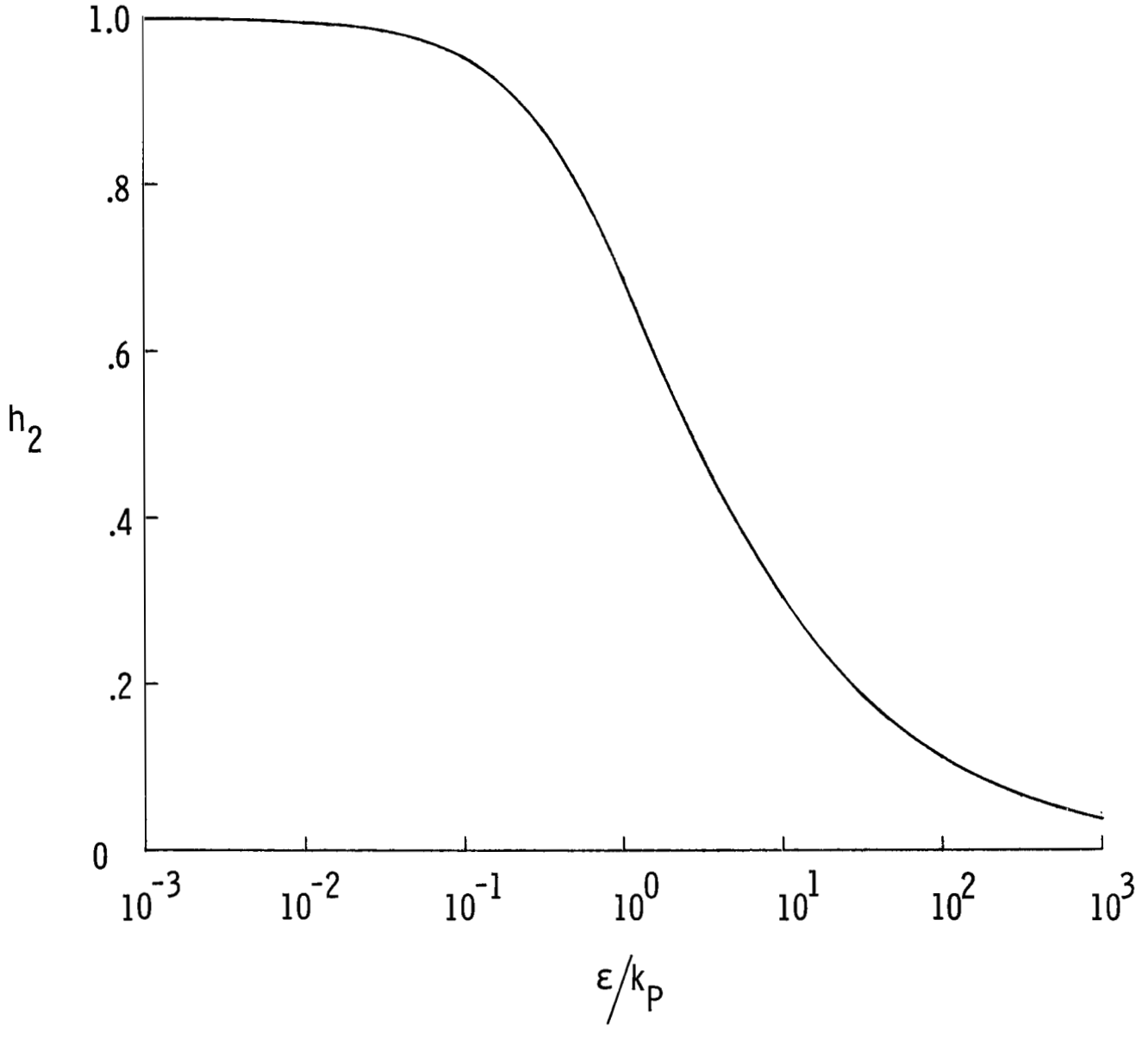

Figure 24.- Variation of h_2 with ε/k_P.

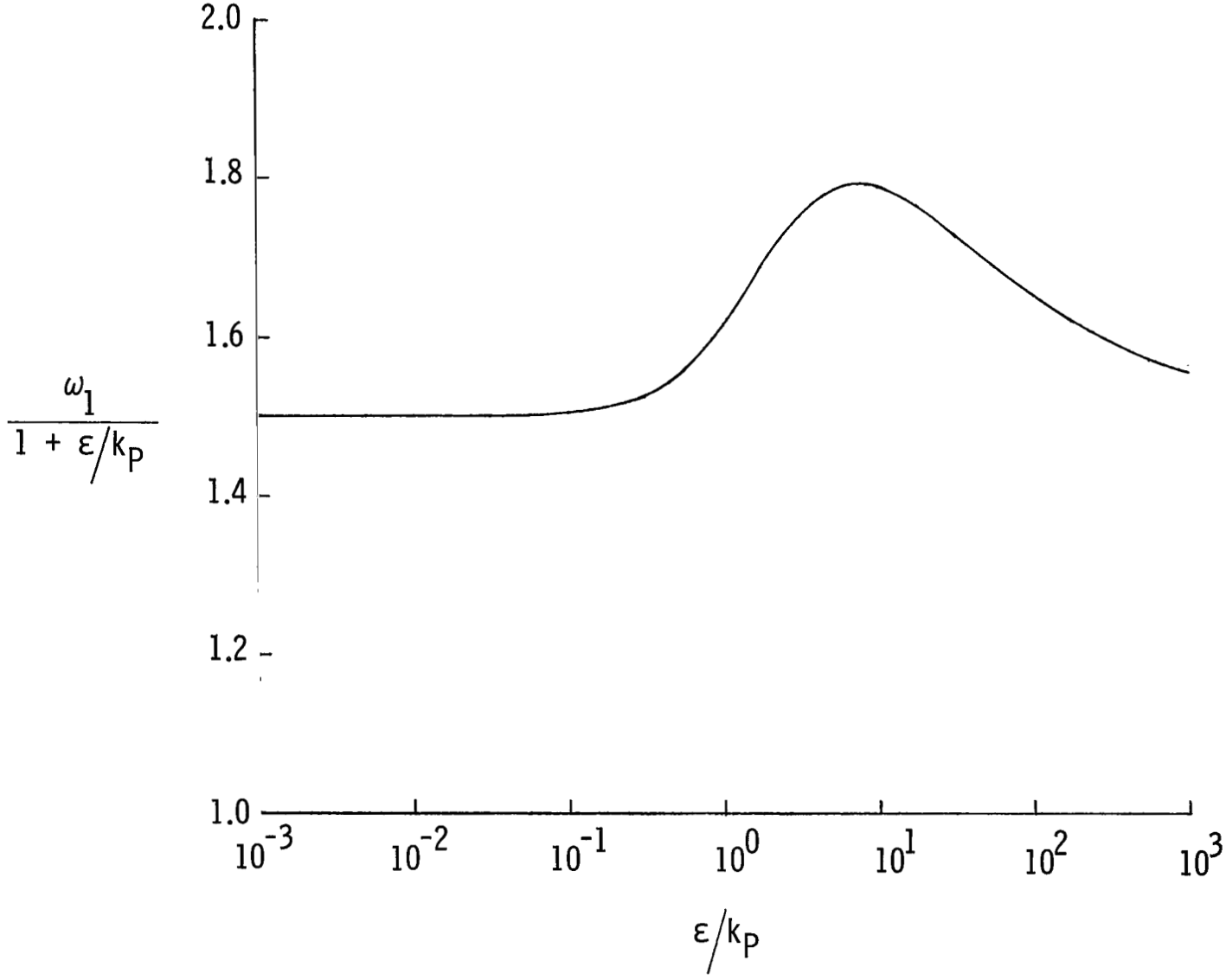

Figure 25.- Variation of $\frac{\omega_1}{1 + \frac{\varepsilon}{k_P}}$ with ε/k_P.

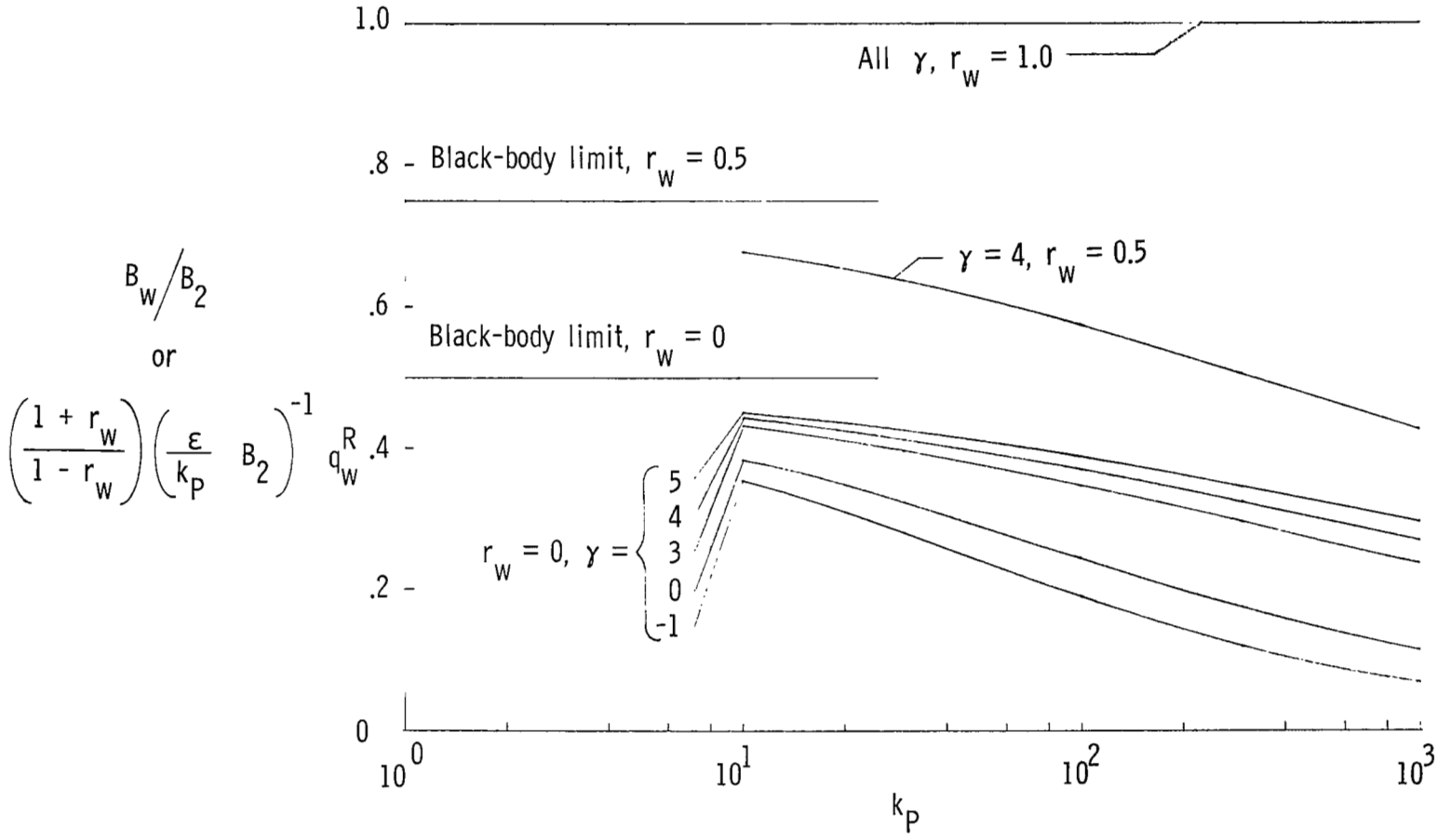

(a) $\varepsilon/k_P = 0.01$, $B_2 = 0.9901$.

Figure 26.- Variation of B_w/B_2 with k_P for various values of γ and r_w.

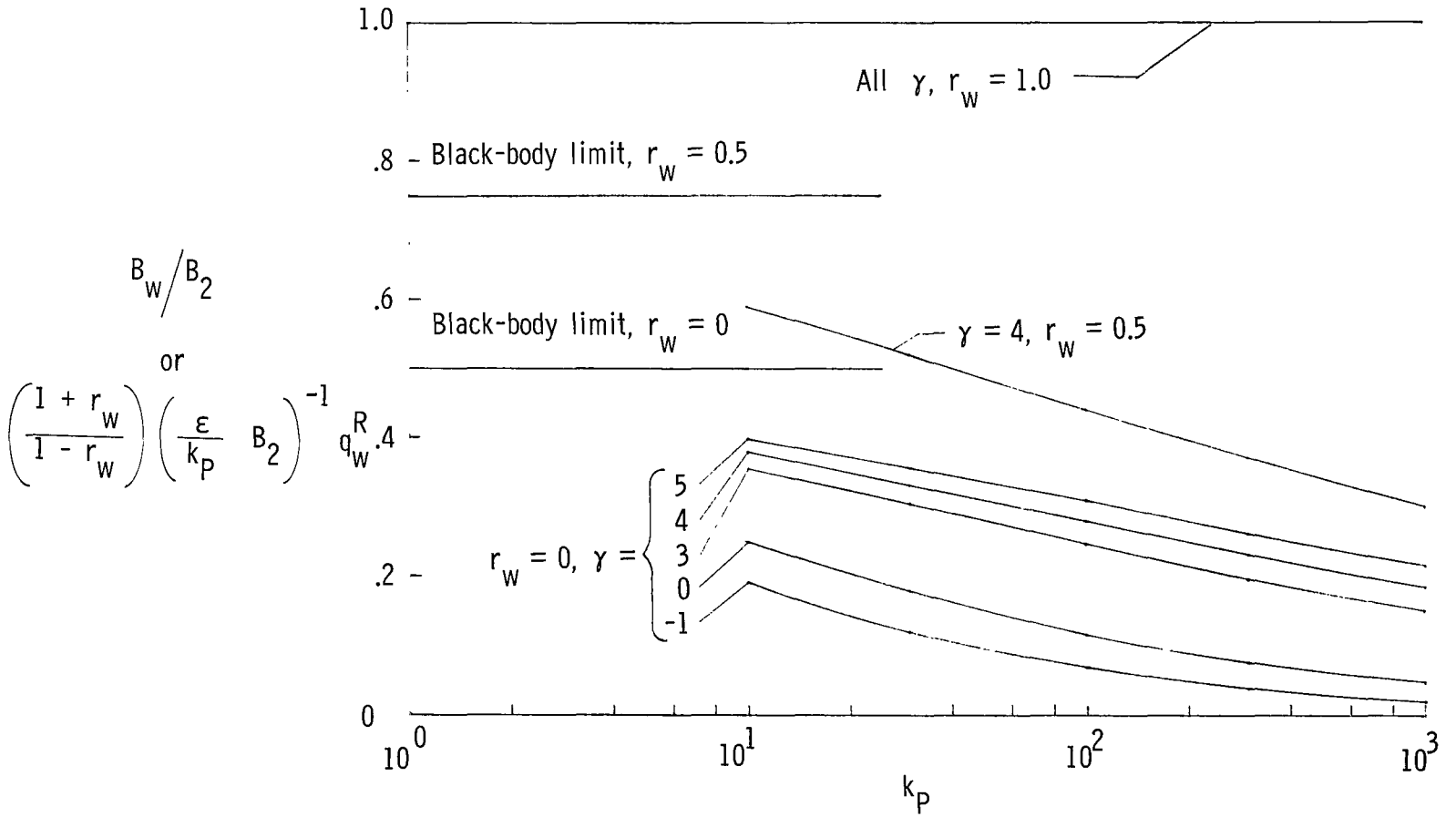

(b) $\varepsilon/k_P = 0.1$, $B_2 = 0.9072$.

Figure 26.- Continued.

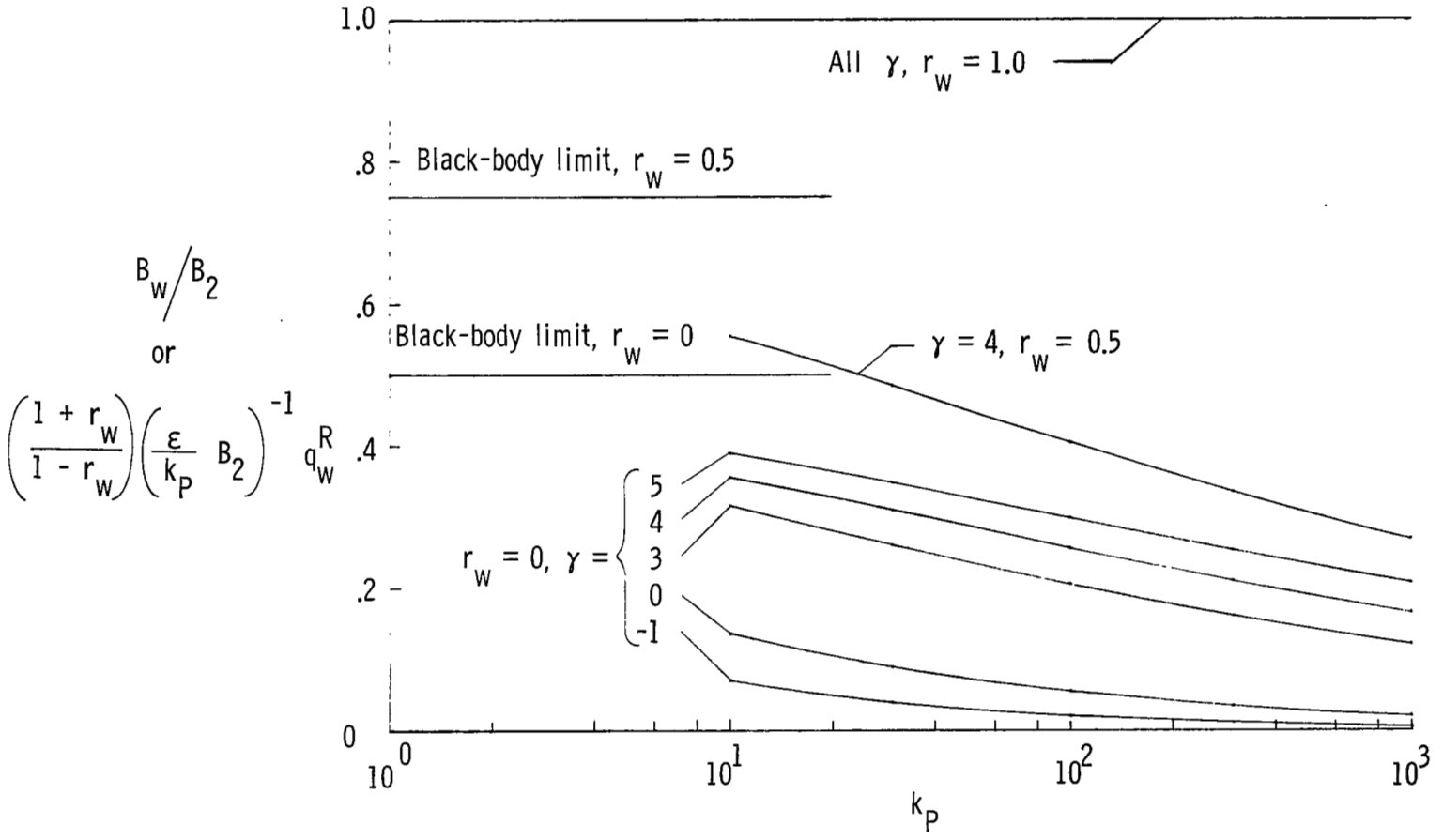

(c) $\varepsilon/k_P = 1.0$, $B_2 = 0.4716$.

Figure 26.- Continued.

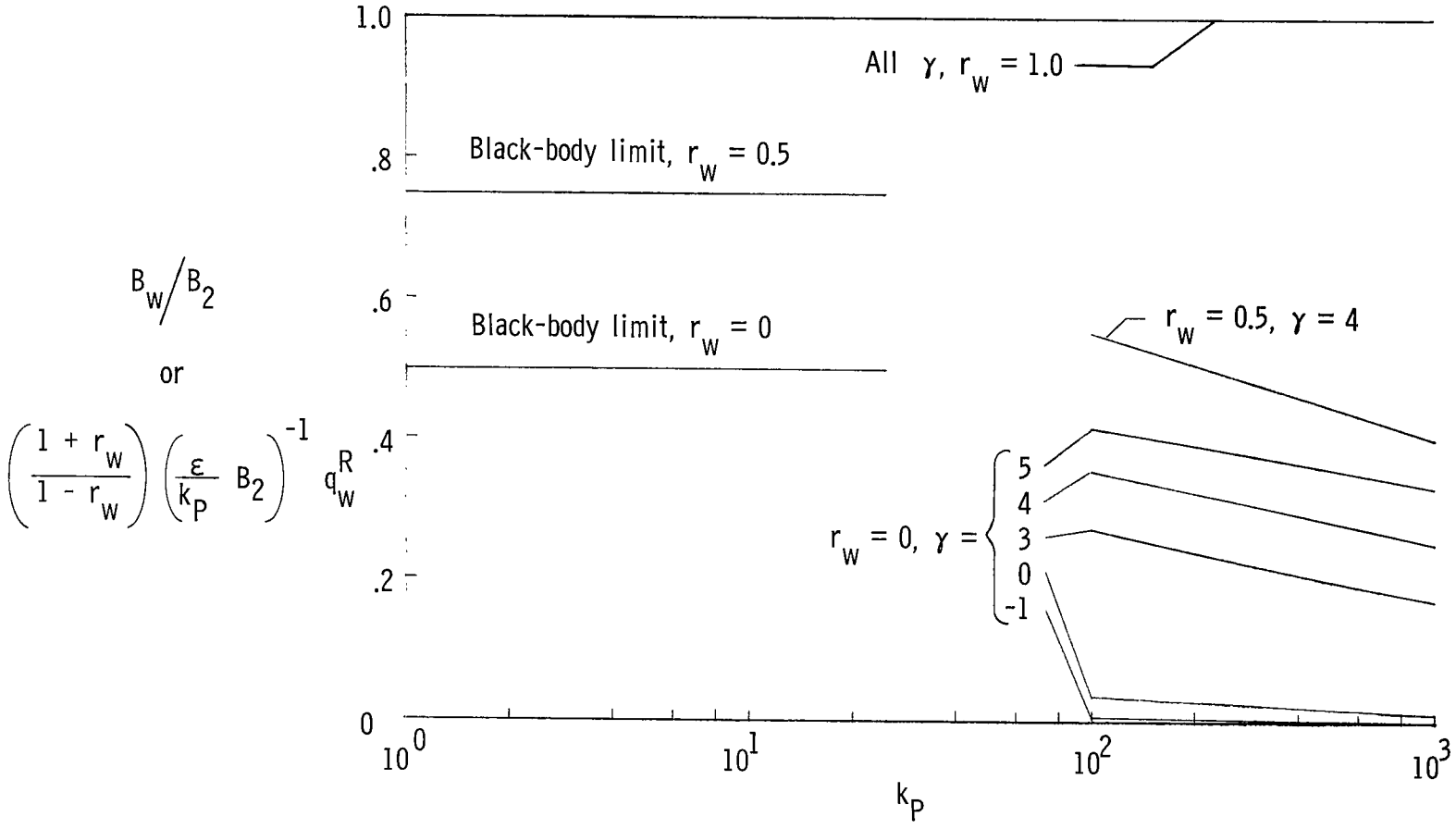

(d) $\varepsilon/k_P = 10$, $B_2 = 0.0916$.

Figure 26.- Concluded.

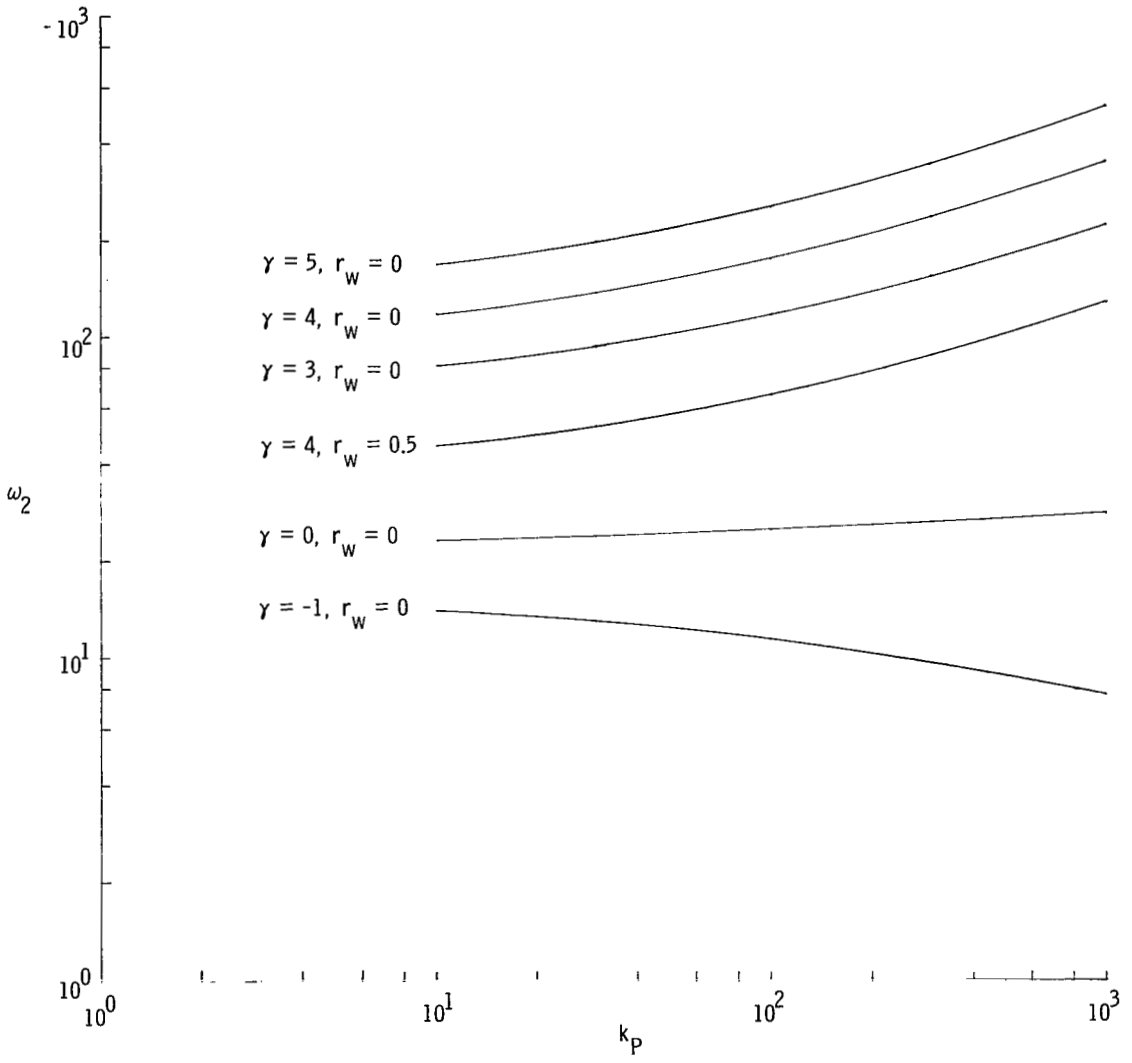

(a) $\varepsilon/k_P = 0.01$.

Figure 27.- Variation of ω_2 with k_P for various values of γ and r_w.

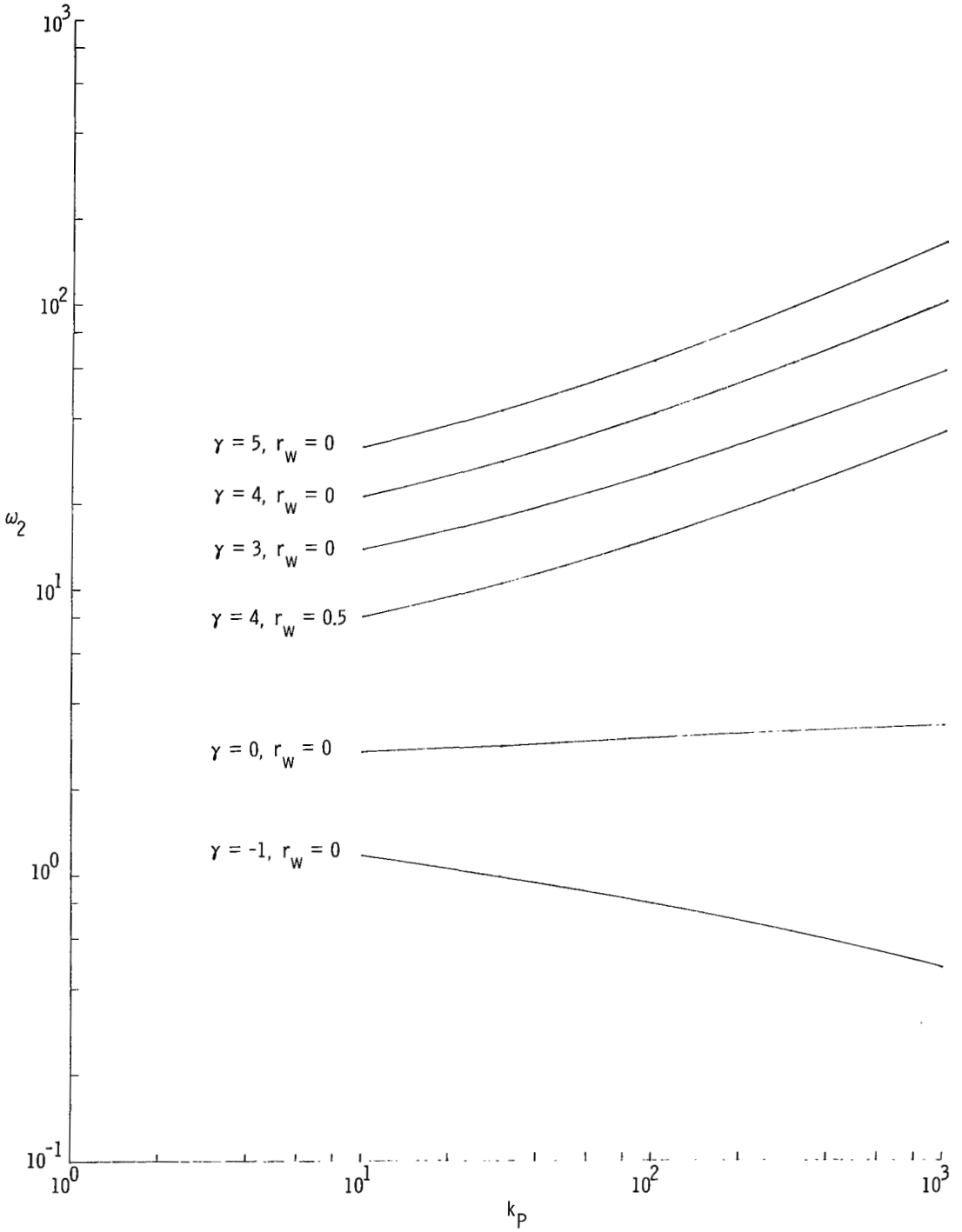

(b) $\epsilon/k_P = 0.1$.

Figure 27.- Continued.

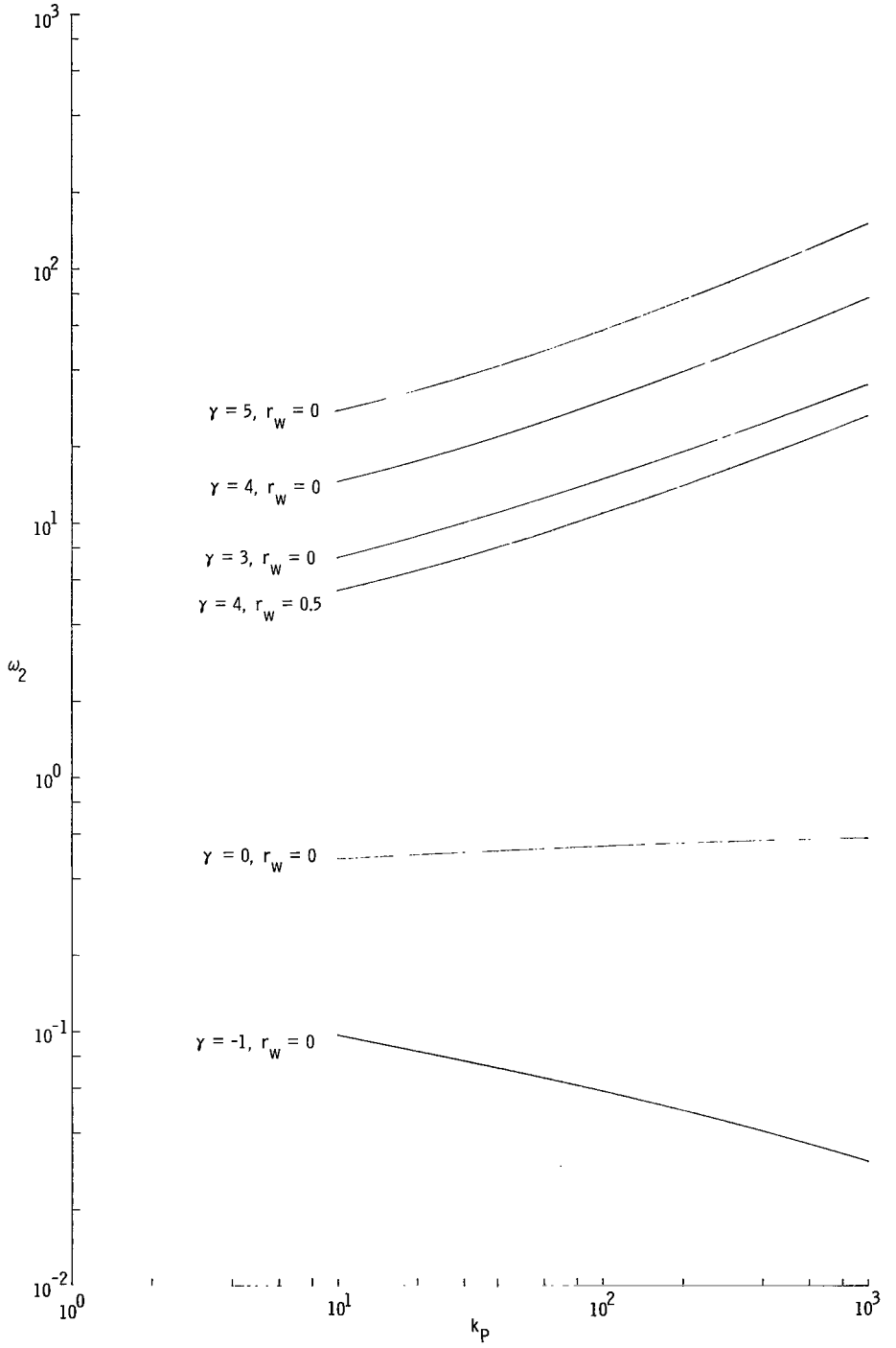

(c) $\varepsilon/k_P = 1.0$.

Figure 27.- Continued.

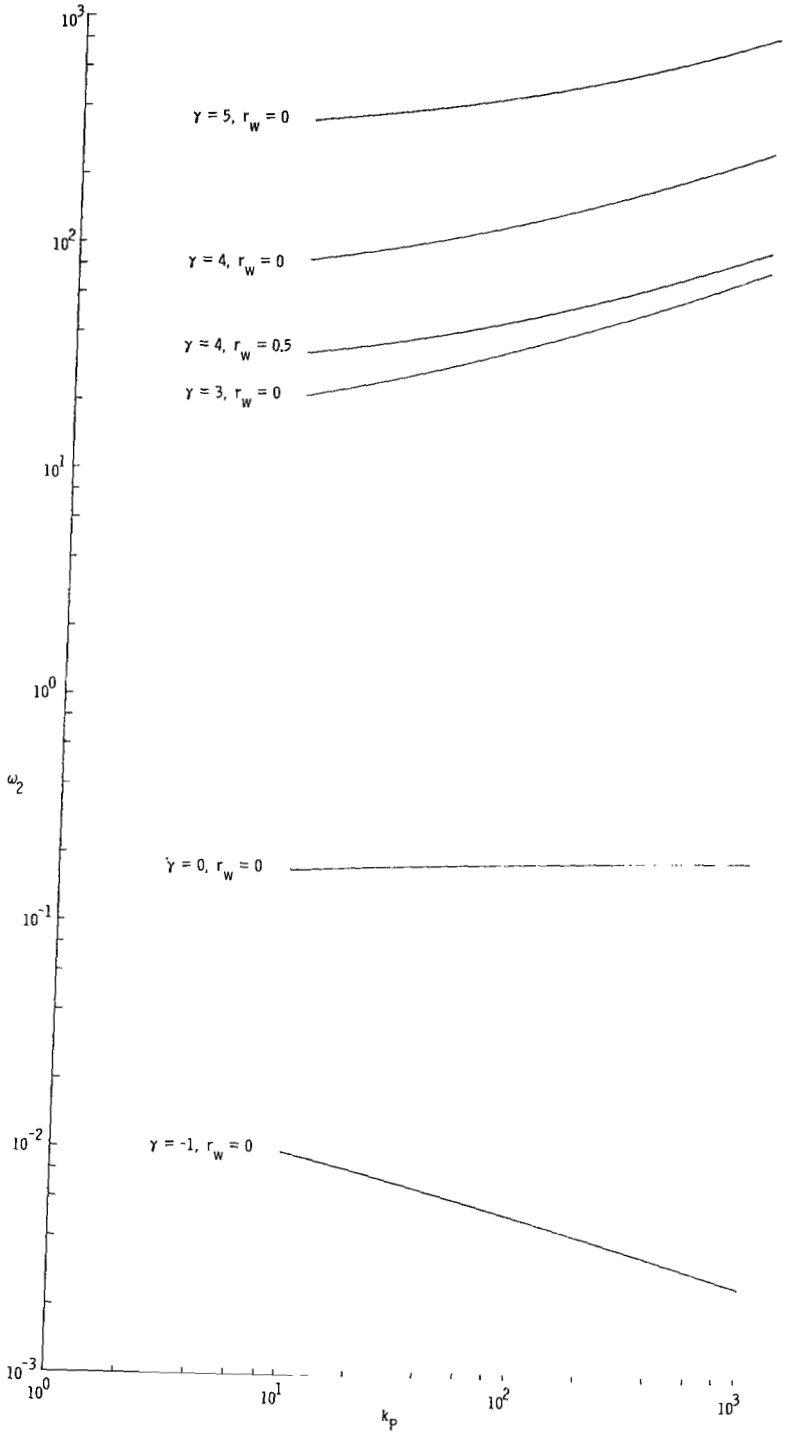

(d) $\varepsilon/k_P = 10.$

Figure 27.- Concluded.

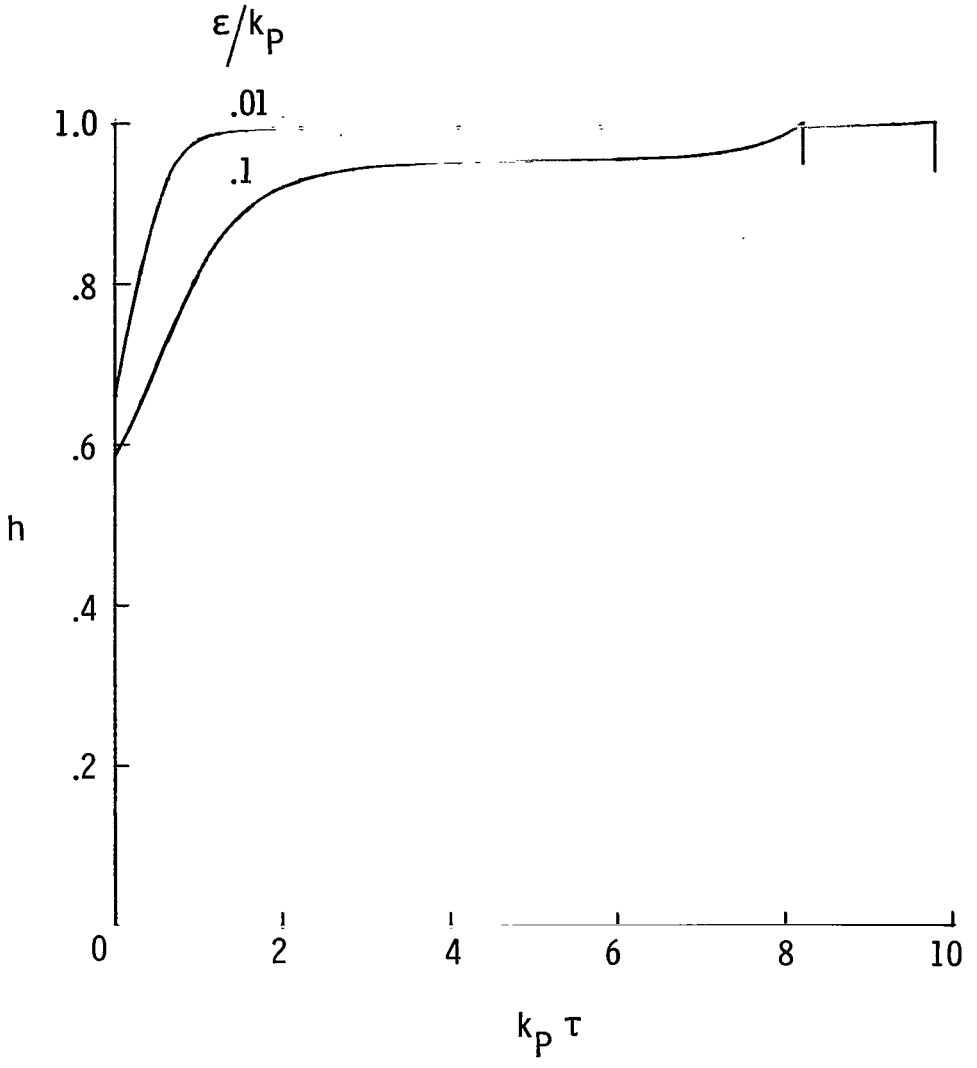

(a) $k_P = 10.$

Figure 28.- Effect of the parameters ε/k_P and k_P on the enthalpy distribution in an optically thick shock layer.

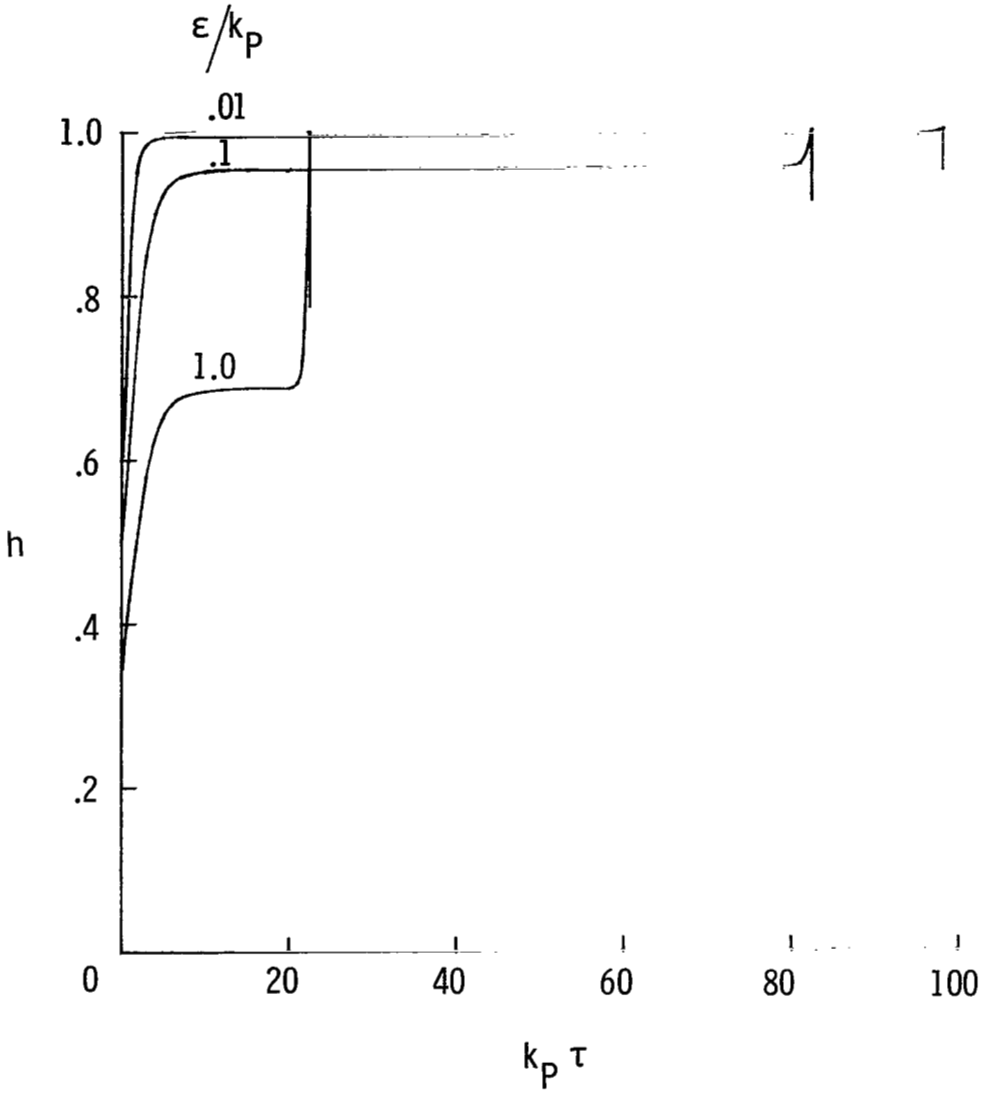

(b) $k_P = 100.$

Figure 28.- Concluded.

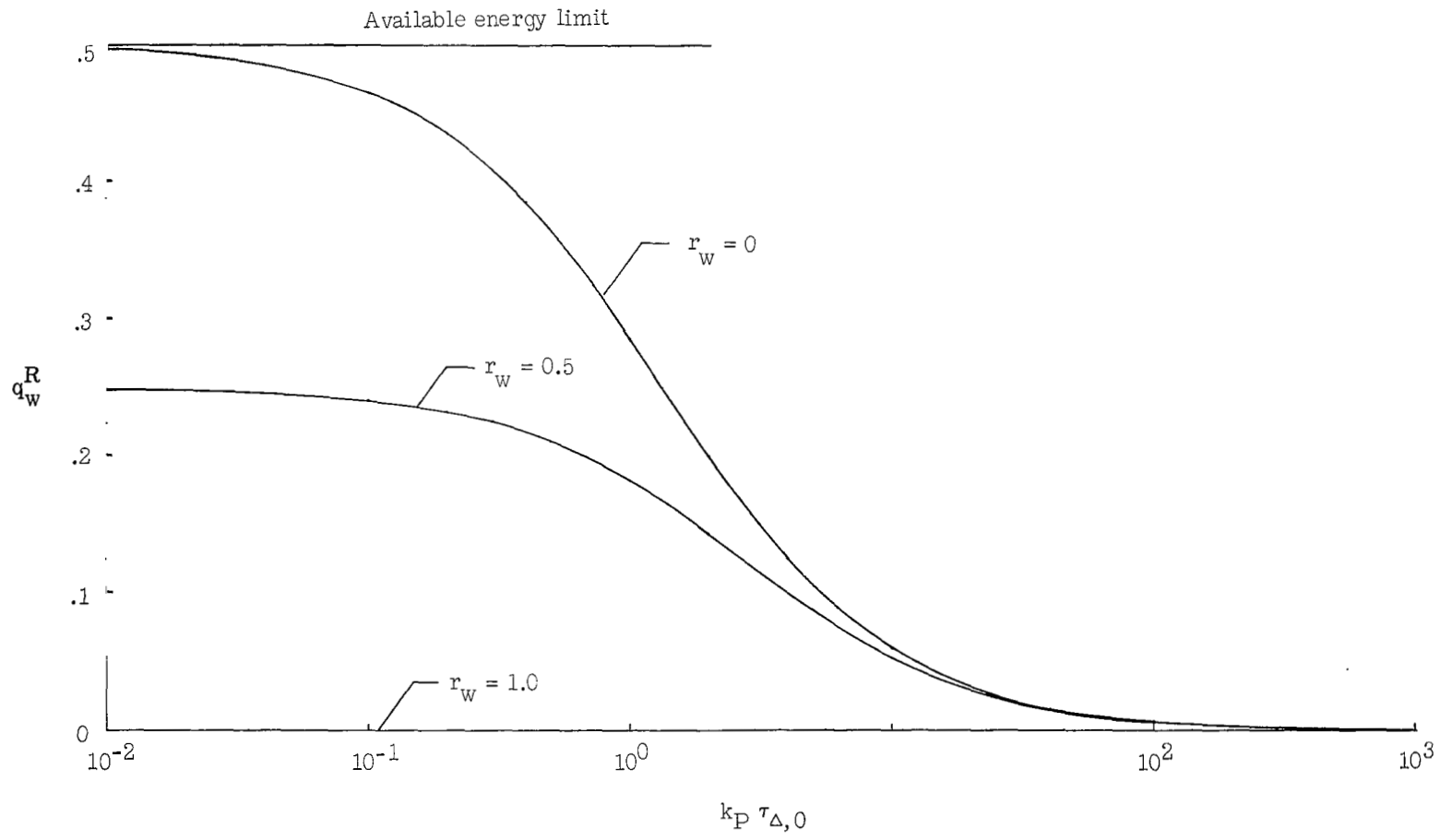

Figure 29.- Radiant heat flux from radiation-depleted shock layer.

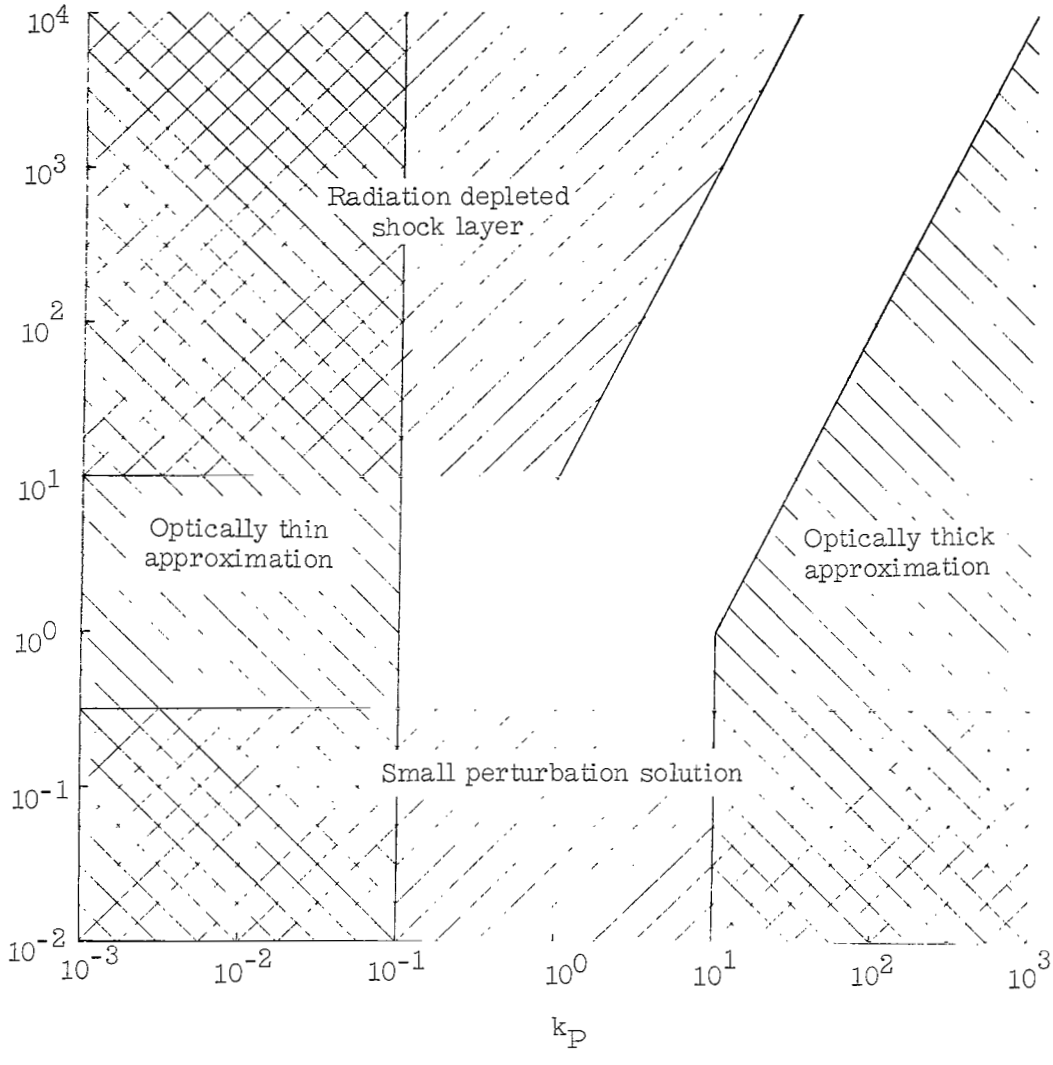

Figure 30.- Radiating shock-layer regimes.

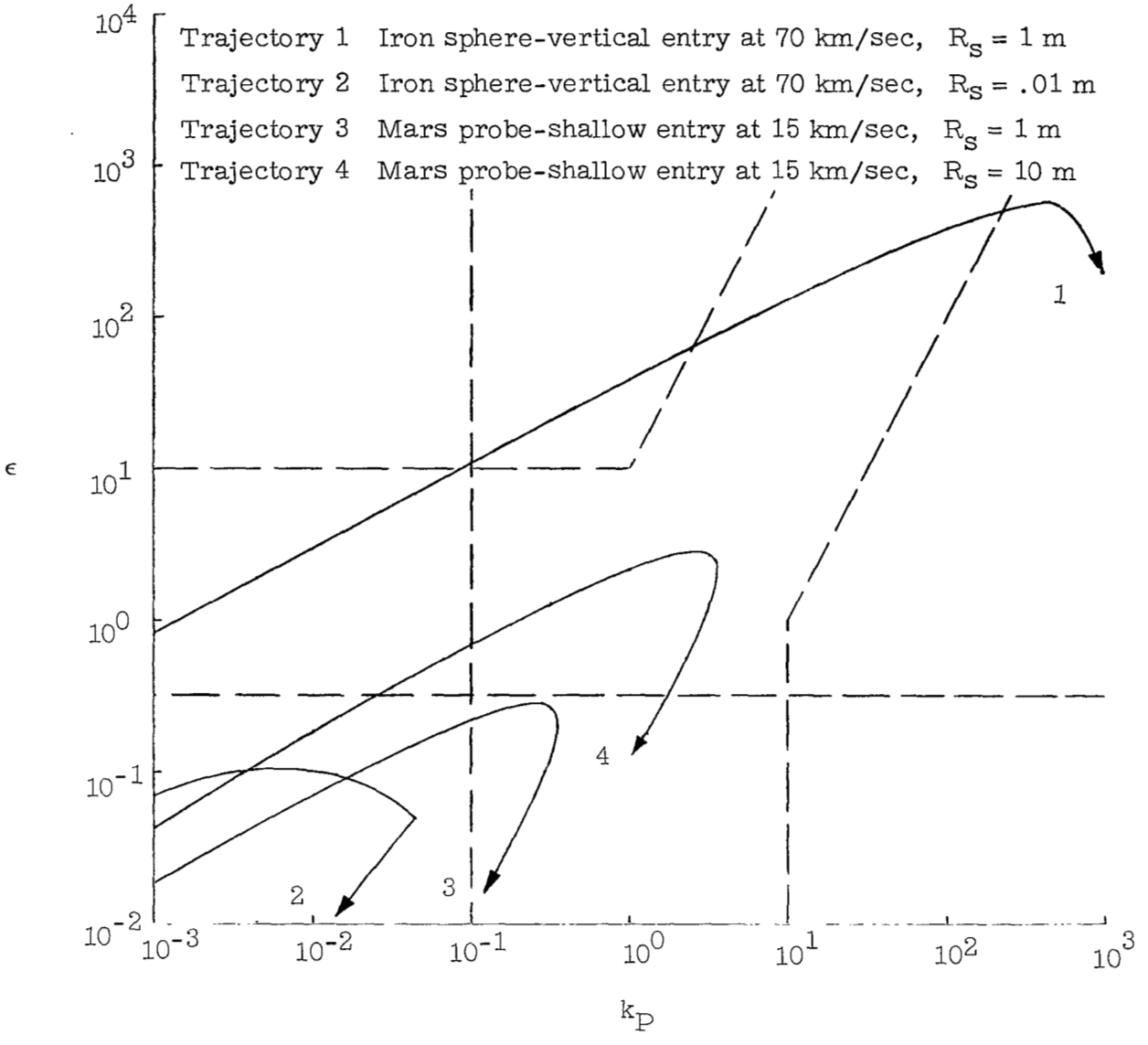

Figure 31.- Entry trajectories in the ϵ, k_p space.

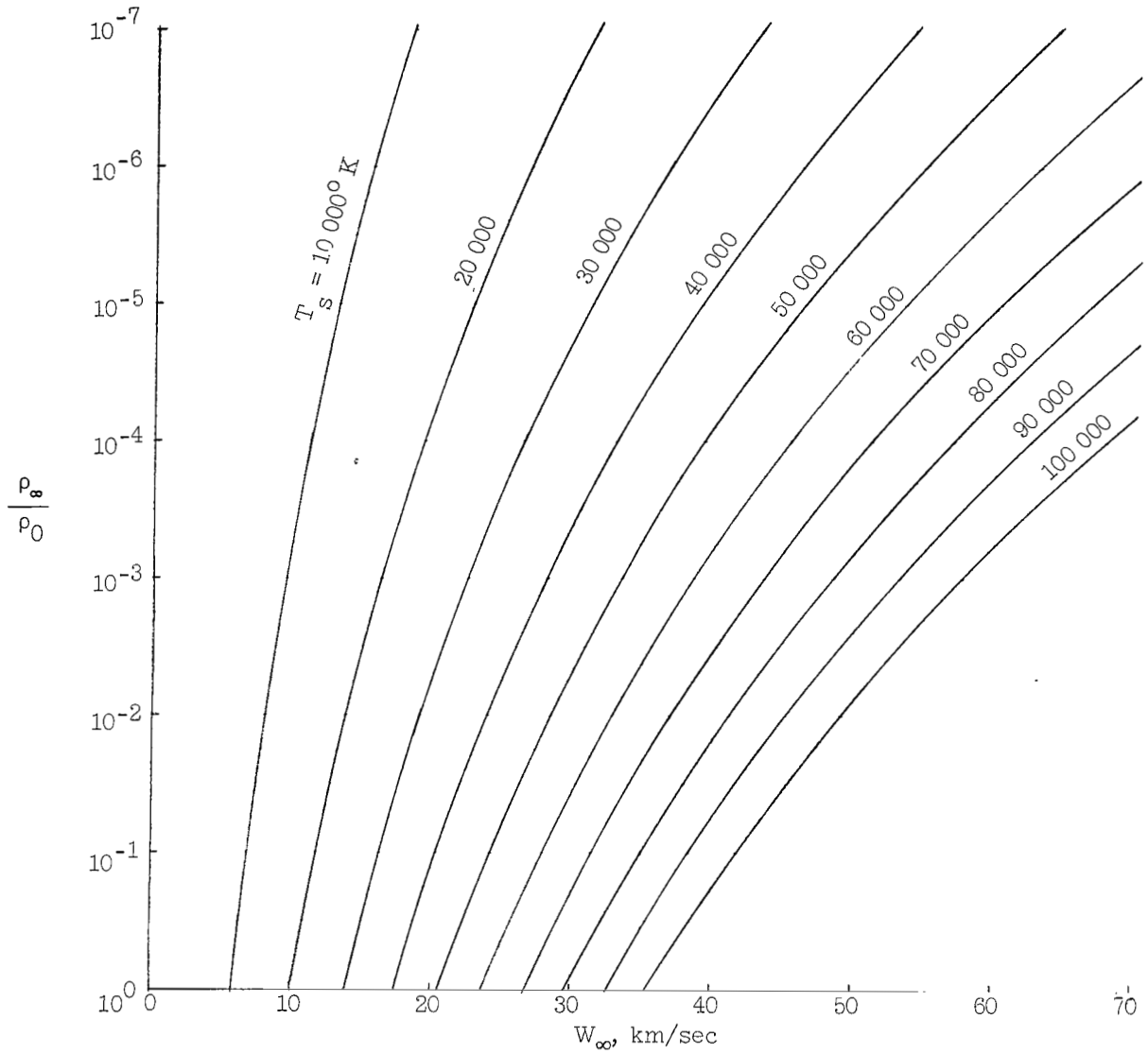

(a) Contours of constant normal-shock equilibrium temperatures.

Figure 32.- The earth-entry environment.

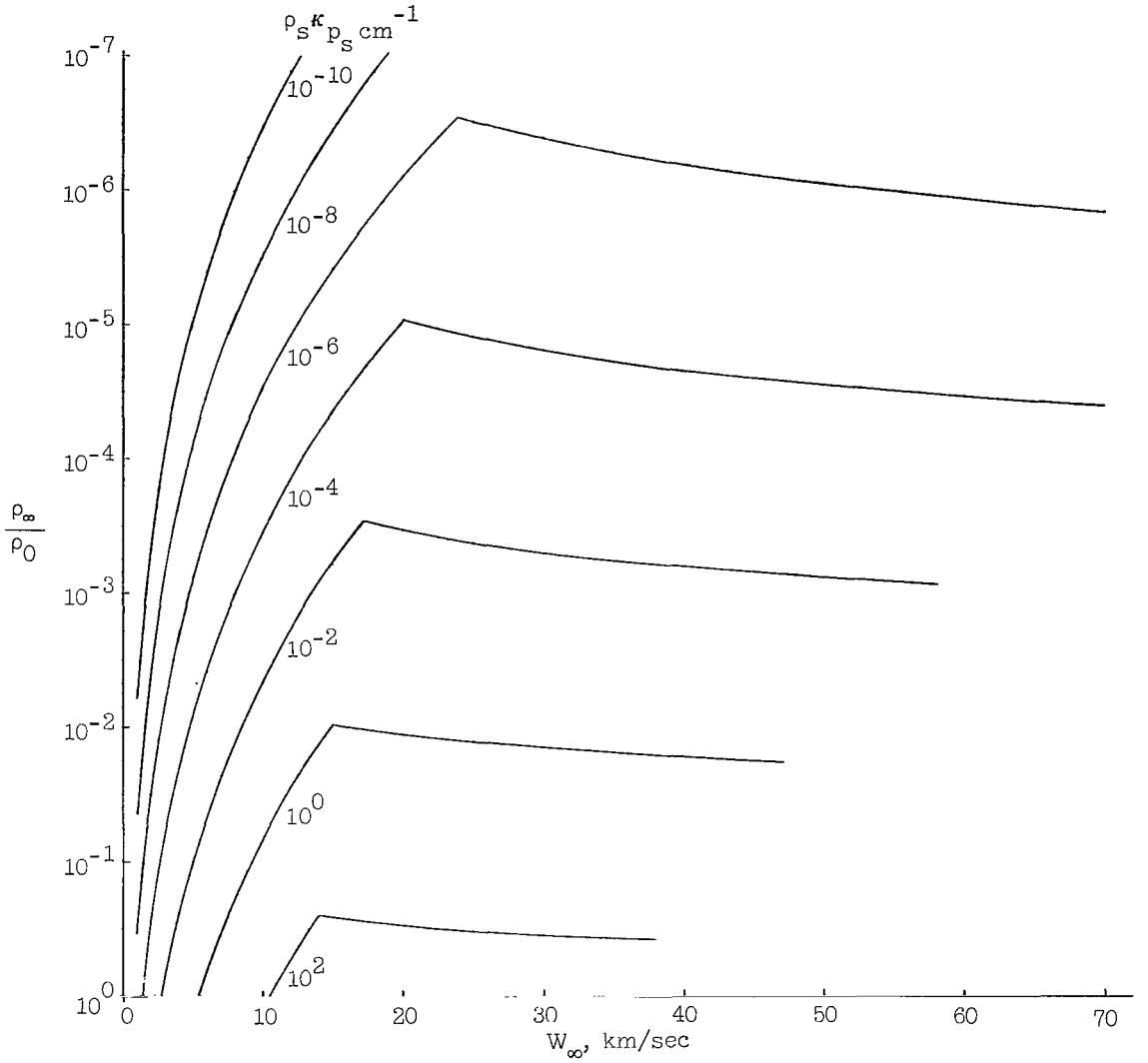

(b) Contours of constant normal-shock equilibrium values of the Planck mean volume absorption coefficient $\rho_s \kappa_{P,s}$.

Figure 32.- Continued.

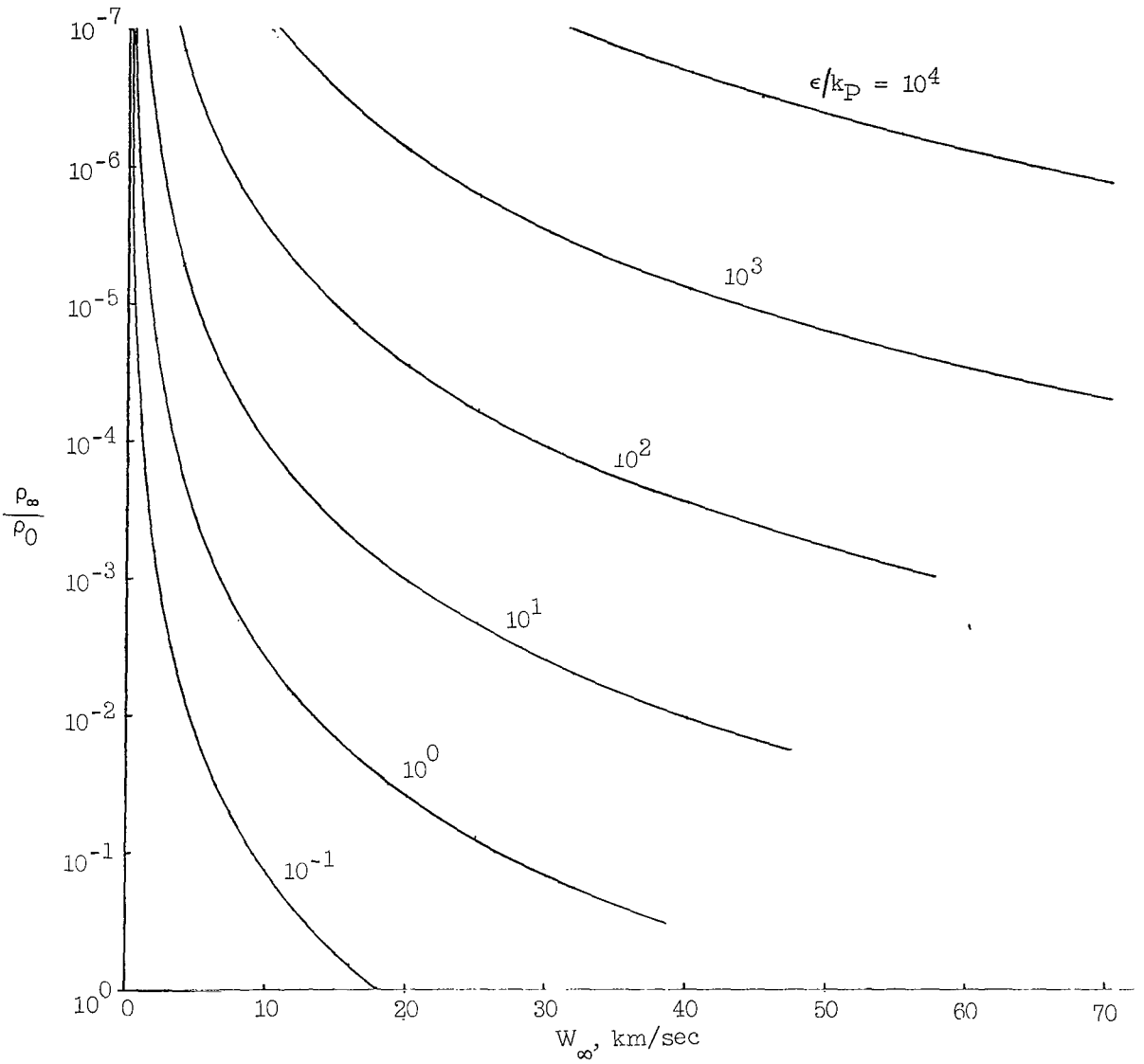

(c) Contours of constant values of $\epsilon/k_P = 4\sigma T_s^4/\rho_\infty W_\infty^3$.

Figure 32.- Continued.

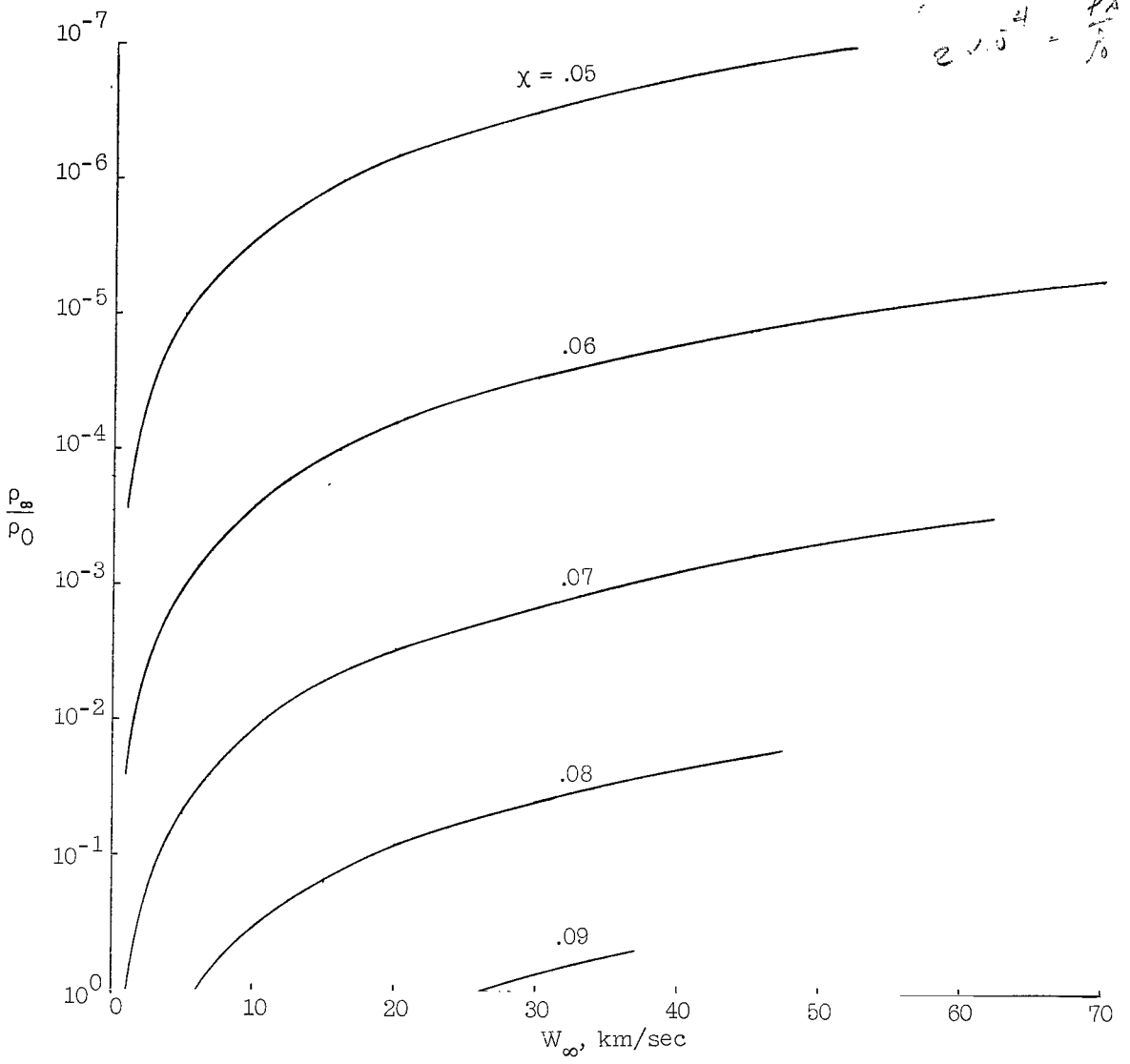

(d) Contours of constant normal-shock equilibrium density ratios.

Figure 32.- Concluded.

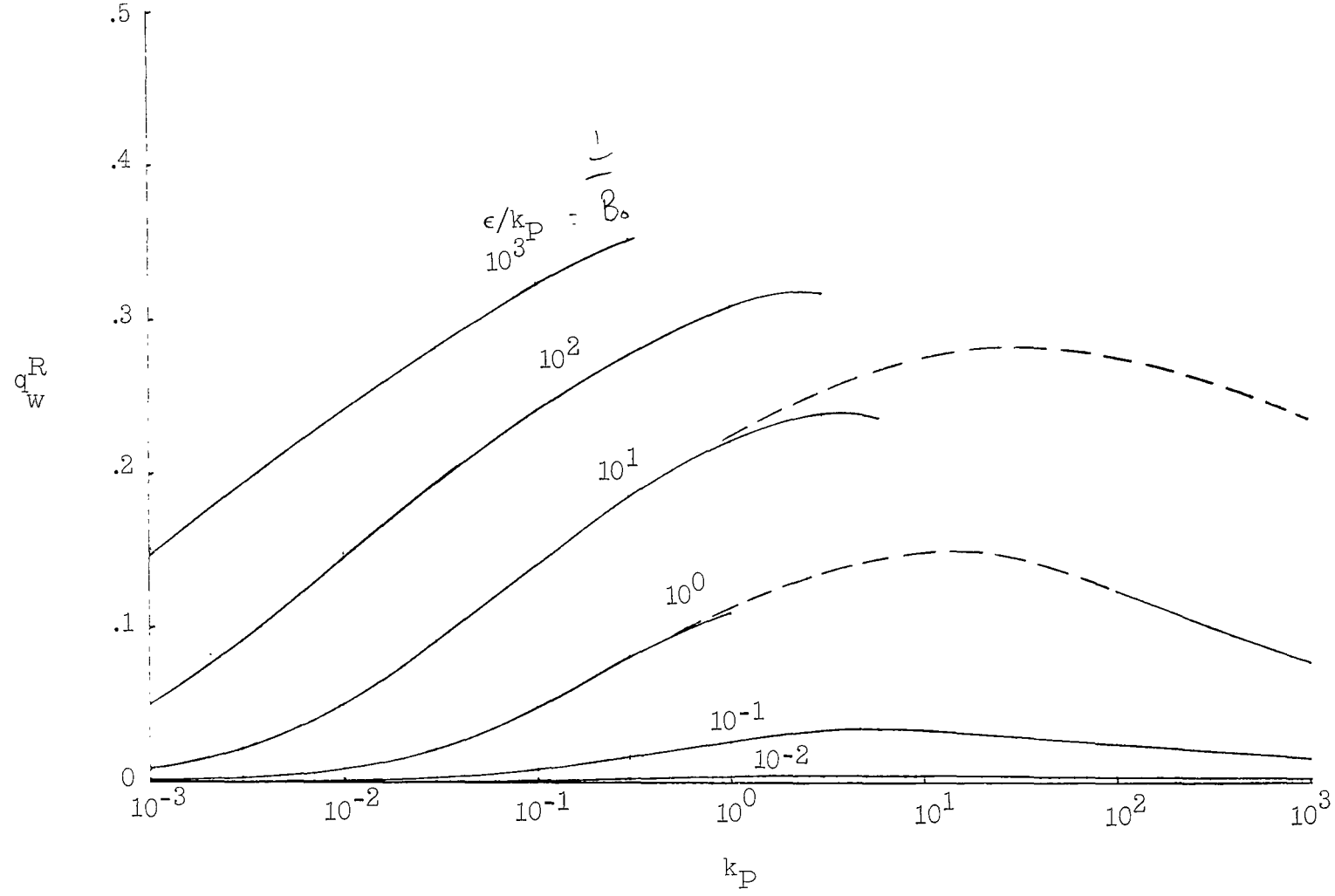

Figure 33.- Stagnation-point radiant heating rate in a model entry environment with a gray absorption coefficient. $\dot{\kappa}_P = 4$; $r_w = 0$.

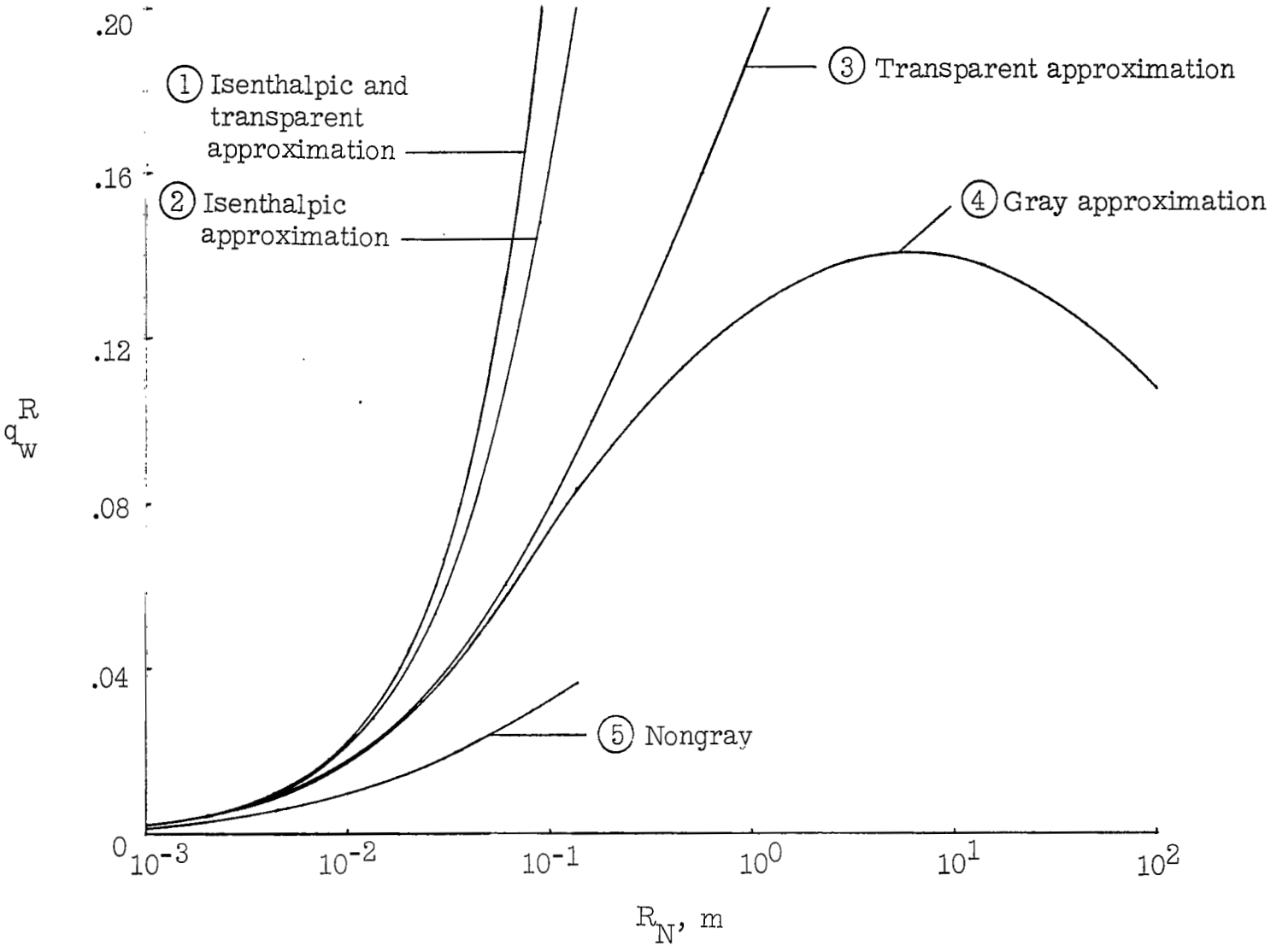

Figure 34.- The effect of body nose radius on the stagnation-point radiant heating rate. W_∞, 14.2 km/sec; altitude, 32.4 km.

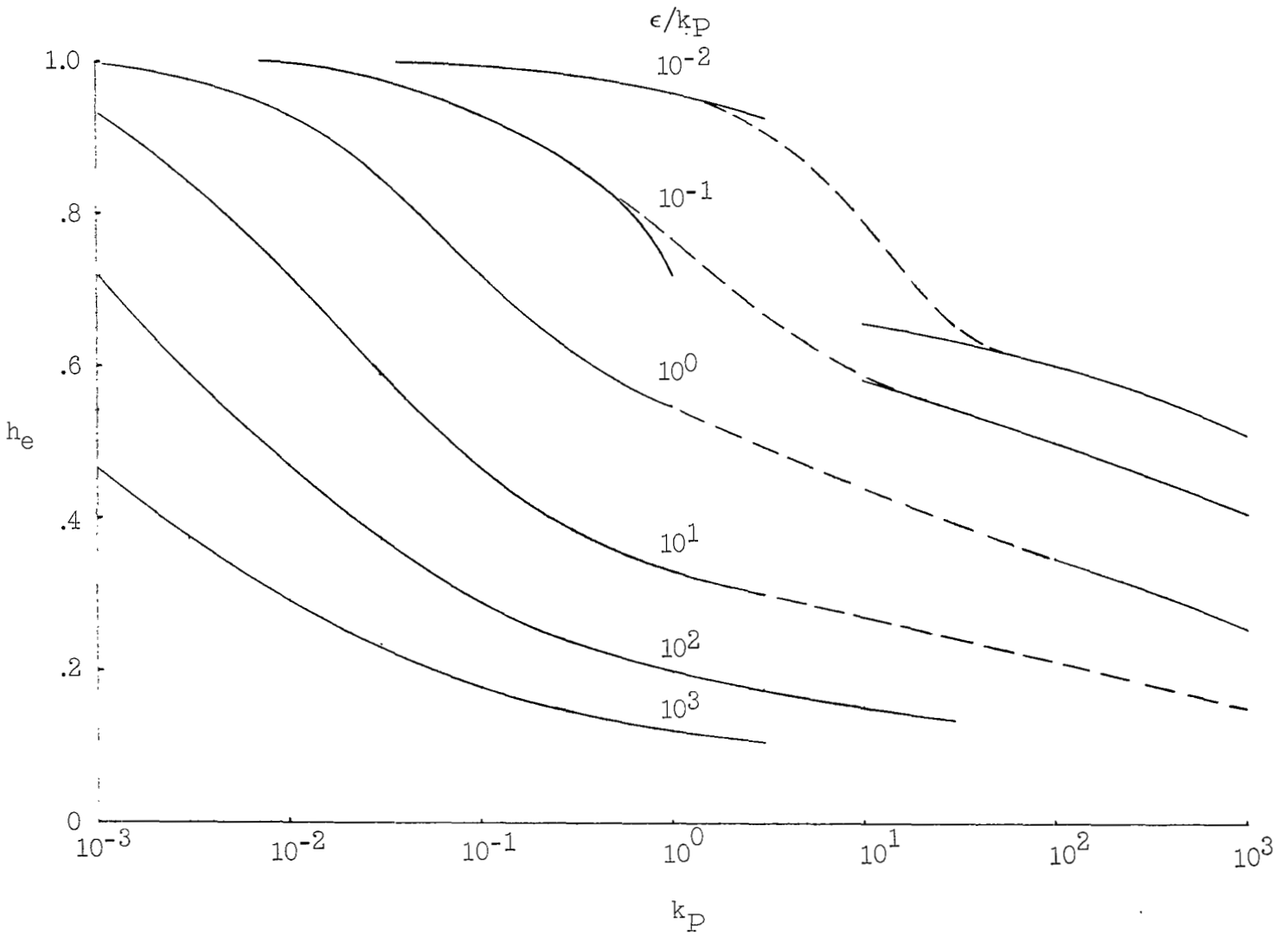

Figure 35.- The effect of radiant energy transport on convective heating.

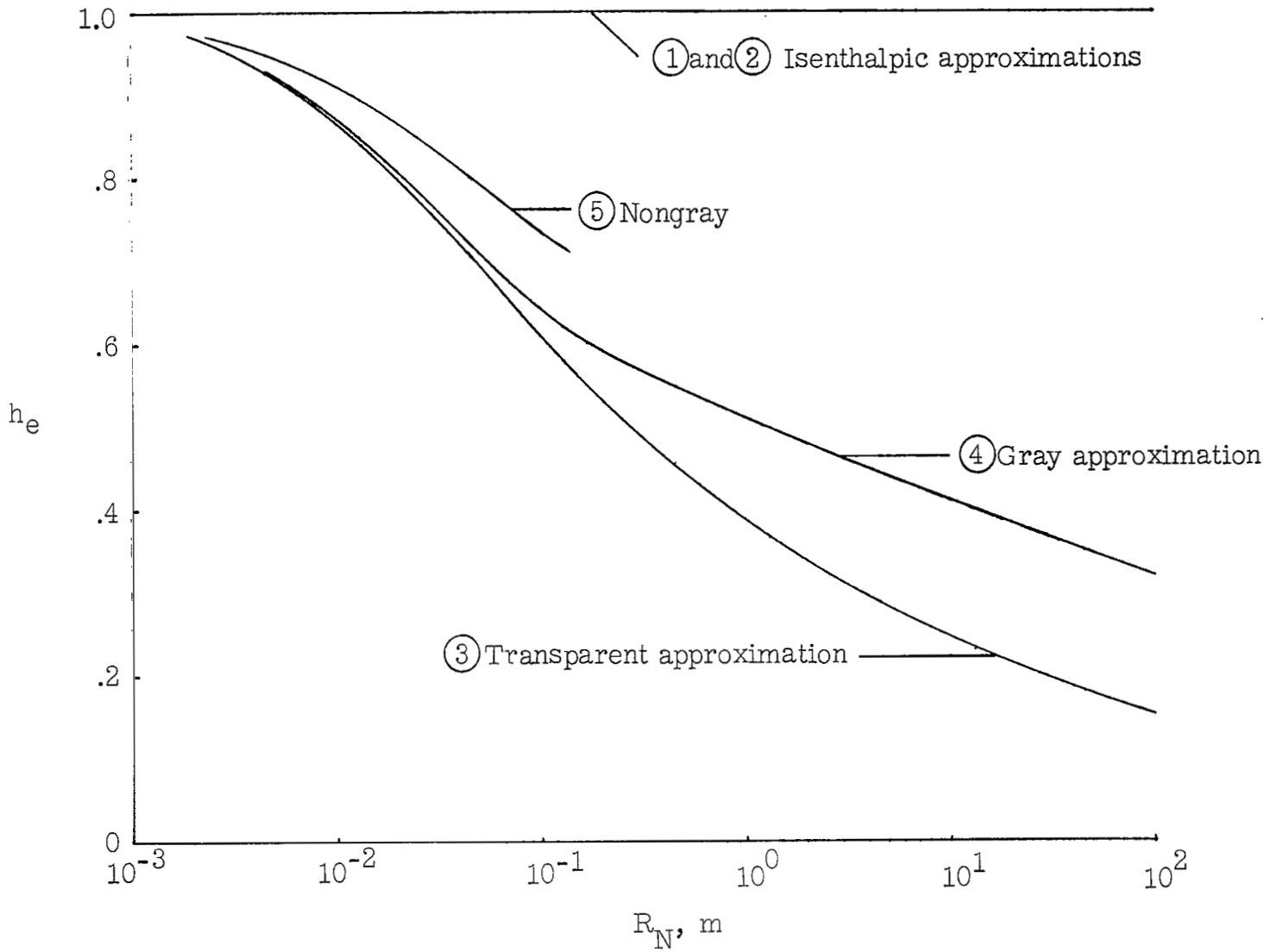

Figure 36.- The effect of body nose radius on the stagnation-point convective heating rate. W_∞, 14.2 km/sec; altitude, 32.4 km.

"The aeronautical and space activities of the United States shall be conducted so as to contribute . . . to the expansion of human knowledge of phenomena in the atmosphere and space. The Administration shall provide for the widest practicable and appropriate dissemination of information concerning its activities and the results thereof."

—NATIONAL AERONAUTICS AND SPACE ACT OF 1958

NASA SCIENTIFIC AND TECHNICAL PUBLICATIONS

TECHNICAL REPORTS: Scientific and technical information considered important, complete, and a lasting contribution to existing knowledge.

TECHNICAL NOTES: Information less broad in scope but nevertheless of importance as a contribution to existing knowledge.

TECHNICAL MEMORANDUMS: Information receiving limited distribution because of preliminary data, security classification, or other reasons.

CONTRACTOR REPORTS: Scientific and technical information generated under a NASA contract or grant and considered an important contribution to existing knowledge.

TECHNICAL TRANSLATIONS: Information published in a foreign language considered to merit NASA distribution in English.

SPECIAL PUBLICATIONS: Information derived from or of value to NASA activities. Publications include conference proceedings, monographs, data compilations, handbooks, sourcebooks, and special bibliographies.

TECHNOLOGY UTILIZATION PUBLICATIONS: Information on technology used by NASA that may be of particular interest in commercial and other non-aerospace applications. Publications include Tech Briefs, Technology Utilization Reports and Technology Surveys.

Details on the availability of these publications may be obtained from:

SCIENTIFIC AND TECHNICAL INFORMATION DIVISION

NATIONAL AERONAUTICS AND SPACE ADMINISTRATION

Washington, D.C. 20546